(12)

ADA111830

VSC-TR-81-14

RESULTS OF THE SDCS (SPECIAL DATA COLLECTION SYSTEM) ATTENUATION EXPERIMENT

VELA SEISMOLOGICAL CENTER

Z.A. Der, T.W. McElfresh, and A. O'Donnell
Seismic Data Analysis Center
Teledyne Geotech
314 Montgomery Street
Alexandria, Virginia 22314

30 OCT 1981

APPROVED FOR PUBLIC RELEASE; DISTRIBUTION UNLIMITED.

DTIC FILE COPY

DTIC
ELECTE
MAR 9 1982
S D
H

Monitored By:
VELA Seismological Center
312 Montgomery Street
Alexandria, VA 22314

82 03 09 042

Sponsored by

The Defense Advanced Research Projects Agency (DARPA)

DARPA Order No. 2551

Disclaimer: Neither the Defense Advanced Research Projects Agency nor the Air Force Technical Applications Center will be responsible for information contained herein which has been supplied by other organizations or contractors, and this document is subject to later revision as may be necessary. The views and conclusions presented are those of the authors and should not be interpreted as necessarily representing the official policies, either expressed or implied, of the Defense Advanced Research Projects Agency, the Air Force Technical Applications Center, or the US Government.

Unclassified

SECURITY CLASSIFICATION OF THIS PAGE (When Data Entered)

REPORT DOCUMENTATION PAGE

READ INSTRUCTIONS BEFORE COMPLETING FORM

1. REPORT NUMBER
VSC-TR-81-14

2. GOVT ACCESSION NO.
AD-A111830

3. RECIPIENT'S CATALOG NUMBER

4. TITLE (and Subtitle)
RESULTS OF THE SDCS (SPECIAL DATA COLLECTION SYSTEM) ATTENUATION EXPERIMENT

5. TYPE OF REPORT & PERIOD COVERED
Technical

6. PERFORMING ORG. REPORT NUMBER
SDAC-TR-80-4

7. AUTHOR(s)
Z. A. Der, T. W. McElfresh, and A. O'Donnell

8. CONTRACT OR GRANT NUMBER(s)
F08606-79-C-0007

9. PERFORMING ORGANIZATION NAME AND ADDRESS
Teledyne Geotech
314 Montgomery Street
Alexandria, Virginia 22314

10. PROGRAM ELEMENT, PROJECT, TASK AREA & WORK UNIT NUMBERS
VT/9709

11. CONTROLLING OFFICE NAME AND ADDRESS
Defense Advanced Research Projects Agency
1400 Wilson Boulevard
Arlington, Virginia 22209

12. REPORT DATE

13. NUMBER OF PAGES
269

14. MONITORING AGENCY NAME & ADDRESS (if different from Controlling Office)
VELA Seismological Center
312 Montgomery Street
Alexandria, Virginia 22314

15. SECURITY CLASS. (of this report)
Unclassified

15a. DECLASSIFICATION DOWNGRADING SCHEDULE

16. DISTRIBUTION STATEMENT (of this Report)

APPROVED FOR PUBLIC RELEASE: DISTRIBUTION UNLIMITED

17. DISTRIBUTION STATEMENT (of the abstract entered in Block 20, if different from Report)

18. SUPPLEMENTARY NOTES
Author's Report Date 01/26/81

19. KEY WORDS (Continue on reverse side if necessary and identify by block number)

Attenuation	Explosion yield
Seismic body waves	m_b
Seismic magnitude	Frequency dependent Q

20. ABSTRACT (Continue on reverse side if necessary and identify by block number)

Investigation of teleseismic arrivals at test sites in the western United States (WUS), a site on the Canadian shield and two sites in the northeastern United States revealed marked differences in mantle attenuation among these sites. All sites in the WUS show high attenuation in the underlying mantle, the sites in the northeastern U.S. appear to be intermediate between the WUS and the shield sites. This pattern fits well into the results of broader regional studies of amplitude anomalies, and spectral variations in both P and S waves.

DD FORM 1 JAN 73 1473 EDITION OF 1 NOV 65 IS OBSOLETE

Unclassified

SECURITY CLASSIFICATION OF THIS PAGE (When Data Entered)

The high frequency content of teleseismic arrivals cannot be reconciled with the results of long period attenuation studies unless a frequency dependence of Q is assumed in the Earth. Preliminary curves for t* vs. frequency are presented for shield and shield-to-tectonic type paths. These results demonstrate that yield estimates of explosions in different tectonic environments have to be corrected for mantle attenuation.

Accession For
NTIS GRA&I
DTIC TAB
Unannounced
Justification
By
Distribution/
Availability Codes
Avail and/or
Dist Special
A
DTIC
COPY
INSPECTED
2

RESULTS OF THE SDCS (SPECIAL DATA COLLECTION SYSTEM) ATTENUATION EXPERIMENT

SEISMIC DATA ANALYSIS CENTER REPORT NO.: SDAC-TR-80-4

AFTAC Project Authorization No.:	VELA VT/9709
Project Title:	Seismic Data Analysis Center
ARPA Order No.:	2551
Name of Contractor:	TELEDYNE GEOTECH
Contract No.:	F08606-79-C-0007
Date of Contract:	01 October 1979
Amount of Contract:	$279,929
Contract Expiration Date:	30 September 1980
Project Manager:	Robert R. Blandford (703) 836-3882

P. O. Box 334, Alexandria, Virginia 22313

APPROVED FOR PUBLIC RELEASE: DISTRIBUTION UNLIMITED

ABSTRACT

Investigation of teleseismic arrivals at test sites in the western United States (WUS), a site on the Canadian shield and two sites in the northeastern United States revealed marked differences in mantle attenuation among these sites. All sites in the WUS show high attenuation in the underlying mantle, the sites in the northeastern U.S. appear to be intermediate between the WUS and the shield sites. This pattern fits well into the results of broader regional studies of amplitude anomalies, and spectral variations in both P and S waves.

The high frequency content of teleseismic arrivals cannot be reconciled with the results of long period attenuation studies unless a frequency dependence of Q is assumed in the Earth. Preliminary curves for t* vs. frequency are presented for shield and shield-to-tectonic type paths. These results demonstrate that yield estimates of explosions in different tectonic environments have to be corrected for mantle attenuation.

TABLE OF CONTENTS

TABLE OF CONTENTS (Continued)

LIST OF FIGURES

LIST OF FIGURES (Continued)

LIST OF FIGURES (Continued)

LIST OF FIGURES (Continued)

LIST OF FIGURES (Continued)

LIST OF FIGURES (Continued)

LIST OF FIGURES (Continued)

LIST OF TABLES

INTRODUCTION

The SDCS attenuation experiment was motivated by indications of differences in the m_b-M_s relationship for explosions at NTS relative to explosions at USSR test sites. These differences can be explained by anomalously high attenuation in the mantle under the various test sites in the Western United States as opposed to a high Q mantle under shield areas of the USSR. This report consists of three parts and summarizes all of the results of the project to date.

The first part discusses the analysis of data from the SDCS station network. This data base is also supplemented by the analysis of some LRSM data in order to extend the areal coverage and to compensate for the fact that only one SDCS station was located on a shield.

The second part consists of a detailed discussion of the results of the SDCS experiment in the framework of research conducted on attenuation by us and others. This section outlines regional variations of Q_α and Q_β under the United States and puts limits on the absolute and relative variations of these quantities. The need for a frequency dependence of Q is also discussed. Since no comparable study of short-period attenuation has been undertaken in the past and since short-period data are influenced by many extraneous factors not related to mantle Q, a methodology had to be created to reduce the effects of these extraneous factors and to choose parameters less sensitive to them and more diagnostic of mantle Q. The data are interpreted in the following framework:

a) Due to the well-documented focusing effects of small scale inhomogeneities in the crust and the uncertainties in the estimation of crustal amplification, short-period body wave amplitude anomalies are likely to be biased and are not reliable indicators of mantle Q.

b) While short-period body wave spectral shapes (especially falloff rates at high frequencies) are extremely sensitive to small variations of mantle Q, they are considerably less affected by other factors.

c) To measure mantle attenuation a combined interpretation of P and S wave amplitude and spectral data is necessary, with more weight being given to spectral measurements.

The third part of this report contains our arguments for using the methods outlined above. We feel that justifying the methodology within the main body of the report would continually divert the reader's attention to side issues; therefore, we have reserved a separate part of the report to demonstrate the validity of points a-c above and to discuss several other factors that need to be addressed to overcome possible objections. This is an essential part of the report and could be read first. Part III consists of Sections A-F, each of which is referred to in the main part of the text.

In this report we describe attenuation in terms of the quantity $t^* = \int \frac{dt}{Q}$, where Q is the quality factor along a certain seismic ray path and t is the travel time. t* is naturally a path-dependent quantity since it is a function of the Q variation in the Earth which in turn is a function of depth and region. It is probably also frequency dependent. t* appears to be the most convenient parameter for characterizing attenuation because for distances greater than 25 degrees it changes little with epicentral distance. Thus, it can be used as a single (although frequency dependent) parameter to characterize regional differences for various types of paths described in terms of upper mantle structures under the source and receiver. For distances less than 20 to 25 degrees, t* increases with epicentral distance due to the fact that the body waves progressively penetrate the low-velocity - low-Q layer (LVZ) in the upper mantle as the distance increases. The contributions from the LVZ (which is coincident with the low Q layer) dominate the integral and thus t* becomes a property that depends almost entirely on the types of upper mantle structures the ray path crosses. Thus:

$$t^* \approx \int_D \frac{dt}{Q} + \int_U \frac{dt}{Q} + t_r^* \qquad (1)$$

where D is the integral along the downgoing leg of the ray path through the LVZ and U is the upgoing part. t_r^* is the contribution from the rest of the path through the crust and the lower mantle. It is relatively small because the crust and lower mantle are high-Q regions.

Alternate representations of attenuation are less convenient. For instance, if the apparent Q is used it has to be specified as a function of travel time and other parameters. It should be understood therefore that t* in this report always refers to values measured at teleseismic distances unless it is clearly associated with near distances.

Throughout this report the mean amplitude, travel time, t* and dominant period differences between stations are not considered significant unless they exceed the 95% statistical confidence levels. The confidence level of some of the data is higher than 99%. This kind of stability is not often found in geophysical literature, and the existence of interstation differentials in the quantities measured can hardly be questioned in such cases.

Details of the experiment that are not essential to the main conclusions of the report are presented in appendices at the end.

PART 1

DATA ANALYSIS FROM SDCS AND SELECTED LRSM STATIONS

The basic theory of the SDCS experiment is that by measuring relative amplitudes and spectral ratios for common events between stations one can infer the degree of anelastic attenuation under each station. The design of the experiment by DARPA is based on an implicit assumption of a degree of seismic reciprocity.

Seismic reciprocity is a general law stated by Knopoff and Gangi (1959), Hudson (1969), and others and is valid for arbitrary inhomogeneous linearly elastic media. This law expresses the interchangeability of source force systems and combinations of receiver displacement parameters. For example, one can state the interchangeability of dilatational force and displacement systems (Hudson, 1969; Knopoff, 1979). Reciprocity requires that the sources and receivers when interchanged occupy exactly the same positions in space. This condition is not satisfied in a strict sense for the SDCS experiment at the NTS sites. This is because, for the m_b -yield application, the sources are at the explosion sites and the receivers are mostly WWSSN and LRSM stations scattered world-wide, whereas for the reciprocal problem, the receivers are close to the explosion site (but not at the same depth) and the sources are located at the seismic belts of the earth. Thus from basic physical grounds alone one cannot expect reciprocity to be exactly valid for the NTS experiment.

The Special Data Collection System network consisted of a variable number of portable seismic stations deployed across the United States and Canada. It is essentially an extension of the LRSM (Long Range Seismic Measurement) network with more up-to-date digital recording systems, although at some sites analog recording was still used. Between 1976 and 1979, these portable stations were deployed at various nuclear test sites in the western United States and at the sites RKON (Red Lake, Ontario), IFME (Island Falls, Maine), and HNME (Houlton, Maine) in order to measure the differences in anelastic attenuation in the mantle under each site. The sites are marked on the map in Figure 1, and relevant site data are tabulated in Table I.

The instrument responses of the short-period systems were identical at all sites except HNME. This makes it impossible to directly compare dominant signal periods and trace amplitudes at this station with the rest of the

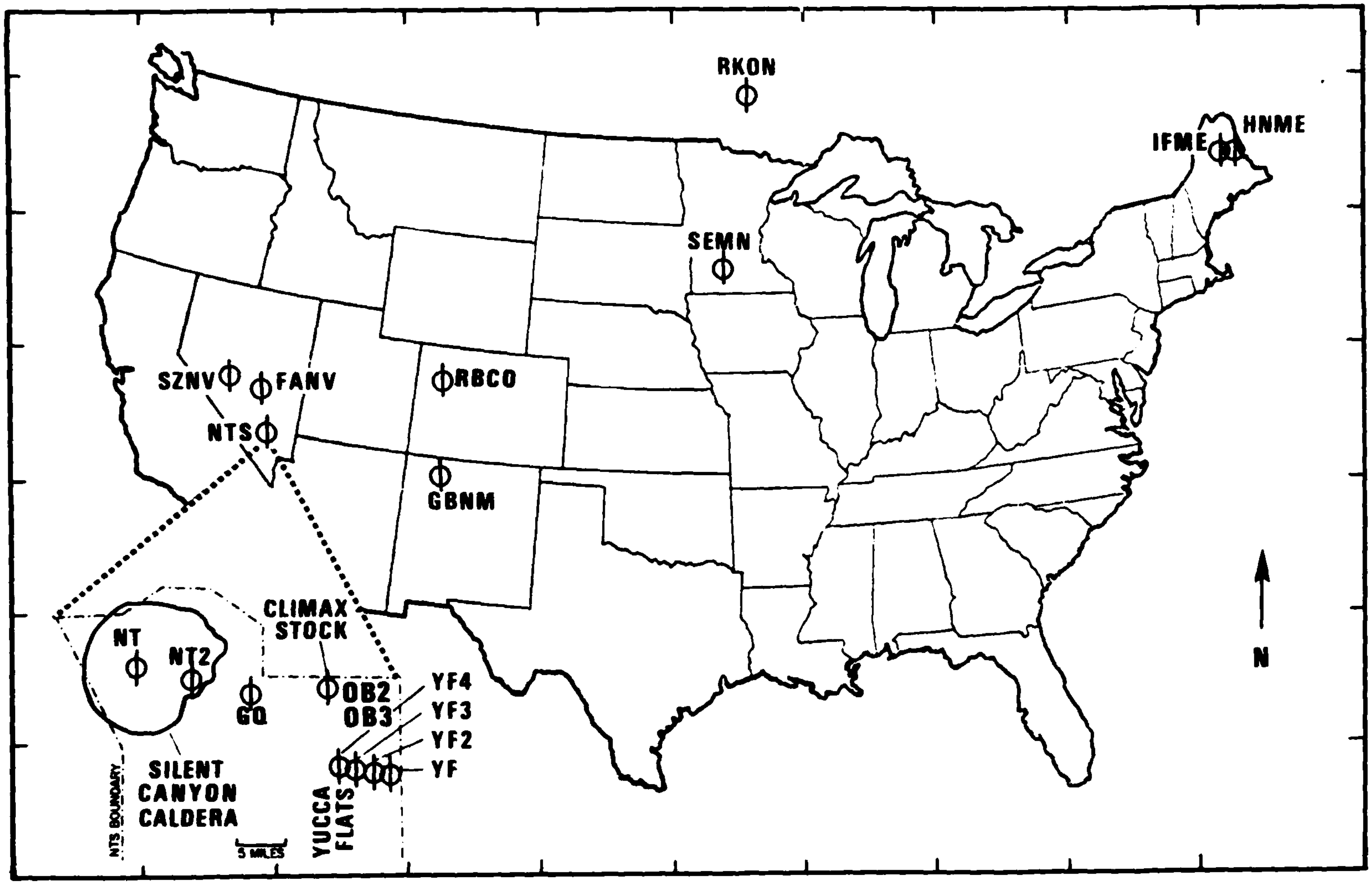

Figure 1 Locations of the SDCS and LRSM stations analyzed in detail in Part I of this report.

TABLE I

Description of SDCS and LRSM stations discussed in Part I of this report

STA	LOCATION	OPERATING PERIOD	SP COMPONENTS*	MODE	CRUST MATERIAL	N LAT	W LONG	ELEVATION M
FANV	FAULTLESS SITE,NEV	6/77-9/77	Z,N,E	ANALOG	ALLUVIUM + TUFF	38.64	116.22	1920
GBNM	GASBUGGY SITE,NM	5/77-8/78	Z,N,E	ANALOG	SEDIMENTS,IGNEOUS DIKES	36.69	107.23	2164
GQNV	GOLD MEADOWS,NTS	10/77-12/77	Z,N,E	ANALOG	GRANITE	37.23	116.21	2057
HNME	HOULTON,ME	2/75-3/76	Z,N,E	DIGITAL	SLATE	46.16	67.99	213
HNME	HOULTON,ME	4/76-8/78	Z,N,E	ANALOG	SLATE	46.16	67.99	213
IFME	ISLAND FALLS,ME	11/77-8/78	Z,N,E	ANALOG	GRANITE	46.03	68.20	232
NTNV	PAHUTE MESA,NTS	8/76-3/77	Z,N,E	DIGITAL	LOW VELOCITY VOLCANICS	31.28	116.42	1987
NT2NV	PAHUTE MESA,NTS	8/76-3/77	Z,N,E	DIGITAL	LOW VELOCITY VOLCANICS	37.25	116.30	2185
OB2NV	CLIMAX STOCK,NTS	8/76-2/78	Z,N,E	DIGITAL	GRANITE	37.23	116.06	1542
OB3NV	CLIMAX STOCK,NTS	4/77-2/78	Z ONLY	DIGITAL	GRANITE	37.23	116.05	1609
RBCO	RIO BLANCO SITE,COLO	12/77-1/79	Z,N,E	DIGITAL	ALLUVIUM + SEDIMENTS	39.81	108.36	1996
RKON	RED LAKE, ONTARIO	3/75-3/78	Z,R_{NTS},T_{NTS}	DIGITAL	GRANITE	50.84	93.67	365
SEMN	SLEEPY EYE, MINN	1/62-6/63	Z,R_{73},T_{163}	ANALOG	GRANITE	44.41	94.67	244
SZNV	SHOAL SITE,NTS	1/63-2/63	Z,R_{319},T_{49}	ANALOG	GRANITE	39.20	118.38	1606
YFNV	YUCCA FLATS,NTS	4/77-9/77	Z,N,E	DIGITAL	ALLUVIUM	37.07	116.00	1271
YF2NV	YUCCA FLATS,NTS	4/77-9/77	Z ONLY	DIGITAL	ALLUVIUM	37.07	116.01	1260
YF3NV	YUCCA FLATS,NTS	4/77-9/77	Z ONLY	DIGITAL	ALLUVIUM	37.07	116.02	1254
YF4NV	YUCCA FLATS,NTS	4/77-9/77	Z,N,E	DIGITAL	ALLUVIUM	37.08	116.04	1244

* SUBSCRIPTS INDICATE ORIENTATION OF R, T COMPONENTS; NTS INDICATES ORIENTATION TOWARD THE NEVADA TEST SITE.

stations. The instrument responses of several kinds of systems discussed in this report are shown in Figure 2.

The approach taken for event selection was to measure events on the first published lists, which were the bulletins of the Hagfors Observatory, that of the French national network or the PDE lists of the USGS. Locations were double checked with later, more accurate event lists. These preliminary locations were sufficient for the purpose of relative magnitude measurements.

Results of Amplitude Studies

During the course of the SDCS experiment the amplitudes and periods of more than 600 events were measured for the purpose of computing interstation m_b differentials. The events were all in the range $25° < \Delta < 85°$ from the stations to ensure traversal of the upper mantle by most of the P wavetrain. A complete listing of the events is shown in Appendix A.

Since the SDCS experiment was designed to resolve problems arising from a study of M_s-m_b, it was necessary to compute the conventional m_b using the maximum amplitude in the first 3 seconds of each signal. The writers are of the opinion, in agreement with Butler (1979), that the amplitude of the first cycle or "b" phase is more meaningful; nevertheless, we shall show that our results agree extremely well with those obtained from "b" phase measurements. Following Cleary (1967) and Butler (1979) we have also compiled differentials of trace amplitudes corrected for distance, and we have abandoned the computation of the uncorrected magnitude m_a' used in previous reports because we feel that it is less meaningful than the trace amplitudes (see section B of Part 3).

Histograms of the m_b and trace differentials are shown in Figures 3 and 4 for the station pair RKON and OB2NV, two stations of great diagnostic value since both of these are located on granite and, presumably, are free of large crustal amplification effects. These figures show the extremely large scatter in the amplitude and magnitude differentials characteristic of short-period data. This is not surprising in view of the comments in section D of Part 3 of this report. A noteworthy data point, the Novaya Zemlya nuclear explosion of 02 OCT 76 (marked as N.Z.), is on the flanks of the distributions in spite of the fact that the source is axisymmetric.

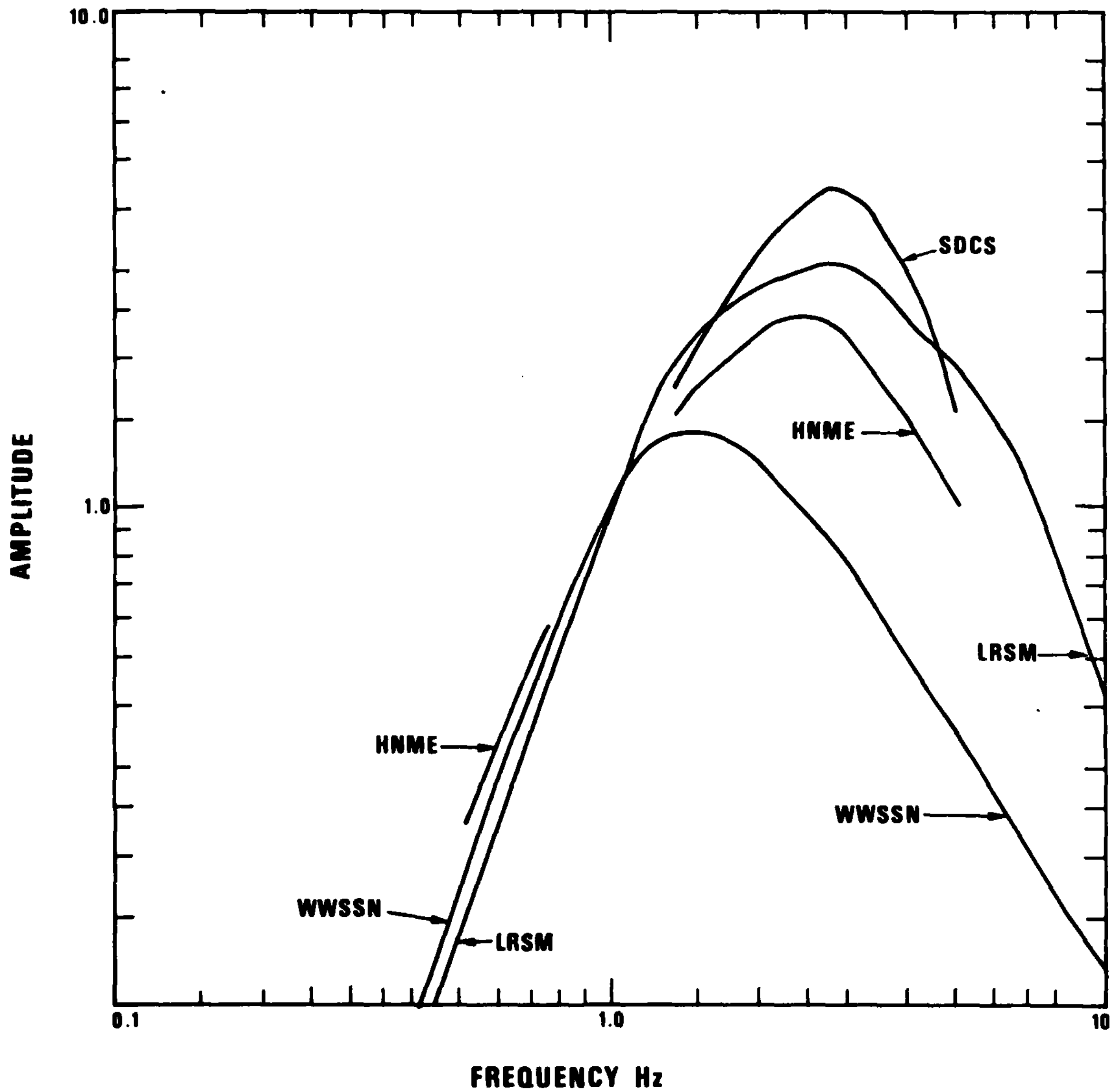

Figure 2 Response curves of the LRSM, SDCS, WWSSN and HNME stations.

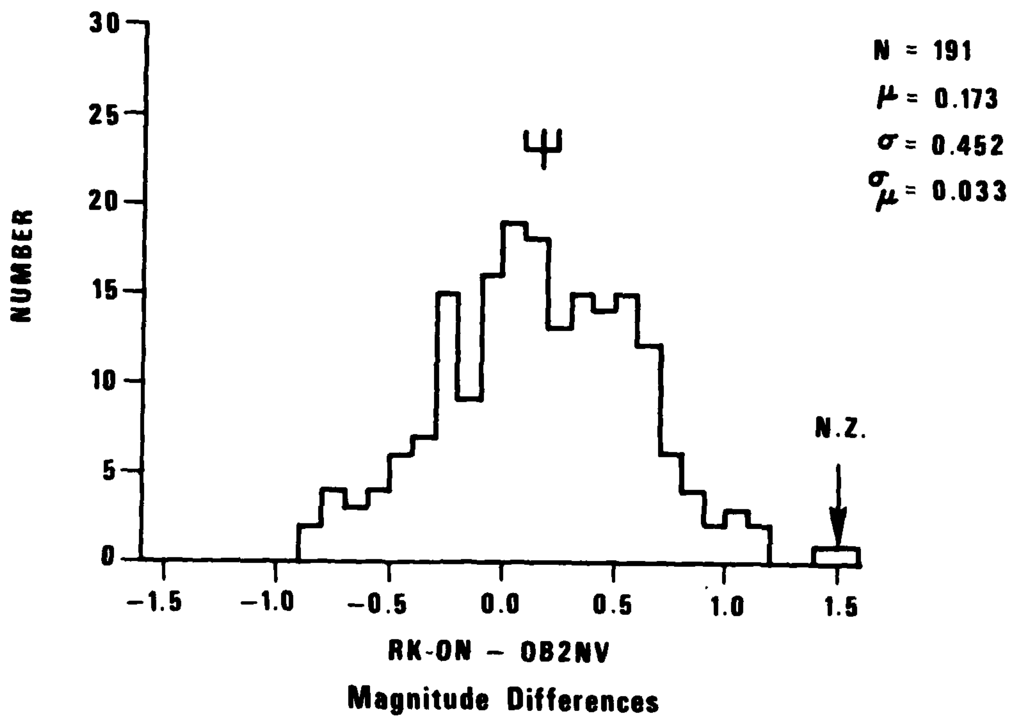

Figure 3 Histogram of m_b differentials between RKON and OB2NV. The mean m_b differential is 0.173 ± .066 (95% confidence) magnitude units. The point N.Z. marks a data point from Novaya Zemlya.

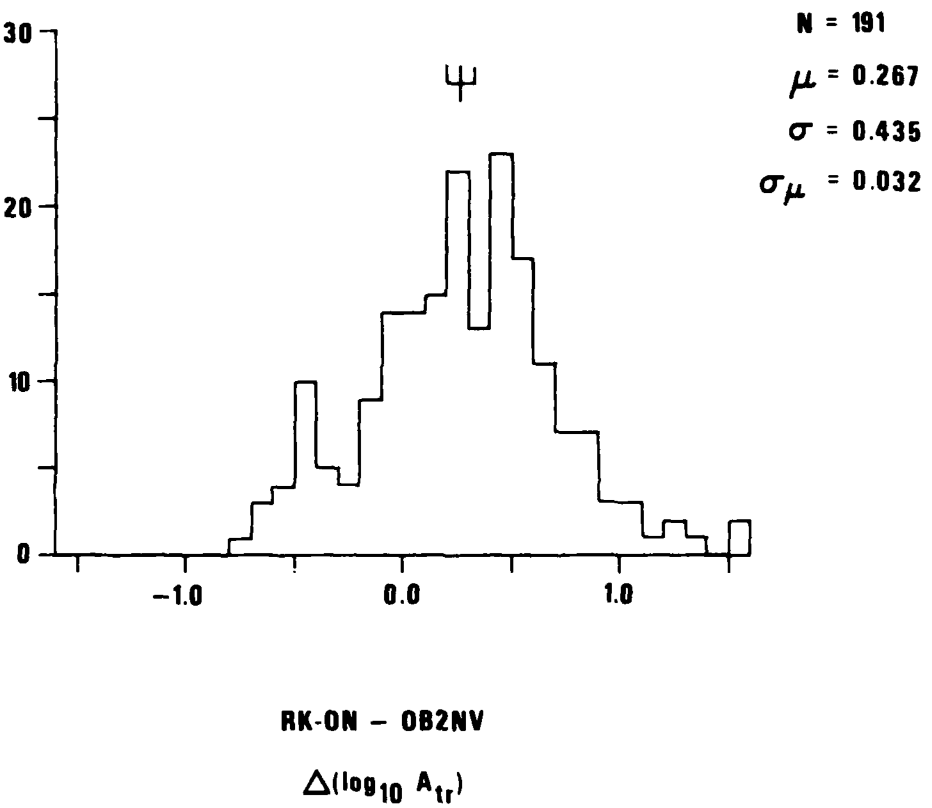

Figure 4 Histogram of P wave trace amplitude differentials between RKON and OB2NV using ten base logarithms of amplitudes as units. The differential is 0.267 ± .064 (95% confidence) showing that the RKON/OB2NV amplitude ratio is about 1.85.

Histograms of the magnitude and trace amplitude differentials for the rest the station pairs are collected in Appendices B and C of this report.

Consider now the standard deviation $\sigma_{\Delta m_b}$ of relative magnitude differentials as a function of the distance between station pairs. Figure 5 is a plot of $\sigma_{\Delta m_b}$ versus log $\Delta°$. A linear empirical relationship appears to exist. The causes of the linear increase in $\sigma_{\Delta m_b}$ are: 1) decreasing signal similarity for the P waveforms as the distance increases so that m_b cannot be consistently picked at similar portions of the P wavetrain, 2) source radiation patterns that cause systematic variations of amplitudes, and 3) increasing effects of focusing and defocusing. In order to take into account the effect of signal coherence evidenced by the $\sigma_{\Delta m_b}$-$\Delta°$ relationship, we make use of a least squares technique which also allows us to incorporate all of our measurements into the determination of magnitude differentials across the SDCS network. For a given event we write the magnitude differentials between pairs of stations i and j in the form

$$\Delta m_b^i - \Delta m_b^j = {}^k\Delta m_b^{ij} + \varepsilon_{ij}(\Delta°_{ij}) \tag{1}$$

where Δm_b^i is the station term (bias) of station i, ${}^k\Delta m_b^{ij}$ is the observed magnitude differential between station i and j for event k and $\varepsilon_{ij}(\Delta°_{ij})$ is an error term dependent upon the distance $\Delta°_{ij}$ between the stations. The expected value of this error term

$$E\{\varepsilon_{ij}^2\ (\Delta°)\} = \sigma_{\Delta m_b}^2\ (\Delta°_{ij}) \tag{2}$$

can be read from the regression line in Figure 5 as a function of distance.

Because taking differences in all possible combinations is redundant, a hierarchy of stations was assigned as follows: OB2NV, OB3NV, YFNV, YF4NV, YF2NV, YF3NV, NTNV, NT2NV, FANV, GBNM, RKON, HNME, and we used the leftmost available station bias term as the reference (positive) term in equation (1). This hierarchy was selected to optimize the distance distribution so that most of the distances used, and consequently the values of $\sigma_{\Delta m_b}$, are as small as possible. Thus OB2NV, at the center of the NTS cluster and located between GBNM and FANV, is the prime candidate for the most commonly used reference station, while RKON and HNME are outliers and rank low.

This least squares procedure causes only minor changes in the relative

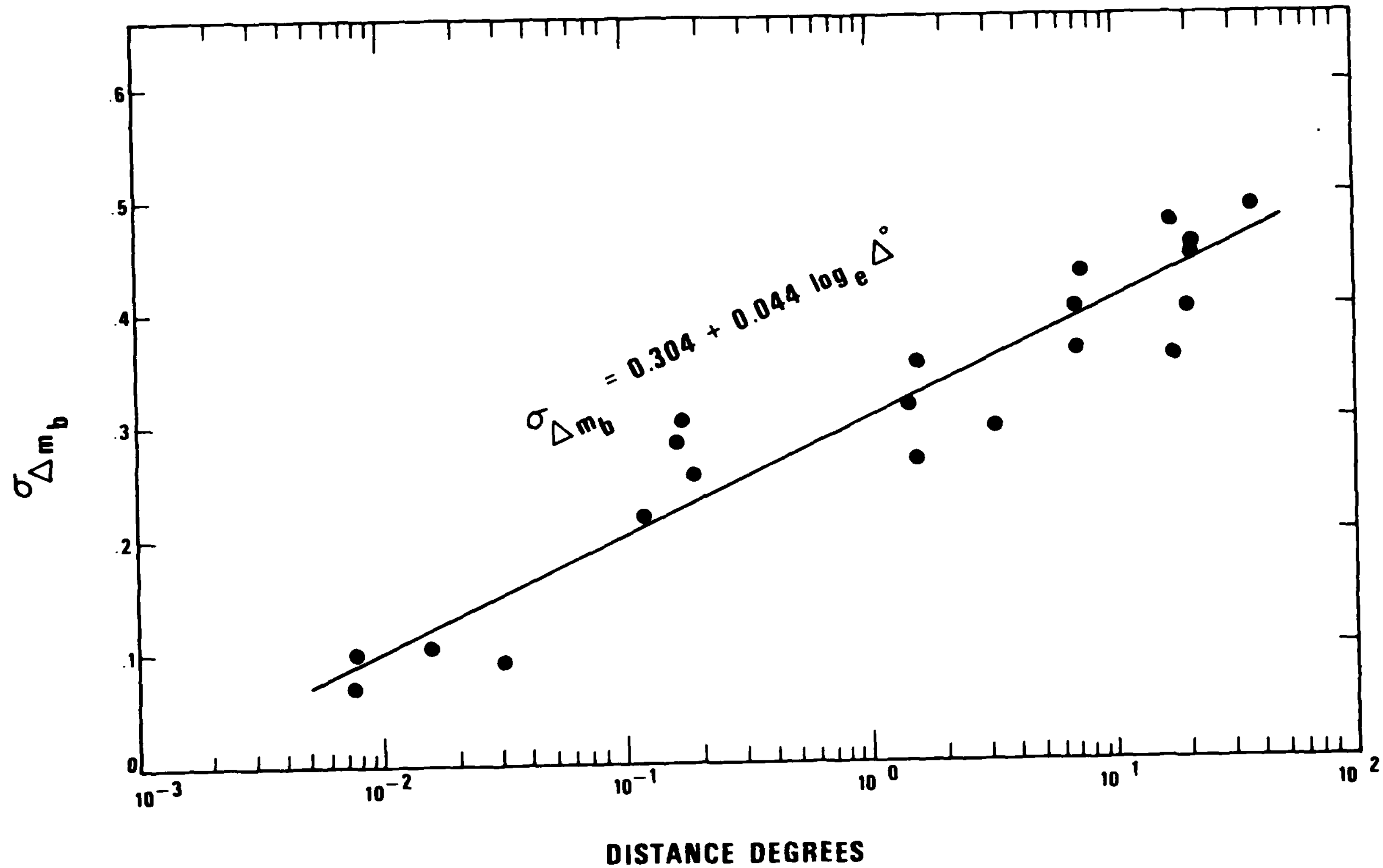

Figure 5 Standard deviation of relative m_b differentials vs. *interstation distance*. The increase reflects increasing variability of m_b readings for more distant station pairs.

m_b and trace amplitude differentials compared to those directly computed from data and given in the histograms in Appendices B and C. The means of the differentials relative to OB2NV of m_b and trace amplitudes are listed in Table II and also shown with their 95% confidence limits in Figures 6 and 7. The most prominent features of these figures are the high amplitudes of m_b values at the stations on Yucca Flats (YF's) and on Pahute Mesa (NT's). The low amplitude of the station IFME in Maine is another feature of Figure 6.

In order to correct for the effect of the crust on these m_b and trace amplitudes we compared changes in synthetic P pulse amplitudes. Pulse shapes for a 50 kt explosion as modeled by von Seggern and Blandford (1972) were computed after passing them through layered halfspace models using the standard Haskell algorithm. Table III lists the model parameters used in the calculations. We attenuated each pulse with a multiplicative spectral factor $\exp(-\pi f t^*)$, where t^* was chosen to be 0.45, a typical value for the WUS. By removing most of the high frequencies, the attenuation factor makes the pulse more rounded. This pulse has a spectrum which, in spectral content, well represents the average teleseismic P-wave arrivals. It is peaked at 1 Hz and falls off at a rate of somewhat more than ω^{-2} at high frequencies. To reduce variations caused by changes in the angle of incidence, we computed the synthetics for three angles (20°, 25°, and 30° measured from the vertical) and then averaged the relative amplification factors between stations obtained for these three angles.

The Yucca Flats sites rest on thick unconsolidated sediments and tuff that cause considerable signal amplification (Houser, 1968; Fernald et al, 1968; Healy, 1968; Ramspott and Howard, 1975; Hays and Murphy, 1971). The FAULTLESS site (FANV) is also located over alluvium and tuff, but according to test site information, the alluvium is more consolidated at this site (McKeown and Dickey, 1969) (Lt. Col. Bulin of ARPA also provided us with data relevant to the FANV site). Alluvium and a thick sedimentary carbonaceous-shale sequence also underlay the GASBUGGY site (GBNM) (Thornbrough, 1971). In all of these cases the part of the structure that primarily determines crustal amplification was found to be near the surface. Consequently, the structures were modeled only down to the basement (Der et al,

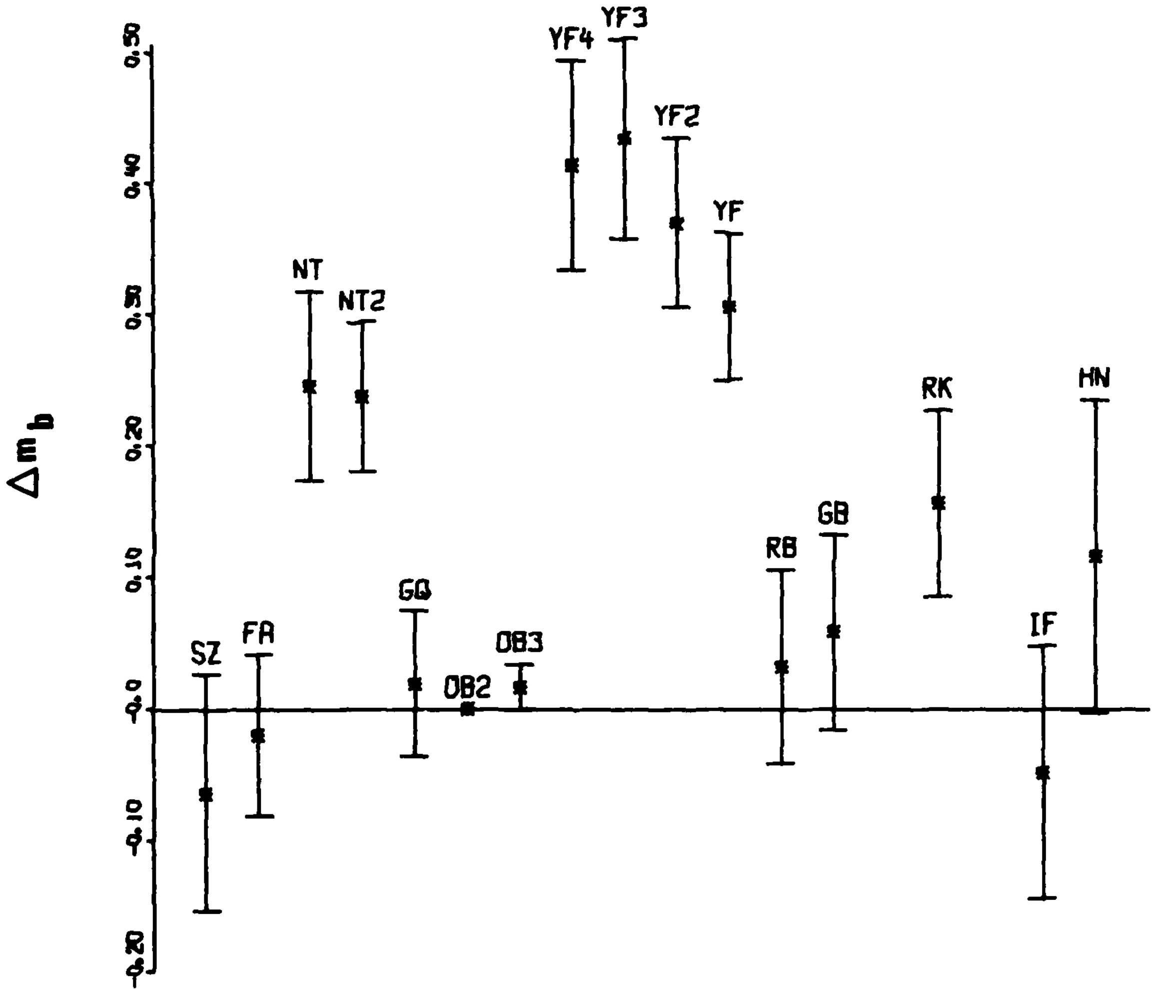

Figure 6 Magnitude bias terms at the various SDCS stations with respect to OB2NV. 95% confidence limits are shown by bars. No corrections for crustal amplification are included.

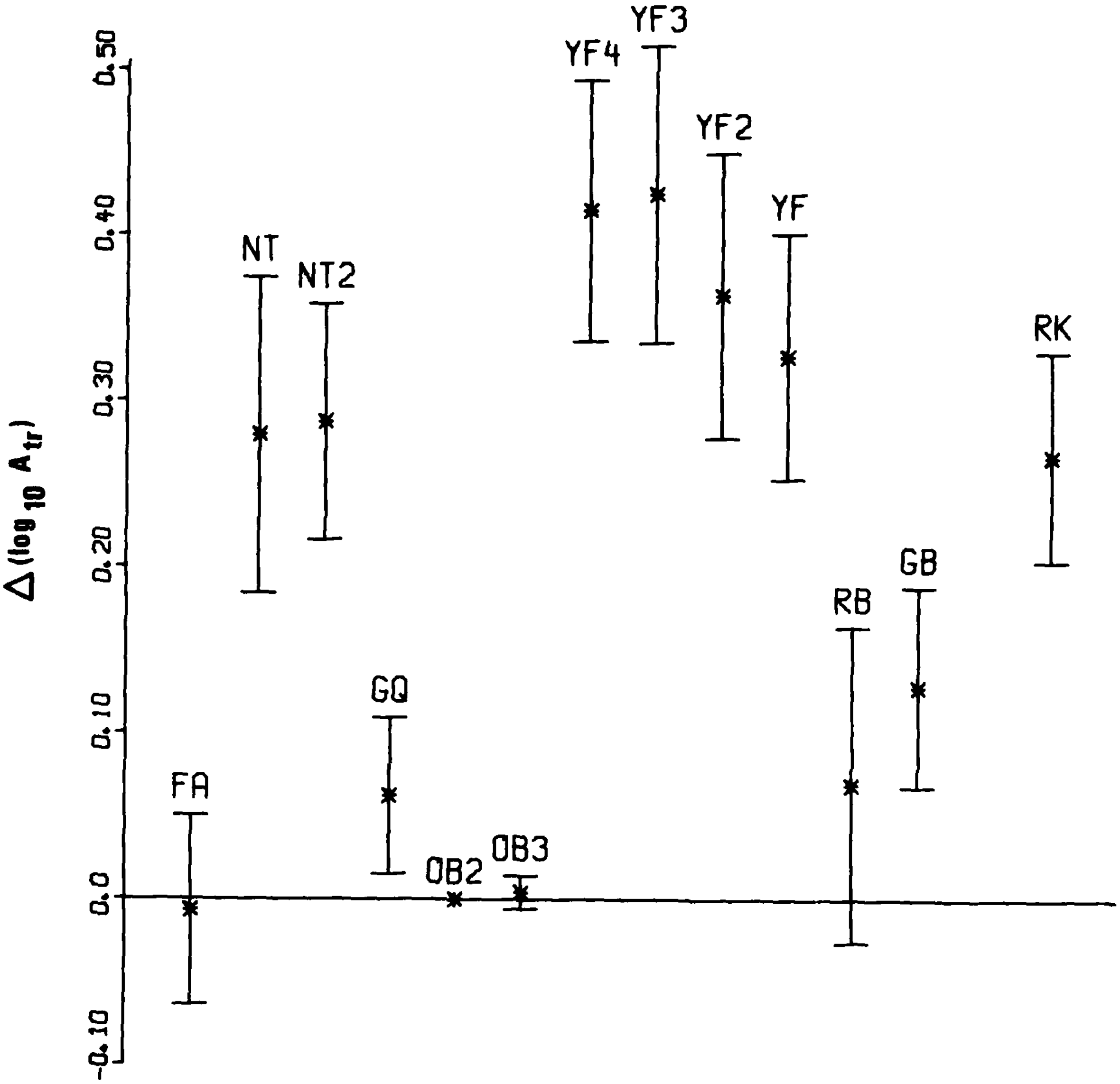

Figure 7 Trace amplitude differentials (expressed in $\log_{10}$ units) relative to OB2NV. No crustal corrections are applied.

TABLE II

Summary of relative magnitudes (Δm_b), trace amplitudes (ΔA_{tr}), crust-corrected values (Δm_b^{corr}, ΔA_{tr}^{corr}), dominant periods (ΔT), and attenuation (Δt^*) with respect to the reference station OB2NV located on the Climax Stock at NTS.

STA	Δm_b	ΔA_{tr}	ΔT	CRUST CORR	Δm_b^{corr}	ΔA_{tr}^{corr}	Δt^*
HNME *	0.116 ± 0.119	N/A	N/A	0.0	0.116	N/A	-0.098 ± 0.030
SEMN RKON *	0.156 ± 0.071	0.267 ± 0.063	-0.192 ± 0.038	0.0	0.156	0.267 ± 0.063	-0.200 ± 0.031
YF *	0.306 ± 0.056	0.327 ± 0.074	-0.051 ± 0.071	0.300 †	0.006	0.027 ± 0.074	-0.040 ± 0.050
YF2 *	0.370 ± 0.065	0.364 ± 0.086	-0.011 ± 0.067	0.330 †	0.040	0.034 ± 0.086	0.014 ± 0.055
YF3 *	0.434 ± 0.076	0.425 ± 0.090	0.032 ± 0.074	0.300 †	0.134	0.125 ± 0.090	-0.016 ± 0.063
YF4 *	0.413 ± 0.080	0.415 ± 0.079	-0.013 ± 0.073	0.310 †	0.103	0.105 ± 0.079	0.006 ± 0.062
FA *	-0.020 ± 0.061	-0.007 ± 0.057	-0.020 ± 0.068	0.268	-0.288	-0.275 ± 0.057	-0.036 ± 0.052
GB *	0.058 ± 0.074	0.128 ± 0.060	-0.068 ± 0.052	0.310	-0.252	-0.182 ± 0.060	0.013 ± 0.050
NT *	0.246 ± 0.072	0.279 ± 0.095	-0.100 ± 0.060	0.216	0.030	0.063 ± 0.095	-0.079 ± 0.052
NT2 *	0.237 ± 0.057	0.287 ± 0.071	-0.100 ± 0.050	0.210	0.027	0.077 ± 0.071	-0.059 ± 0.050
OB3 *	0.016 ± 0.018	0.004 ± 0.010	0.007 ± 0.027	0.0	0.016	0.004 ± 0.010	-0.036 ± 0.019
SZ *	-0.064 ± 0.090	N/A	N/A	0.0	-0.064	N/A	-0.030 ± 0.091
GQ	0.019 ± 0.055	0.062 ± 0.047	-0.086 ± 0.050	0.0	0.019	0.062 ± 0.047	-0.052 ± 0.042
IF	-0.048 ± 0.096	N/A	N/A	0.0	-0.048	N/A	-0.112 ± 0.040
RB	0.032 ± 0.074	0.069 ± 0.095	-0.014 ± 0.078	0.134	-0.102	-0.065 ± 0.095	0.035 ± 0.035

* Δm_b Adjusted by least squares technique over these stations

† Average of finite difference and Haskell results

TABLE III

Crustal models used for estimating crustal amplifications at the SDCS stations

	d(km)	α(km/sec)	β(km/sec)	$\rho(g/cm^2)$
FA-NV	0.44	2.50	1.06	2.30
	1.00	3.00	1.60	2.30
	1.00	3.50	1.73	2.30
	1.525	4.00	2.20	2.50
	∞	5.70	3.29	2.70
GB-NM	0.700	2.00	1.06	2.00
	0.150	3.25	1.63	2.00
	0.200	3.45	1.73	2.00
	0.120	3.90	2.16	2.28
	0.600	4.40	2.48	2.49
	0.625	4.80	2.73	2.55
	∞	5.70	3.29	2.70
GQ-NV	2.0	6.10	3.60	2.70
	∞	6.10	3.60	2.70
HN-ME	10.0	5.90	3.36	2.70
	∞	6.35	3.62	2.72
IF-ME	2.0	6.10	3.60	2.70
	∞	6.10	3.60	2.70
NT-NV	1.0	3.00	1.80	2.00
	4.0	3.60	2.00	2.20
	5.0	5.70	3.36	2.70
	∞	6.10	3.60	2.80
NT2NV	1.0	2.86	1.75	2.00
	4.0	3.60	2.00	2.20
	5.0	5.70	3.36	2.70
	∞	6.10	3.60	2.80
OB2NV	10.0	5.70	3.36	2.70
	∞	6.10	3.60	2.80
OB3NV	10.0	5.70	3.36	2.70
	∞	6.10	3.60	2.80
RB-CO	1.0	3.80	2.10	2.30
	∞	6.10	3.60	2.70
RK-ON	6.0	5.64	3.47	2.70
	∞	6.15	3.64	2.80
SZ-NV	2.0	6.10	3.60	2.70
	∞	6.10	3.60	2.70
YF-NV	0.18	1.30	0.659	1.75
	0.55	2.00	1.07	1.196
	∞	5.70	3.36	2.70
YF2NV	0.24	1.30	0.659	1.75
	0.58	2.00	1.07	1.196
	∞	5.70	3.36	2.70
YF3NV	0.29	1.30	0.659	1.75
	0.61	2.00	1.07	1.196
	∞	5.70	3.36	2.70
YF4NV	0.29	1.30	0.659	1.75
	0.70	2.00	1.07	1.196
	∞	5.70	3.36	2.70

1977), which was assumed to have the same elastic properties as the granite stock at OB2NV (which was modeled by a simple homogeneous halfspace). This similarity makes the pulse sizes of the computed synthetic records comparable with correction for halfspace properties below the layered stack.

Finite difference methods were also used to estimate crustal amplification at the four stations on Yucca Flats (the method is described in the paper by Kelly et al, 1976). We attempted to model Yucca Flats with a structure derived from Hays and Murphy (1971), utilizing Ramspott's and Howard's (1975) and Fernald et al's (1968) velocity and structural data. The results of both methods are shown in Table IV. Both the Haskell matrix and the finite difference methods suggest considerable amplification at Yucca Flats, and the two methods yield about the same result.

Plots of m_b differentials relative to OB2NV corrected for crustal effects, Figure 8, show major changes compared to the uncorrected data of Figure 6. The differences between OB2NV and the Yucca Flats (YF) and Pahute Mesa (NT) stations are drastically reduced with the exception of YF3 and YF4 to a level below significance. The m_b values for FANV, RBCO and GBNV are reduced below the level of OB2NV. The thin ($h < 50$ m) weathered layer at HNME does not justify any crustal correction relative to IFME since, in our experience, such thin layers do not amplify teleseismic waves. However, any such correction could move HNME to slightly lower m_b values. The relative positions of RKON and OB2NV, the two key stations on granite, are unchanged, and the differential in m_b, 0.17 m.u., is statistically significant - at higher than the 99% confidence level.

The crust-corrected trace amplitudes expressed in base 10 log units behave similarly as shown in Figure 9. The crustal corrections for trace amplitudes are the same as for m_b since there is no apparent change in period in the synthetic calculations. The OB2NV-RKON differential of 0.267 is highly significant statistically and is in excellent agreement with the results of Butler (1979).

TABLE IV

Results of finite difference and Haskell algorithm calculations of crustal response at Yucca Flats

Stations	Magnitude Differential Relative to OB2NV		
	Observed	Layered (Haskell)	FINITE DIFFERENCE 1 Hz
YF	0.306	0.34	0.26
YF2	0.370	0.34	0.32
YF3	0.434	0.32	0.27
YF4	0.413	0.32	0.30

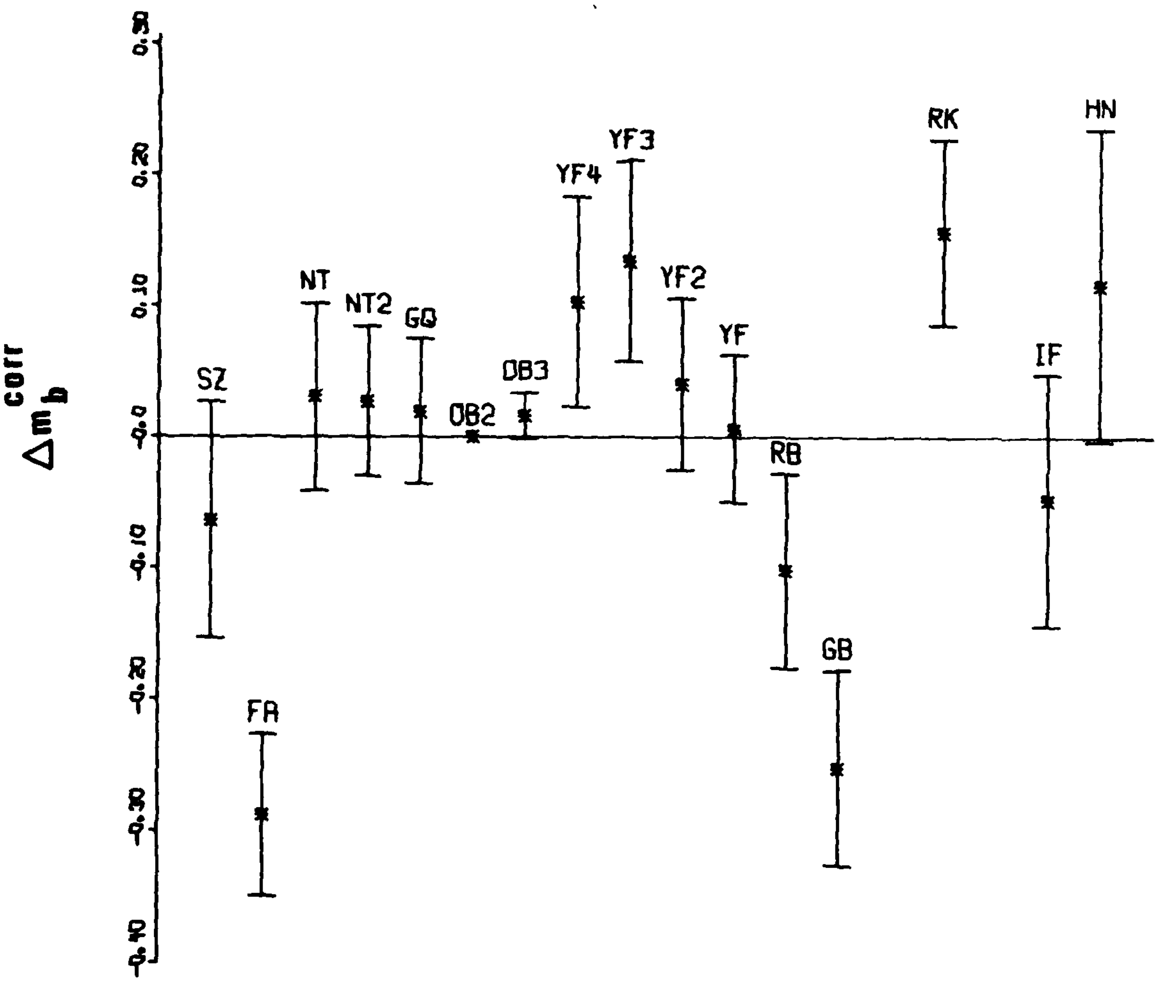

Figure 8 Magnitude bias terms relative to OB2NV with crustal corrections. The m_b levels at Yucca Flats and Pahute Mesa (NTNV and NT2NV) are greatly reduced.

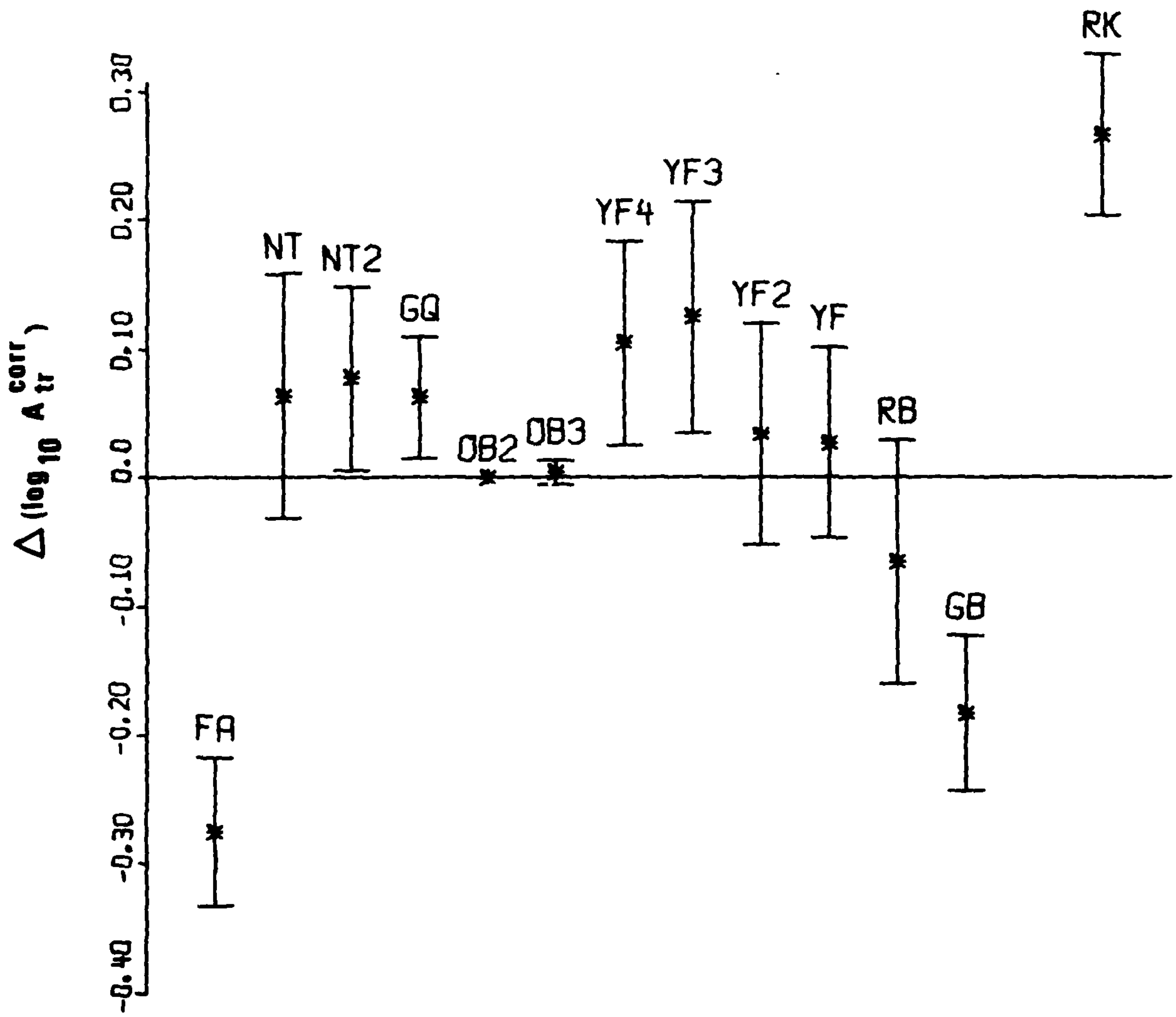

Figure 9 Trace amplitude levels relative to OB2NV ($\log_{10}$ units) with crustal corrections applied.

Possible Bias Effects in m_b Due To Variable Thresholds, Noise Level and Source Region

Since relative and absolute amplitude measurements can be biased by threshold and source region effects (von Seggern and Blandford, 1972; Ringdal, 1976), we have tested our data to determine the extent of any possible bias. The criteria we have used for amplitude measurement require that S/N be greater than 3. Thus, event pairs were eliminated when one of the stations, e.g. station A, has S/N < 3. Because this condition could result from low signal at station A relative to station B, the average amplitude at A could be overestimated relative to B at low magnitudes. Only if the great majority of all readings are considerably above the 3:1 S/N level can such bias in the average be ruled out. To test for this bias, we plotted the differentials of m_b for selected stations pairs against the average m_b for the same two stations. Pronounced trends in plots such as these would indicate biases in the procedures used for determining Δm_b. A slight change of Δm_b with increasing magnitude might also suggest a shift of corner frequency of seismic sources of lower frequencies. This shift would be more visible at a high Q than at a low Q station. Absence of a clear trend indicates that bias in Δm_b from variable noise levels is not significant.

Figures 10 through 16 show such plots for a selected set of key station pairs. None of these plots, including the critical pair RKON-OB2NV, suggest a clear trend. Therefore, bias effects from our procedure are probably negligible. Note that the noise level is approximately 0.3 m. u. higher at RKON than at OB2NV. However, the raw amplitudes on the film (magnitude at 1 Hz, not amplitude corrected at T or at A/T) also average 0.3 m. u. at RKON. Thus, the average expected S/N is the same, and no bias would be expected.

To test for the effect of source region biases on the measured relative m_b, we divided the RKON-OB2NV interstation differentials into four groups marked with different symbols as follows:

Symbol		
A	$(\Delta m_b - \mu) < -\sigma$	high amplitude at OB2NV
B	$-\sigma < (\Delta m_b - \mu) < 0$	
C	$0 < (\Delta m_b - \mu) < +\sigma$	
D	$(\Delta m_b - \mu) > +\sigma$	low amplitude at OB2NV

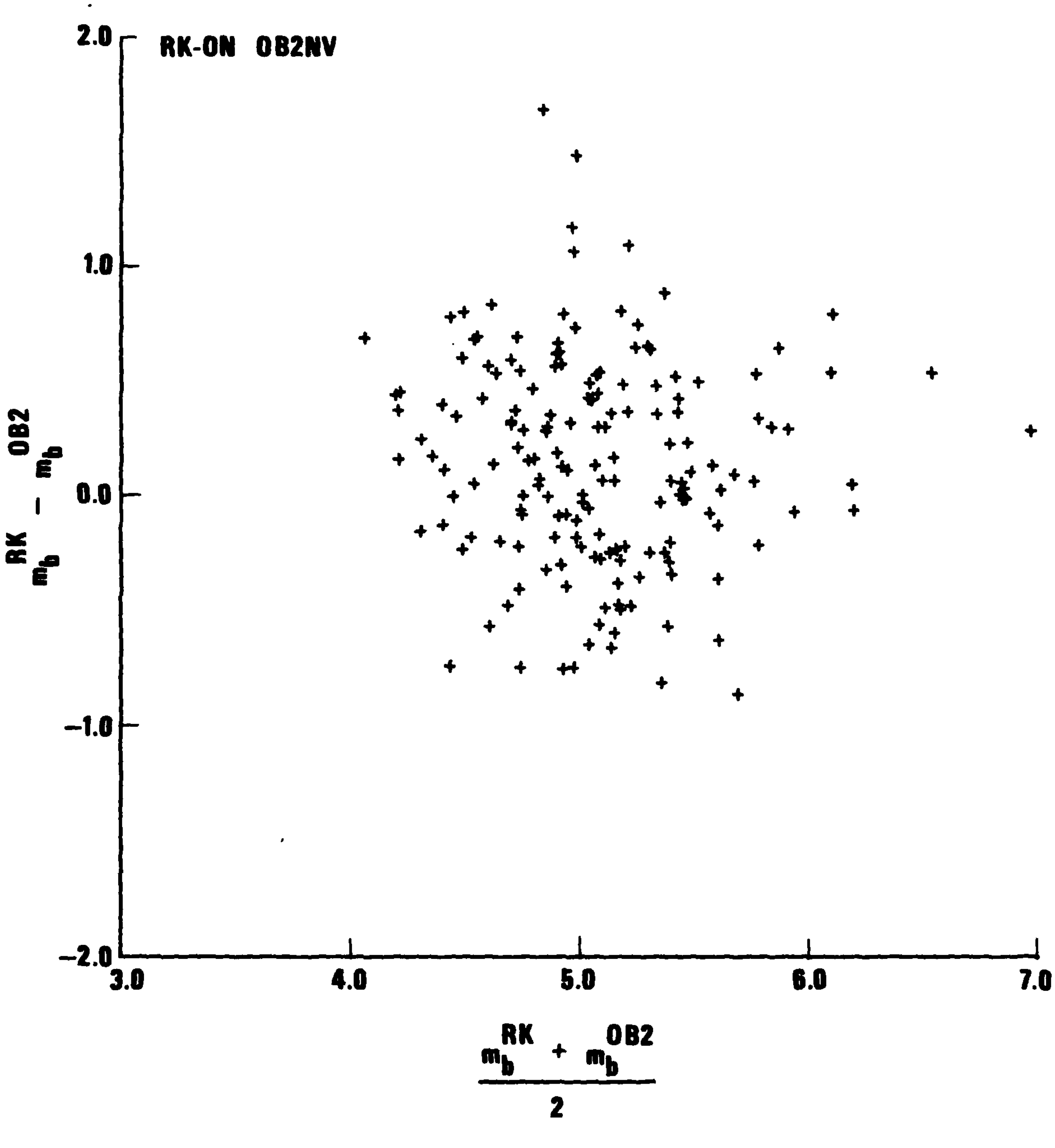

Figure 10 Interstation m_b differentials plotted against the two-station average m_b for station pair RKON - OB2NV. The absence of any clear increasing or decreasing trend indicates that magnitude threshold biases are not present (see text).

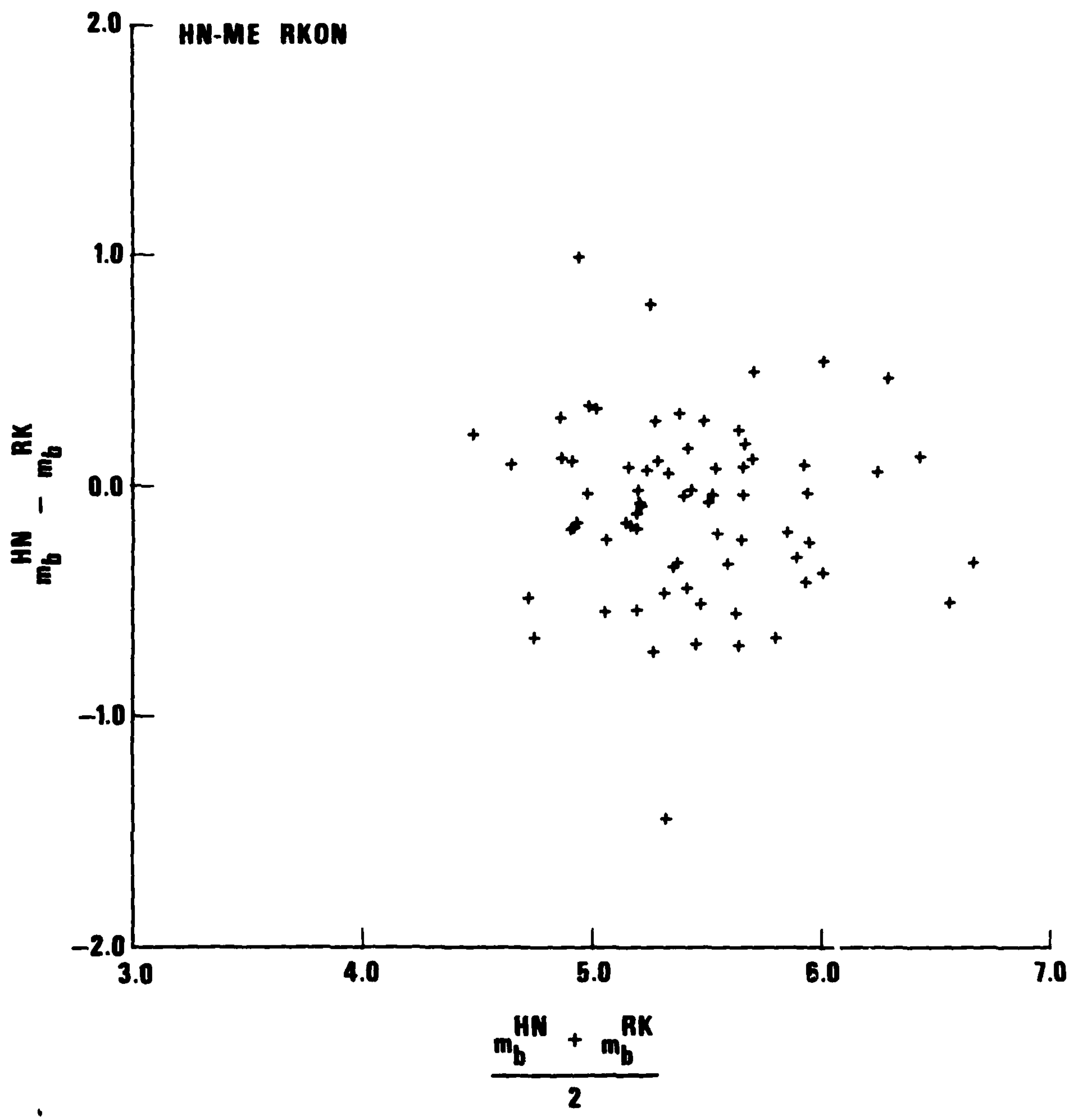

Figure 11 Interstation m_b differentials plotted against the two-station average m_b for the station pair HNME - RKON. The absence of any clear increasing or decreasing trend indicates that magnitude threshold biases are not present (see text).

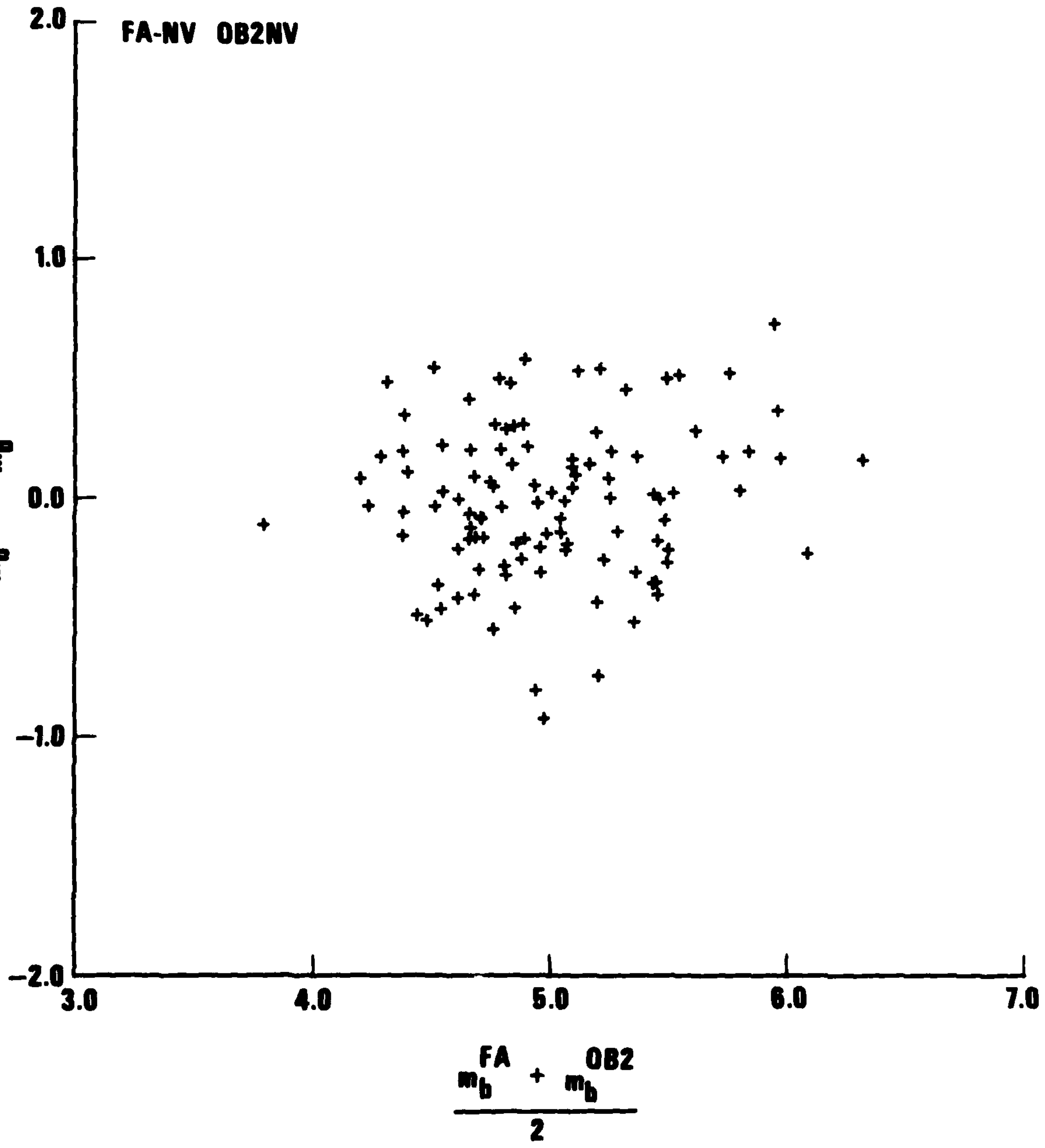

Figure 12 Interstation m_b differentials plotted against the two-station average m_b for the station pair FANV - OB2NV. The absence of any clear increasing or decreasing trend indicates that magnitude threshold biases are not present (see text).

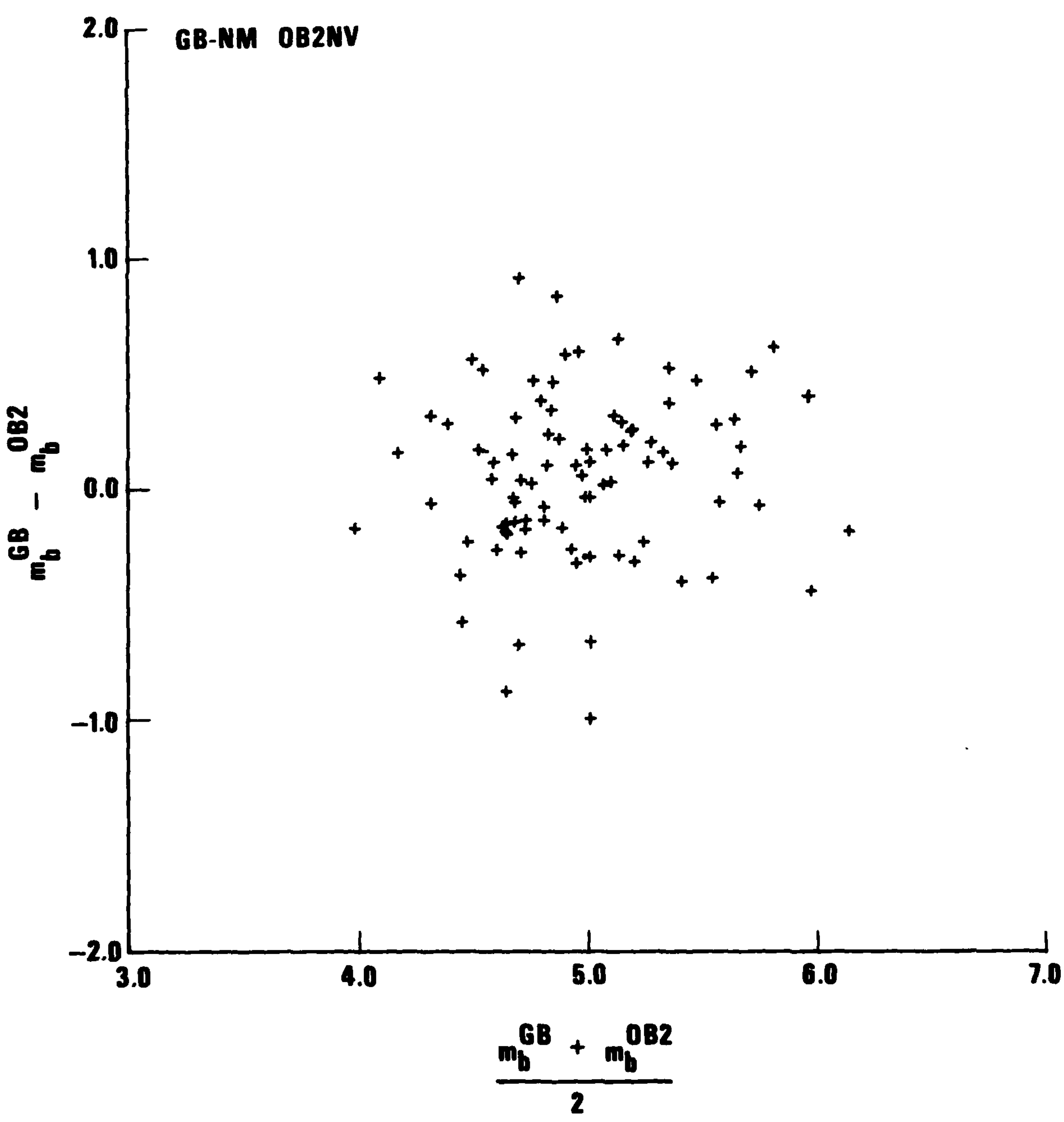

Figure 13 Interstation m_b differentials plotted against the two-station average m_b for the station pair GBNM - OB2NV. The absence of any clear increasing or decreasing trend indicates that magnitude threshold biases are not present (see text).

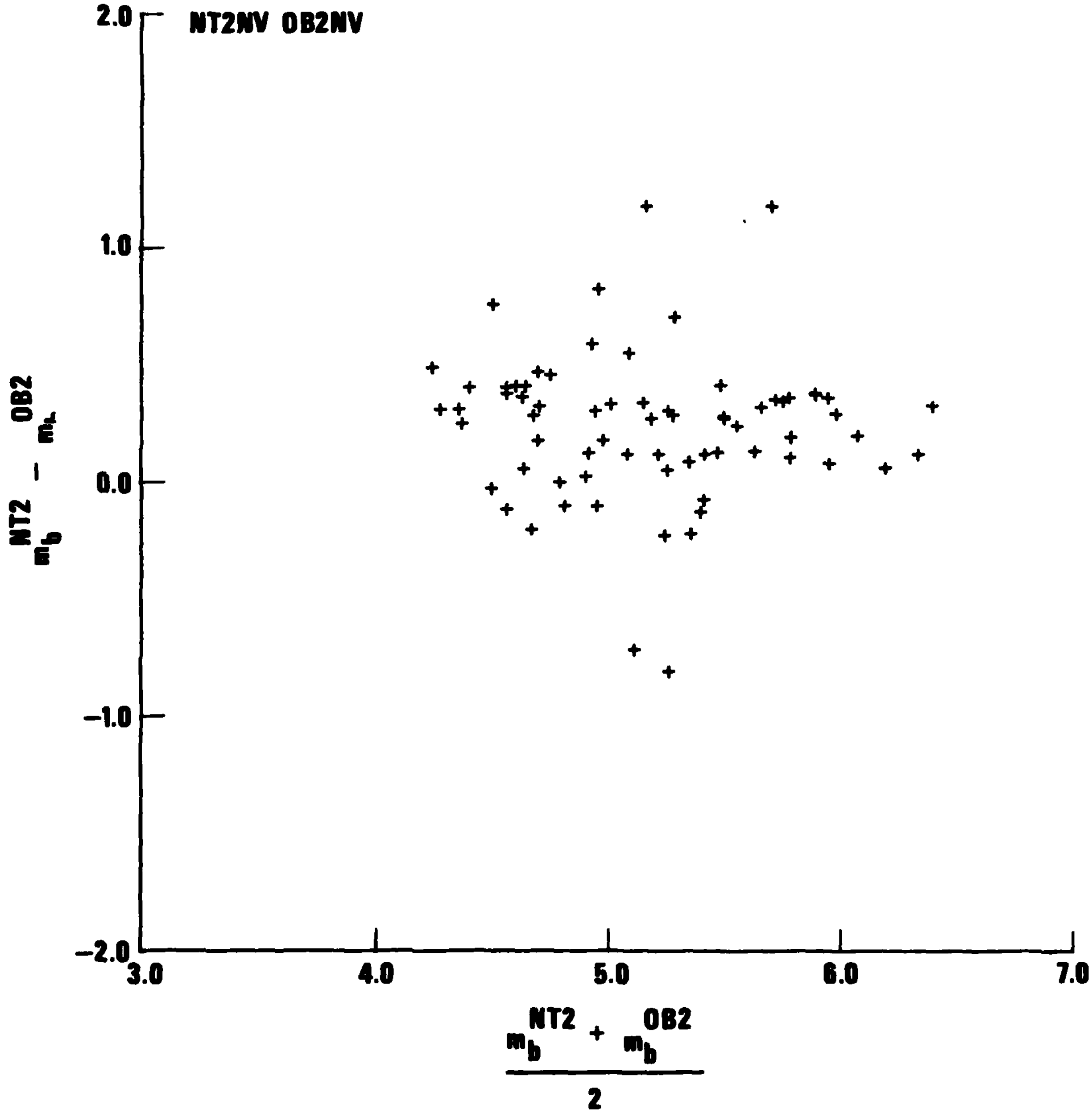

Figure 14 Interstation m_b differentials plotted against the two-station average m_b for the station pair NT2NV - OB2NV. The absence of any clear increasing or decreasing trend indicates that magnitude threshold biases are not present (see text).

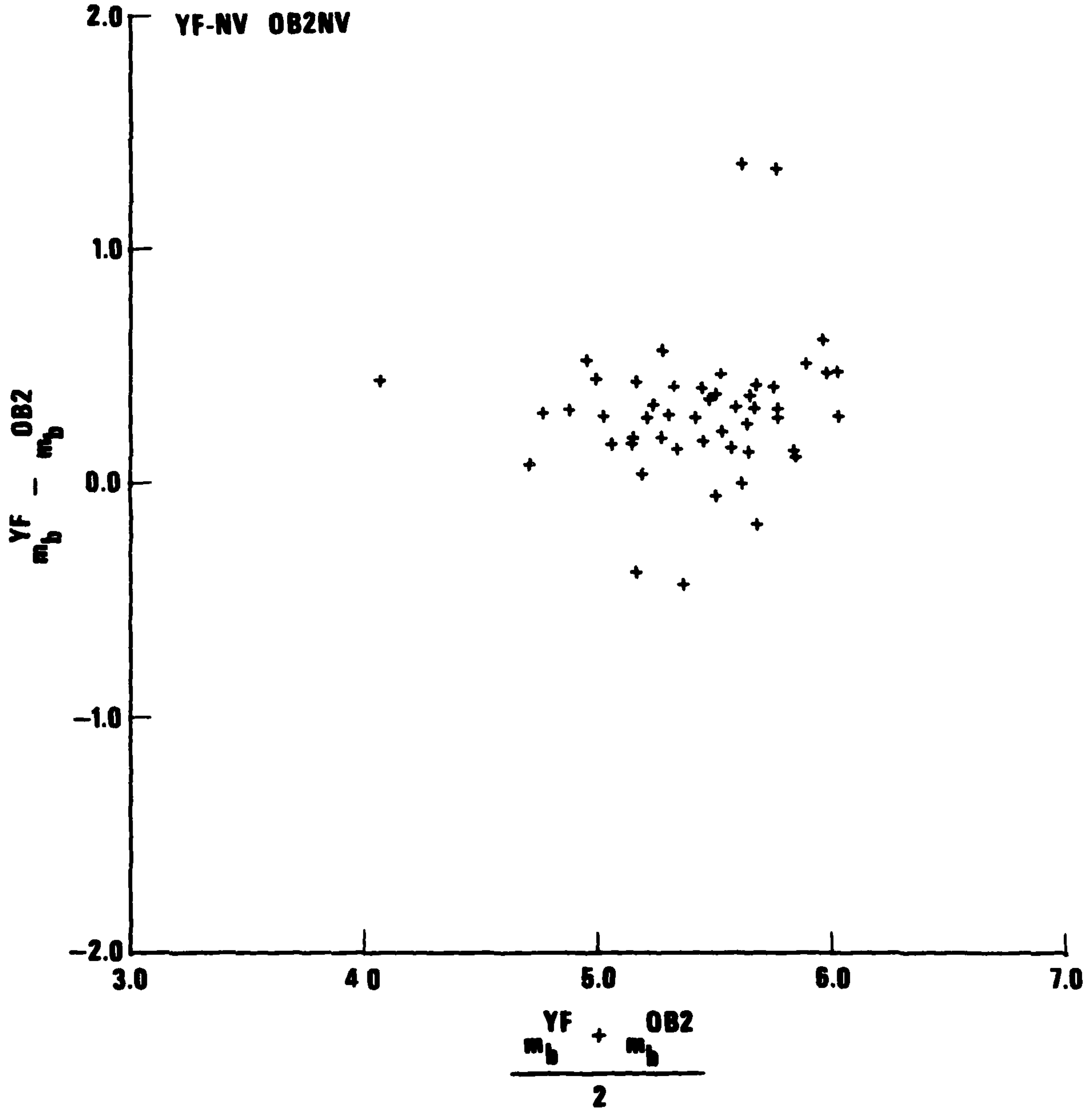

Figure 15 Interstation m_b differentials plotted against the two-station average m_b for the station pair YFNV - OB2NV. The absence of any clear increasing or decreasing trend indicates that magnitude threshold biases are not present (see text).

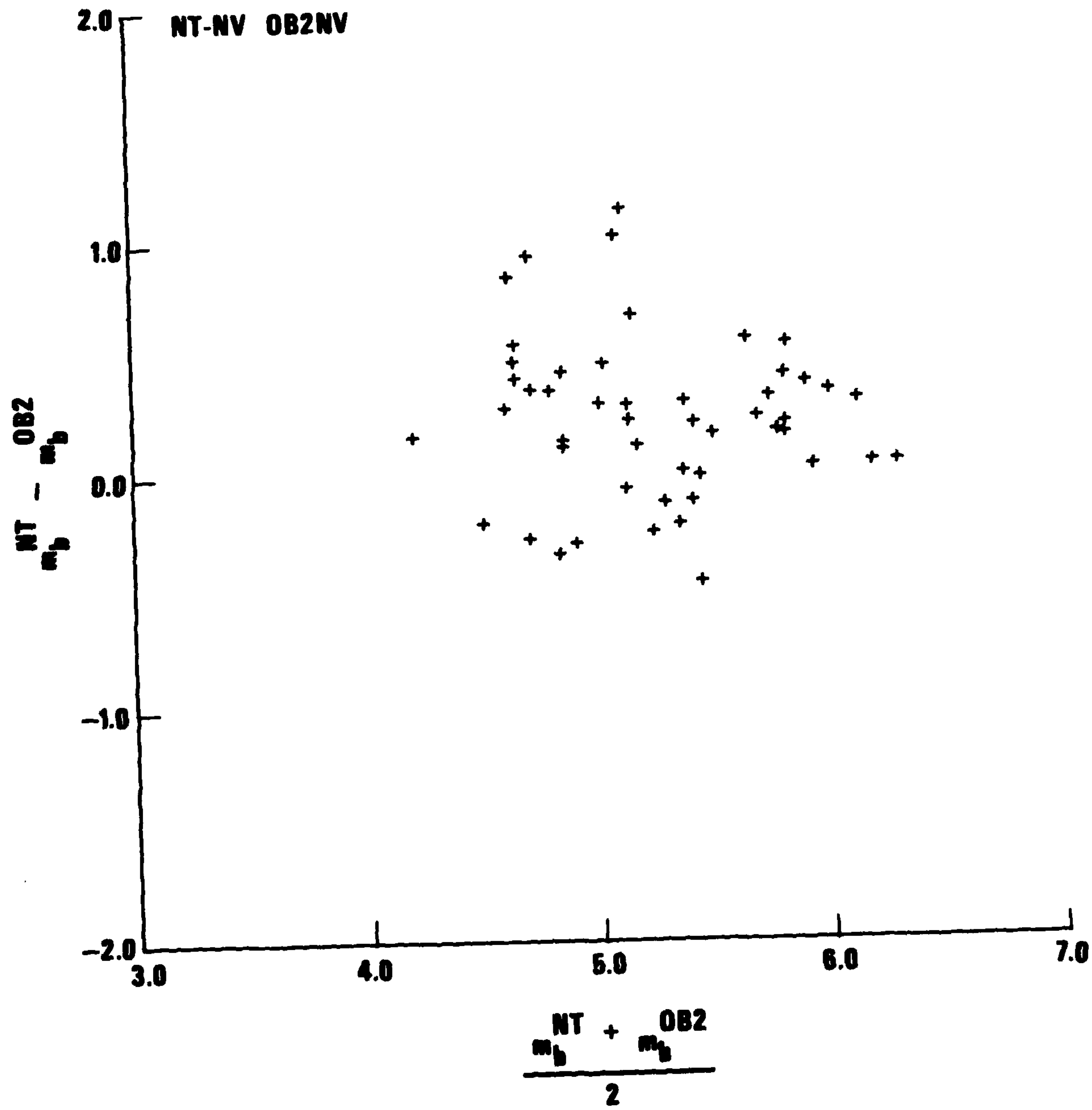

Figure 16 Interstation m_b differentials plotted against the two-station average m_b for the station pair NTNV - OB2NV. The absence of any clear increasing or decreasing trend indicates that magnitude threshold biases are not present (see text).

and plotted these symbols against azimuth and distance to OB2NV. Any regional bias such as a consistent orientation of fault planes would cause similar symbols to cluster in some regions. No such clustering is discernible on the diagram shown in Figure 17, and therefore there are no indications of source related biases.

Elimination of source region bias does not mean that near-station azimuthally dependent focusing on small scale crustal inhomogeneities is not present in the data. Such biases cannot at present be removed from these data sets since most of the events occur in belts of seismicity, and thus the azimuth-distance distribution of events is uneven.

Anelastic Attenuation as the Cause of the RKON-OB2NV Magnitude Differential

Having demonstrated the existence of magnitude differentials at the various SDCS stations, we turn now to their cause. In our opinion, anelastic attenuation is responsible for most if not all of the observed differentials. However, since station amplitude or magnitude anomalies are subjected to biases by such factors as crustal inhomogeneities, it is important to find diagnostics that indicate that the magnitude differentials are indeed due to anelastic attenuation.

Concentrating on the critical RKON-OB2NV pair (often used in key arguments in this report), strong support for anelastic attenuation can be found by the simple technique of subdividing the event population at RKON into high frequency (broad band) signals and low frequency (narrow band) signals based on the dominant period. The two populations are identified as $T \leq \overline{T}$ and $T > \overline{T}$, where $\overline{T}$ is the average period for the station for all events. These populations should behave as predicted in the discussion in section B of Part III of this report. This appears to be the case. As shown in Figure 18, the histogram of base 10 logarithms of trace amplitude differentials corrected for distance shows that the differential in trace amplitude is greater for the population $T \leq \overline{T}$, which agrees with the hypothesis that high frequency events undergo greater attenuation. Histograms of $\Delta m_a'$ (magnitudes computed without dividing by the period) show reduced differentials for both populations, and at the same time the difference in the means of the two populations also decreases. This is due to the over-correction associated with the assumption of a monochromatic signal (see section B). Finally, the last line of

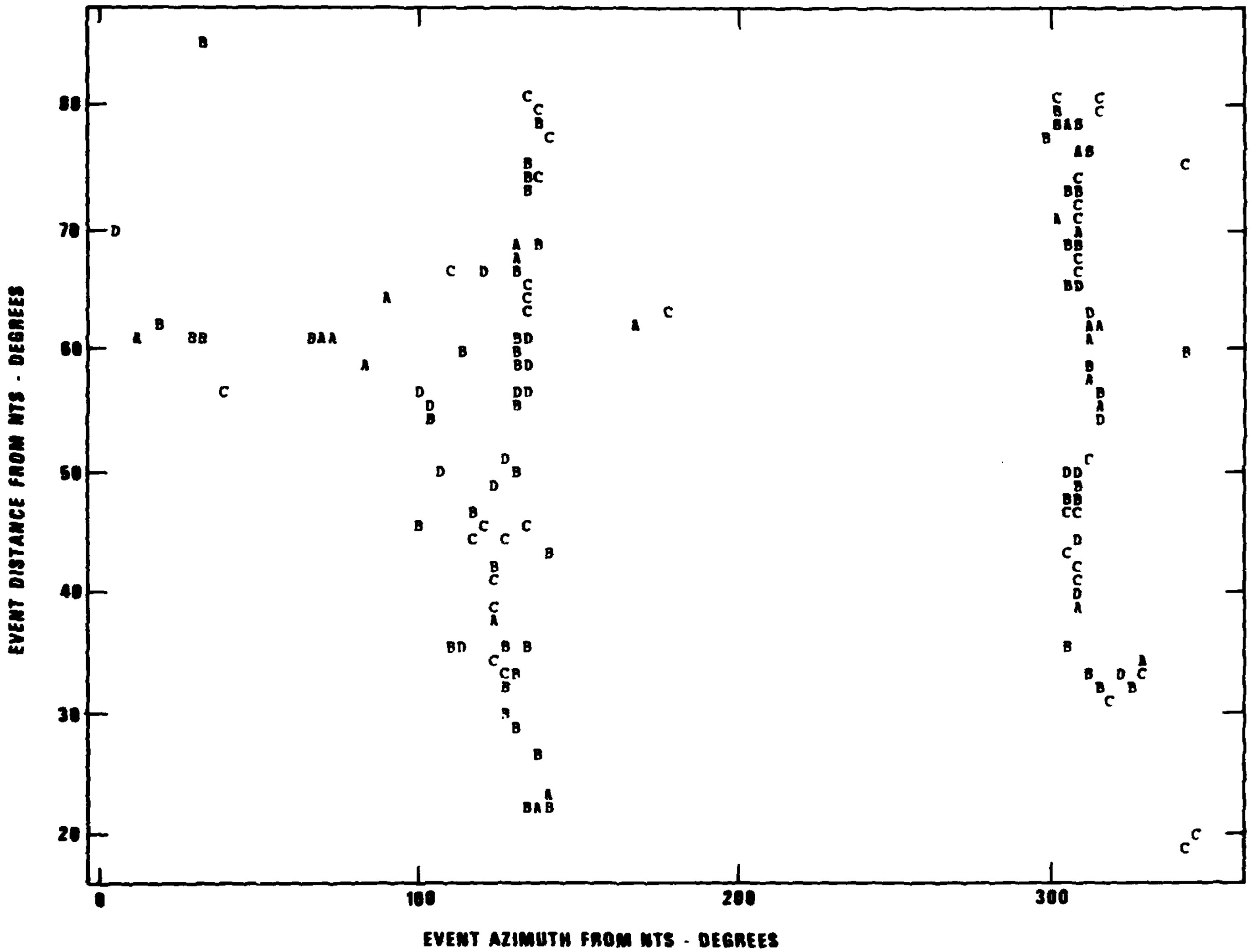

Figure 17 Plot of magnitudes of *interstation* m_b differentials for the RKON–OB2NV pair *against distance* and azimuth of OB2NV. The absence of any clear clustering of symbols in any region indicates that there are no source region biasing effects due to dominant source orientations (see text).

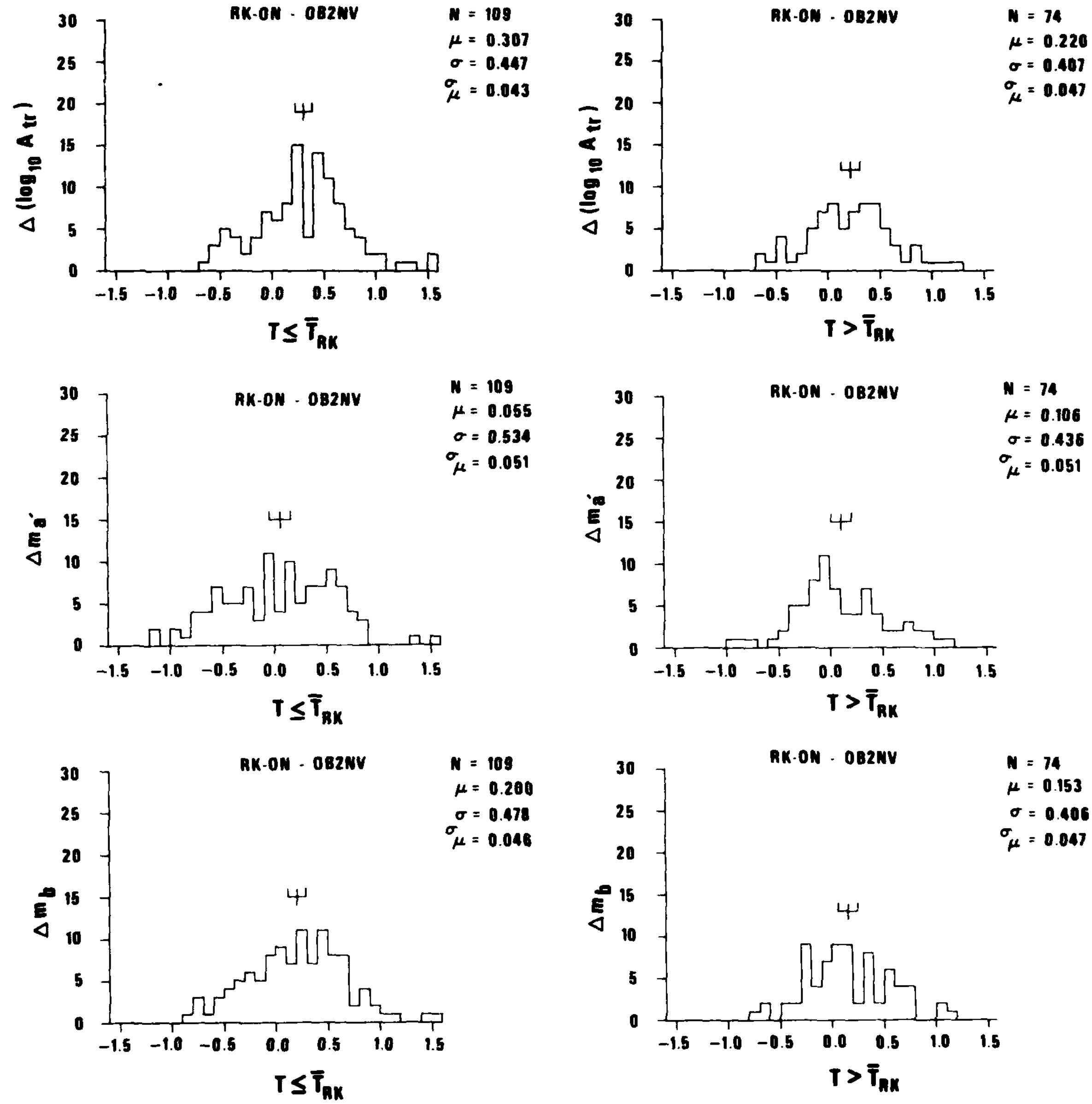

Figure 18 Subdivision of the event population into wide band and narrow band signal populations shows that a) the RKON-OB2NV trace amplitude differential is less for narrow band longer period signals (top row), b) the differential is reduced in m_a', trace amplitude divided by the instrument magnification at the dominant period measured. This reduction is greater for wide band signals (middle row) and c) division by period T causes the increase of m_b differential relative to that of m_a', and the increase is greater for wide band signals. This behavior is diagnostic of attenuation as a cause for the RKON-OB2NV magnitude differential (see text and section B of Part III).

Figure 18 shows the m_b computed by dividing by the period. This tends to restore the regional differential since the period is shorter at RKON than at OB2NV. The period differential is also greater for the population $T \leq \overline{T}$ as predicted in section B and judging by the increase of Δm_b versus $\Delta m_a'$.

This behavior is quite consistent with the interpretation of the OB2NV-RKON magnitude differential as an attenuation effect, and it effectively rules out many other interpretations such as accidental local focusing. One feature of this reasoning is that it is based entirely on time domain measurements and should suit those who dislike spectral arguments.

SPECTRAL ANALYSIS

Relative t* values (Δt^*) for the SDCS stations have been computed by the spectral ratio method. Because computing spectral ratios for all possible pairs of stations is redundant, we computed ratios for station pairs directly connected by lines in Figure 19. Differentials in t* and their standard deviations ($\sigma_{\Delta t^*}$) for other station pairs can be derived easily from these results. This approach takes advantage of the fact that for closely located station pairs, $\sigma_{\Delta t^*}$ has smaller variance than for distant pairs of stations. (This will be discussed in more detail later.) Thus, for example, determining Δt^* for the RKON-OB2NV and OB2NV-YFNV pairs is more reliable than determining Δt^* directly from the few events common to RKON and YFNV alone. This approach is also the most practical because during the project's two phases many events for the RKON-OB2NV pair were available to reduce the variance of their mean Δt^*, while only a few events were sufficient to define Δt^* for the OB2NV-YFNV pair to the same accuracy.

The histograms of the measured Δt^* are given in Appendix D. In addition to those involving the new stations of Phase III, updated versions of histograms for the OB2NV-RKON and HNME-RKON pairs are presented. In all cases, an accuracy ($2\sigma_{\Delta t^*}$) of $\sim$0.05 sec was the goal.

The easiest way to discuss the Δt^* values is to compare them to a common standard station. Figure 20 summarizes the results using OB2NV as the standard. As mentioned above, some of these Δt^* mean values and their standard deviations were derived indirectly. This figure also includes some relative t* data at SZNV (SHOAL site, on granite) and SEMN with the assumption that t* at SEMN is the same as at RKON. This can be justified easily by S wave data shown later in this report. Figure 20 shows that all WUS stations have essentially the same t* as OB2NV except stations NTNV and NT2NV, which have slightly lower t* than OB2NV. On the other hand, the RKON-OB2NV differential in t* is about 0.2 sec and highly significant statistically. The HNME-OB2NV differential is less (0.1 sec), but it is also significant at the 95% confidence level. This lower value indicates some attenuation under the northeastern U.S., a possibility suggested by Solomon

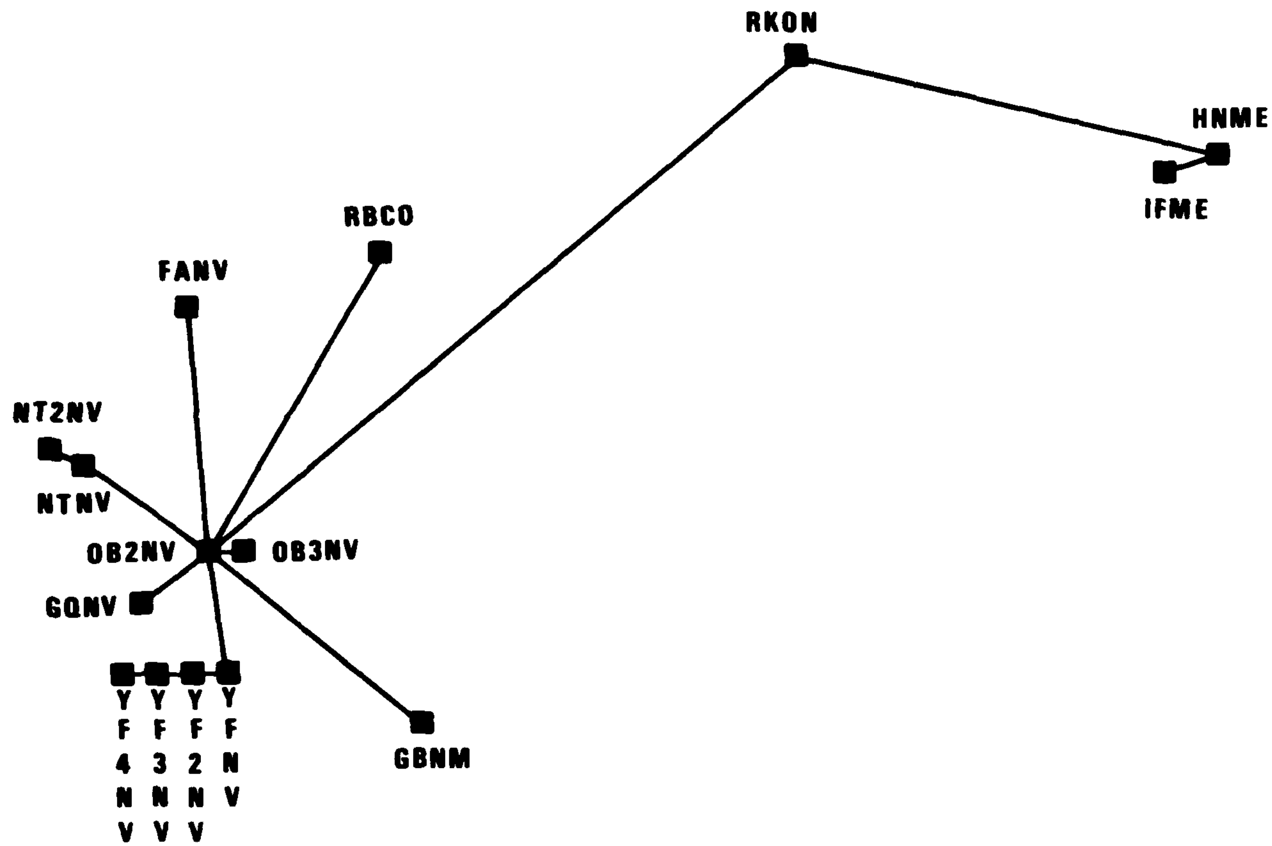

Figure 19 Hierarchy of station pairs selected for spectral ratio computation.

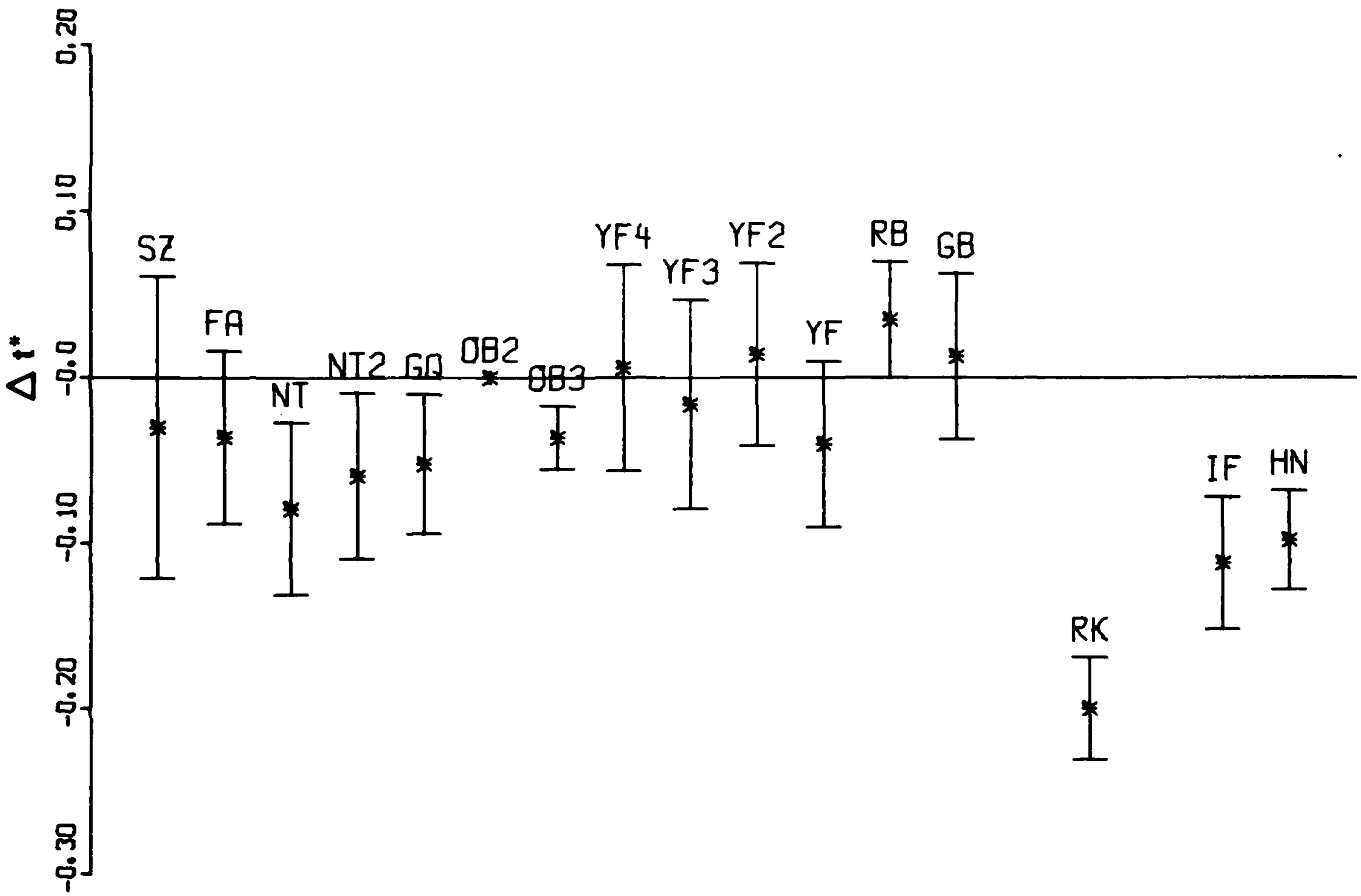

Figure 20 Δt* values of selected *SDCS* and *LRSM stations relative* to that of OB2NV. RKON on a shield has the lowest t*, while the WUS stations have the largest. 95% confidence limits are indicated by bars.

and Toksöz (1970) and Der et al (1975). The t* at IFME is comparable to that at HNME.

There was some difficulty with the Yucca Flat stations in reliably determining t*. This difficulty resulted from high unstationary noise levels due to drilling. As a result, the standard procedure for estimating noise in the signal window (taking spectra of time windows prior to the arrival of the P wave) failed repeatedly. Many of the spectral ratios supposedly show points with high S/N (around 4 Hz) that disagree with the trend at lower frequencies. This can be attributed to nonstationary noise rather than to real signal energy at 4 Hz, which should be far beyond the corner frequency expected for most events. Moreover, crustal response calculations rule out major enhancements of high frequency energy. Thus, the reader should assign less weight to the t* determination at YF stations.

Returning to Figure 20 the OB2NV-OB3NV differential, although small, is significant statistically. t_p^* for stations NTNV, NT2NV and GQNV appears to be smaller than that at OB2NV and Yucca Flats although significantly higher than that of RKON. A high-Q high-velocity plug may be present under Pahute Mesa as suggested by Spence (1974), and this could also affect measurements at nearby GQNV. The high frequency content of L_g is also visibly enhanced at Pahute Mesa (Barker et al, 1980). Since L_g propagates entirely in the crust, this may indicate that the apparently low t* at NTNV and NT2NV could be no more than a local crustal resonance effect. We have no preferred interpretation of this.

As shown in Figure 21, the dominant periods of P waves behave similarly to the Δt_p^* values of Figure 20. ΔT is smaller at NTNV, NT2NV, and GQNV than at OB2NV and the Yucca Flats stations. Moreover, all of the WUS stations have ΔT values significantly higher than that of RKON. Periods at HNME are not comparable to those of other SDCS stations due to the difference in instrumentation at HNME. Histograms of ΔT for the rest of the SDCS Network are compiled in Appendix E.

As mentioned earlier, the standard deviation of relative t* values also depends upon mutual distance between stations in a manner similar to that shown by the magnitude residuals. A plot of $\sigma_{\Delta t^*}$ versus $\Delta°$ is shown in Figure 22. Note that the numerical values of $\sigma_{\Delta t^*}$ are smaller and increase

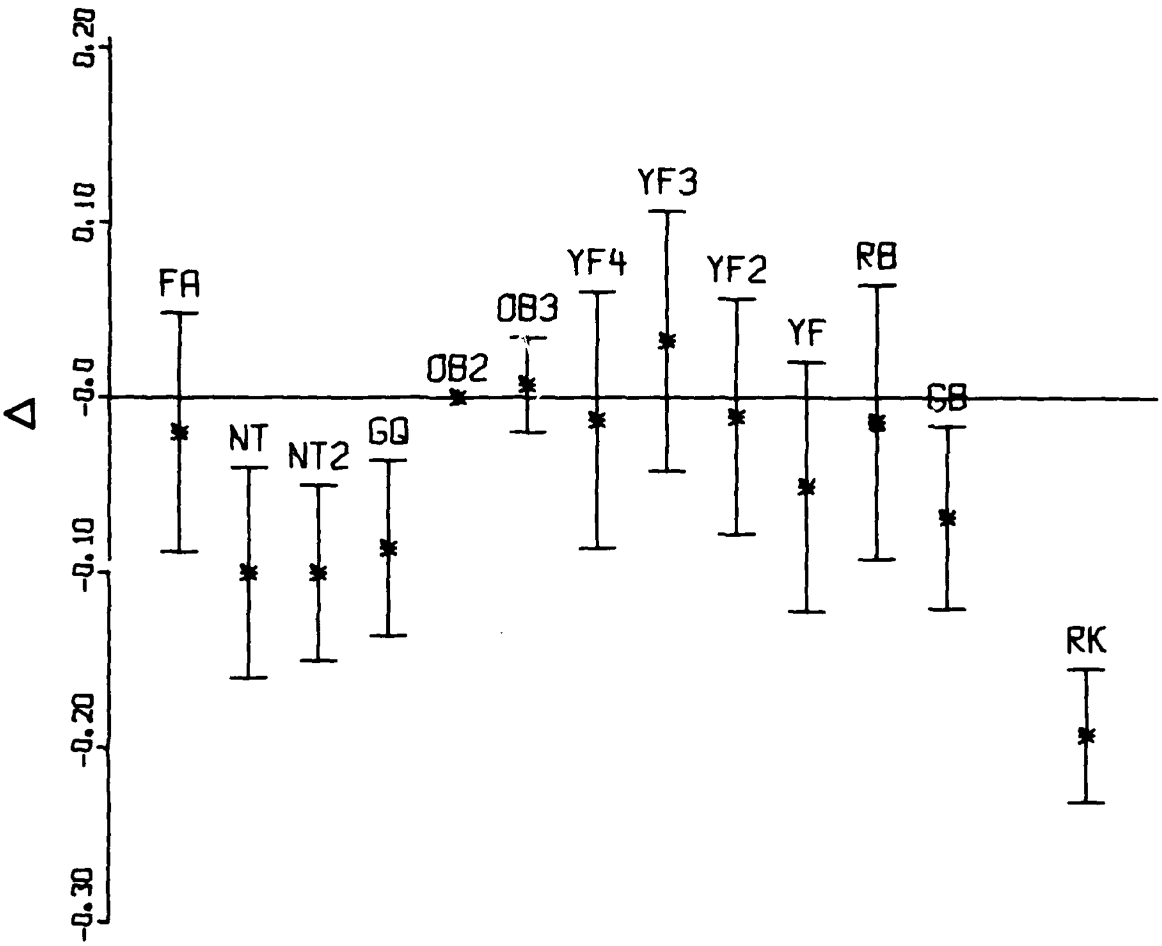

Figure 21 Differentials in dominant period T relative to OB2NV. 95% confidence limits are indicated by bars. RKON has the shortest dominant period. HNME is omitted because its instrument response is different from that of the other stations. No direct comparison of IFME with the rest of the stations was possible.

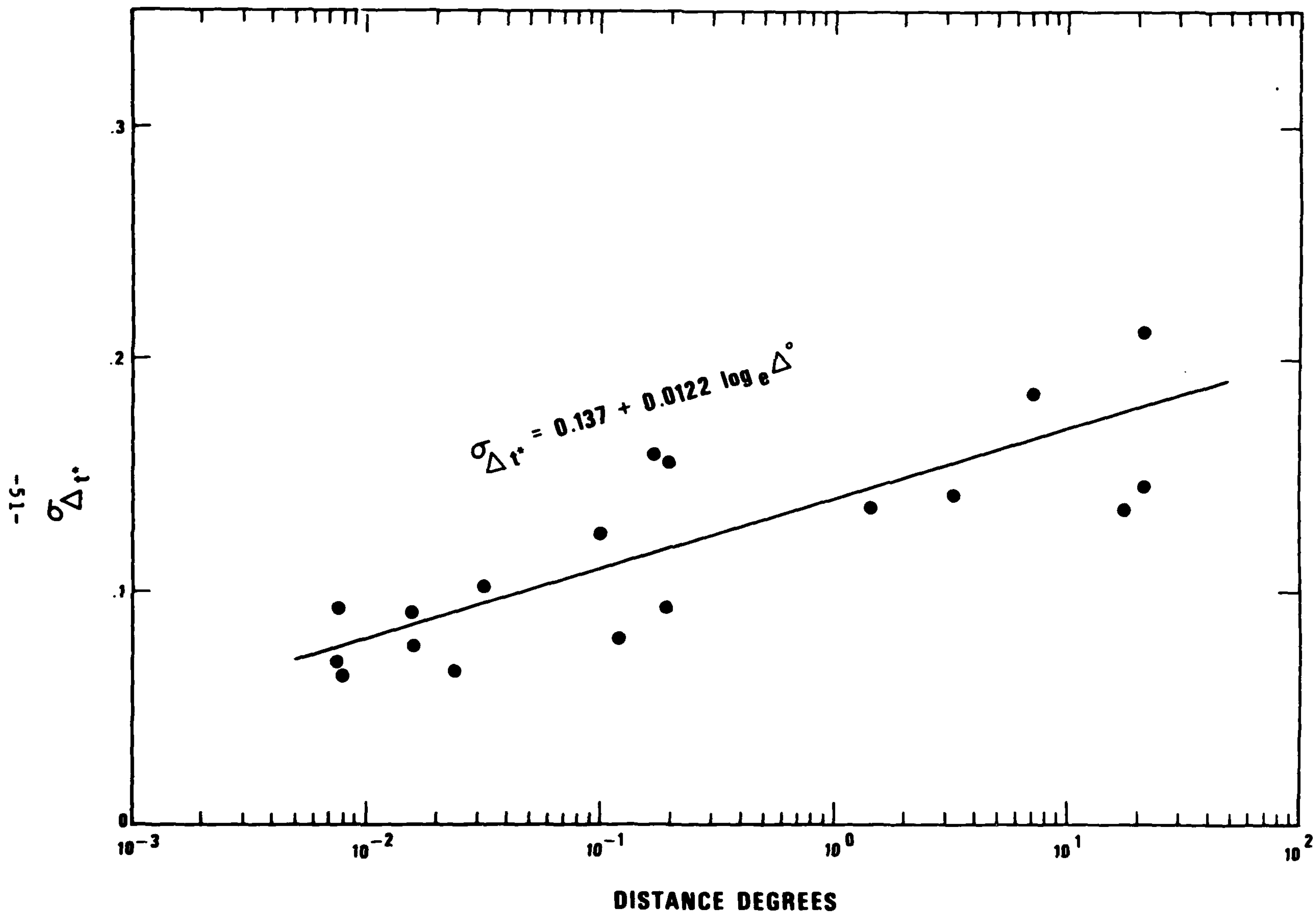

Figure 22 Standard deviation of relative t* differentials vs. interstation distance.

more slowly with distance than $\sigma_{\Delta m_b}$. Because absolute numerical values of Δm_b and Δt^* are both of the order of a few tenths in magnitude units and seconds, respectively, fewer measurements are needed to establish Δt^* between stations than to determine magnitude residuals. This result is in agreement with experience at seismic arrays and shows that Δt^* is numerically a more stable quantity than Δm_b in terms of multipathing and other disturbances (Der et al, 1977).

Narrow Band Determination of t* Differential for RKON and OB2NV

In order to see whether the Δt^* value we computed depends excessively on the low level high frequency end of the spectrum (3 to 4 Hz), we recomputed the relative t* between RKON and OB2NV using spectral slope fits in the narrower 0.5 to 2 Hz band. A strong frequency dependent variation in the relative t* differential between OB2NV and RKON would result in a drastically different t* differential for this narrower band. Figure 23 shows that this is not the case--the relative t* differential 0.24 ± .06 sec is not significantly different from the wider band value of 0.20 ± .03 sec. This demonstrates that our results do not depend on low level high frequency energy, the existence of which is questioned by some researchers. This statement is also supported by the fact that time domain measurements that depend primarily on the 1 to 2 Hz band are also indicative of t*, variation between RKON and OB2NV. The above result also rules out a rapid change with frequency in the interstation t* differential above 1 Hz.

Testing for some Biases in Relative t^*_p Measurements

To see whether any source region bias is apparent in the measured relative t*, we separated the RKON-OB2NV Δt^* values into four groups designated by different symbols as follows:

Symbol	
A	$(\Delta t^* - \mu) < -\sigma$
B	$-\sigma < (\Delta t^* - \mu) < 0$
C	$0 < (\Delta t^* - \mu) < +\sigma$
D	$(\Delta t^* - \mu) > +\sigma$

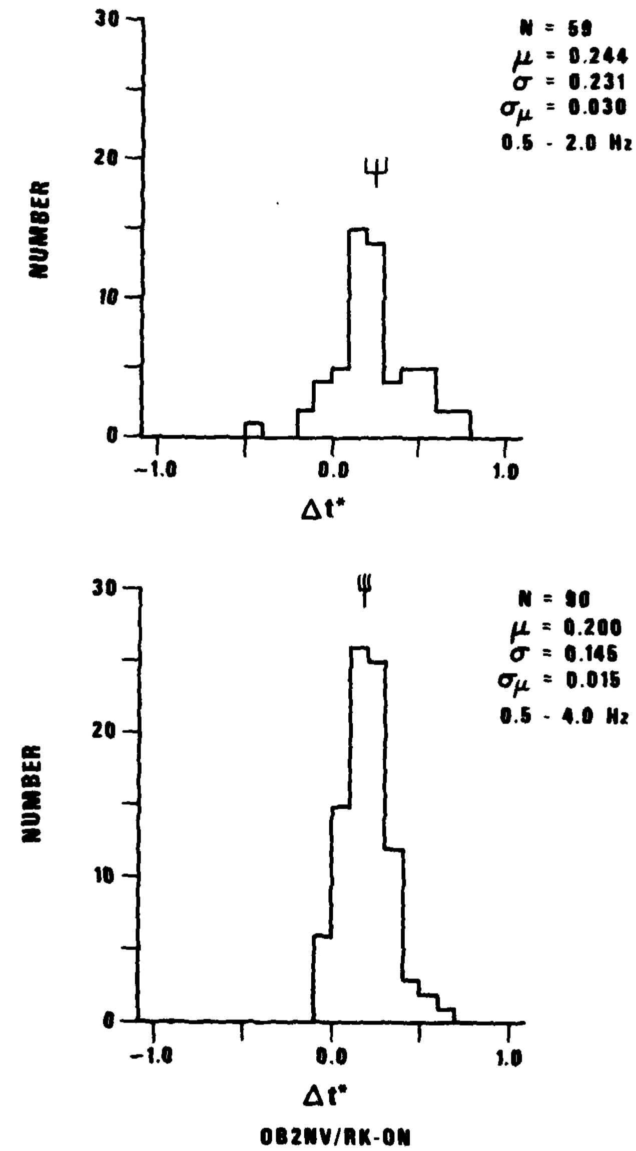

Figure 23 Histograms of OB2NV-RKON t* differentials computed in the 0.5 to 2.0 Hz and the 0.5 to 4.0 Hz bands. The fact that the narrow-band average differential is about the same as that computed in the 0.5 to 4.0 Hz range (0.244 versus 0.200) rules out rapid change of relative t* with frequency in this range, and shows that our t* results do not depend critically on low level high frequency energy. Note that the scatter in these t* histograms is small compared to that in Figures 3 and 4 for m_b and trace amplitudes, demonstrating the greater consistency of spectral measurements.

and plotted these symbols against azimuth and distance to OB2NV in Figure 24. This subdivision assigns the letter D to the largest t* difference and A to the least. The resulting pattern shows no convincing evidence of regional biases. Such biases could in theory be due to directionality of finite sources that would result in consistent regional patterns of Δt^* if the fault planes were oriented in any consistent manner relative to the station pair studied. The lack of any such bias effect is not surprising since, although the geographical distribution of sources used is clearly non-random, the orientation of the trends of seismic belts, island arcs and the like relative to the OB2NV-RKON station pairs varies enough to eliminate such bias even if the source mechanism of all events were the same. But the fact is that sources in the seismic belt include a variety of mechanisms, and this further reduces chances for finding overall, consistent source related biases in the determination of Δt^* from averages of many events.

To demonstrate further that Δt^* behaves consistently, consider the recordings of a Novaya Zemlya explosion in Figure 25. On the left is the recording at OB2NV and on the right at RKON. This source is supposedly symmetrical azimuthally, but the trace amplitudes differ by a factor of 30, a dramatic illustration of the instability of amplitude measurements. The filtered traces shown below demonstrate that the P wave is richer in high frequencies at RKON than at OB2NV. The S/N ratio is high for this event. This figure also demonstrates that the concept of "transparency" used in time domain work is not a physically meaningful one. OB2NV was regarded as a "transparent" station in much of the time domain work of Butler et al (1979) and it is clearly not in this case. The waveform of P is quite complex. Experience at seismic arrays indicates that "transparency" is a function of near receiver focusing and thus varies with the azimuth of the events observed.

Studies of S Waves at SDCS Stations

Although the prime emphasis in this project was on P wave amplitude residuals and spectra, a limited search was made for short-period S waves recorded in the SDCS data base. The S wave data thus found is limited, and the S/N ratio of these signals is generally not good. In Figures 26 through

31 we show a few examples of short-period S waves and the spectral ratios computed from them. D· to the poor S/N ratios of these signals most of the spectral ratios are ..ed over a frequency range of only 0.75 Hz. Nevertheless, the available data indicate that RKON is richer in high frequency content, and GBNM appears to have t_s^* values comparable to OB2NV. Due to the sparse data and the emphasis on m_b, S wave amplitude residuals were not studied at SDCS stations.

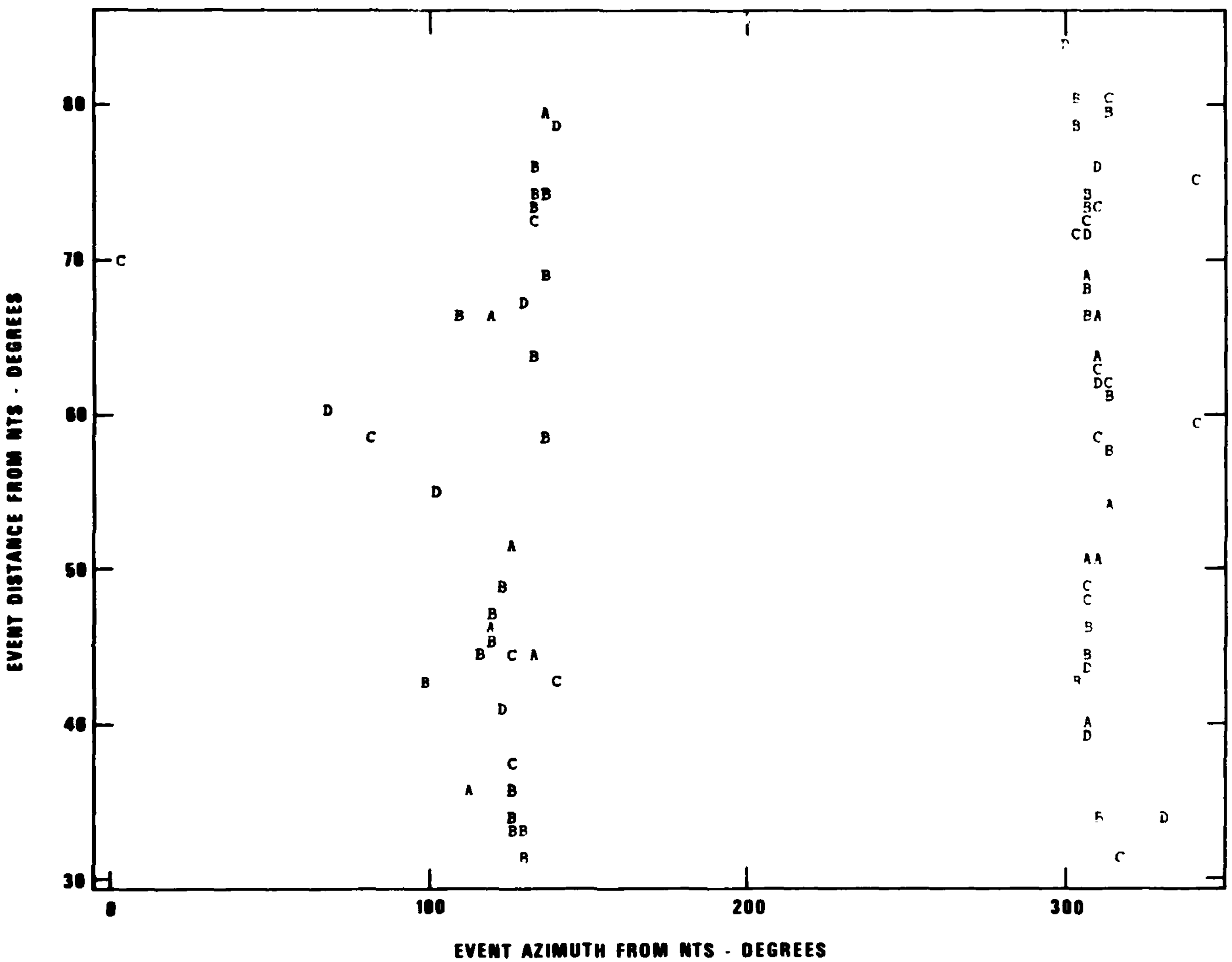

Figure 24 Magnitudes of t^*_p differentials for the OB2NV/RKON station pair plotted against distance and azimuth to OB2NV. The absence of clear clustering of symbols shown rules out any dominance of a preferred fault directivity in any region (see text).

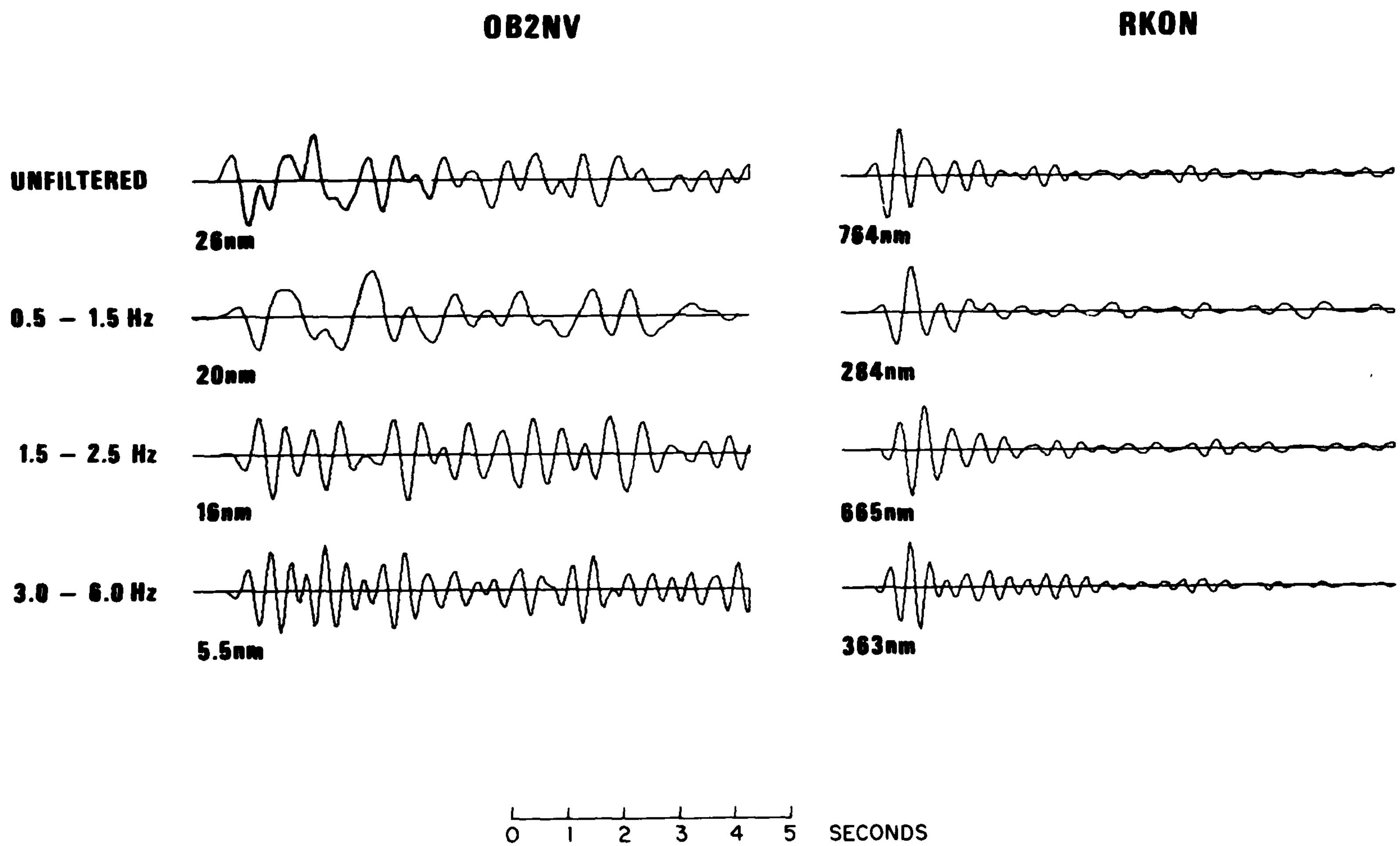

Figure 25 Comparison of signals from a Novaya Zemlya shot recorded at OB2NV and RKON.

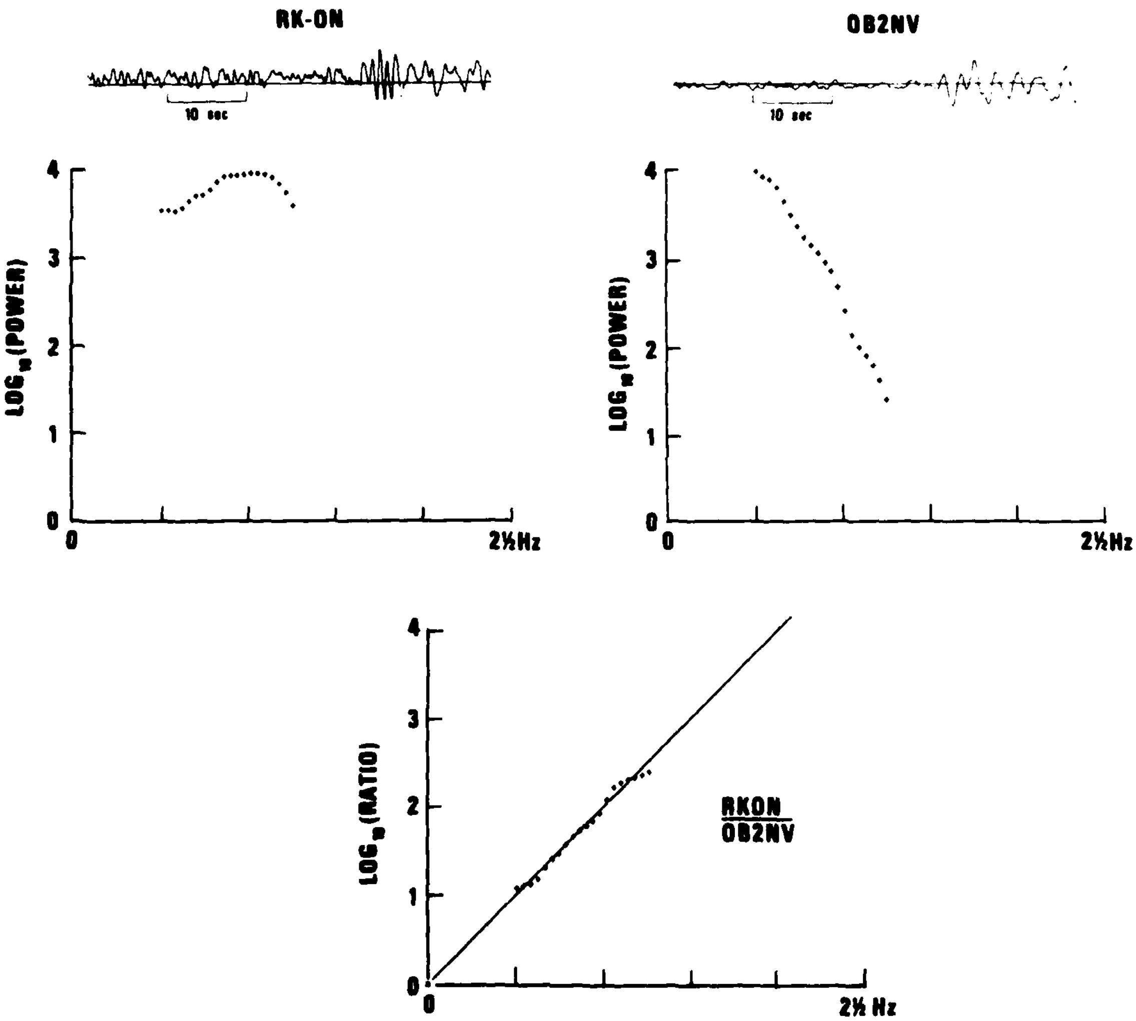

Figure 26 S wave spectra and spectral ratio for the station pair RKON - OB2NV (radial component), 4 September 1977 23:20:48.0, Aleutian Islands.

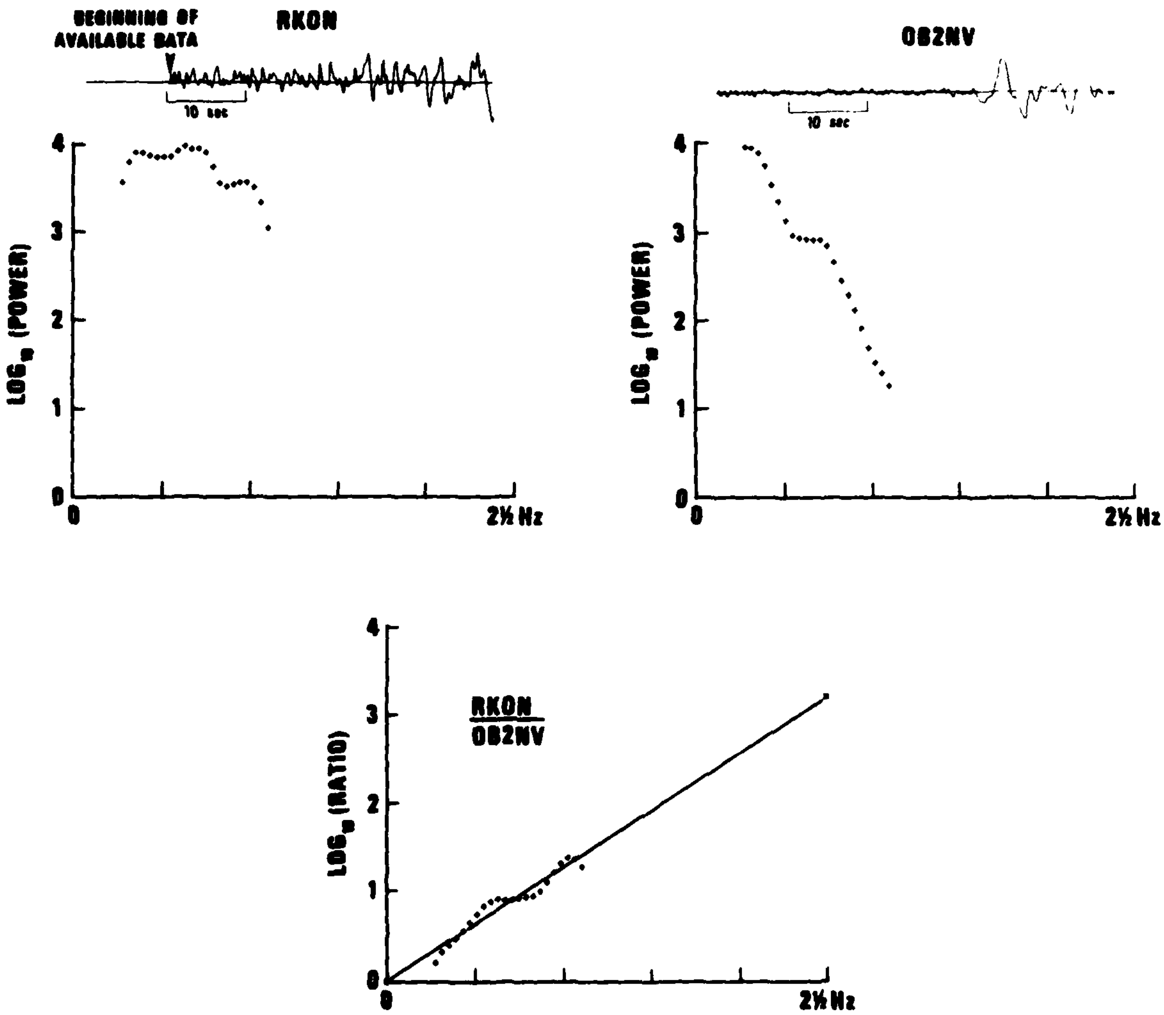

Figure 27 S wave spectra and spectral ratio for the station pair RKON - OB2NV (transverse component), 4 September 1977 15:40:59.7, Aleutian Islands.

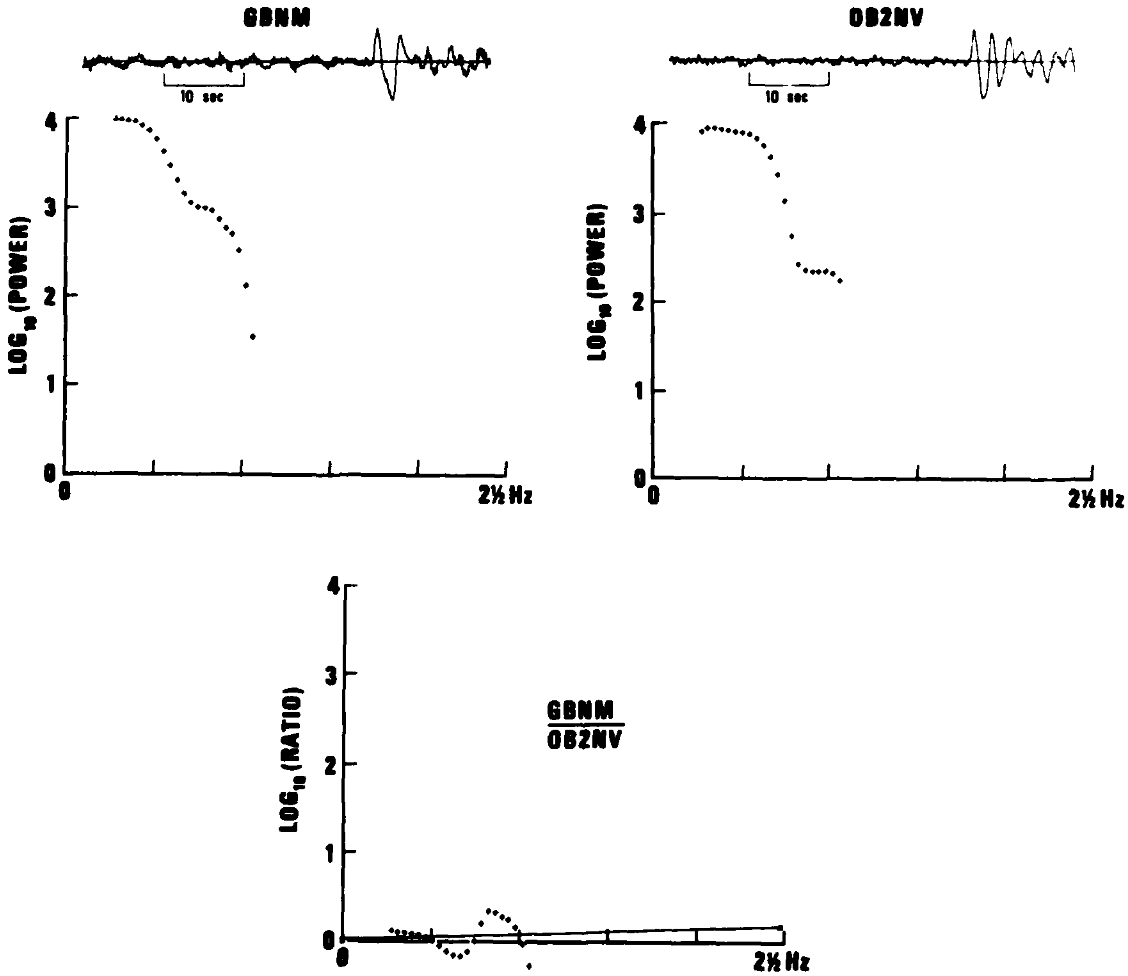

Figure 28 S wave spectra and spectral ratio for the station pair GBNM - OB2NV (transverse component), 19 June 1977 11:47:22.3, Kurile Islands.

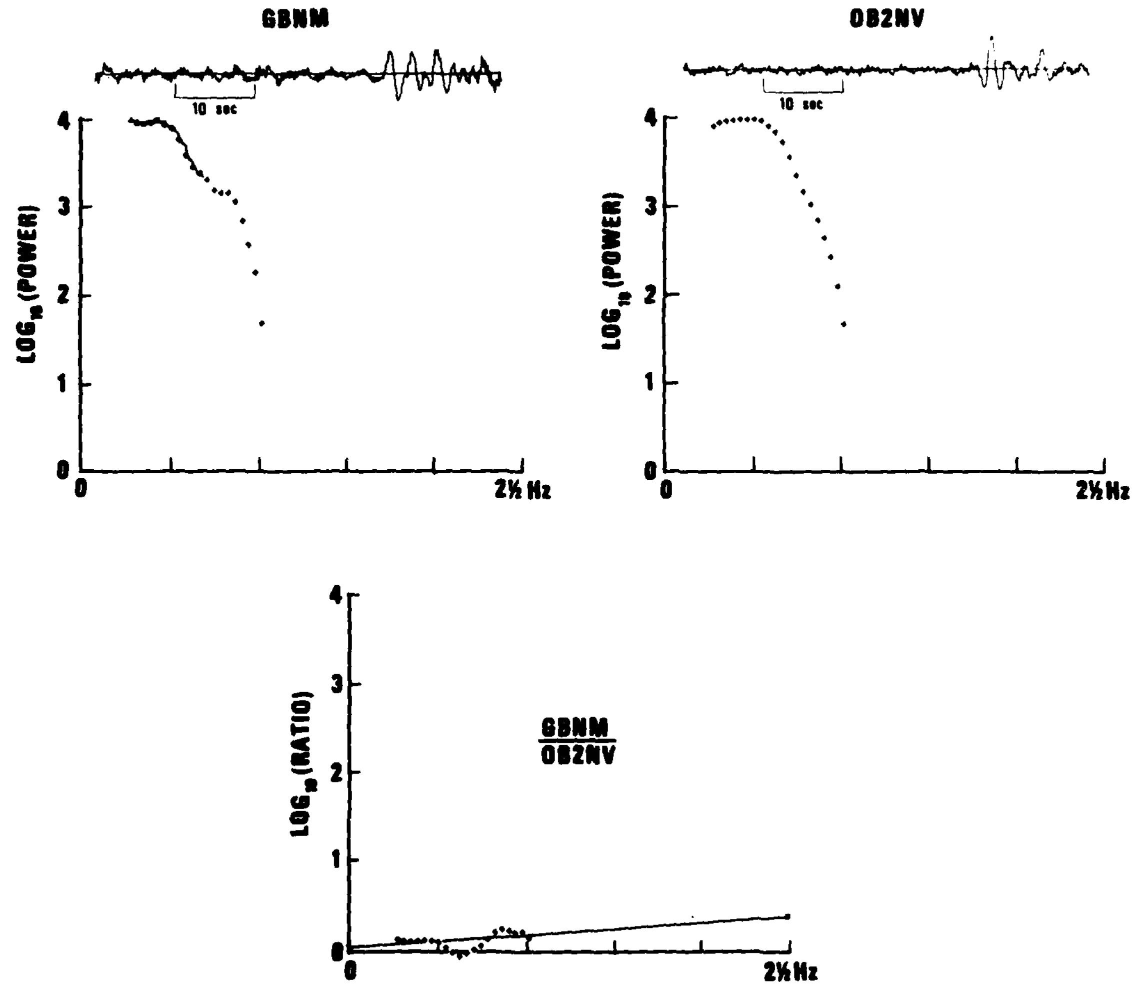

Figure 29 S wave spectra and spectral ratio for the station pair GBNM - OB2NV (radial component), 19 June 1977 11:47:22.3, Kurile Islands.

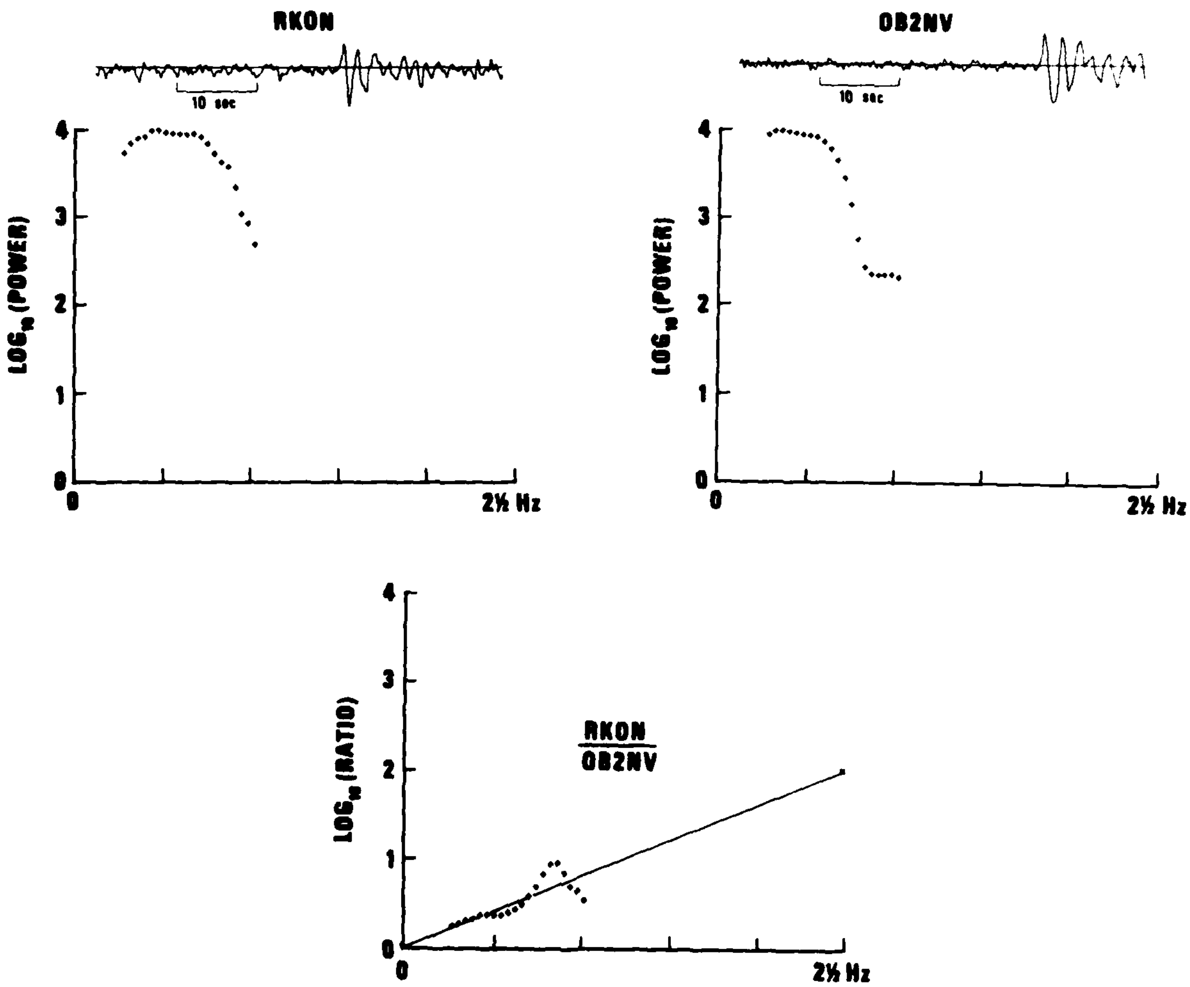

Figure 30 S wave spectra and spectral ratio for the station pair RKON - OB2NV (transverse component), 19 June 1977 11:47:22.3, Kurile Islands.

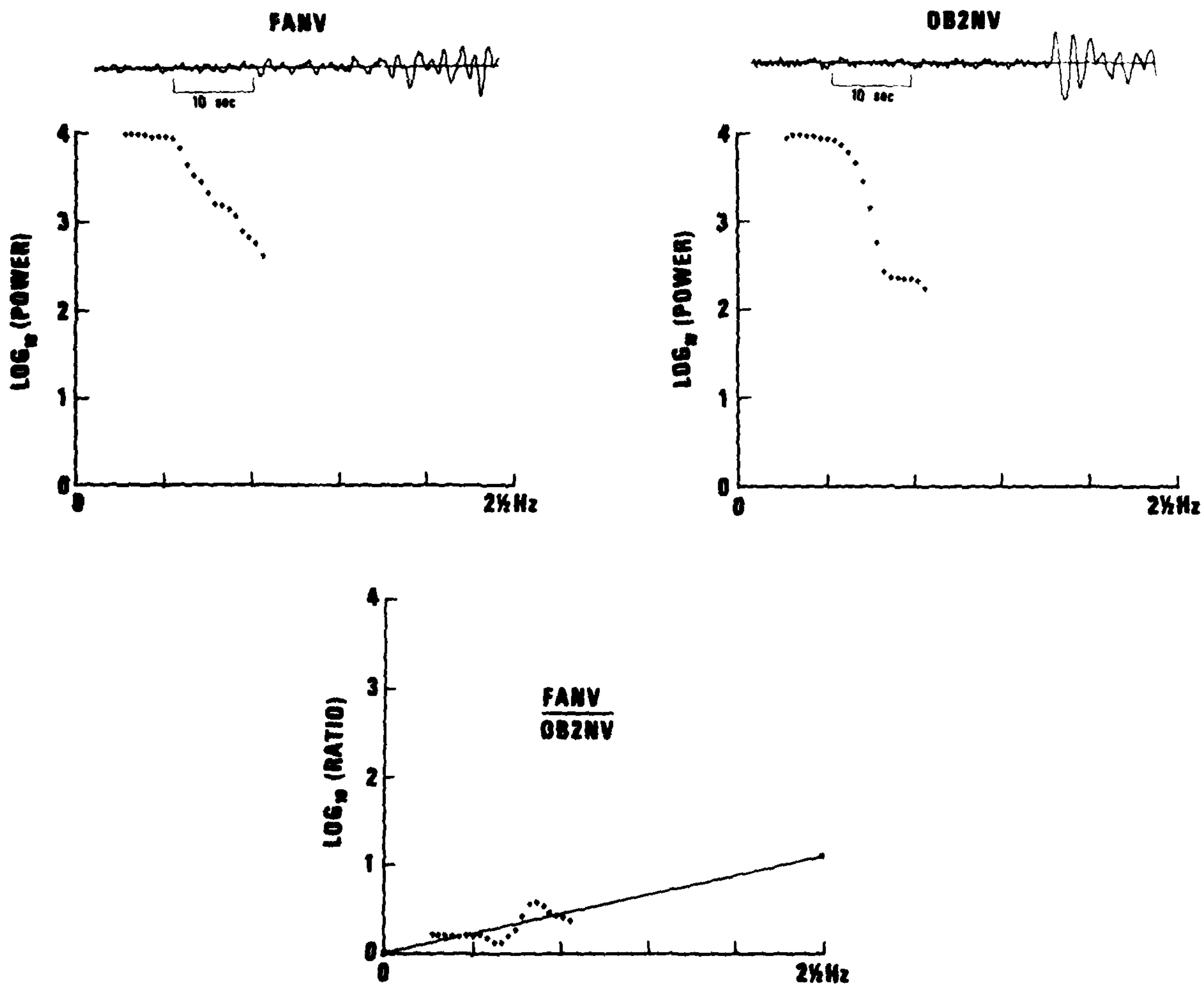

Figure 31 S wave spectra and spectral ratio for the station pair FANV - OB2NV (transverse component), 19 June 1977 11:47:22.0, Kurile Islands.

TRAVEL TIME RESIDUALS

Since P wave travel time residuals constitute an additional parameter that characterizes the physical state of the mantle under a given station, we have computed relative travel time residuals for all SDCS stations with sufficient data base. Late arrivals are commonly associated with high upper mantle attenuation and the presence of a low velocity layer in the upper mantle. Worldwide observations support the correlation of travel time residuals with highly attenuative properties and other diagnostic geophysical measurements such as S wave delays, heat flow, and electrical conductivity. In view of this fact, it is important to measure the relative travel time residuals among the SDCS stations in order to further evaluate the condition of the upper mantle under each station. Travel times for P waves were routinely compiled throughout the SDCS project, but it is only recently that we have accumulated sufficient data to compute travel time residuals.

The stations of prime interest are OB2NV, RKON and IFME, all of which are located on granite, though great distances apart. Determination of relative residuals between the members of this group is complicated by large scatter in the results of the computation. Generally speaking, the greater the distance between stations the greater the scatter. Thus, the problem is less serious for the group of stations located throughout the WUS (OB2NV, FANV, GBNM) since the relative distances are less. Finally, the stations at NTS constitute a tightly spaced group for which the measurement of relative residuals constitutes no difficulty.

In all travel time studies one also has to deal with some measurements which are grossly in error. This did not prove to be extremely difficult. In most cases, as a large number of readings was compiled, we found a tight group resembling a normal distribution with some very obvious outliers. We followed the standard statistical practice of computing the standard deviation σ for the tight group and omitting all points removed by more than 3σ from this group. The mean travel time residuals were then computed from the purged data set. Histograms of travel time differences for various station pairs are given in Appendix F. The differentials and their 95% confidence limites are tabulated in Table V.

TABLE V

Travel time residuals for selected SDCS stations relative to OB2NV

STATION	ΔTT	ΔTT^{corr}
FANV	0.03 ± 0.16	-0.52
GBNM	-0.05 ± 0.25	-0.49
HNME	-1.28 ± 0.63	-1.04
NTNV	0.43 ± 0.23	-0.23
RKON	-1.89 ± 0.29	-1.68
YFNV	0.61 ± 0.22	0.37

As mentioned above, the standard deviations of travel time differentials have a distance dependence similar to those of the magnitude and t* differentials. This is shown in Figure 32. The physical causes for this phenomenon are the increasing effect of mislocation of events with distance and the increasing probability of misreading the first arrivals due to the decreasing visual similarity of the signals.

Table V also shows the residuals corrected for elevation and local geology and adjusted relative to OB2NV (OB2NV is assumed to be zero). The table shows that all WUS stations are late relative to RKON, which agrees with results obtained by other workers (Sengupta and Julian, 1976). Stations in the northeastern United States, HNME and IFME, are later than RKON but not by as much as the WUS stations. This picture is in perfect agreement with other studies and also conforms to our evaluation of relative t* differentials, assuming that LVZ is associated with low Q.

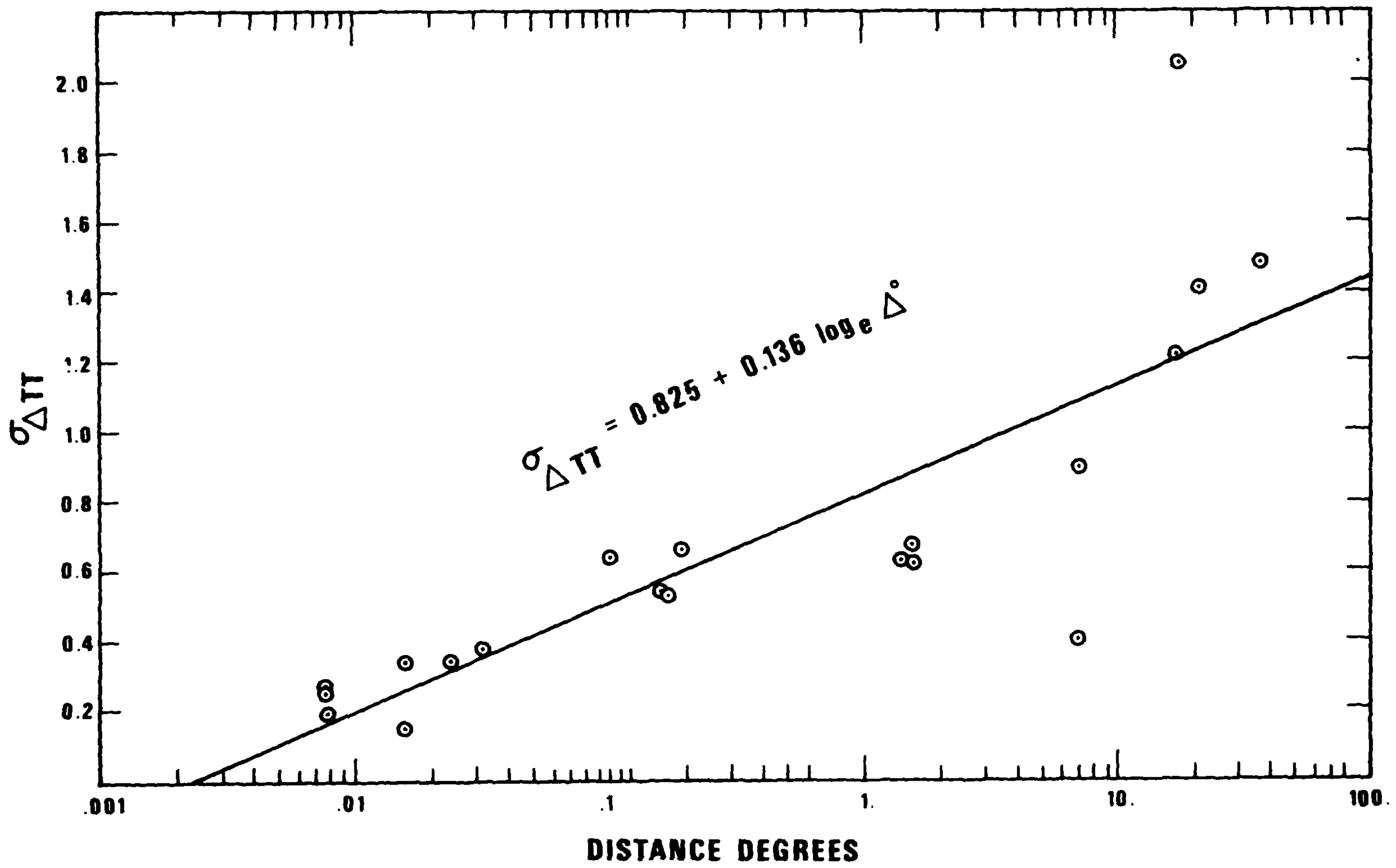

Figure 32 Standard deviation of relative travel time difference as a function of interstation distance.

SUMMARY

Numerical values of the most relevant diagnostic parameters obtained in the data analysis are summarized in Table II. The data indicate that after crustal corrections are made, P wave amplitudes tend to be lower at the WUS test sites than at RKON. The NEUS stations, HNME and IFME, appear to be intermediate in amplitude between the two groups, but large scatter in the data does not permit the determination of a significant m_b difference between these stations and either OB2NV or RKON. Crustal corrections leave large differences between the stations in m_b or trace amplitudes which are unexplained in terms of t* or known structures and are presumably caused by local focusing effects.

Spectral measurements indicate a significant loss of high frequency content at all WUS test sites relative to RKON. The NEUS stations, HNME and IFME, occupy an intermediate position in frequency content. The t* determined from spectral ratios shows a good qualitative agreement with the dominant periods measured by analysts.

Travel time residuals shown in Table V indicate that after local crustal and elevation corrections, P waves arrive late at all WUS test sites relative to RKON. The NEUS stations, HNME and IFME, again appear to be intermediate in their relationship.

The significance of these results will be discussed in the next part of this report in the broader context of related work by SDAC and other researchers.

PART 2

EVALUATION OF THE RESULTS OF THE SDCS PROJECT IN THE CONTEXT OF RELATED WORK BY SDAC AND OTHER RESEARCHERS

The first part of this report presented the results of data analysis from the SDCS and a few LRSM stations. The areal coverage of this station set is limited; only one of the stations, RKON, is located on a shield. Thus it is extremely important to show that RKON is not in any way anomalous lest our conclusion concerning the other shield regions be seriously in error. The station in Maine should also be tested in the same context. Since there have been other studies of amplitude and magnitude anomalies of teleseismic P waves, our results must be interpreted in the framework provided by these. For example, some recent broad regional studies of P wave anomalies were interpreted in a manner that seemed to be in conflict with our conclusions. We shall show that no real conflict exists if some errors and unintentional misrepresentations are corrected. We also include here some results of our own spectral and amplitude studies of P and S waves. In addition, we shall outline regional variations of Q_α under the contiguous United States. In the last part of this section we shall put some limits on the <u>absolute</u> values of t^*_p and t^*_s and discuss possible forms of frequency dependence of t^* for two types of paths.

Discussion of the Results of the SDCS Experiment in the Context of Amplitude and Spectral Studies of Short-Period P and S Waves

Although we pointed out in the previous part of this report that the SDCS data can be interpreted in terms of decreased Q_β in the upper mantle, there is still a need to integrate these results into a framework of other regional studies to confirm our interpretation. Any lateral decrease of Q_β in the mantle would cause the following suite of phenomena all of which have to be present:

a) Decrease of P wave amplitudes resulting in a magnitude anomaly for P waves.

b) Decrease of high frequency content in P waves.

c) A regional anomaly for S wave amplitudes. The effect should be greater than that for P waves.

d) High frequency content of S waves should decrease at a greater degree than that for P waves since $t^*_s \sim 4t^*_p$.

We shall discuss manifestations of these phenomena and show that all of these are present in much of the western United States.

P-Wave Amplitude Anomalies

It would be expected that in the regions underlain by a low Q mantle the P-wave amplitudes from observed teleseisms would be reduced. This has been confirmed in several studies of magnitude variations across the U.S. (Evernden and Clark, 1970; Cleary, 1967; North, 1977; Booth et al, 1974). The various studies all show a negative bias in amplitudes in most of the WUS relative to the EUS as a whole. The methods of data selection and amplitude measurement methods vary, and the reported bias values for common stations in many cases also differ considerably.

Figure 33 shows the regional pattern obtained by Booth et al (1974). This map shows strong negative magnitude residuals in the southwestern United States and positive residuals in the north central section of the country. A study of these residuals (Der et al, 1979) showed that crustal amplification alone cannot explain this pattern, and that even after correcting for crustal effects, a 0.33 m.u. EUS-WUS regional bias remains. Figure 34 from this study shows that magnitude residuals plotted against logarithms Δm_b^c of multiplicative crustal amplification factors A_c tend to cluster around two regression lines for the WUS and EUS populations respectively. Therefore, a multiple regression using both the crustal amplification factor A_c and t_p^* is necessary to reduce the variance. The regression on the set of stations gave for an assumed EUS-WUS t* difference

$$\Delta m_b \simeq (1.35 \pm 0.32)\ \Delta t^*$$

at the 95% confidence level.

This coefficient is of the same order as

$$\pi f/\ln 10 = 1.36 \text{ (for } f = 1 \text{ Hz)}$$

which would be the multiplicative coefficient between t* and the 10 base logarithms of amplitudes for an attenuated 1 Hz wave. This equation shows that average regional variations of amplitudes in short-period P and t* are closely tied together and cannot be specified independently.

Consider now some results of a study by Butler and Ruff (1980) in the same context. Figures 35 to 39 show logarithmic plots of P wave amplitudes

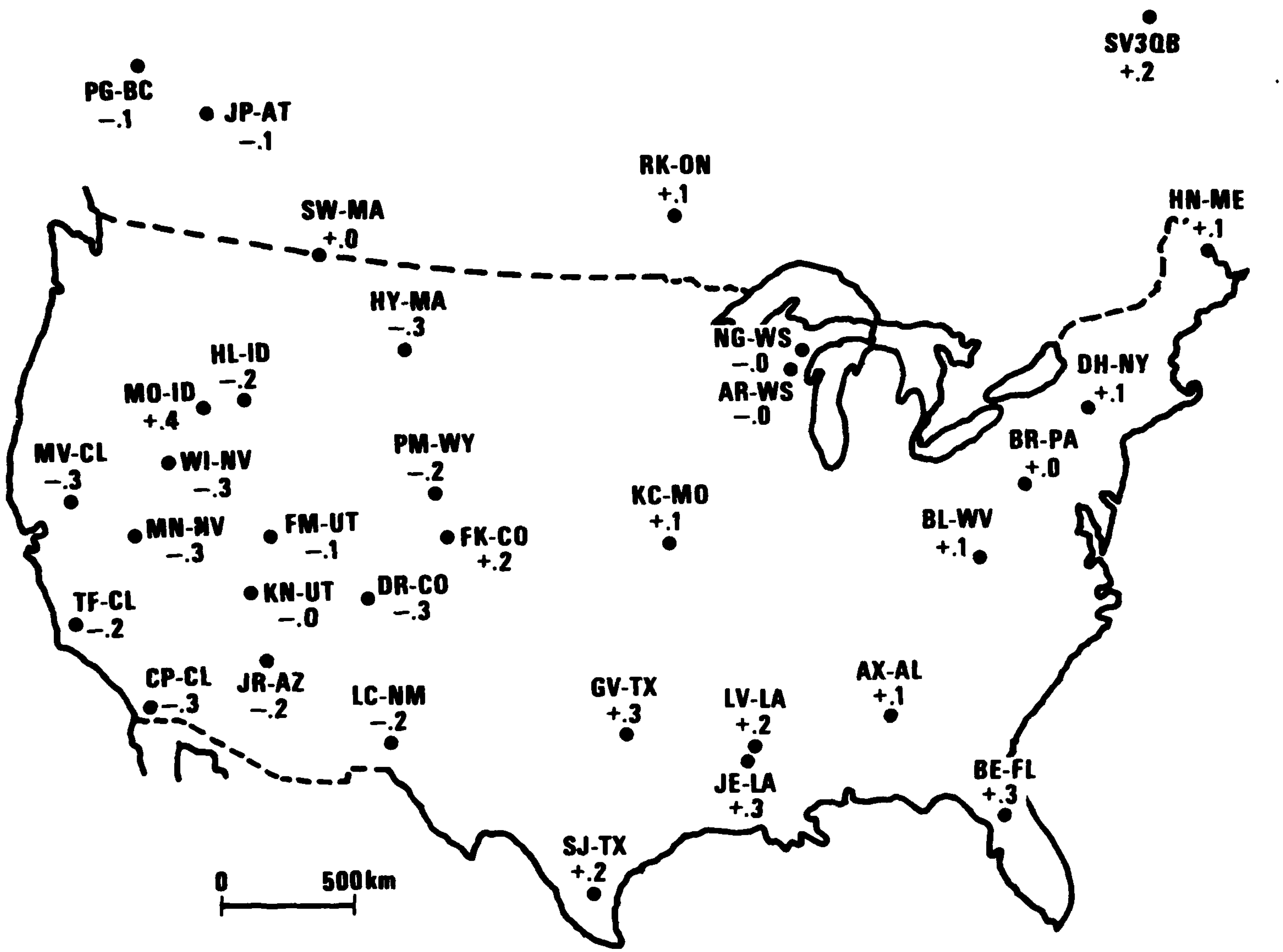

Figure 33 Magnitude residuals for LRSM stations (after Booth et al, 1974).

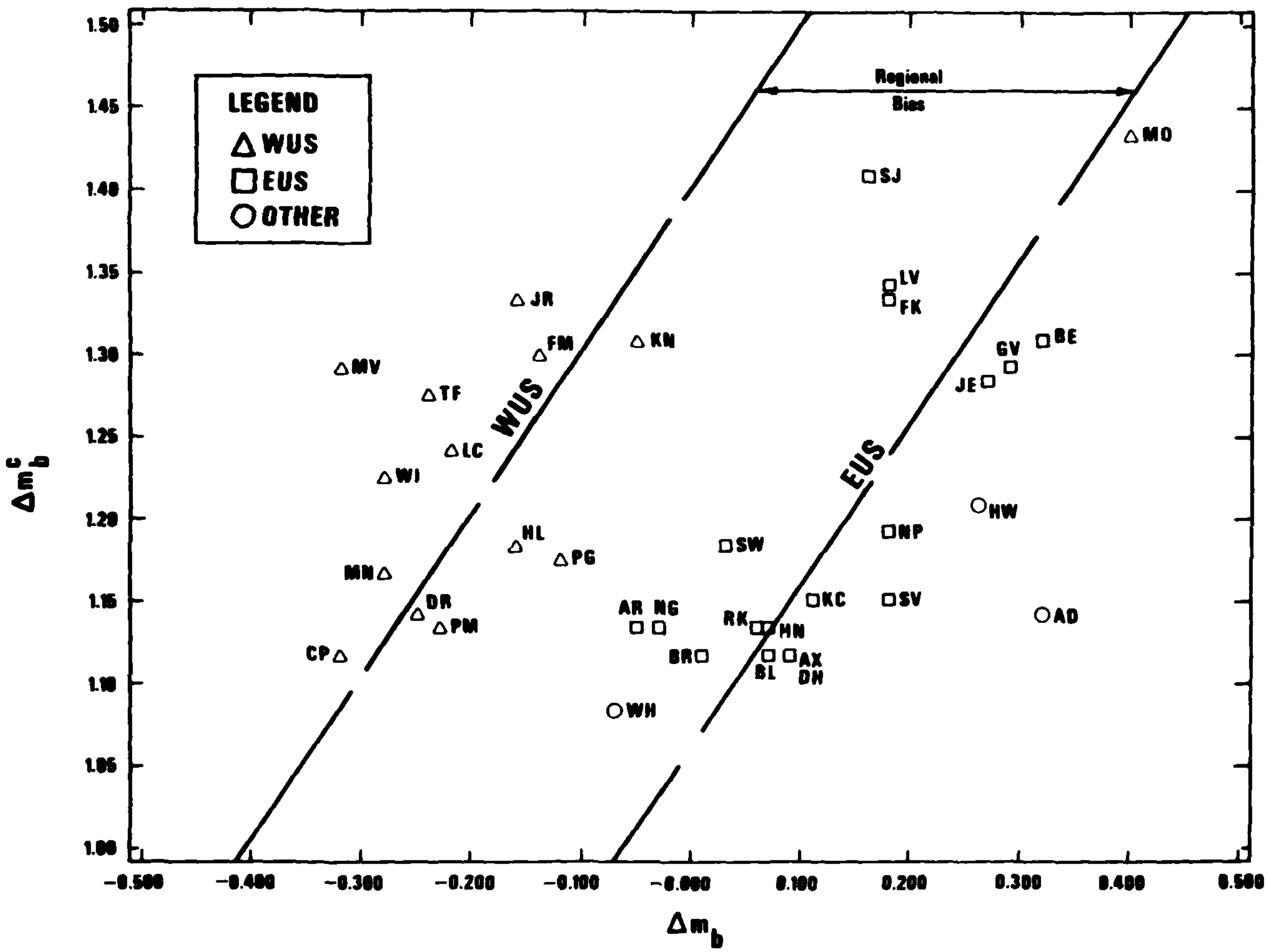

Figure 34 Magnitude residuals for Booth et al (1974) plotted against the logarithms of crustal amplification factor A_c. The data points tend to cluster around two regression lines, one for the EUS, the other for the WUS.

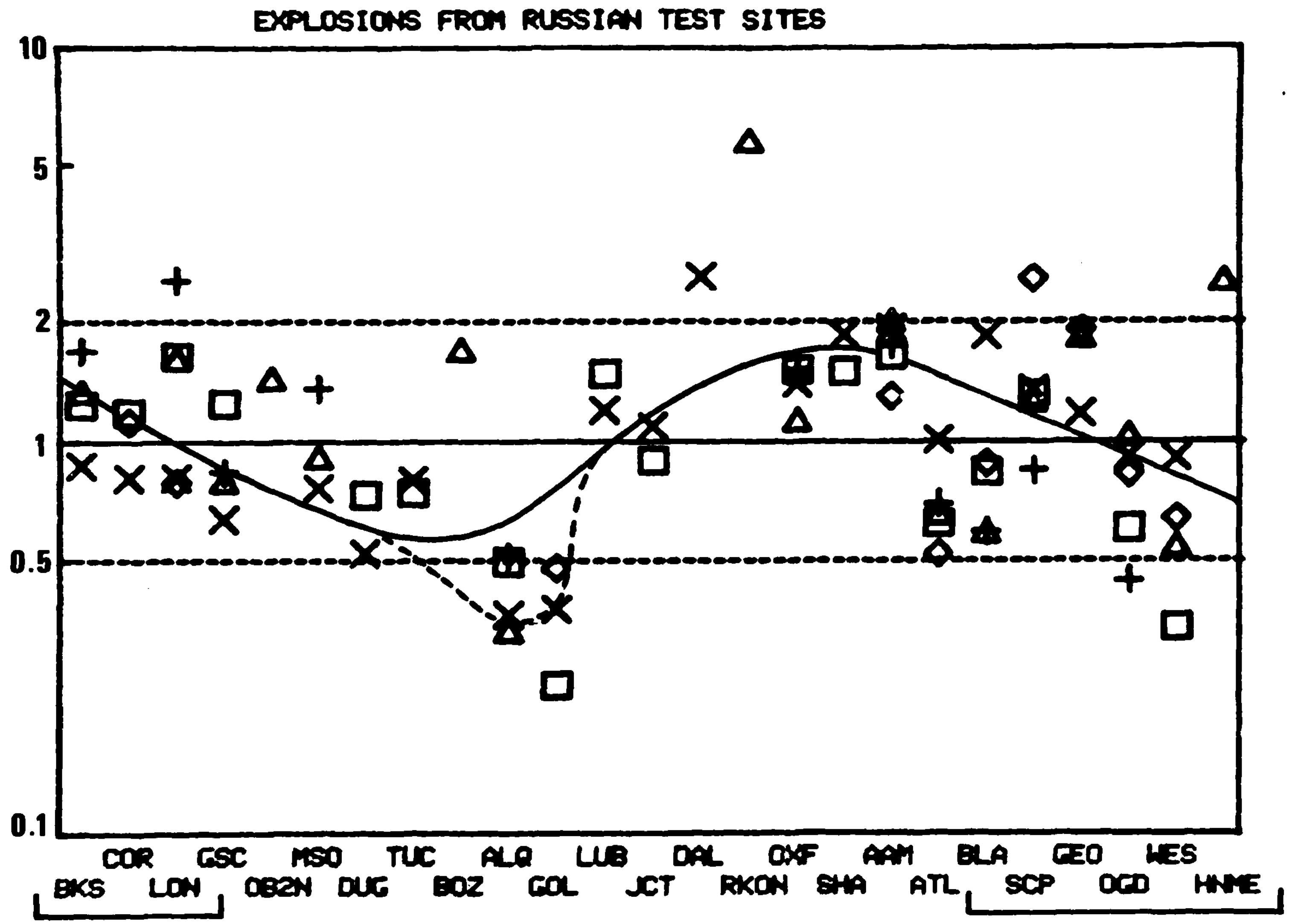

Figure 35 Logarithms of P wave trace amplitudes of WWSSN and SDCS stations (after Butler et al (1980)). Common shapes of the anomaly pattern are sketched for these stations (see text). NEUS stations and some Pacific coastal stations are given disproportional weight in these plots. The data shown are from events at Russian test sites.

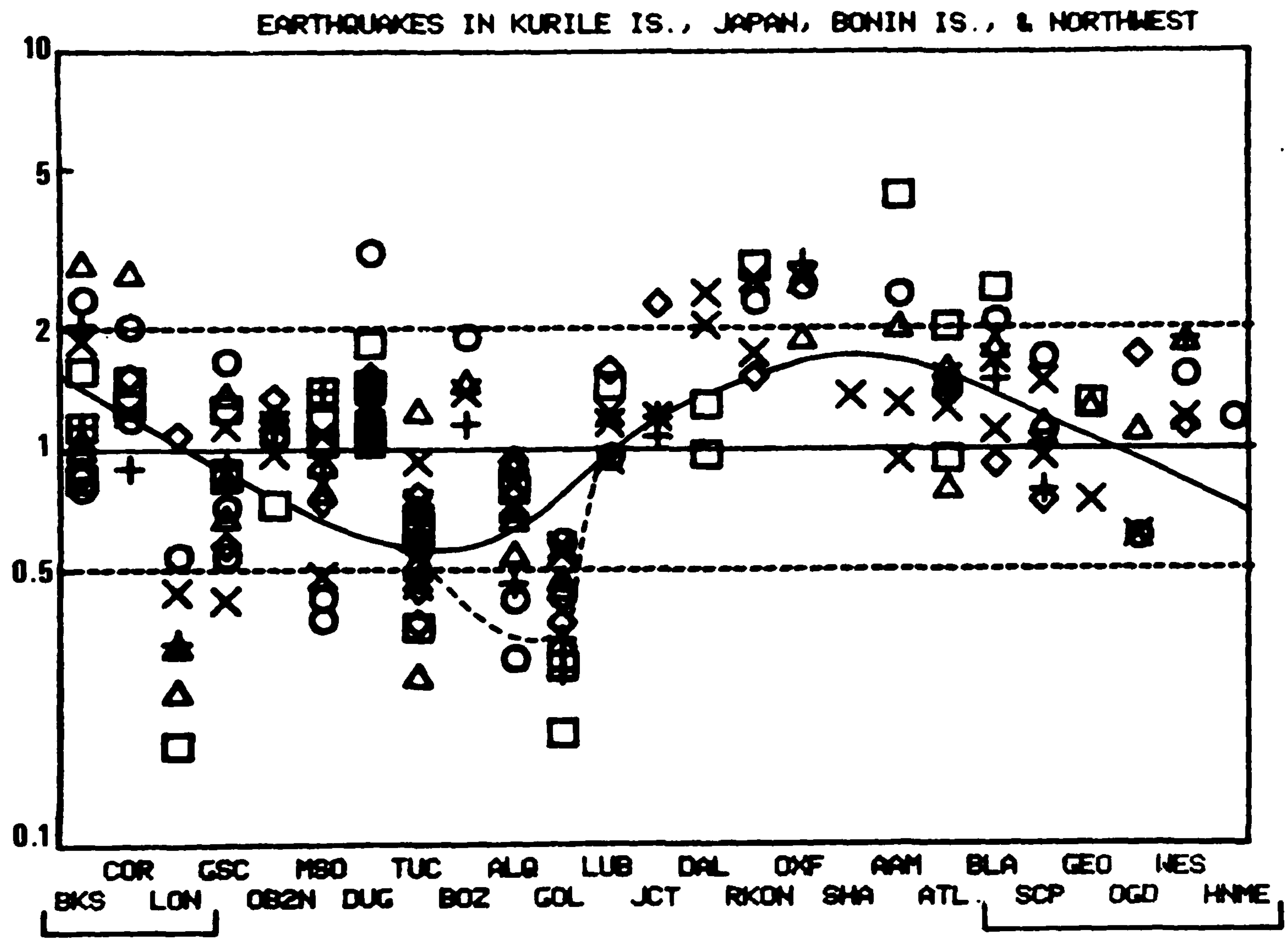

Figure 36 Logarithms of P wave trace amplitudes for WWSSN and SDCS stations (after Butler et al, (1980)). Common shapes of the anomaly patterns are sketched for these stations (see text). NEUS stations and some Pacific coastal stations are given *disproportional weight in* these plots. The data shown are from Kurile Islands, Japan, Bonin Islands and other northwestern events.

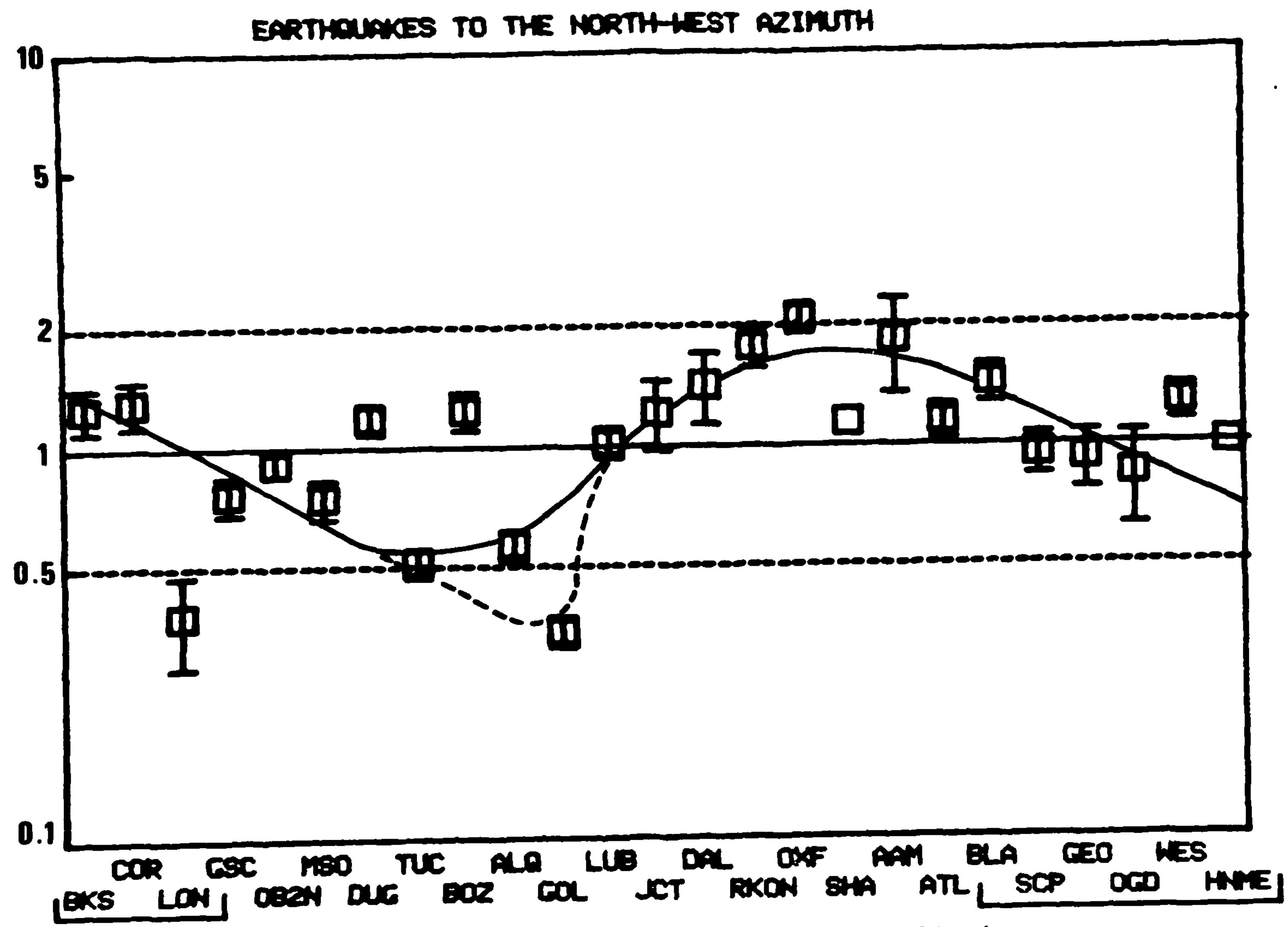

Figure 37 Logarithms of P wave trace amplitudes for WWSSN and SDCS stations (after Butler et al, (1980)). Common shapes of the anomaly pattern are sketched for these stations (see text). NEUS stations and some Pacific coastal stations are given disproportional weight in these plots. The data shown are from earthquakes along the northwest azimuth.

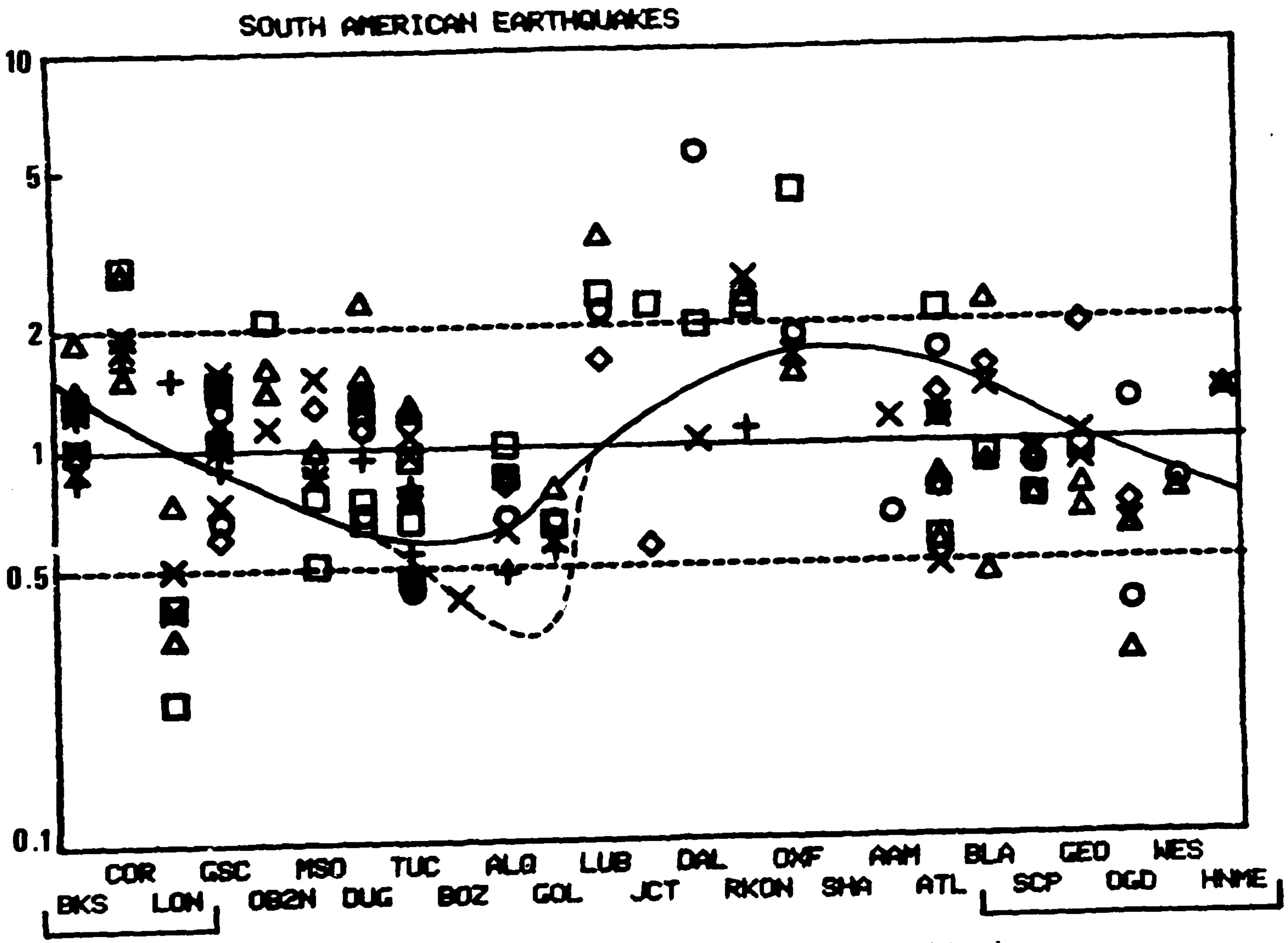

Figure 38 Logarithms of P wave trace amplitudes for WWSSN and SDCS stations (after Butler et al, 1980)). Common shapes of the anomaly pattern are sketched for these stations (see text). NEUS stations and some Pacific coastal stations are given disproportional weight in these plots. The data shown are from South American earthquakes.

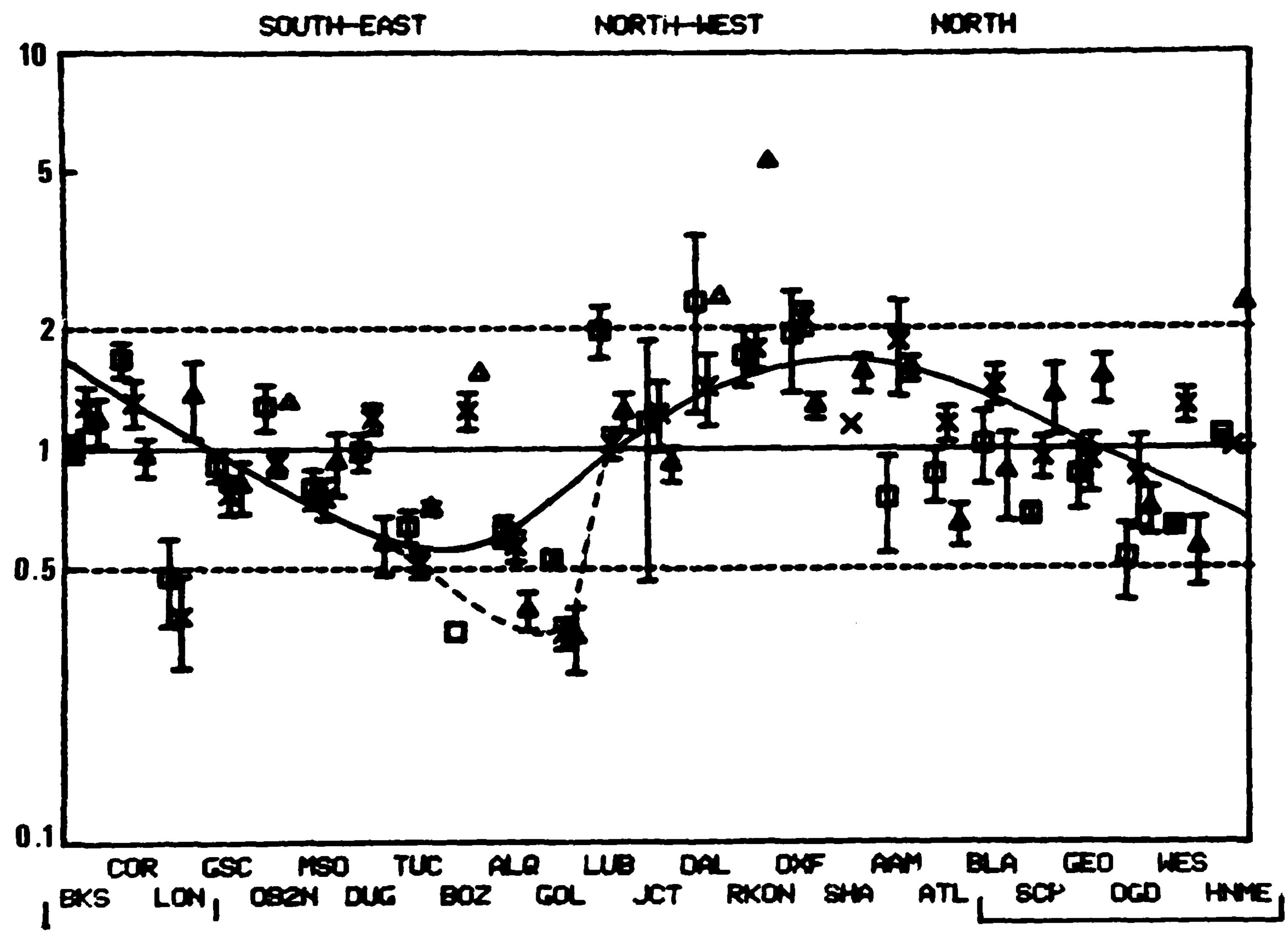

Figure 39 Logarithms of P wave trace amplitudes for WWSSN and SDCS stations (after Butler et al, (1980)). Common shapes of the anomaly pattern are sketched for these stations (see text). *NEUS stations and some Pacific* coastal stations are given disproportional weight in these plots. The data shown are from all events from the SE, NW, and N azimuths.

as E-W cross sections of sorts across the United States. These represent amplitude patterns for Russian test sites, earthquakes from the Kuriles, all earthquakes for the NW azimuth, South American earthquakes, and the sum of all of the data. For convenience of presentation they spaced the stations equally on the plots, a practice that gives an enhanced visual weight to some groups of stations that is out of proportion to the small areas they occupy (ie, the BLA-SCP-GEO-OGD-WES-HNME group and the BKS-COR-LON group). We shall refer to this fact later. Inspecting these figures in succession one can see a common pattern (sketched in freehand with a solid line) that is clearly associated with the crust-mantle structure under the United States. The wide variations from azimuth to azimuth and source region to source region are not surprising in view of the focusing phenomena described in Section D of the last part of this report. There is an indication of another detail, a low amplitude region along the Rocky Mountain front (dashed line).

Another curious feature of Figures 35 to 39 is that on most of these plots the SDCS stations OB2NV, RKON and HNME are high in amplitude relative to their surroundings. This arouses the suspicion that in Butler's work, when data from the two networks, SDCS and WWSSN, were assembled together, the mean m_b levels of the two networks were not adjusted properly. To investigate this we attempted to tie OB2NV in with this pattern by computing the magnitude differential at the common station OB2NV and station ANMO (ALQ). Readings of trace amplitude differentials at corresponding portions of the P wavetrain for 72 events resulted in the histogram of $\log_{10}$ (Amplitude) shown in Figure 40. The mean differential -0.15 ± .058 (95% confidence) indicates that the relative positions of WWSSN and SDCS stations in the study of Butler et al (1979) are not correct since Butler's differential between OB2NV and ALQ is much larger; it is outside the confidence limits indicated. This confirms our suspicion. Within each network, the relative differences in m_b levels are, however, correct in Butler's study and for the SDCS network his results agree well with ours.

Figure 35 to 39 were interpreted by Butler et al (1979) as showing that no average EUS-WUS regional difference in amplitudes exists, and the visual impression from these figures appears to confirm this if one averages the levels in the WUS and EUS in their graphs. However, if one considers the relative areas covered by the stations in the northeastern United States,

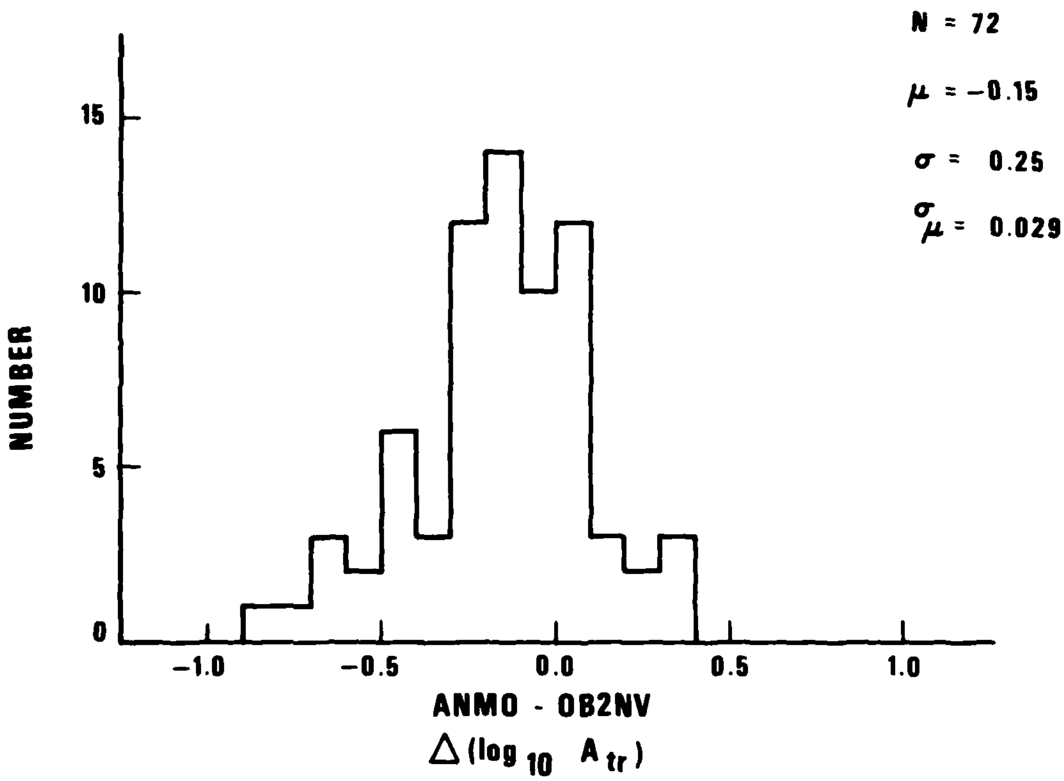

Figure 40 Histogram of trace amplitude differentials of P waves at OB2NV and ALQ (ANMO). This differential is significantly different from the value given by Butler et al, (1980).

about 1/20 of the total area, the visual weight given to the stations in the NEUS in Butler's figures (where they are evenly spaced) is excessive. Therefore these figures are highly deceptive. If one takes averages weighted with respect to the areas covered, the conclusion of many researchers that the EUS as a whole has larger m_b or amplitude levels than the WUS still stands.

P Wave Spectral Anomalies

Due to the sensitivity of high frequency body waves to variations of t*, spectral slopes are strong diagnostics of regional variations of attenuation. While body wave magnitude measurements involve mostly 1 Hz energy, spectra of P waves often show significant energy up to 4 Hz that is considerably more sensitive to variations of Q than 1 Hz energy. This fact, together with the greater stability of spectral slopes with respect to lateral inhomogeneities, makes spectral measurements extremely important in evaluating mantle Q under any location.

Spectral measurements can be used in various ways to estimate t_p^* in the earth. Spectral ratios of the observed P spectra to the estimated source spectrum can be used to estimate the absolute value of t_p^*. In most cases, absolute strengths of sources are not well known for either earthquakes or explosions; however, the slopes of source spectra are well enough specified to put reasonable limits on t_p^*. For explosions, near source measurements are often available to estimate the source spectrum from a reduced displacement potential. In the absence of near source data it appears that source models such as those of von Seggern and Blandford (1972) or Mueller and Murphy (1971) describe explosion spectra with sufficient accuracy to permit the computation of t_p^* to within 0.1 second. For earthquake observations, basic physical arguments require that the spectra fall off beyond a specific (although ill defined) corner frequency at rates of ω^{-2} or ω^{-3}, a condition that immediately puts limits on the possible range of absolute t_p^*.

In addition to estimating absolute t_p^*, spectral ratios of body waves observed at various stations for common events can be used to determine regional variations of anelastic attenuation. The ideal sources for such studies are nuclear explosions because, except for possible strain release, they are non-directional sources essentially radiating the same spectrum in all directions.

In our previous papers (Der and McElfresh, 1976, 1977) we compiled t* estimates for a group of paths crossing the mantle under the United States, mostly for nuclear explosions. Paths not crossing the mantle under the WUS were associated with signals of significant energy in the 3 to 4 Hz range. Paths crossing the mantle under the WUS showed a great reduction of the high frequency content. The t* for shield paths was found to be around 0.2 sec while for paths crossing the upper mantle under the WUS the t* was between 0.4 and 0.5 sec. None of our data showed t* equal or larger than 1 sec, although it is possible that some paths from the WUS to other tectonic regions might have $t^*_p \sim 1$ sec. Spectral ratios computed at the SDCS stations also fall into the pattern outlined above. All WUS test sites show relatively high t^*_p compared to RKON, while the stations in the northeastern U.S. are intermediate with regard to t^*_p, a position that correlates with the regional amplitude patterns.

S Wave Amplitude Anomalies

An additional measure of regional attenuation is provided by amplitude anomalies of short-period S waves. Short-period S waves are commonly not observed for shallow focus events, but are fairly common for deep earthquakes. This fact by itself puts some limitation on the values of t^*_s that we shall discuss later.

If regional P magnitude anomaly patterns are caused by variations of Q, then regional amplitude anomaly patterns of S should resemble those of P. This appears to be the case. In Figure 41 we show average SH trace amplitude residual terms expressed in units of $\log_{10}$(Amplitude) from the seven deep earthquakes listed in Table VI. The amplitudes were corrected for SH radiation pattern using the double couple representation of the sources. Data points close to nodal lines and requiring a large correction were omitted to avoid overcorrections due to uncertainties in source orientation. The average event magnitude was used for normalizing the amplitudes for each event. The SH residuals clearly show patterns similar to those for the P waves in Figure 33 (Booth et al, 1974). Furthermore, as Figure 42 shows, correction for crustal amplification effects on SH using flat layered models of crust under LRSM stations does not remove the anomalies. The approach used is identical to that presented by Der et al (1979). The scatter

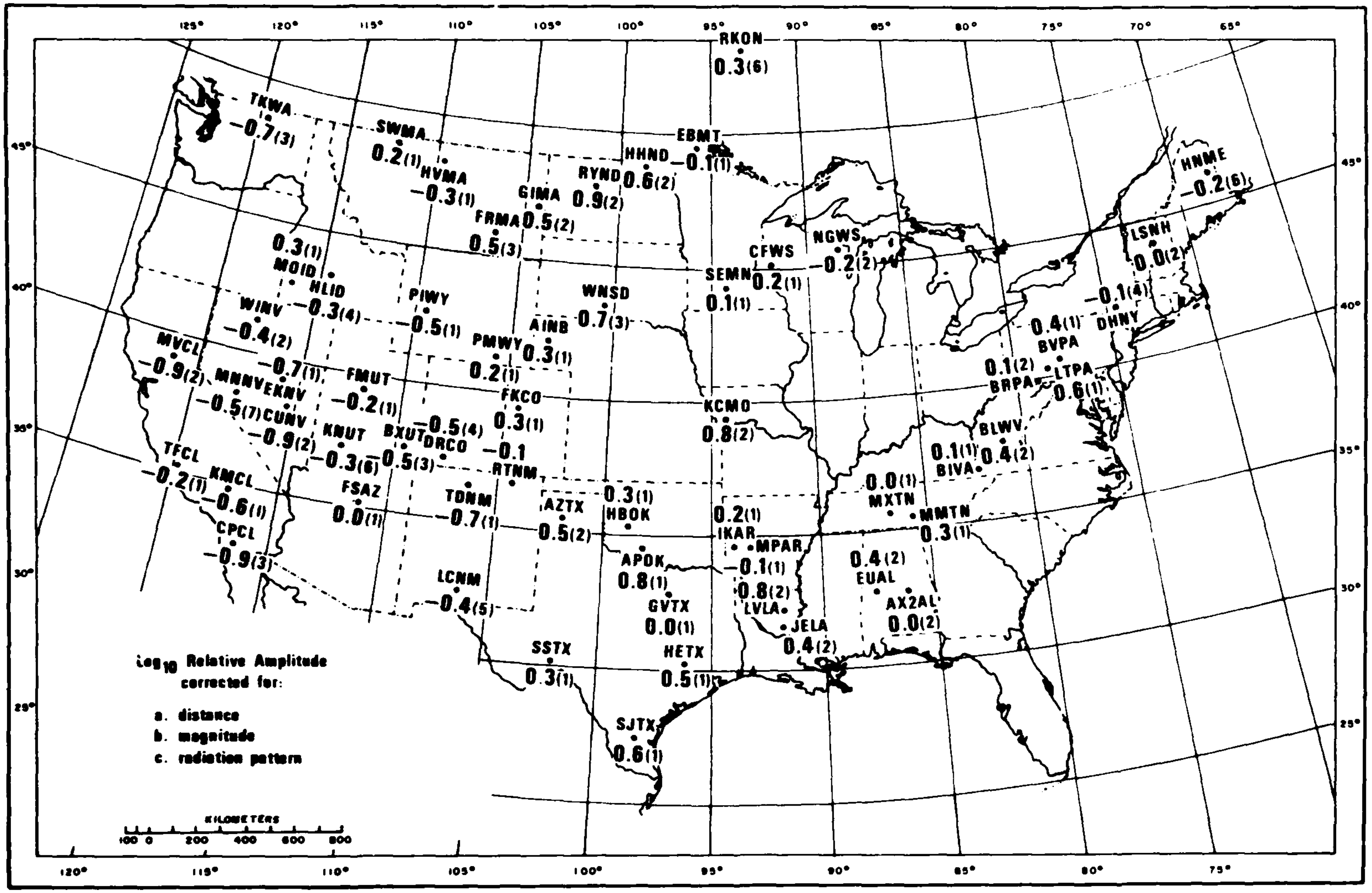

Figure 41 Short-period SH wave amplitude anomalies corrected for double couple radiation patterns and adjusted for relative magnitudes and distances for seven deep earthquakes listed in Table VI. The anomalies are given in units of ten base logarithms of amplitude. Large negative anomalies occur in the southwestern United States.

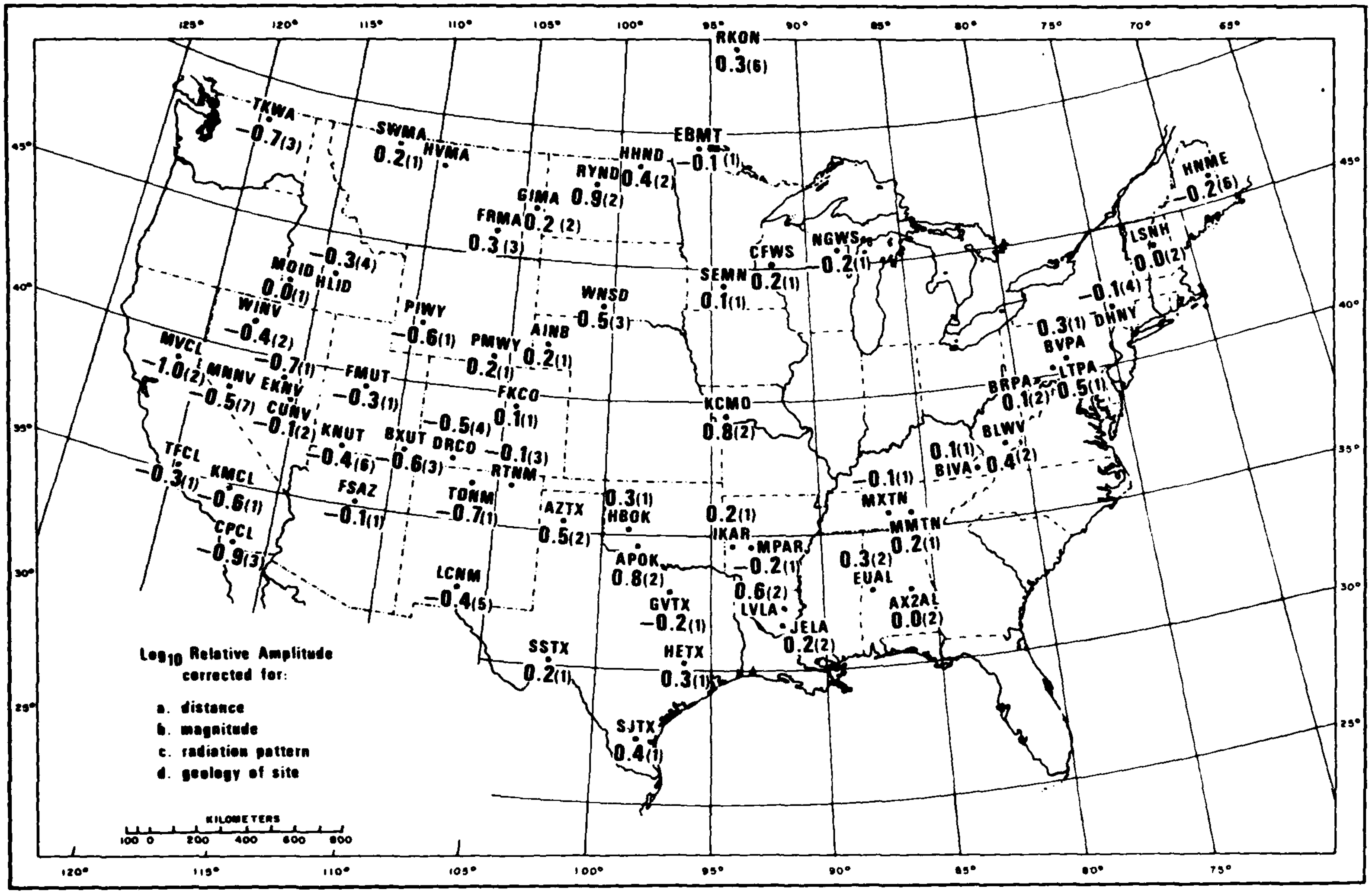

Figure 42 Short-period SH wave amplitude anomalies corrected for radiation patterns and adjusted for relative magnitudes, distance and estimated crustal amplification. Large negative values occur in the southwestern United States indicating the diminution of amplitudes in this region by anelastic attenuation.

TABLE VI

Seven deep earthquakes used for Figures 41 and 42

DATE	ORIGIN TIME	LOCATION	DEPTH (km)	LATITUDE	LONGITUDE	m_b	FOCAL MECHANISM		
							RAKE	DIP	STRIKE
08 DEC 62	21:27:18.0	NE ARGENTINA	620	27.0S	63.0W	7.0	241.21	85.02	164.75
09 NOV 63	21:15:30.0	WESTERN BRAZIL	600	9.0S	71.5W	7.0	258.10	66.89	104.01
10 NOV 63	01:00:38.8	PERU-BRAZIL BORDER	600	9.2S	71.4W	5.6	259.92	61.47	126.60
18 MAR 64	04:37:26.9	NW OF KURILES	438	52.5N	153.6E	5.6	270.00	85.00	50.00
22 AUG 66	14:21:14.0	SEA OF OKHOTSK	653	50.3N	147.7E	5.1	270.00	90.00	20.00
22 NOV 66	06:29:53.1	SEA OF OKHOTSK	469	48.0N	146.8E	5.7	90.00	55.00	190.00
12 OCT 67	12:53:46.9	NW OF KURILES	483	52.2N	152.5E	5.5	298.71	79.16	43.10

is still quite large, a fact that is not surprising since S waves are also subjected to the same lateral inhomogeneity effects as P waves, but the pattern is clear nonetheless. Unfortunately, short-period S waves are not sufficiently abundant to achieve the same accuracy in the estimation of station terms, but most of the negative residuals, especially the large ones, are in the western United States.

S Wave Spectral Measurements

According to most evidence, $t_s^* \sim 4\ t_p^*$ appears to be valid for regional as well as teleseismic changes in t* (Solomon and Toksöz, 1970; Der et al, 1980). Consequently, spectral changes in S should be quite noticeable from region to region. This appears to be true also. In Figures 43 to 49 we show tracings of short-period S waves at various LRSM stations across the U.S. Pointers show the location of the recording LRSM station on the map, and the instrument gains are given above each trace. Since one of the perpendicular horizontal components of the LRSM stations is oriented towards NTS, the tracings were done on the component closest to the transverse direction (SH) to the event. Although a few of these components may be misoriented by as much as 45°, the figures show a clear tendency for the stations in the southwestern U.S. to have lower amplitudes and lower frequencies. These are typical examples of this phenomenon and are not accidents of fault plane orientation and directivity. All broad band S waves (sometimes containing significant signal energy up to 2.5 Hz) show this phenomenon regardless of fault plane orientation. These events, not previously analyzed in our recent study (Der et al, 1980), demonstrate that visible regional differences in the frequency content of S waves are the rule and there is nothing exceptional about the data presented by Der et al (1980). We have inspected S waves from large numbers of deep events all showing similar variation.

Differential attenuation manifests itself in various ways in the time domain. Wide band signals with considerable high frequency content undergo a significant lengthening of dominant periods by the preferential reduction of the high frequency end of the spectrum. Narrow band signals containing less high frequency show little change in waveform. For both types of signals the overall trace amplitude is reduced, and this reduction is greater for the

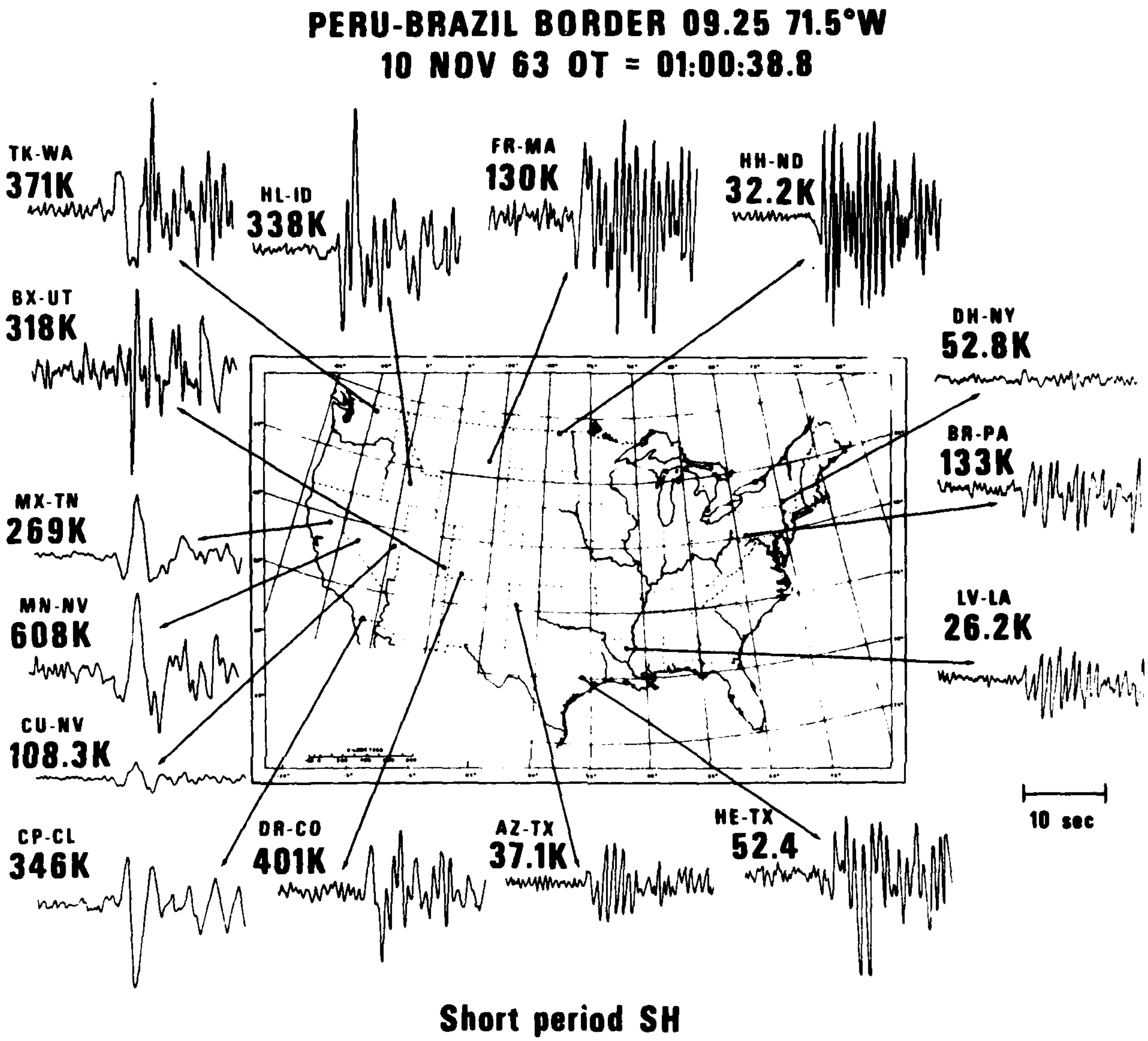

Figure 43 Tracings of short-period SH phases at LRSM stations across the United States. Depending on the frequency content of the signals, the time domain manifestations of anelastic attenuation vary, but the overwhelming majority of the signals show a diminution of amplitudes and the decrease of high frequency content in most of the WUS with especially severe effects in the southwestern United States. No corrections for radiation patterns were made in these figures. Instrument gains are shown on each trace.

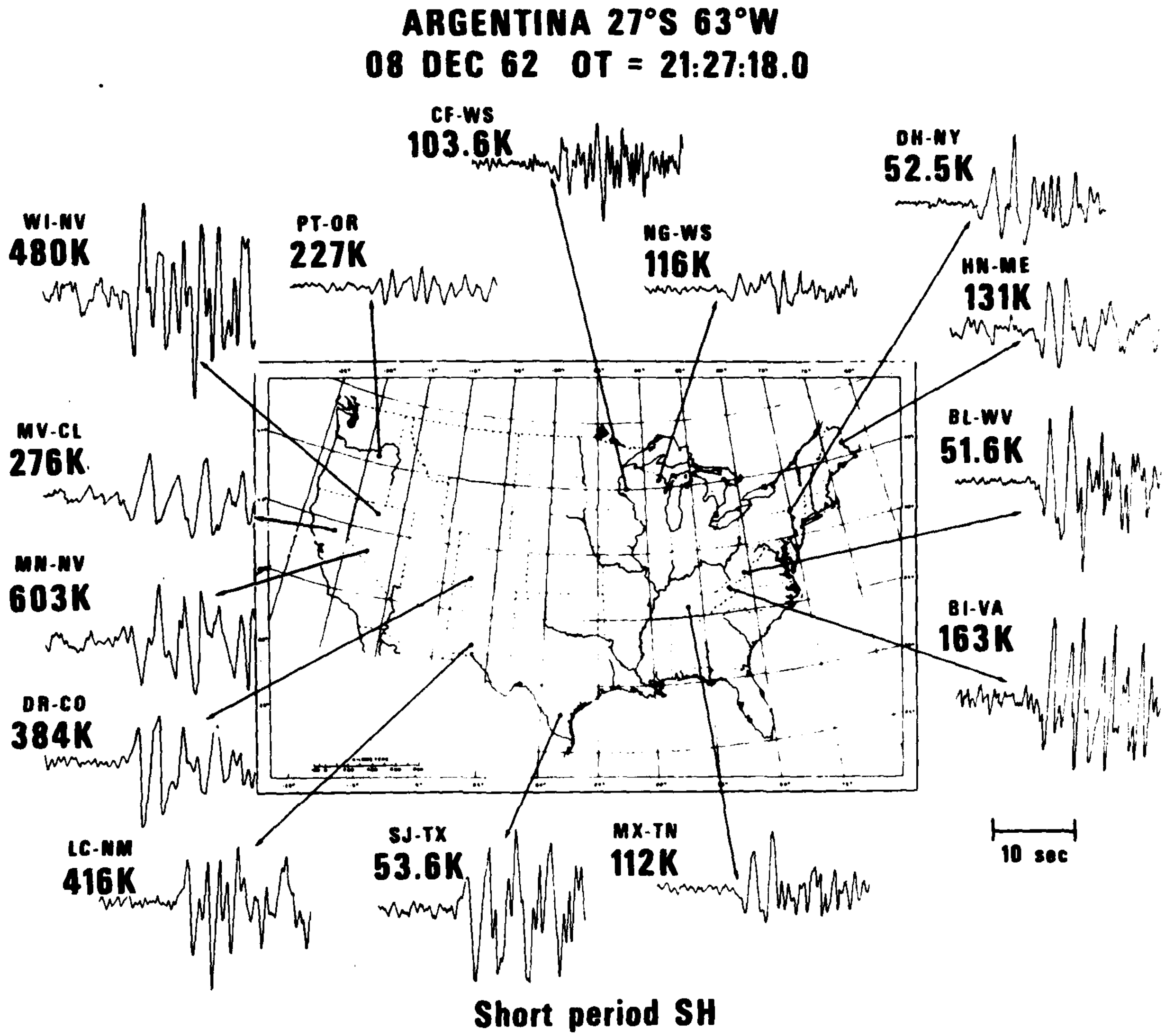

Figure 44 Tracings of short-period SH phases at LRSM stations across the United States. Depending on the frequency content of the signals, the time domain manifestations of anelastic attenuation vary, but the overwhelming majority of the signals show a diminution of amplitudes and the decrease of high frequency content in most of the WUS with especially severe effects in the southwestern United States. No corrections for radiation patterns were made in these figures. Instrument gains are shown on each trace.

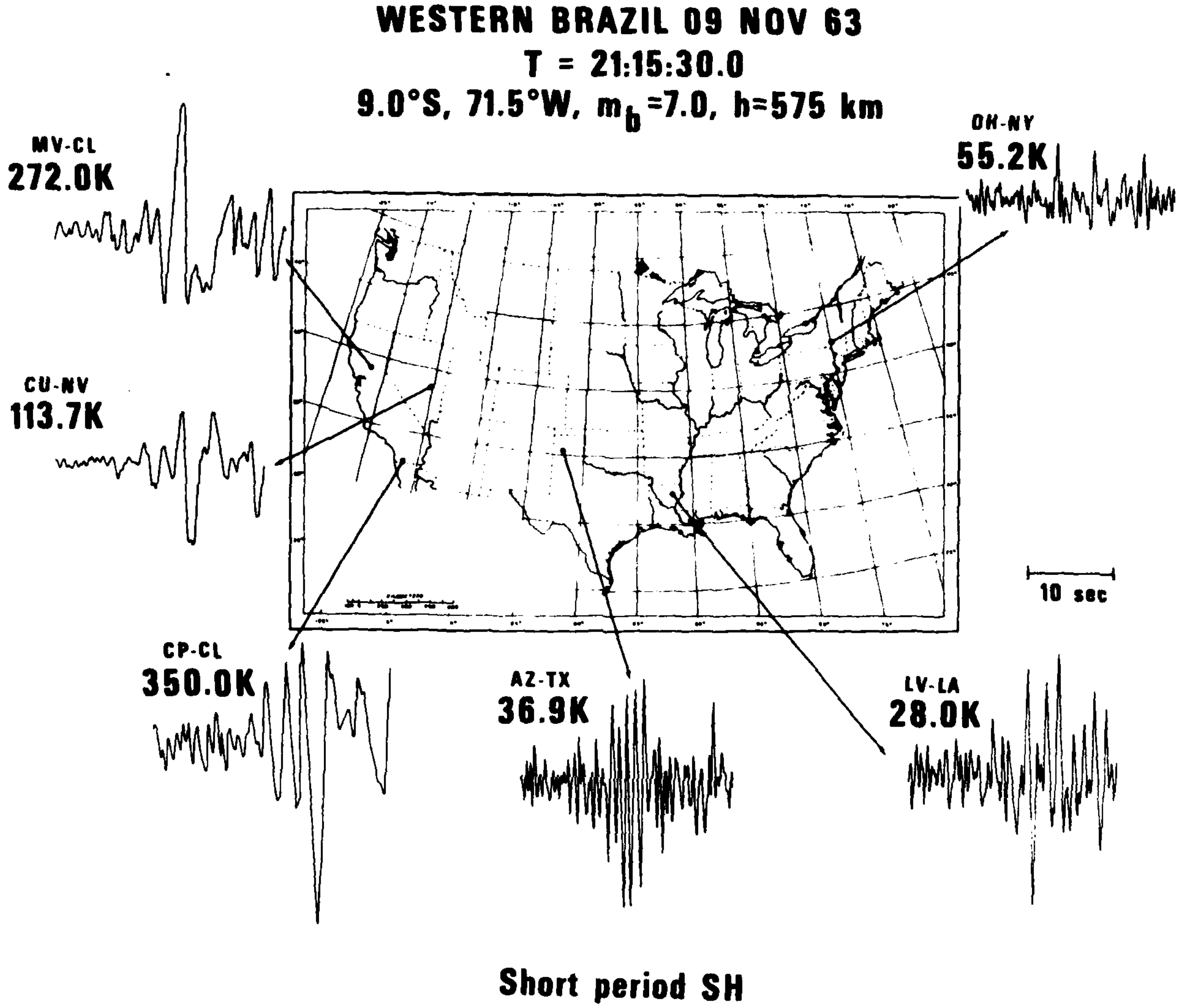

Figure 45 Tracings of short-period SH phases at LRSM stations across the United States. Depending on the frequency content of the signals, the time domain manifestations of anelastic attenuation vary, but the overwhelming majority of the signals show a diminution of amplitudes and the decrease of high frequency content in most of the WUS with especially severe effects in the southwestern United States. No corrections for radiation patterns were made in these figures. Instrument gains are shown on each trace.

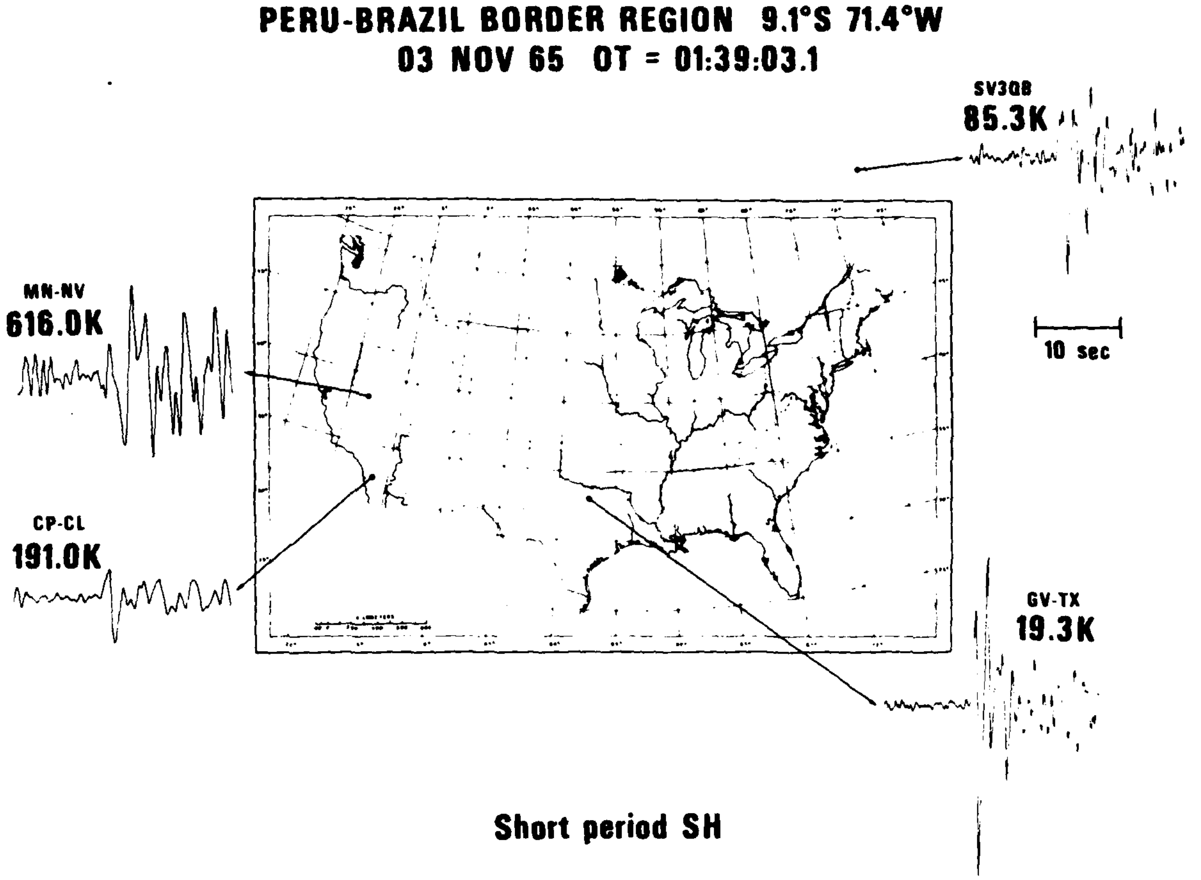

Figure 46 Tracings of short-period SH phases at LRSM stations across the United States. Depending on the frequency content of the signals, the time domain manifestations of anelastic attenuation vary, but the overwhelming majority of the signals show a diminution of amplitudes and the decrease of high frequency content in most of the WUS with especially severe effects in the southwestern United States. No corrections for radiation patterns were made in these figures. Instruments gains are shown on each trace.

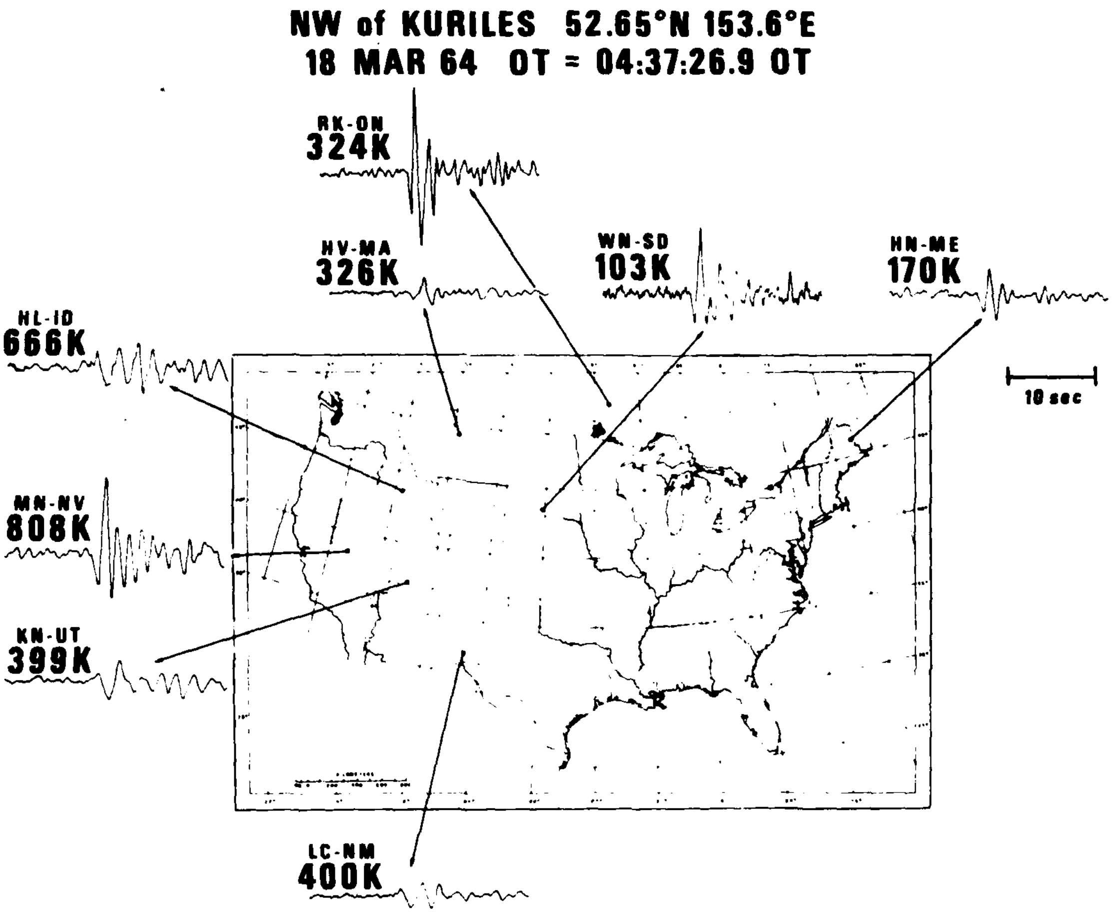

Short period SH

Figure 47 Tracings of short-period SH phases at LRSM stations across the United States. Depending on the frequency content of the signals, the time domain manifestations of anelastic attenuation vary, but the overwhelming majority of the signals show a diminution of amplitudes and the decrease of high frequency content in most of the WUS with especially severe effects in the southwestern United States. No corrections for radiation patterns were made in these figures. Instrument gains are shown on each trace.

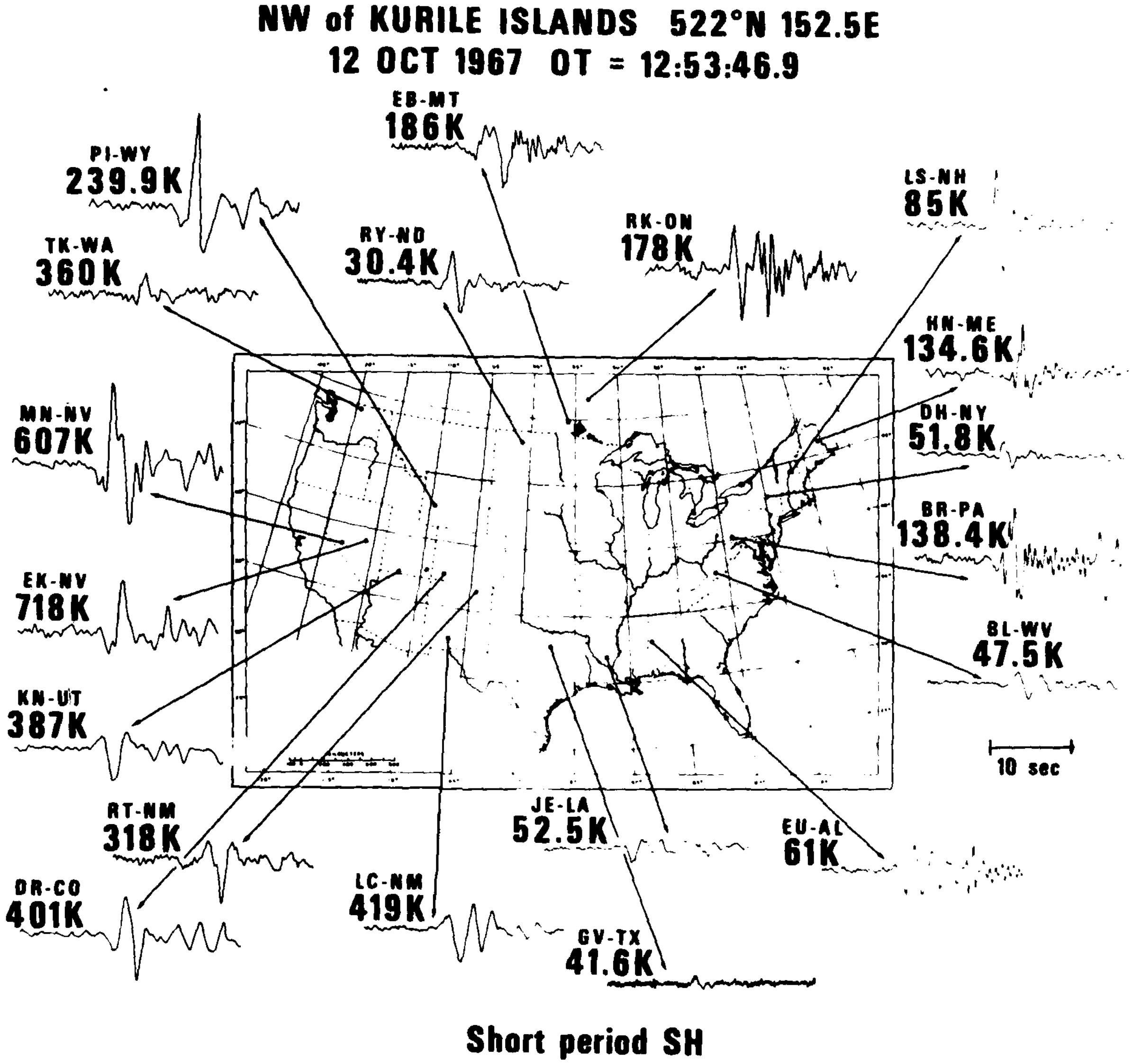

Figure 48 Tracings of short-period SH phases at LRSM stations across the United States. Depending on the frequency content of the signals, the time domain manifestations of anelastic attenuation vary, but the overwhelming majority of the signals show a diminution of amplitudes and the decrease of high frequency content in most of the WUS with especially severe effects in the southwestern United States. No corrections for radiation patterns were made in these figures. Instrument gains are shown on each trace.

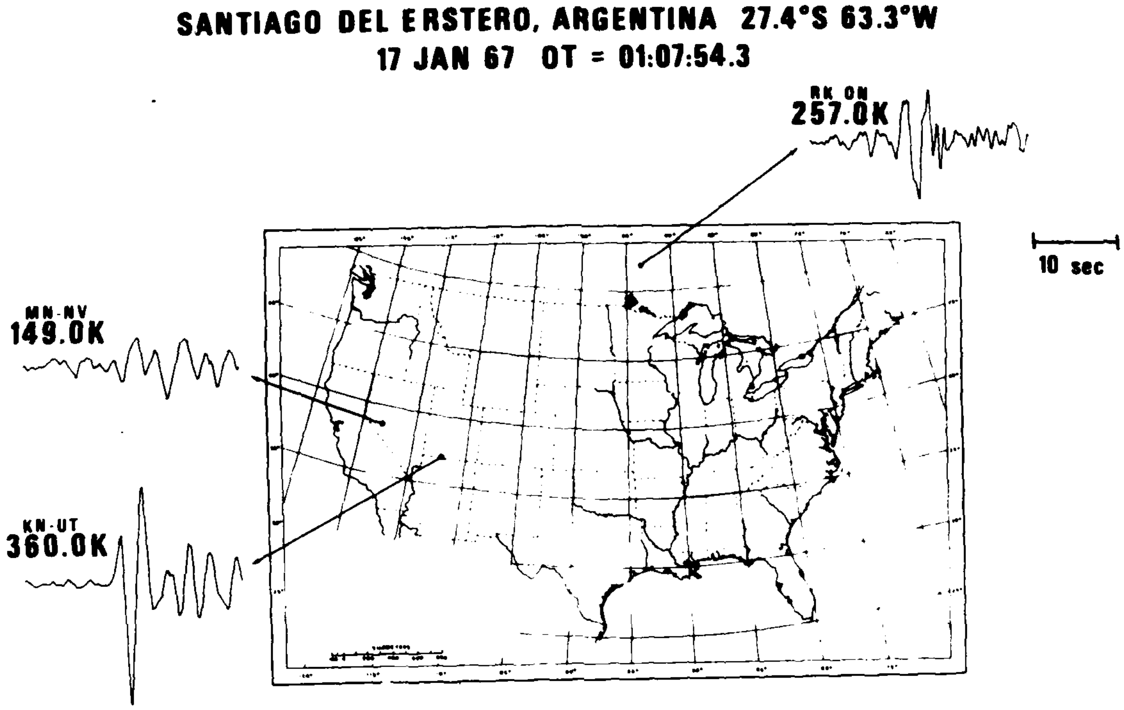

Short period SH

Figure 49 Tracings of short-period SH phases at LRSM stations across the United States. Depending on the frequency content of the signals, the time domain manifestations of anelastic attenuation vary, but the overwhelming majority of the signals show a diminution of amplitudes and the decrease of high frequency content in most of the WUS with especially severe effects in the southwestern United States. No corrections for radiation patterns were made in these figures. Instrument gains are shown on each trace.

wide band signals (Der and McElfresh, 1980). The above-mentioned tracings show examples of both types of behavior. The nature of signals can be easily judged by their appearance at the high Q shield sites. WWSSN records show similar variations, but the high frequency content riding over lower frequency waves is suppressed somewhat relative to those shown due to the different instrument response.

The differential in SH wave trace amplitudes reflects the regional Q differential to a lesser extent than would the amplitude at the dominant frequencies of the signals in the low Q regions. Many S signals in the north central U.S. have dominant frequencies at slightly less than 1 Hz; such frequencies appear to be completely absent in the southeastern U.S. The Q differential can effectively be measured only in the frequency domain, of course.

In a previous study (Der et al, 1980) we have shown that the regional averages of t_s^* differentials are 3 to 4 times larger than the average t_p^* differentials.

Outlining the Regional Variations of Q Under the United States

In spite of the many uncertainties with regard to source spectra, source mechanism, absolute source strengths and the precise determination of Q in the Earth, reasonable limits on the values of Q can be established in the short-period band by utilizing the great sensitivity of high frequency energy to Q. Consider the consequences of $t_p^* \sim 1$ sec and $t_s^* \sim 4$ sec, values widely used in long-period simulations and also claimed to be valid in the short-period band. Figure 50 shows spectra of P and S waves from some deep events observed in the north central United States. If one generously allows for the source depth by halving the t* values to $t_p^* \sim 0.5$ and $t_s^* \sim 2$ sec and plots the expected spectral falloff rates of ω^0, ω^{-1}, ω^{-2}, and ω^{-3} in the source spectra (solid lines), there is a sizable discrepancy at the high frequency end in each case. This discrepancy is especially obvious in the S waves where it amounts to more than two orders of magnitude. Furthermore, for S waves it is clearly prevalent even in the vicinity of 1 Hz. The observed spectra in all cases are incompatible with $t_p^* \sim 0.5$ and $t_s^* \sim 2$ and require considerably lower values for these quantities.

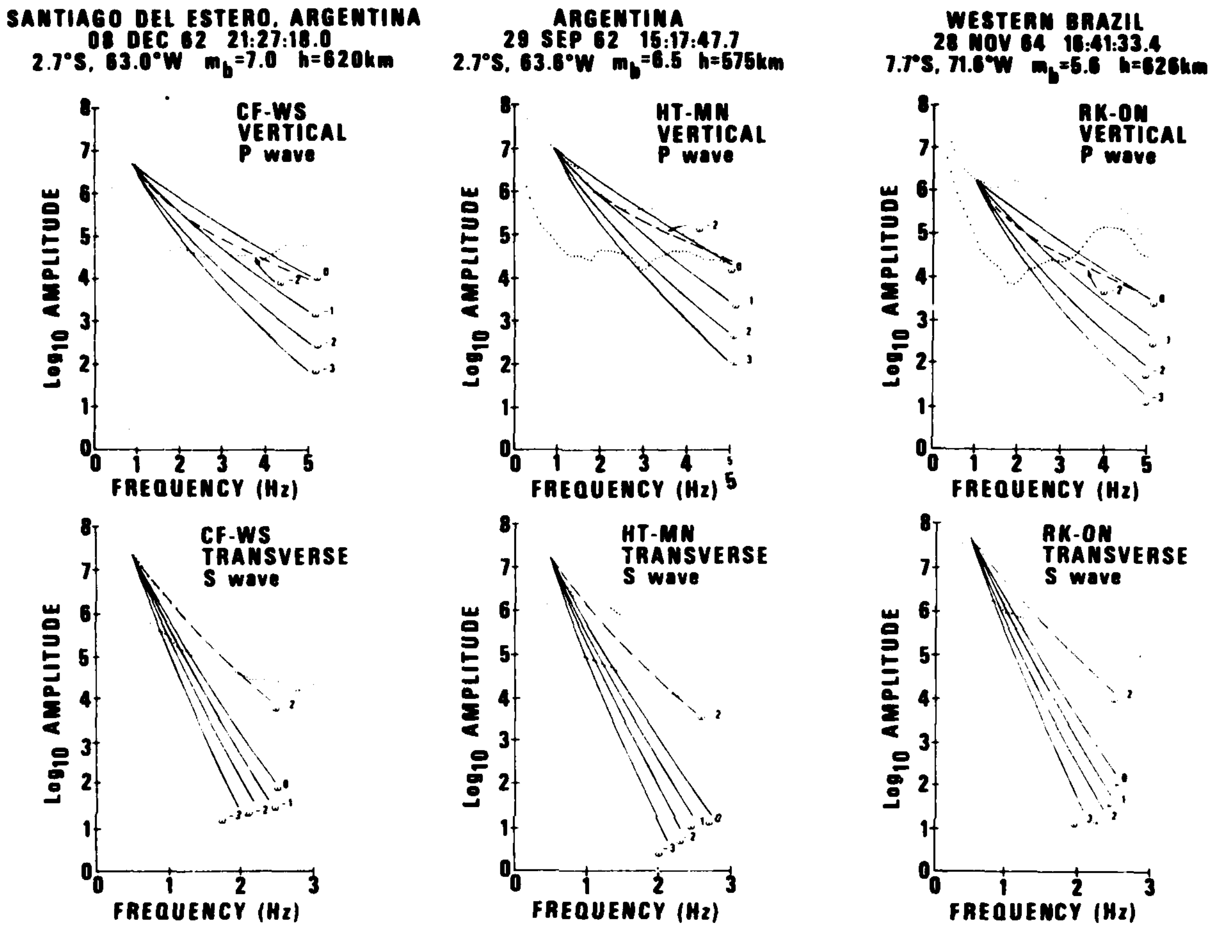

Figure 50 Spectra of signal and noise (upper and lower dotted lines) of selected P and S waves from deep earthquakes observed in the north-central U. S. The spectra were corrected for instrument response. The falloff rates of theoretical spectra (solid lines) (assuming various falloff rates for the source spectrum with $t^*_p = .5$ and $t^*_s = 2.$ and also allowing for the source depth) lead to discrepancies of several orders of magnitude. These values of t*, commonly used in time domain work, are therefore unacceptable. The values of $t^*_p = 0.2$ and $t^*_s = 0.8$ (dashed lines) with an ω^{-2} falloff in the assumed source spectra fit better, but even these values may be too high.

We estimate from a larger data set that $t_p^* < 0.2$ and $t_s^* < 0.8$ sec is needed to satisfy these data. This is illustrated by the dashed lines in Figure 50 assuming a falloff rate of ω^{-2}, which is the most likely value for large events such as these. This implies that $t_p^* \leq 0.2$ and $t_s^* \leq 0.8$ for deep events and that for shallow events in this type of upper mantle (shield) at both ends of the paths, $t_p^* \leq 0.4$ and $t_s^* \leq 1.6$. This result, together with the long-period result of $t_p^* \sim 1$ and $t_s^* \sim 4$ along similar paths by other workers, implies that t* is frequency dependent. We must point out, however, that most results in the long-period band are not applicable to shields, and the possibility remains that t* is low but not dependent on frequency for shields.

Consider again an additional constraint that limits the regional variation of t_p^*--the size of P wave magnitude anomalies. Since these are of the order of 0.3 magnitude units, the corresponding t* variation must be of the order of 0.2 sec (Der et al, 1979). This is the same result that one arrives at by using spectral ratios (Der and McElfresh, 1977; this report). This implies $t_p^* \sim 0.6$ for paths crossing the mantle under the western United States and terminating in a shield type of structure at the other end. Values such as $t_p^* = 1.3$ (Hadley, 1979) are therefore too high and cannot be accepted in the short-period band.

As far as measured relative regional variations of short-period t_s^* in the U.S. are concerned, these are of the order of 0.8 or maybe somewhat less. The existing constraints are not too tight on these (Der et al, 1980).

t_s^* must also satisfy another condition imposed by observations, namely that for shallow earthquakes short-period S is usually not seen. This condition is quite unspecific since it is not clear how the amplitude of S compares to that of P in the short-period band at the source. Assuming the S amplitude to be five times that of the P (double [illegible]), one gets the result that for $t_s^* = 2$ sec, S will have 5% of the am[illegible] of P at 1 Hz. A slightly higher $t_s^* \sim 2.4$, corresponding to tectonic-to-shield type paths and the known phenomenon of corner frequency shift of S to lower frequencies, can easily account for the observed disappearance of S into the P coda. Therefore our values appear to satisfy this condition without the need for $t_s^* \sim 4$, a high value commonly claimed by some researchers.

It is conceivable that one could occasionally observe a t_s^* considerably larger than what we consider representative from deep events. For example, a body wave could encounter pockets of attenuating material close to the source (Sacks and Okada, 1974). Such observations, however, cannot be considered representative for the mantle under the north central United States, a common medium for all arrivals observed in this region. Observations of high frequency S wave energy from deep events would be unlikely if any observed low Q is attributed to the mantle under the observing station, unless we presuppose lateral Q variations of extremely small scale. This is because the raypaths sample a relatively small region under the station.

All of the data presented here appear to be compatible with an apparent t_p^* of 0.1 to 0.2 second for shield to shield type paths and 0.4 to 0.5 sec along paths from a shield to the WUS. The data are also compatible with the measurements for explosions listed by us (Der and McElfresh, 1977) and the relative t_s^* measurements from deep events (Der et al, 1980).

Correlation with Travel Time Delays and the Extent of the Mantle Low Velocity Layer

It is not necessary for travel time delays to correlate with regional variations of Q since seismic wave velocities are also dependent on chemical composition. Nevertheless, the correlation between the regional variations of Q outlined above and travel time delays reported by Sengupta and Julian (1976) is extremely good. The major features of their results, shown in Figure 51, include large delays in the Basin and Range and SWUS in general, early arrivals in the shield, and slightly late arrivals along the Atlantic seaboard and in New England. The late P arrivals in New England have since been studied in more detail (Taylor and Toksöz, 1979). The P wave travel times at OB2NV are 1.7 sec late relative to RKON after elevation correction, and because of this NTS fits well into the regional pattern presented by Sengupta and Julian. The same observation can be made with regard to the S wave delays in North America as compiled recently by Wickens and Buchbinder (1980). The larger S delays in the southwestern corner of the United States appear to coincide in area with the most severe attenuation of S waves apparent in our Figures 43 to 49. There are also indications that the

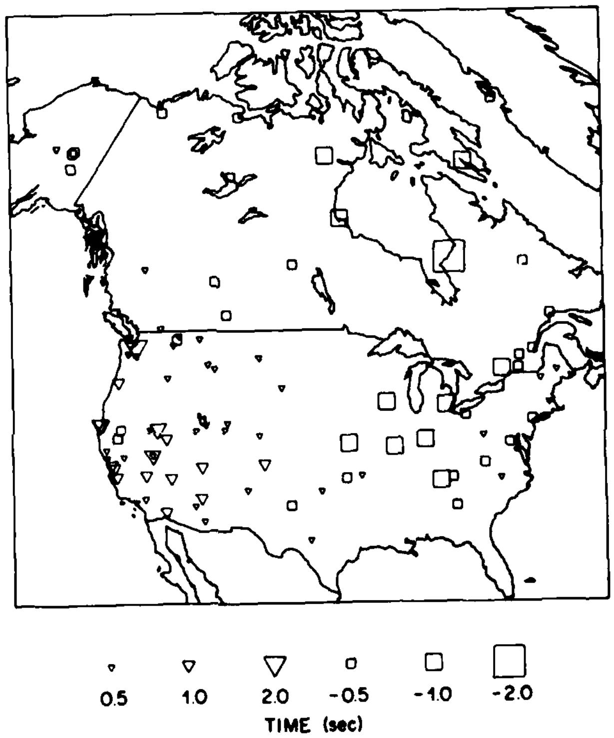

Figure 51 Travel time delays for P waves from deep events across the United States (after Sengupta and Julian, 1976).

relationship between P and S delays is different in the EUS versus the WUS (Romanowitz and Cara, 1980), indicating that the travel time delay pattern cannot be associated with changes in thickness of simple low velocity layers without changes in velocity contrast. Low velocities in the upper mantle also manifest themselves in the diminution of phase velocities of surface waves with significant particle motion in the mantle. There appears to be a correlation between low surface wave Q and low phase velocities worldwide (Lee and Solomon, 1979; Nakanishi, 1979). The low Q-low mantle velocity regions are also characterized by negative m_b residuals (North, 1977). Low mantle velocities and low Q thus appear to be areally correlated worldwide.

Frequency Dependence and Worldwide Implications

Strictly speaking, frequency dependence of Q can only be established if attenuation is measured in a wide frequency band using short- and long-period instruments over the same paths. Consideration of frequency dependence introduces a large number of additional parameters into studies of attenuation. It is possible that the form of frequency dependence changes from region to region, and the depth distribution of Q may be different at various frequencies (Solomon, 1972; Lundquist, 1979). These uncertainties can be resolved only by further detailed studies. A large number of reported t* determinations within the U.S. in the long-period band were obtained by time domain methods, but these cannot be accepted as valid until the controversies surrounding them are resolved. We have shown above that in the short-period band values of $t^* \approx 1$, as often obtained by time domain techniques, are unacceptable.

In the following we shall outline possible frequency dependence of t^*_p using three assumptions. The first assumption is that the Q and velocity structures are basically identical for all shields, so that absolute attenuation measurements in other shield regions can be applied to the north central U.S. The second assumption is that $t^*_s \approx 4t^*_p$. This assumption is supported by most of the data in the literature, and the slight modification due to losses in compression proposed by Sailor and Dziewonski (1978) does not affect the following argument. The third assumption is that most of the losses in the mantle occur in the upper 200 km and that the contribution of any low Q region at the core mantle boundary is relatively small. All of these assumptions agree well with the findings of research to date.

We now proceed to describe attenuation in terms of t_p^* as a function of frequency along two types of teleseismic paths. The first type of path crosses a shield-stable platform type structure at both the downgoing and upgoing legs of the path. We call these paths "shield paths" in the following discussion. The second type crosses a WUS (tectonic) type of mantle on either leg of the path. We term these paths "shield-to-tectonic". In the previous section we put several bounds on the possible values of t_p^* and t_s^* in the short-period band within the U.S. These are:

- t_p^* is of the order of 0.1 to 0.2 sec for shield paths in the 0.5 to 4 Hz range (from spectral measurements).
- $t_s^* \sim 2$ for shield paths around 1 Hz.
- The t_p^* differential between shield and shield-to-tectonic paths is of the order of 0.2 sec.

These constraints are supported by short-period t_p^* measurements from other regions. Spectral measurements of short-period P waves having shield type paths from Asia to NORSAR imply $t_p^* \sim 0.1$ (Noponen, 1975, Ringdal, 1976; Filson and Frasier, 1972). The spectral differences between WUS and central Asia earthquakes and explosions at NORSAR imply a t_p^* differential of the order of 0.2. Spectra of teleseismic P waves for a wide variety of paths observed on shields contain significant high-frequency energy in the 3 to 4 Hz range, essentially ruling out any constant $t_p^* \sim 1$ for most such paths.

Having put limits on t_p^* and t_s^* within the short-period band, we can proceed now to review the evidence in the long-period band. The studies by Solomon and Toksöz (1970) and Solomon (1972) give a regional t_p^* differential of $\Delta t_p^* \sim 0.5$ sec or more in the two types of paths. The studies of Lee and Solomon (1975 and 1979) result in Q_β structures that imply a long-period t_p^* differential of only 0.25. Ray tracing through the Q models given would yield t_p^* of the order of 0.6 to 1.7 in the eastern U.S. (EUS) and close to unity for an EUS-WUS path. This by itself would imply frequency dependence of Q, but the absolute Q values in these models are rather uncertain due to the inherent difficulties of measuring Q of surface waves over short paths. In any case, these studies indicate that the upper mantle Q also varies regionally in the long-period band. Therefore, the fitting of absorption band models that do not allow for this by shifting the high-frequency limit

only (Lay and Helmberger, 1980) unnecessarily constrains the results. The work of Nakanishi (1979) provides further indications that the upper mantle Q measured in the 150 to 300 sec period range is high under shields. It appears from his work that, on the average, anelastic losses under shields are less than those associated with model MM8 of Anderson et al (1965). At teleseismic distances model MM8 gives a t_p^* of the order of 0.6 to 0.8 sec; thus those values should be considered as upper limits of t_p^* for a long-period band also.

The ideal measurement of Q_β under shields would be provided by multiple ScS phases. Unfortunately, there are no studies of ScS that could be clearly associated with purely shield type paths (and none under the eastern United States). Nevertheless, the average Q_β ScS values for the whole mantle of 600 by Kovach and Anderson (1964) and 580 by Sato and Espinosa (1967) may be indicative of Q values in regions above the downgoing slab in South America that may have Q characteristics similar to shields (Sacks and Okada, 1974). These Q values are considerably higher than those obtained from multiple ScS studies elsewhere (Sipkin and Jordan, 1980), but the corresponding t_p^* at teleseismic distances in such structures would still be 0.4 to 0.5 sec, twice the apparent t* from spectral ratios in the short-period band. Thus even these high Q values imply some weak frequency dependence of Q for shield type of paths. If the average Q under shields turns out to be lower, as suggested by the average mantle Q_{ScS} of 225 for continents (Sipkin and Jordan, 1980), the frequency dependence would, of course, be stronger.

The above constraints allow one to draw the preliminary sketch shown in Figure 52 of frequency dependence of t_p^* for the two types of paths discussed above. The most natural assumption is a smooth variation that appears to be supported by indications of smooth changes in both the short- and long-period bands (Archambeau et al, 1969; Sato and Espinosa, 1967; Brune, 1977; Yoshida and Tjusiura, 1975). Such a gradual change does not greatly bias any relative or absolute t* measurements from spectral ratios although to allow for such bias the curves are drawn higher than the t* determined from spectral ratios assuming a constant Q. Details of the regional and frequency dependence of Q under the United States must still be worked out.

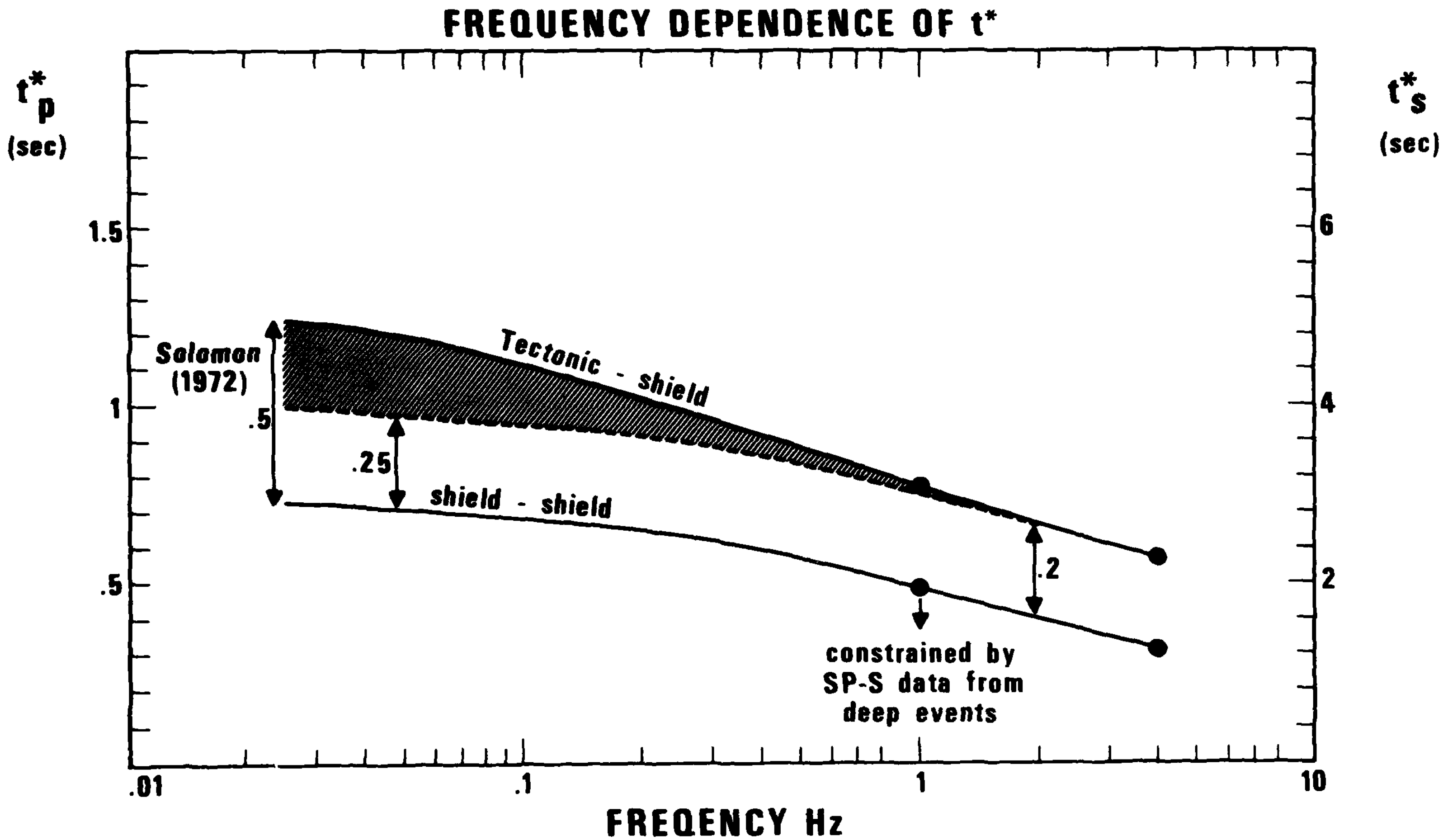

Figure 52 Proposed variation of t^*_p and t^*_s with frequency *for* purely shield type of paths (lower curve) and for a mixed WUS-shield path.

We now discuss briefly some worldwide measurements of Q in the context of frequency dependence and regional variations. Worldwide measurements of Q_{ScS} and mantle waves (Sipkin and Jordan, 1979, 1980; Nakanishi, 1979) show that the regional variation of Q in the long-period band is similar to that observed in the short-period band (Barazangi et al, 1975; Oliver and Isacks, 1967; Solomon, 1972). Attenuation is extremely high behind island arcs in certain areas, under mid-ocean ridges and in tectonic regions. It is low under shields and old ocean basins. This appears to be true throughout the 0.003 to 4 Hz band. In most regions of the Earth, attenuation measurements in the long-period band indicate Q values that would give $t_p^* \sim 1$ and $t_s^* \sim 4$. Most Q models derived from free oscillation data also imply $t_p^* \sim 1$ and $t_s^* \sim 4$ (Anderson and Hart, 1977). On the other hand, observations of high frequency energy in the 3 to 5 Hz range are quite common over a wide variety of teleseismic paths (Asada and Takano, 1963; Takano, 1971; Felix et al, 1971; Noponen, 1975) providing the observations were made using instrumentation peaked at high frequencies and having suitable recording systems. A large number of worldwide Q_p estimates are given by Rivers and Der (1980) indicating $t_p^* \sim 0.5$ for most of the paths studied. Reports of similar observations in the literature are too numerous to quote them all. There is thus a clear conflict between short- and long-period Q measurements that apparently can be resolved only by assuming a frequency dependent Q that doubles within the range of 0.01 to 2 Hz.

CONCLUSIONS

- Large scale regional amplitude anomalies exist for teleseismic P and S waves in the United States. The regional distribution of P and S wave amplitude anomalies is essentially identical, but the range of variation is greater for S waves. The amplitude patterns cannot be explained by crustal amplification, and corrections for crustal amplification leave a pattern of high amplitudes in the north central United States and low amplitudes in the western United States--especially in the southwestern part of the country. The northeastern United States is characterized by moderately depressed amplitude levels.

- The regional amplitude anomalies correlate with spectral changes in both P and S waves; low amplitudes are accompanied by losses in high frequency energy. These spectral changes are quite dramatic in S waves from deep events observed across the United States. The regional variation of teleseismic t* across the United States is of the order of 0.2 seconds for P and about three to four times that for S.

- The existence of these anomalies confirms the hypothesis that the causes of these variations are lateral changes in Q_β in the mantle under the United States.

- The data presented indicate that mantle attenuation is greatest under the southwestern United States, including the Basin and Range province, and it is the least in the shield region of the north central United States. As a whole, the western United States mantle is more attenuating than the mantle under the eastern United States. The northeastern United States appears to be characterized by mantle attenuation greater than that of the shield region but less than that of the Basin and Range province. The SDCS results fit well into the regional pattern outlined.

- The regional variations in Q correlate well with travel-time residuals and variations in the upper mantle LVZ that are derived from surface wave studies that indicate that the LVZ is also a low Q region.

- The amount of high frequency energy in short-period teleseismic P and S waves in the U.S. and worldwide is incompatible with the values of $t_p^* \sim 1$ sec

and $t_s^* \approx 4$ sec derived from long-period attenuation studies and commonly used in synthetic simulations. This appears to indicate that Q is frequency dependent and doubles in value somewhere in the range of 0.01 to 2 Hz.

PART 3

BASIC QUESTIONS RELATED TO THE ANALYSIS OF SHORT-PERIOD DATA AND THE MEASUREMENT OF ATTENUATION IN THE 0.5 TO 5 HZ BAND

Interpretation of short-period data and the determination of Q from such data presents special problems that are of no concern in the long-period band. In the short-period band the scale of inhomogeneities in the crust and the surface topography become comparable to the wavelength, and that introduces complications due to focusing of seismic energy, crustal amplifications of signals and scattering. In addition, the frequency content of signals becomes a critical and sensitive determinant of Q at high frequencies. The tools seismologists use in analyzing signals are the measurement of wave amplitudes and spectra and the matching of waveforms. In the following sections we shall evaluate the relative effects that various factors have on these signal characteristics. We shall discuss the effects of Q on amplitude and spectral measurements and critically evaluate time domain methods of waveform matching. We shall also estimate the possible effects of instrument nonlinearity on Q measurements. As dictated by the diversity of subjects, this part of the report consists of separate sections discussing the above topics. These are referred to when appropriate in the previous parts of this report.

Section A: The Effect of t^* on the Absolute Level of Spectra in the Short-Period Band

For a constant t^* the effect of attenuation is described by the formula

$$A \sim \exp(-\pi f t^*) \tag{1}$$

where A is the wave amplitude, f is frequency and $t^* = T/Q_{av}$. T is travel time and Q_{av} is the average quality factor. Let us examine this function for some values of t_p^* and t_s^* frequently mentioned in the literature. Figure 53 shows a plot of equation (1) for various t_p^*. As the figure shows, $t_p^* = 1$ implies that 4 Hz amplitudes are reduced by a factor of more than 10^4 relative to those at 1 Hz. Thus the assumption of $t_p^* = 1$ rules out the observation of 4 Hz energy in P waves for all practical recording systems presently in use since lower frequencies would saturate the system before 4 Hz energy would be observable.

Now let us consider the consequences of various constant t_s^* on the spectra of S waves, as shown in Figure 54. The factor of 4 increase of t_s^* relative to t_p^* essentially shifts the frequency axis by the same factor to the range around 1 Hz. This effect is even more severe than the value $t_s^* = 3$ sec claimed for deep earthquakes by Burdick (1978) and, in spite of the counter-balancing effect of most short-period instrument responses, effectively rules out any observation of 1 to 2 Hz energy in S waves from deep events.

It appears, however, that 4 Hz energy is routinely observable from P waves even at low Q sites such as OB2NV. This is demonstrated in Figure 55, where we show five typical spectra from this site. Furthermore, 1 to 2 Hz energy is often observed in S waves from deep earthquakes as shown in Figure 50 of part 2 of this report. Observational evidence, therefore, precludes the general use of such high values as $t_p^* \sim 1$ and $t_s^* \sim 4$ since, as we have shown above, such values would depress the higher frequencies by <u>many orders of magnitude</u> and thus render them unobservable.

In view of the fact that <u>spectra of short-period body waves are extremely sensitive to even small variations of Q</u>, we must conclude that studies claiming these high values are incorrect. We shall show in section C that distortion of the shape of the spectra, especially the falloff rate toward high frequencies, is also primarily determined by t^*.

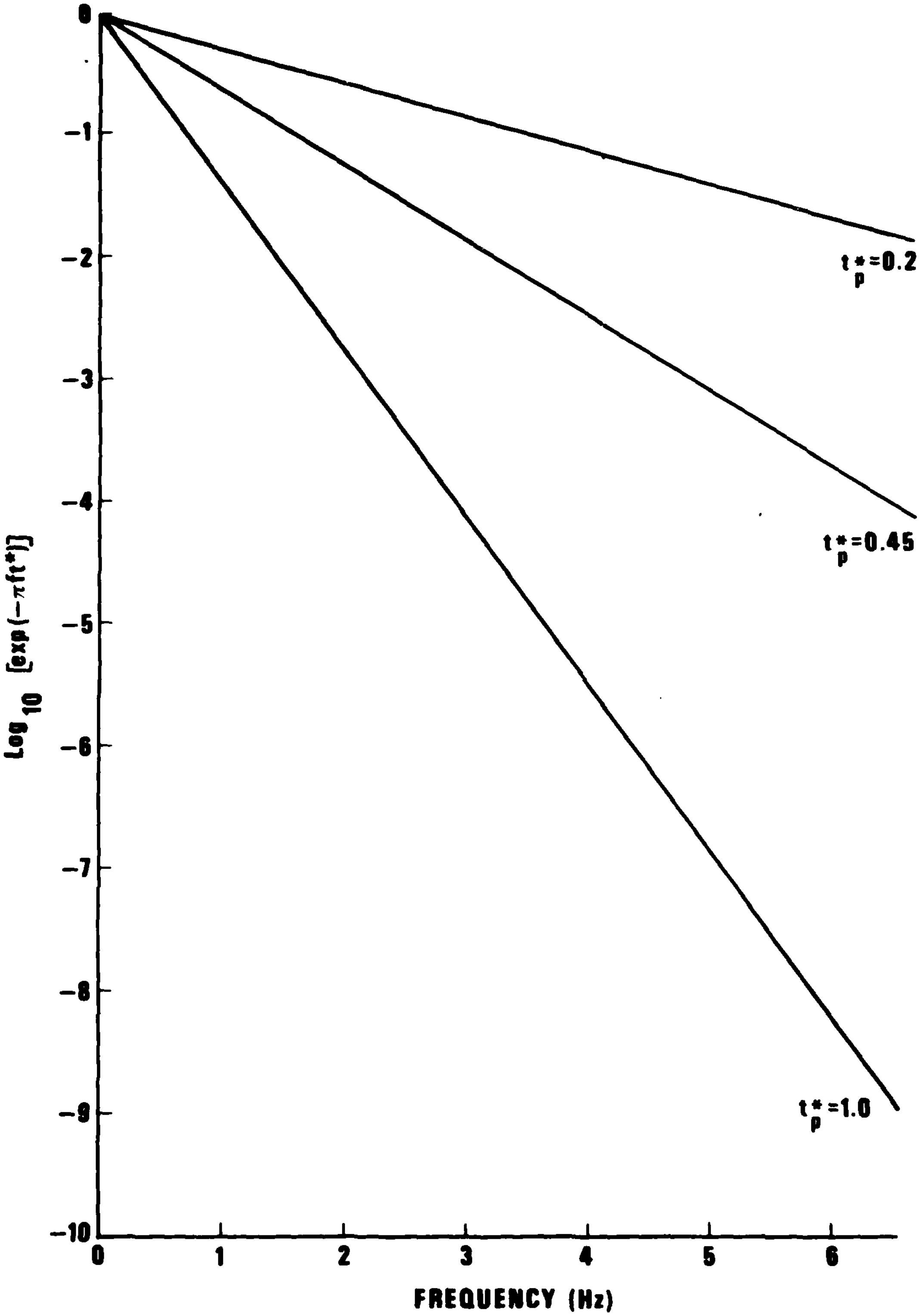

Figure 53   Diminution of P wave amplitudes as a function of frequency for various values of t_p^*.

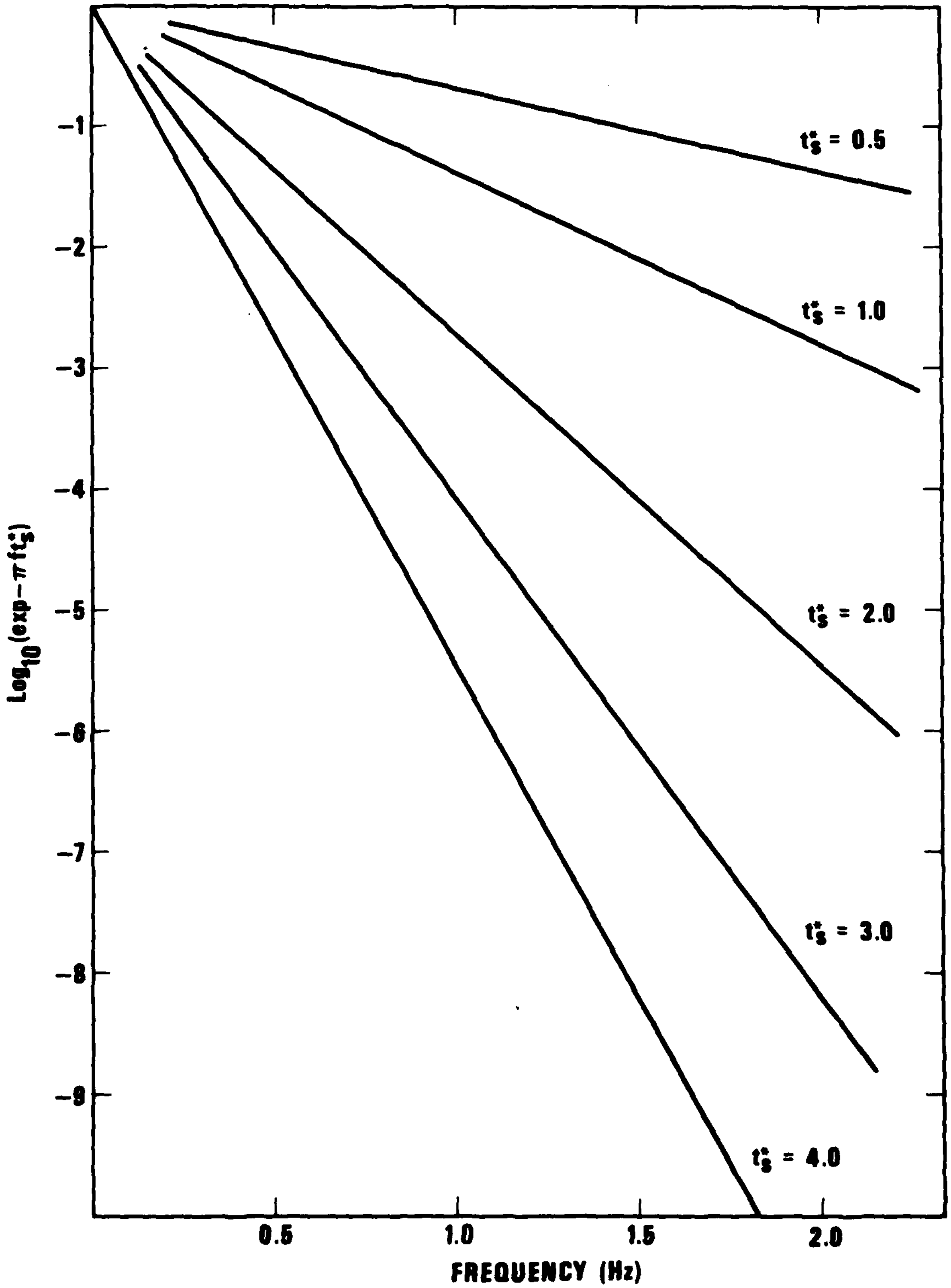

Figure 54 Diminution of S wave amplitudes as a function of frequency for various values of t_s^*.

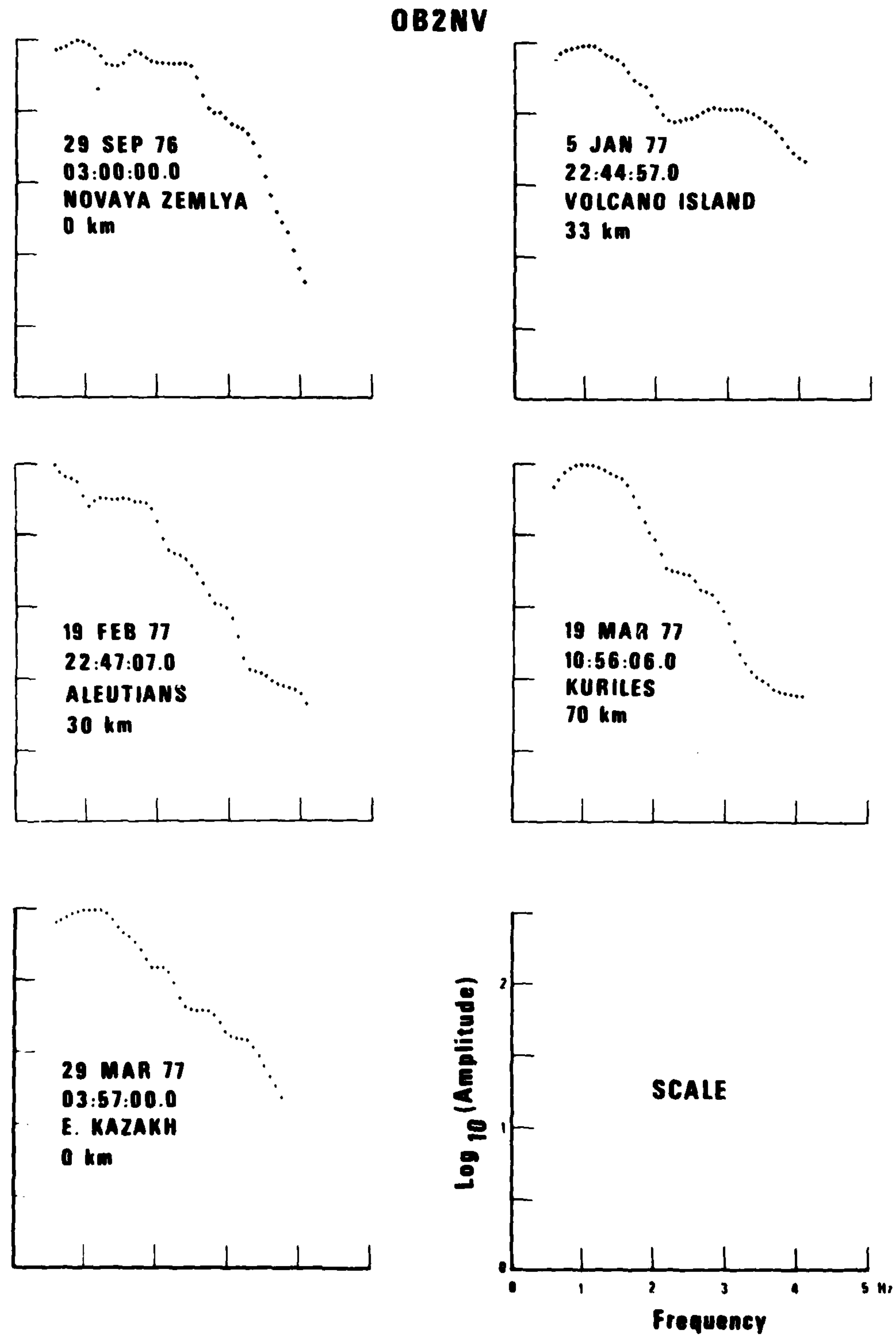

Figure 55 P wave spectra at OB2NV showing significant signal energy at 4 Hz. (All these spectra have a minimum of 3:1 ratio of signal to noise power.)

Section B: Time Domain Manifestations of Varying t_p^* and Their Biasing Effect on the Computation of m_b

The first order visible effects of t* in the time domain are changes in the amplitudes and dominant periods of the body waves affected. These changes can be seen to various degrees, depending on the spectral characteristics of the seismic sources. Figure 56 illustrates this. This figure shows a wide band (left) and a narrow band (right) signal causally filtered by various t*. The narrow band signal, typical of large events used in time domain simulations, is quite insensitive to t_p^*. Note that its waveshape and dominant period change little. The wide band signal, on the other hand, shows a drastic change in general appearance with increasing t_p^*, and the dominant period changes from 0.5 sec to 1.8 sec. The maximum trace amplitude changes by a factor of ten for the wide band signal and by a factor of five for the narrow band signal over the entire range of 0.8 sec in t*. Thus the effect of t* on two time domain representations can be visually quite different, and not all signals will show a major change in dominant period.

When a change of period does occur it will introduce a paradox if m_b is computed from such signals using the standard formula

$$m_b = \log_{10} \frac{A_{tr}}{m(T)\cdot T} + B(\Delta°)$$

where A_{tr} is the trace amplitude, m(T) is the magnification of the instrument at the dominant measured period T, and B is a distance-dependent correction factor. For example, if m_b is computed for the wideband signals associated with $t_p^* = 0$ and $t_p^* = 0.6$ at the left of Figure 56, one obtains the result that m_b is larger for $t_p^* = 0.6$. This is the reverse of what one would expect on physical grounds for high frequency signals. The cause of this is the period dependent instrument (LRSM in this case) factor m(T) that overcorrects due to the implicit assumption that the time domain amplitude measurement is associated with a single frequency. This paradox affects the body wave magnitude and amplitude results whenever the standard m_b procedure is adhered to. For moderate changes of t* the actual reversal of m_b values does not occur, but for wide band signals the m_b procedure tends to de-emphasize the attenuation effect. These considerations caused us to abandon the measure

$$m_a' = \log_{10} \frac{A}{m(T)} + B(\Delta°)$$

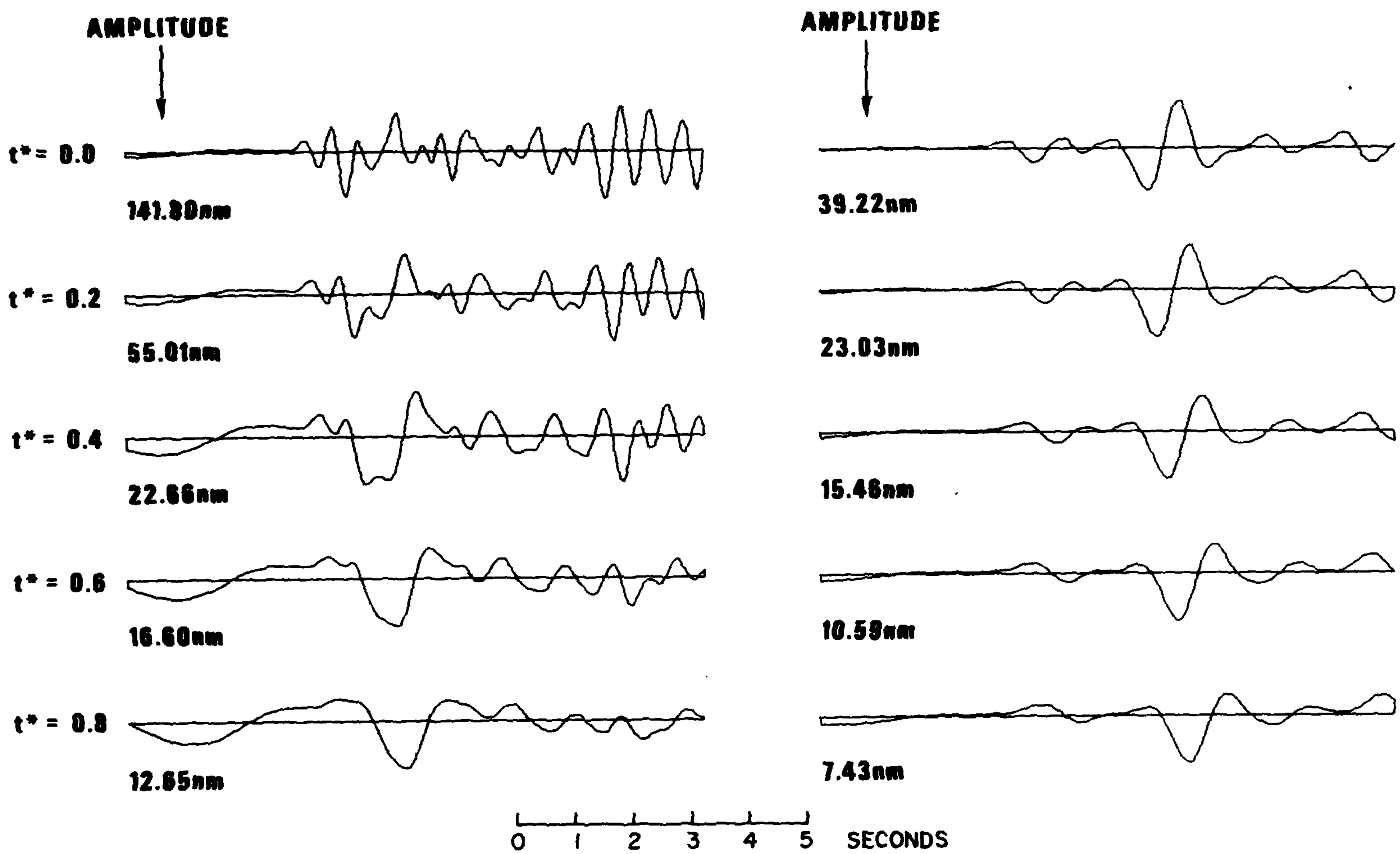

Figure 56 Different manifestations of the same t* on wide band and narrow band signals in the time domain. The wide band signal shows more change in amplitude and dominant period (left) than the narrow band, low frequency signal (right).

used in our previous reports and to substitute trace amplitudes A_{tr} in our discussions.

That this effect is not a hypothetical presupposition but actually does occur is shown in Figure 18 of Part I and the accompanying discussion (page 42 of this report). The fact that the effect of attenuation on m_b critically depends on source spectra makes a search for more meaningful spectral measures of body wave energy necessary.

These remarks were made in order to point out how deceptive purely time domain observations and simulations can be. These problems do not exist, on the other hand, if comparisons are made in the spectral domain. The advent of high quality recording stations with large dynamic ranges makes purely time domain comparisons obsolete, since spectral calculations are more sensitive and reliable indicators of variations of t* with frequency and geographical region. Time domain comparisons fail to utilize the broad band information available in signals recorded with systems of high dynamic range.

Section C: Various Effects on Body Wave Spectral Shapes (Excluding Attenuation)

Taking ratios of observed body wave spectra at various sites in order to measure relative attenuation and taking ratios of observed spectra to model source spectra in order to obtain values of t* are widely used methods in seismology. These techniques utilize the slope of the spectra by fitting straight lines to spectral ratios on a semilogarithmic plot, discarding the absolute amplitude, the high variability of which is unrelated to anelastic attenuation (see Section D of this report). In this section, we shall list and evaluate various effects not related to t* that might seriously bias the results of such studies. We do not claim that these effects on rare occasions cannot be important, but we merely wish to consider their relative importance compared to t*. In Section A, we demonstrated the drastic effect of t* on body wave spectra. In the following, we shall demonstrate that the effect of other factors is much smaller.

The most prominent crustal perturbation of spectral slopes at the source is the effect of surface reflections. Compared to these, the internal reverberations have a small effect (Fuchs, 1966). For earthquakes, this includes the phases pP and sP, the relative amplitudes of which depend on the surface reflection coefficients and the orientation of the source mechanisms. For explosions, the pP and any possible spall phase can affect the spectrum. However, pP and the corresponding clear spectral nulls are mostly absent in the observed seismograms, indicating that either the effective surface reflection coefficient is small (due to either scattering or nonplanar surfaces) or that multipathing effects obscure the surface reflections. In any case, the P wave spectra may be affected by the surface reflections.

It must be pointed out that synthetic results based on elastic flat layer models are often demonstrably not valid. Such calculations generally predict a large free surface reflection. In contrast, the actual data for most explosions do not show such large secondary arrivals, and the spectral minima (nulls) to be expected are weak or not detectable (Der and McElfresh, 1976). It appears that the effective reflection coefficient of the free surface is much less than unity at most places. The physical reasons for

this are that the free surface is not flat and that there exist inhomogeneities close to the source that distort the waveforms. The reduction of effective surface reflection coefficient means that the nulls in the spectra disappear, and the effect on the t* measurements becomes negligible. Furthermore, in the few cases when these nulls are apparent in the data, it is easy to correct the spectra for pP interference and eliminate this factor. For earthquakes, pP and sP both occur with amplitudes varying relative to direct P. In such situations clear spectral nulls usually do not appear. The variants of such simulations may include the spall phase or a pP with the spectra modified by near-surface layers. In any case, none of these models can consistently mimic the effect of anelastic attenuation that consistently suppresses the high frequency end of the spectrum.

Another possible effect on spectra and waveforms is that of multipathing and focusing. Studies of seismic arrivals at arrays reveal that secondary arrivals of energy delayed in time and (often) deflected in the direction of arrival are present in most teleseismic body waves (Mack, 1969). Some of these can be deterministically modeled by an uneven Moho or deep structures in the mantle (Berteussen et al, 1975; Capon, 1974; Capon and Berteussen, 1974; Christofferson, 1975; Dahle, 1975; Dahle et al, 1975; Haddon and Husebye, 1978; Hadley, 1979; Chang and von Seggern, 1980 and many others) or by the theory of waves in homogeneous random media. The effect of identical multipath arrivals with random amplitudes at random times is to introduce fluctuations in the body wave spectra, but it cannot introduce a consistent decrease of amplitudes with frequency similar to the factor $\exp(-\pi f t^*)$.

To assess the effect of such random variations we computed spectral ratios between individual sensor pairs belonging to various subarrays at NORSAR for ten events. Since we do not believe that t* actually changes across the array, the observed fluctuations in the slopes of the spectral ratios between 0.5 to 4 Hz must reflect the random effect due to multipathing. Figure 57 shows the histogram of slopes of spectral ratios expressed in terms of apparent t*. The standard deviation of this population is 0.06 sec, showing that the spectral ratios are quite stable and the scatter is quite small. Using the empirical formula $\Delta m_b \approx 1.35\ \Delta t^*$ (Der et al, 1979), this would translate into $\Delta m_b \sim 0.08$. The actual variation of

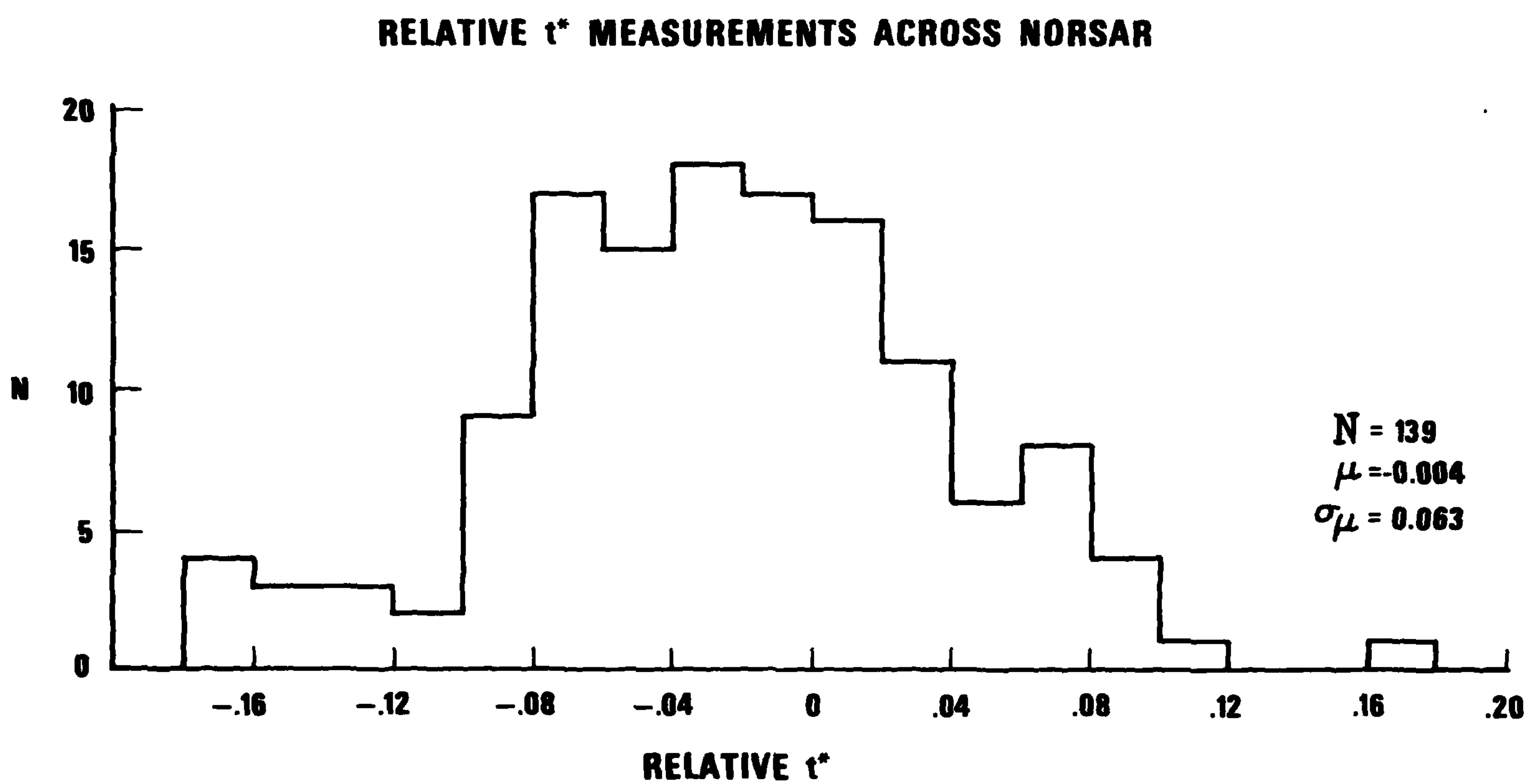

Figure 57 Relative t* between subarrays at NORSAR for ten teleseismic events. The histogram shows that the scatter of Δt^* compared to that of amplitudes is small (σ = 0.06 sec). *This illustrates the relative* stability of spectral measurements.

Δm_b measured directly is about 0.4 magnitude units at NORSAR. This demonstrates that spectral slopes are more stable than signal amplitudes. Large variations of amplitudes across LASA were also reported by Chang and von Seggern (1980). These are generally distance and azimuth dependent.

The receiver crust is another factor to consider when evaluating studies that involve spectral ratios. The effect of the receiver crust manifests itself in the increase of the peak amplitude of the signal and the prolongation of wavetrains (ringing) at sites with thick low-velocity sedimentary cover. In the frequency domain, the slopes of amplitude responses of most crustal models are flat when fitted with least squares lines over the 0.5 to 4.0 Hz range. Over shorter frequency ranges these slopes will be greater. In general the presence of the receiver crust does not seriously affect the spectral ratios.

A few remarks need to be made about detailed slopes of crustal responses. In computing synthetic seismograms, specific crustal structures are routinely used to model the crustal reverberations in detail in the time domain. This, on the surface, conveys an impression of precision. Experience with short-period spectral work indicates, however, that the details of such calculations both in the time and frequency domains cannot be trusted. An indication of this is that for short-period waves Phinney's (1964) radial to vertical spectral ratio method never worked, the probable reason being that at most places the near-surface geology is horizontally heterogeneous giving different spectral ratios in various directions. The dominant effect of the crust is associated with acoustic impedence changes due to variations in the near-surface materials (Der et al, 1979) that causes considerable changes in the amplitude levels while leaving the gross spectral slopes unaffected.

Another objection often voiced against spectral calculations is that scattered high frequency energy in the coda can significantly bias the t* measurements. First of all, it must be pointed out that while scattering near the receiver may apparently enhance high frequencies by some mechanism such as P conversion to Rayleigh waves, such scattering cannot generate high frequency energy. Any such signal energy observed must have come from the source. The simplest test to assess the relative contribution of the P-wave coda to the high frequency part of the spectra is band pass filtering

of P-wavetrains. Figures 58 to 60 show some examples of this. In filtering these traces, a set of causal band pass filters with a flat response in the band indicated on the figures and a 24 dB/octave falloff outside the band were used. Algorithms for causal digital filtering are described in many textbooks (Oppenheim and Schafer 1975 for example). In most of the cases shown, the envelopes of the wavetrains are essentially similar in all bands. This indicates that our use of a 9-second signal window is not only representative of the signal spectra, but it also has the beneficial effect that the spectra are more stable than those computed from shorter windows. Any enhancement of high frequency energy in the coda is not comparable in effect to that of even small changes of t*. Thus, the claim that the scattering effect is significant has no basis in fact.

Finally, an effect that can significantly alter both the observed relative amplitudes and the spectra is directionality of earthquake sources. Although considerable work has been done in the long-period band to model such effects, and fair success has been achieved in modeling waveforms, not all of the problems have been solved to date. Modeling of unequal P and S corner frequencies is still deficient (Molnar et al, 1973; Hanks, 1980), and source time functions are over-simplified. In the short-period band, simulation of waveforms is largely unsuccessful for earthquakes and doubtful for explosions. It is likely that short-period radiation patterns are extremely complex for large and moderate sized earthquakes. While at long-periods, with wavelengths comparable to the fault length, an earthquake may resemble a double couple source with some directionality component added, this is much less likely to be true in the short-period band where the details of source motion in space and time play a more significant role. We conclude that modeling of large earthquakes in the 0.5 to 5 Hz frequency range is beyond the state-of-the-art since no one has done it successfully. In the absence of modeling capability one has to rely on averaging over many events to reduce the source directionality effects in order to estimate path characteristics. Fortunately, all seismic regions contain enough variability in source mechanisms to make this possible.

We tabulate the main conclusions of this section in Table VII.

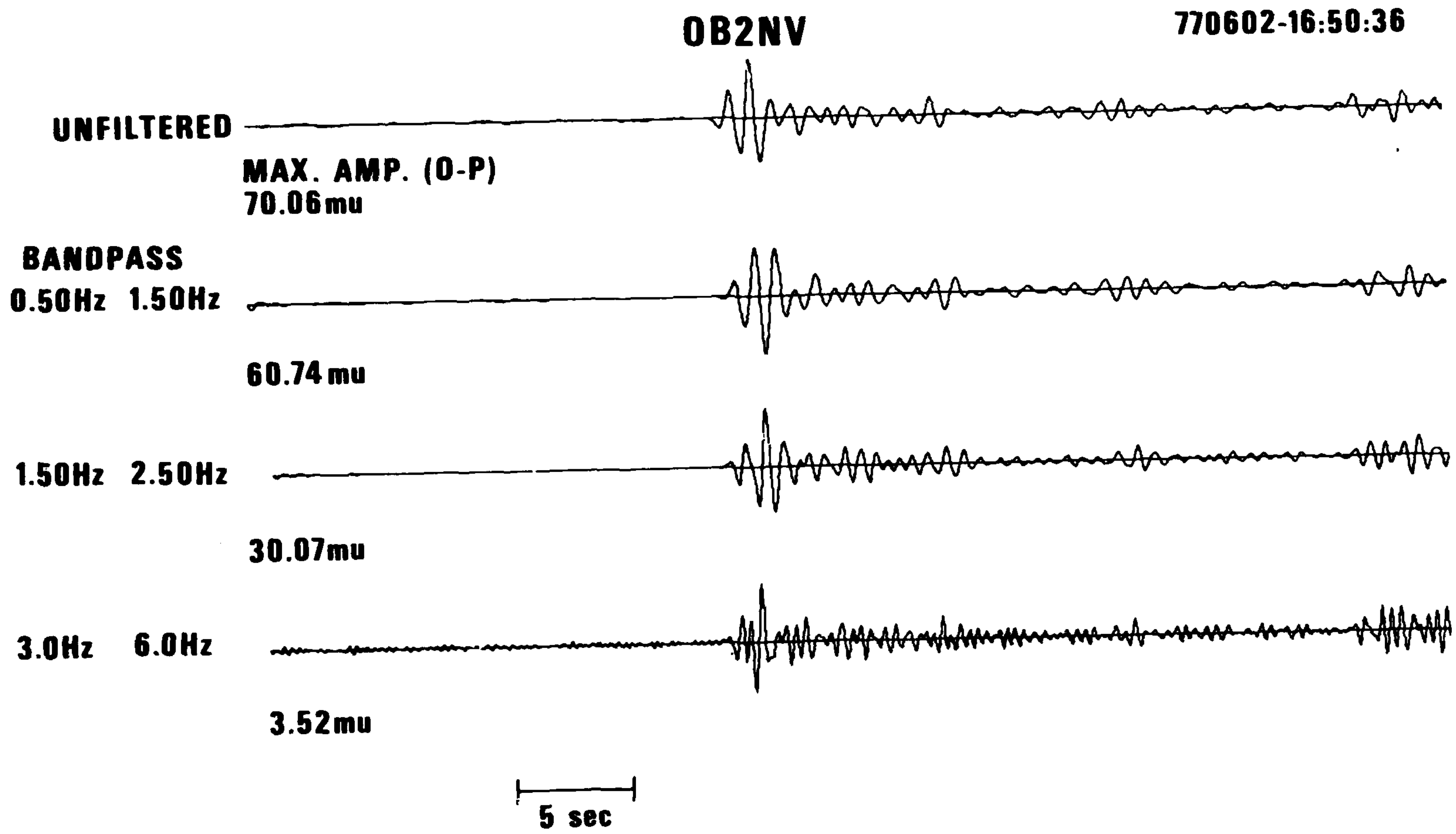

Figure 58 Band pass filtered P wave seismograms at the NTS station OB2NV. The figures show that the frequency content in P waves does not change much in the first 10 sec of the signal. Therefore taking spectra of the first 9 sec of P does not introduce a significant bias in t* relative to that computed from shorter windows.

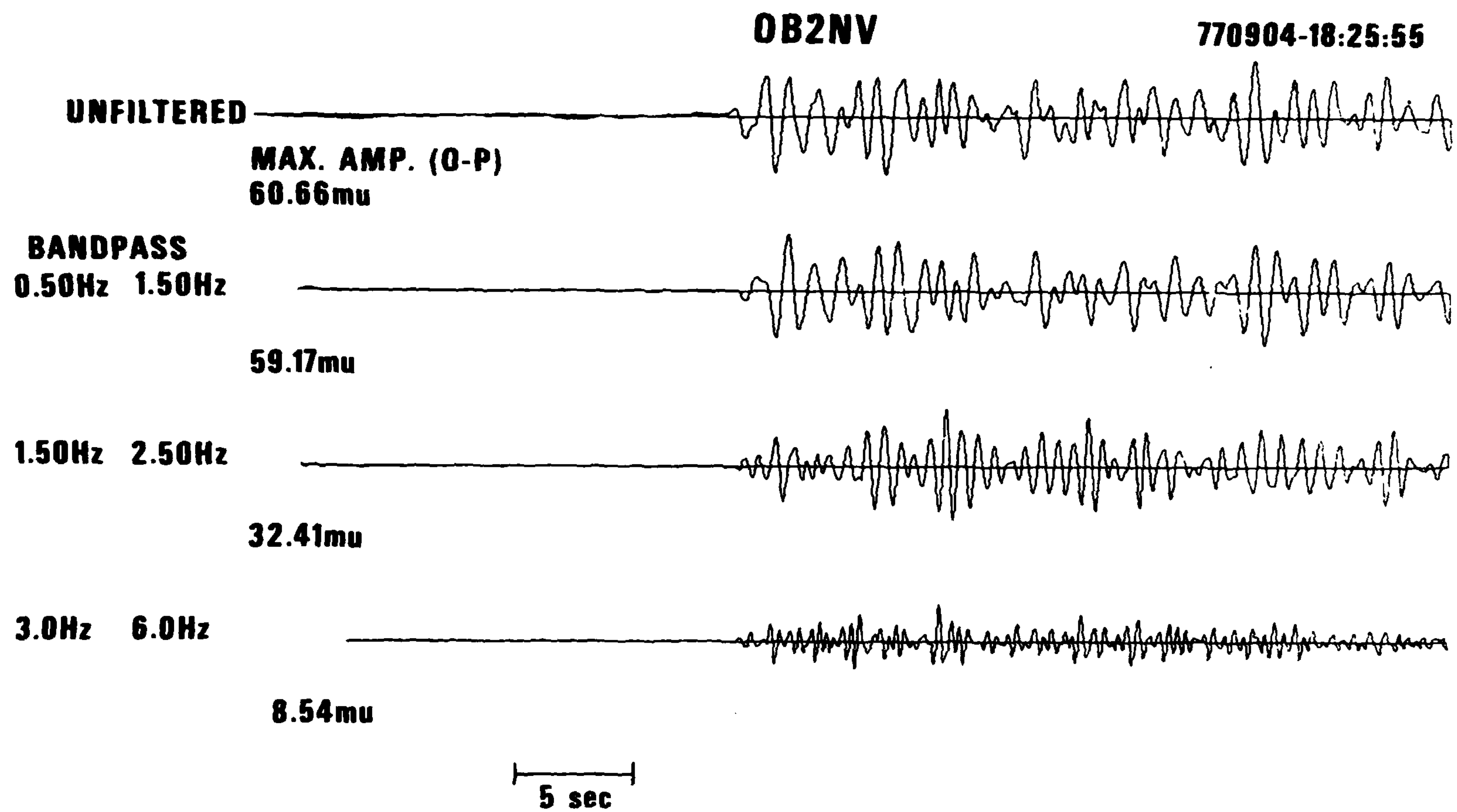

Figure 59 Band pass filtered P wave seismograms at the NTS station OB2NV. The figures show that the frequency content in P waves does not change much in the first 10 sec of the signal. Therefore taking spectra of the first 9 sec of P does not introduce a significant bias in the relative to that computed from shorter windows.

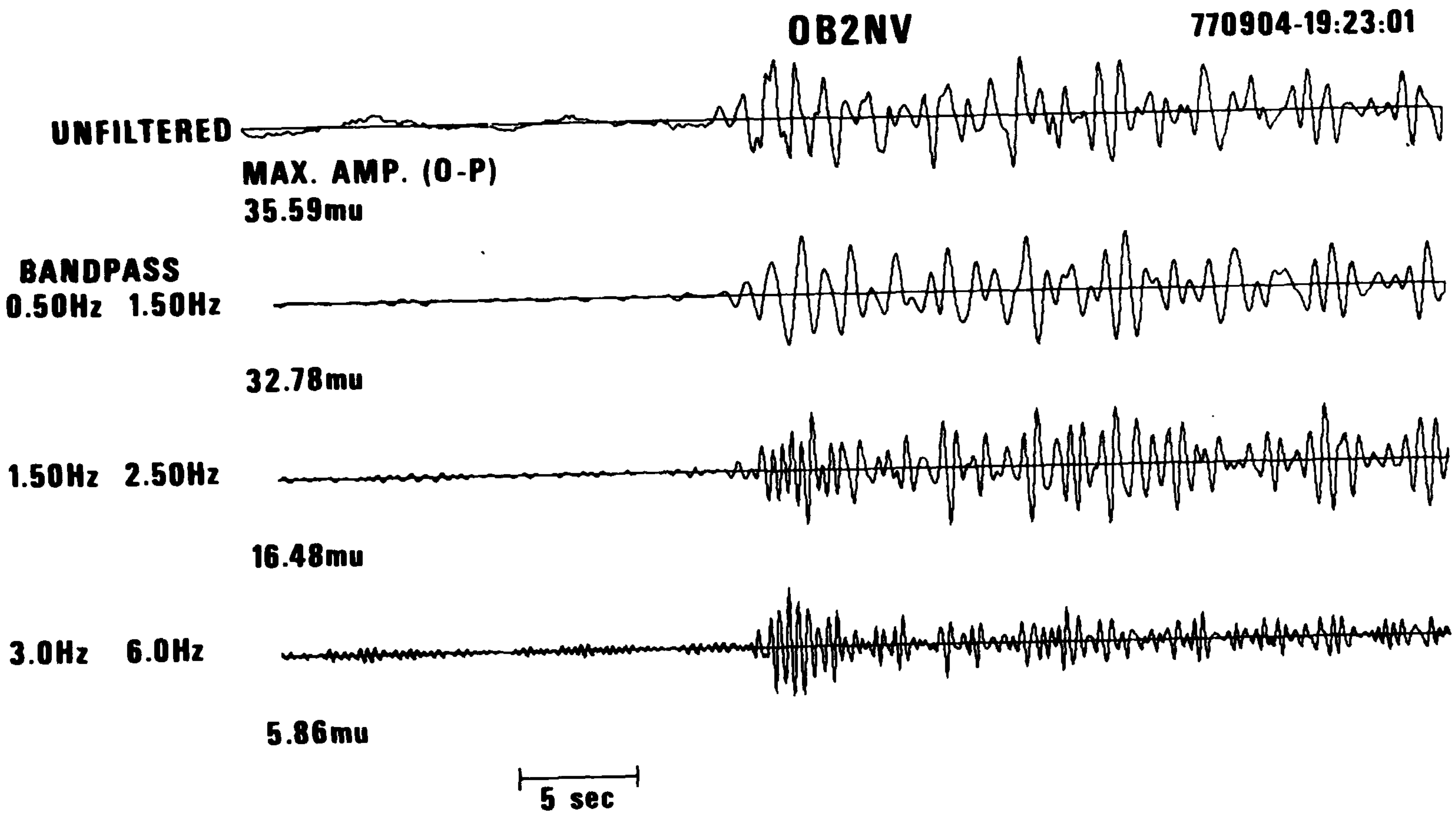

Figure 60 Band pass filtered P wave seismograms at the NTS station OB2NV. The figures show that the frequency content in P waves does not change much in the first 10 sec of the signal. Therefore taking spectra of the first 9 sec of P does not introduce a significant bias in t* relative to that computed from shorter windows.

TABLE VII

The Effect of Various Factors on Spectral Slopes
(falloff rates with frequency disregarding absolute amplitudes)

Factor	Properties	Relative Importance
Anelastic attenuation	Causes a falloff of spectra $\exp(-\pi f t^*)$ with frequency	First order large effect (several orders of magnitude at high frequency end of spectrum)
Crustal amplification	Distorts spectrum	Rarely it can cause an error in t* up to .1 sec on sediments, negligible at most hard rock sites
Surface reflections (pP, sP, etc)	Introduce nulls in the spectra	If detectable it can be easily corrected for. Negligible in comparison to t* effect if surface reflection coefficient is considerably less than unity
Scattering	May enhance high frequencies	Negligible in comparison to t*
Multipathing	Changes spectral slope	Negligible in most cases (Wald's theorem)
Source directivity	Changes spectra with azimuth,. Poorly understood in the short-period band.	Can be large for earthquakes, can be averaged but with large sets of events, negligible for pure explosions
Near surface or receiver focusing	May change spectrum	Probably negligible (It cannot suppress or enhance high frequencies similarly to t*)

Section D: Perturbing Effects Influencing Body Wave Amplitudes (Excluding Attenuation)

Some discussion of amplitudes was presented in the previous section where perturbations of the spectra were compared to those of the signal amplitudes as a result of various extraneous factors. In this section, we shall discuss these factors in more detail and at the same time critically examine the proposition that averaged P-wave amplitude levels at any location can be used as the sole measure of attenuation in the mantle underlying that location.

We have examined the effect of varying constant t* on amplitude, and it appears that the measured amplitude differential due to t* variations is dependent on the source spectrum. It is larger for high frequency signals and smaller for low frequency signals. This in itself makes it difficult to relate t* directly to amplitude residuals, although it can be done either empirically (Der et al, 1979) or by synthetic simulation.

The effect of the source crust can be reliably modeled if the source is known to be linear elastic and if the crust is a laterally homogeneous flat layered medium. In most cases, neither criterion is satisfied. The effect of an unknown effective surface reflection coefficient on the time domain amplitudes can be quite severe, and small variations in the reflection coefficient and the source depth can cause large changes in amplitude. This can be avoided by picking amplitudes prior to the arrival of surface reflections.

The receiver crust has a large effect on amplitudes. At sites located on thick unconsolidated sediments the body wave amplitudes can be several times larger than at sites on solid rock, and this amplification is more severe for S waves. The regional geology under the average seismic station is usually not known well enough to model such effects with sufficient accuracy, although crustal corrections computed by flat layered models achieved a statistically significant reduction of variance in average amplitude measurements for a larger set of stations (Der et al, 1979). This does not mean, however, that corrections computed for individual stations are accurate. This is not surprising since, even if the site is carefully surveyed with refraction profiles or borehole measurements, the shear velocity-depth distribution is usually unknown.

Let us consider now the effect of randomness of the medi⌟ around the sources and receivers. Lateral horizontal inhomogeneities around sources appear to be the cause of broad regional systematic variations of amplitude that can be associated with the source locations. The existence of such effects has been verified by several studies (Hadley, 1979; Butler, 1979), and this implies that in order to measure t* on amplitudes this random effect must be removed by averaging measurements from many source regions.

The effects of inhomogeneities close to the receiver are also well documented. These effects, well known to researchers involved with analysis of array data, manifest themselves as large azimuthally dependent relative amplitude variations between even closely situated sites. The relative amplitude patterns are repeatable for groups even at similar azimuths and distances, and even the intersite modifications of waveforms are repeatable and describable in terms of transfer functions (Filson and Frasier, 1972; Chang and von Seggern, 1980; Butler and Ruff, 1980; Lay et al, 1979). These phenomena were recognized early in array work and have been analyzed extensively using various models (Berteussen et al, 1975; Capon, 1974; Capon and Berteussen, 1974; Christofferson, 1975; Dahle, 1975; Dahle et al, 1975; Haddon and Husebye, 1978; Chang and von Seggern, 1980 and many others).

The existence of focusing phenomena is also consistent with the picture of the crust provided by the COCORP studies (Schilt et al, 1978), which clearly demonstrate the widespread occurrence of lateral inhomogeneities in the crust. It is not unusual for sensors spaced only a few km apart to show fairly large amplitude ratios. This hardly comes as a surprise since the geology is complex enough at most locations and such effects due to focusing and defocusing of seismic waves are to be expected. It was found by Chang and von Seggern (1980) that at NORSAR such anomalies tend to average out to zero if amplitude measurements at a large range of distances and azimuths are taken. However, this cannot be done at most stations that operate for limited lengths of time due to the non-random geographical distribution of sources. This means that such effects cannot always be removed. Besides, there is no guarantee that the average of such site anomalies approaches zero in all cases, even if equal weights are given to a wide range of azimuths and distances.

The expected consequence of the near source and receiver inhomogeneities is that magnitude levels, even at closely spaced stations, may exhibit differences that cannot be explained and that P-wave magnitude anomalies at individual stations cannot be used by themselves to determine the degree of attenuation in the mantle under any location. The attached Table VIII summarizes the effect of various factors influencing trace amplitudes. Most of these are of the first order.

TABLE VIII

The Effect of Various Factors on Absolute Signal Amplitudes

Factor	Properties	Relative Importance
Anelastic Attenuation	Changes signal amplitudes	First order, but less for low frequency ($f < 1$ Hz) signals
Crustal Amplification	Amplifies signals	Large, comparable in size to that of t* variations to be expected. Can be estimated to some degree
Surface Reflections	Change amplitude	Can be estimated but time domain estimation is nonunique
Scattering	Unknown	Unknown
Multipathing	Unknown	Unknown, can be large
Source Directionality	Unknown	Few demonstrated examples in the short-period band, no adequate methods exist to estimate its importance in the short-period band. Can be removed by averaging over many events
Near Source or Receiver Focusing	Changes signal amplitudes	Larger than that of t* variations in question. Great obstacle to estimation of yields. Absolute level of change cannot be established at most locations

Section E: A Critique of Time Domain Methods

A large number of papers in recent literature employ time domain matching of synthetic waveforms with observed waveforms, during which attenuation (t*) is estimated in a deterministic multiparametric scheme. The common approach begins with the source by computing some fault model or an RDP, then continues the computation of the waveforms through deterministic models of the crust, upper mantle, receiver crust and instrument response. Several free parameters, including t*, are adjusted in the process to obtain the "best" visual fit in the time domain. Those values thus obtained are assumed to constitute a valid description of the source and path properties.

This method achieved fair-to-good success in modeling seismograms in the long-period band; consequently, researchers were emboldened to apply the technique to short-period data. Unfortunately, the methodology as applied thus far has so many flaws that most of the results should be declared invalid in the short-period band and doubtful in the long-period band. We summarize some general criticisms below (more specific objections are given elsewhere in this report):

1. The quality of the matching of two time domain waveforms in the short-period band primarily depends on the low frequency end of the spectrum for large events, thus ignoring the high frequencies. Waveforms for such events are extremely insensitive to t* (Der and McElfresh, 1980) and cannot reliably measure variations in t* of the order of a few tenths of a second (See Figure 56).

2. The practitioners of this method create the overall impression that the mantle, crust and source parameters are well known and precisely controlled in their simulations. We submit that this is not the case. Short-period data are characterized by large spatial fluctuations in waveshapes, amplitudes and spectra brought about by small scale inhomogeneities in the earth. Simple parameterization cannot adequately describe these fluctuations.

3. The high variability and scatter inherent in short-period data requires statistical techniques for the extraction of meaningful information. In particular, analysis of variance of the parameters in the problem, such as t* in our case, should be considered. In much of the synthetic work no

statistical evaluation of the stability of results is given, and the data sets fitted in the short-period band are often unreasonably small.

4. There is a tendency to extrapolate successful theoretical models to the short-period band or to use theoretically defined but restrictive models for simulating the data. The validity of each type of theoretical model should be independently demonstrated using carefully chosen data sets. Only models that have clearly been validated should be used in fitting parameters. Unfortunately, this is frequently not the case. For example, the Haskell type of propagating fault model that cannot adequately simulate the frequently observed inequality of P and S corner frequencies is used uncritically in many simulations (Molnar et al, 1969; Hanks, 1980). Another example: fitting Minster's absorption band model to data (Lay and Helmberger, 1980) unnecessarily restricts the class of obtainable solutions.

5. As far as attenuation studies are concerned, a considerable amount of detail in time domain modeling is irrelevant. Since we are interested primarily in the spectral content of the source versus that of the observed waveform, details of time domain waveforms depending mostly on phase properties of spectra are of no interest. Simple limiting arguments with regard to spectra are sufficient to put reasonable bounds on attenuation.

6. Time domain methods often end up with the same $t^*_p \sim 1$ and $t^*_s \sim 4$ in the long-period band for travel paths involving a variety of upper mantle structures. This conflicts with the observed regional variations of surface wave attenuation (Nakanishi, 1979; Mills, 1978; Lee and Solomon, 1979). It also appears that if one considers only the attenuation results obtained by <u>not</u> using the time domain methodology, these correlate well with the regional patterns of surface wave and short-period body wave attenuation in the studies just quoted. It seems, therefore, that results of time domain studies with regard to attenuation do not make sense in the broad geophysical context, which indicates that the methodology is not suitable for measuring attenuation.

7. In the short-period band, the t^*_p obtained by time domain methods is often demonstrably wrong (pages 105 to 107 of this report). Furthermore, t^* reported by various authors for similar paths using the time domain methods

differ greatly. For teleseismic paths to NTS, Burdick and Helmberger (1979), Hadley (1979), and Helmberger (1973) use t_p^* values of 1.0, 1.3 and 0.7 respectively. Besides the fact that two of these values are clearly impossible (pages 93 and 108 of this report), the range of variation is such that, if true, they would imply an m_b variation of about 0.67. Since the regional magnitude variations we are attempting to explain are of the order of 0.2 to 0.3, such instability in the results cannot be tolerated, and time domain methods as practiced today thus have no place in magnitude-yield studies. We must point out that spectral methods yield short-period t* that are repeatable and quite close in value, as reported by several authors quoted in the literature and in this report.

8. A variant of time domain waveform matching is the use of synthetics in both the short- and long-period bands (Burdick, 1978; Hadley, 1979). This is, in effect, a variation of the spectral ratio method. Although this approach has a potential for usefulness, no conclusive results have been produced thus far that can be applied to the short-period band. Burdick's results for short-period S are outside the frequency range of interest (the dominant frequency of these short-period S waves is 0.25 Hz). Hadley's result of $t_p^* \sim 1.3$ is not unique. Der and Blandford (1979) showed that plausible modifications to more reasonable values of insufficiently constrained parameters in Hadley's simulations can reduce t* to 0.6. It appears again that the time domain amplitudes in these simulations are too sensitive to the various unconstrained factors.

Summarizing this section, it appears that although time domain methods have contributed a great deal to our knowledge of earth structure and, to a lesser degree, of source mechanisms, they are not suitable for studying attenuation unless radical changes are made in the methodology. For the reasons listed above and in the discussions elsewhere in this report, we shall disregard all results with respect to attenuation produced by such methods.

Section F: The Possibility of Generation of High Frequencies in the Recorded Signal by Instrument Nonlinearity

In a recent paper Sacks (1980) suggested that the high frequency energy observed in short-period seismograms may not be actual signal energy but rather an artifact caused by nonlinear distortion in the system when a high amplitude but low frequency P or S wave excites it. This, if true for the LRSM, SDCS, or LASA-NORSAR systems, would be quite serious, especially with regard to attenuation studies. Although it seems implausible that work over the course of 20 years has overlooked such an effect, and although recording non-linearities are routinely recognized and avoided, we have re-examined this question and concluded that with such instrumentation there is no serious possibility of such effects.

We have analyzed some constant amplitude harmonic (constant current, equivalent to constant ground acceleration) calibration signals that were routinely run for the LRSM system at high equivalent ground motion amplitude levels. These high levels resulted in the FM analog high-gain recording system being close to the nonlinear (clipping) levels. The selected station was MNNV for 31 August 1963. We computed amplitude spectra on the calibrations as well as on the preceding noise background. Some examples of these are shown in Figures 61 to 64. The calibration frequencies range from 0.33 to 5.0 Hz. These calibrations were run routinely on the last day of each month at every LRSM station, and the resulting system response was plotted in the logs. The signal spectra all show clear peaks at the center frequency of the calibrations, and the calibration spectra quickly descend to noise level. Side lobes above noise level are visible only for 1.0 and 1.5 Hz. These signals are less than a factor of two below the visible FM clipping levels. In fact, the 1.0 and 1.5 Hz spectra had to be computed from the radial channels because the vertical channels (for these frequencies only) did clip. Inspection of the film, however, shows no clipping. This proves that the clipping is in the FM system and not in the instrument. Clipping of this sort is routinely recognized, and the standard procedure in these cases is to use the low gain recording channels.

Another approach to the question of non-linearity is to observe signals having equal levels of 1 Hz but different levels of 5 Hz energy. Such observations would seem to rule out the possibility that the 5 Hz energy was

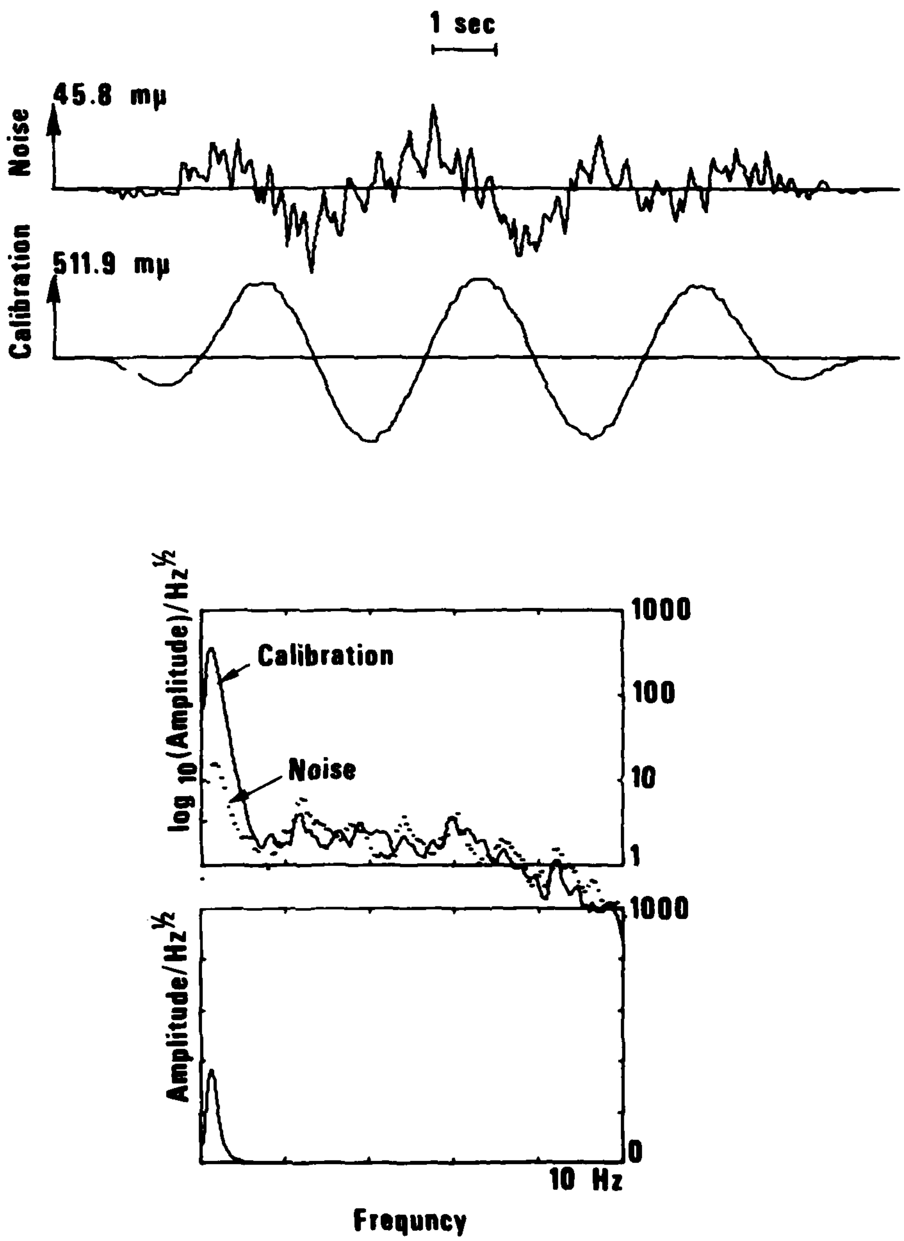

Figure 61 Spectra of steady state calibration signals at LRSM stations. The spectra are dominated by the frequency of the input signal with only minor contamination by harmonics presumably generated by nonlinearity.

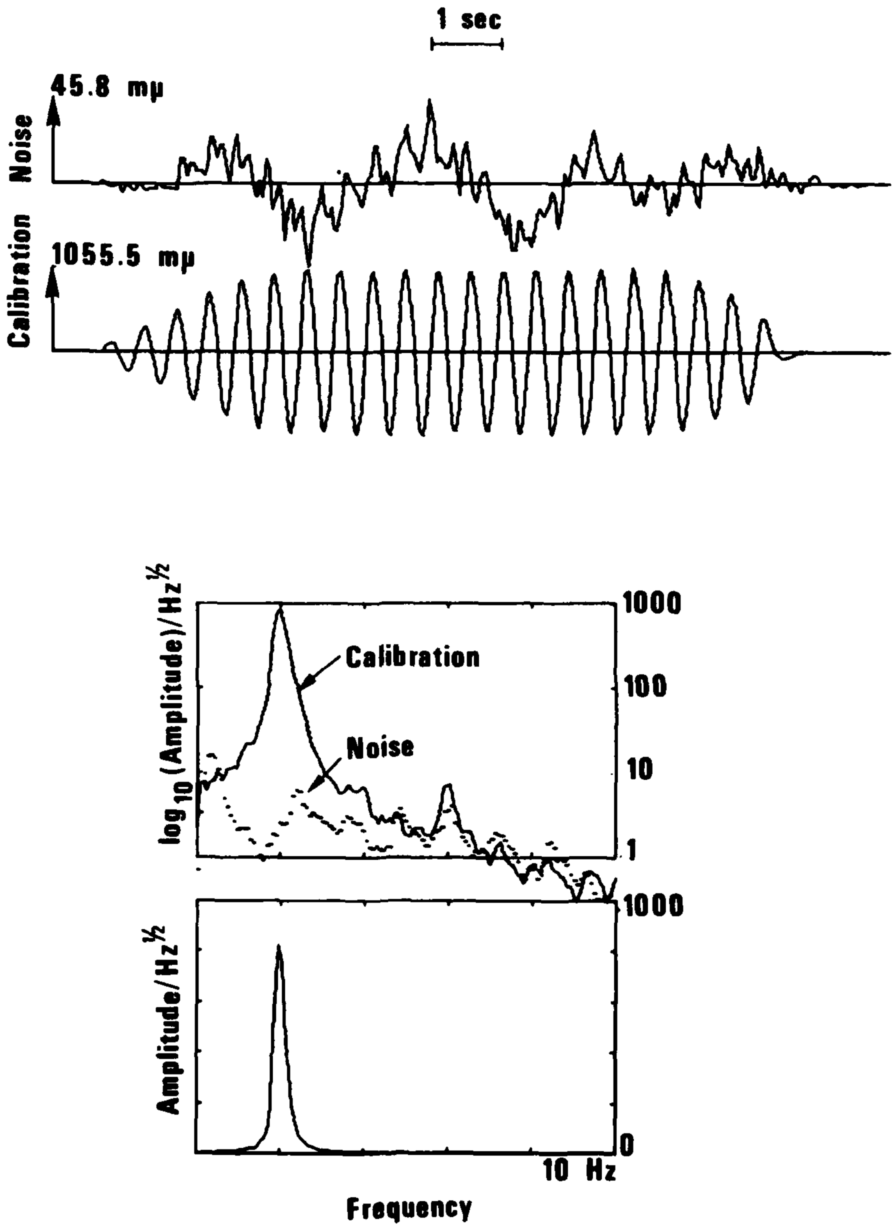

Figure 62 Spectra of steady state calibration signals at LRSM stations. The spectra are dominated by the frequency of the input signal with only minor contamination by harmonics presumably generated by nonlinearity.

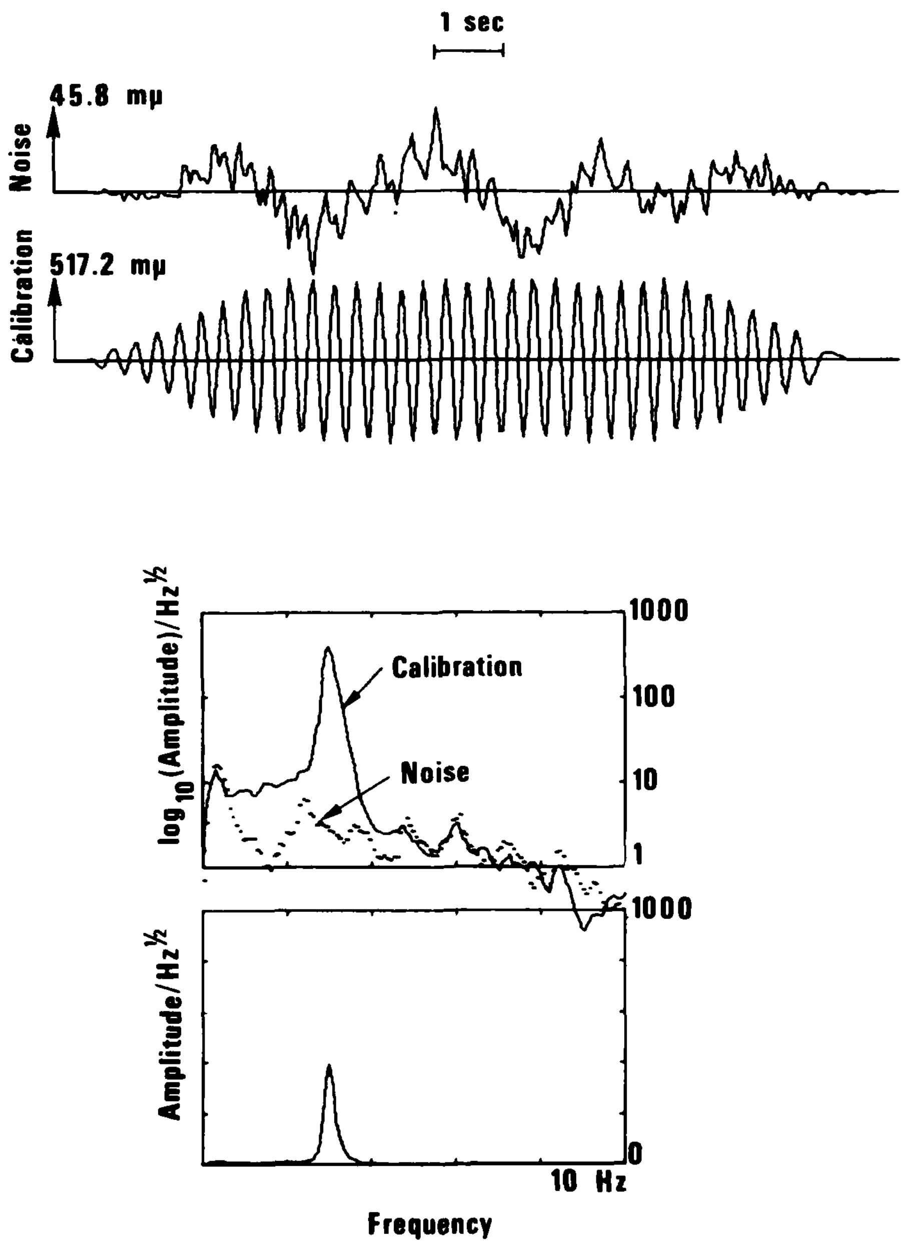

Figure 63 Spectra of steady state calibration signals at LRSM stations. The spectra are dominated by the frequency of the input signal with only minor contamination by harmonics presumably generated by nonlinearity.

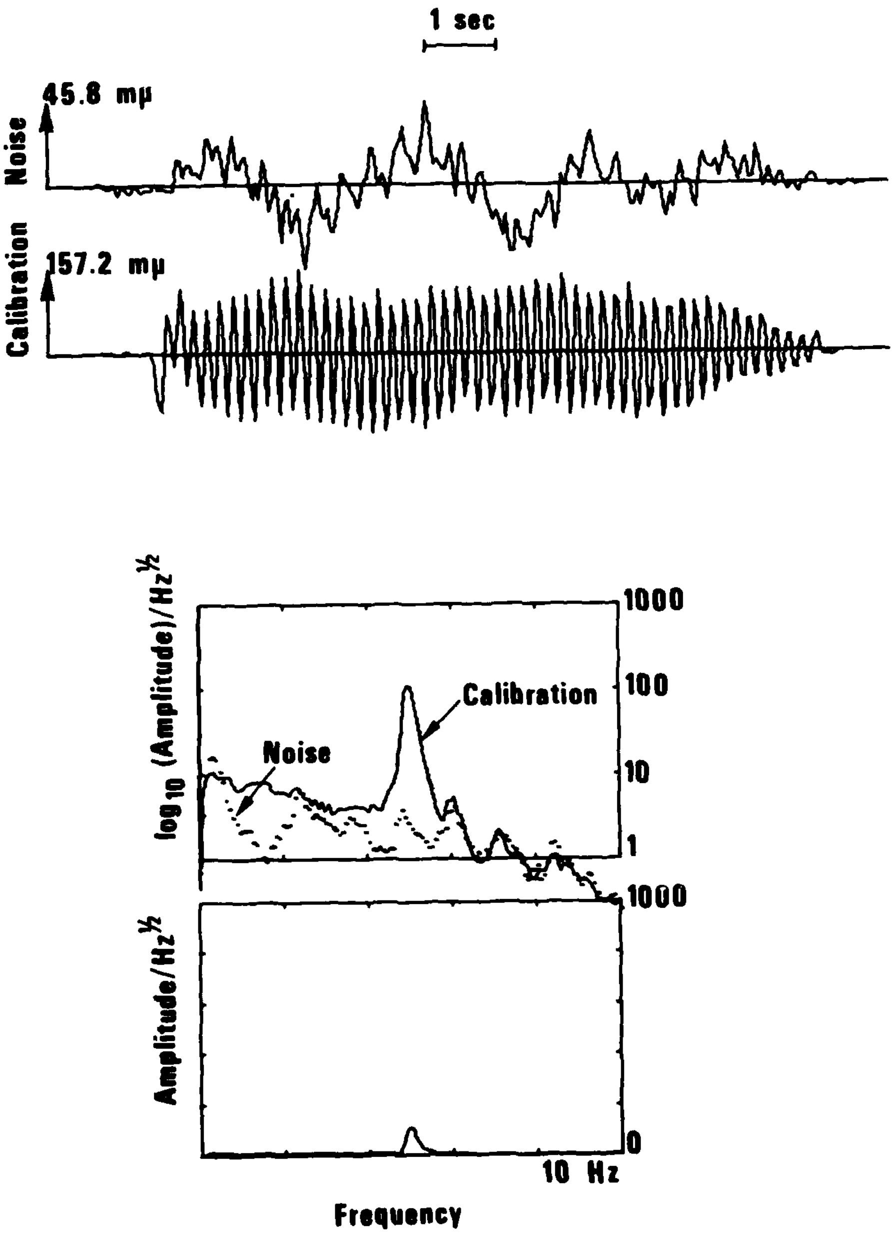

Figure 64 Spectra of steady state calibration signals at LRSM stations. The spectra are dominated by the frequency of the input signal with only minor contamination by harmonics presumably generated by nonlinearity.

created by the 1 Hz energy. Figures 65 and 66 are two events as recorded at the center element of the C3 subarray of NORSAR. These signals show no indication of clipping or nonlinear distortion. Low t* values are based on spectra such as that seen in Figure 65. The spectra as seen through the system response are nearly flat so that a small non-linear side lobe cannot account for the high frequency energy. Compare Figures 65 and 66 which have about equal 1 Hz levels but which differ at 5 Hz by a factor of about 30 in amplitude. These differences in spectra cannot be associated with non-linearity.

Additional evidence is offered by close-in observations of NTS explosions with the same instrumentation. Figure 67 shows recordings at KNUT and MNNV, at distances of about 200 and 300 km from explosions of 1100 kt (BENHAM) down to perhaps less than 1 kt (BUTEO). Note that the smaller BUTEO event has the higher frequency and the recorded amplitude for BUTEO is equivalent to a large-magnitude earthquake teleseismically, while the BENHAM amplitude through the system response is 100 times larger. Figure 68 shows the raw unsmoothed spectra. For BUTEO the spectrum is nearly flat. We see directly that in BENHAM as compared to BUTEO the high frequencies are dramatically absent above 3 Hz. Also, for frequencies below about 7 Hz the amplitude spectra are down only about 30 dB even for BENHAM. In Figure 69 we show the spectral ratio of these two events. Note that it is in excellent agreement with cube root scaling theory, ranging from a ratio of over 1000 at low frequencies to a ratio of about 10 at 5 Hz. For these events the FM systems do not clip because resistors are added in the circuit as necessary to keep the voltage in range. This does show that the basic seismometer system must be linear to much higher amplitude levels than those encountered in teleseismic practice.

Many of our arguments are also based on short-period S waves, such as those shown in Figures 43-49 of the first section of this report. First of all, the most severe clipping could not cause a change in the dominant periods of the signals unless the nonlinearity is clearly seen (by reversing the peaks). Even this becomes impossible if one considers the instrument gains in these figures, if the S amplitudes are equal everywhere as some claim. The instruments with the highest gains, thus having the highest

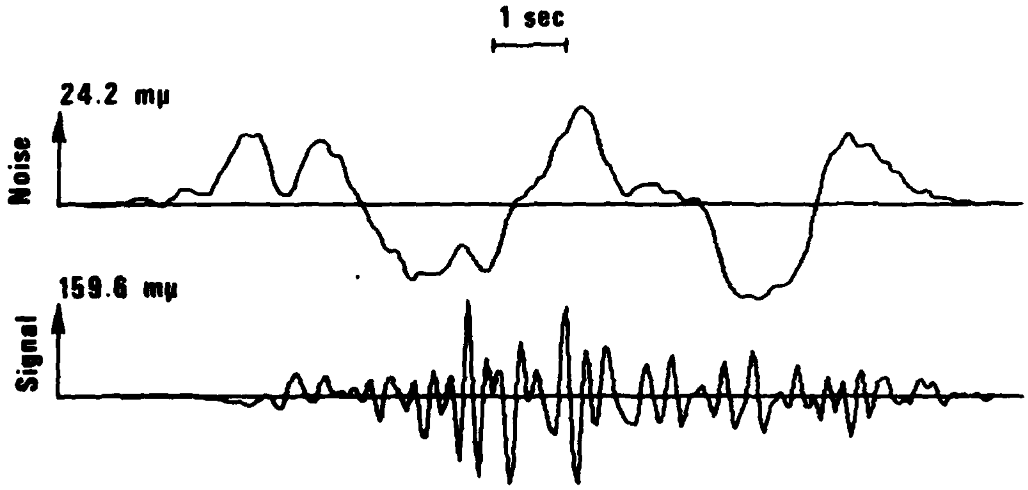

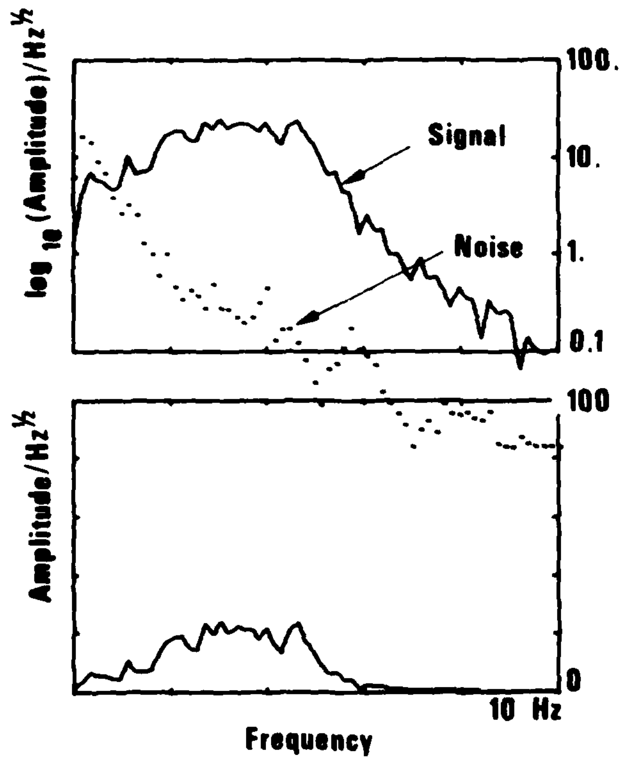

Figure 65,66 Spectra of two events at the C3 subarray of NORSAR. For the same amplitude level at 1 Hz, the level at 5 Hz differs considerably. If nonlinearity were the source of 5 Hz energy for the various events these levels should be the same.

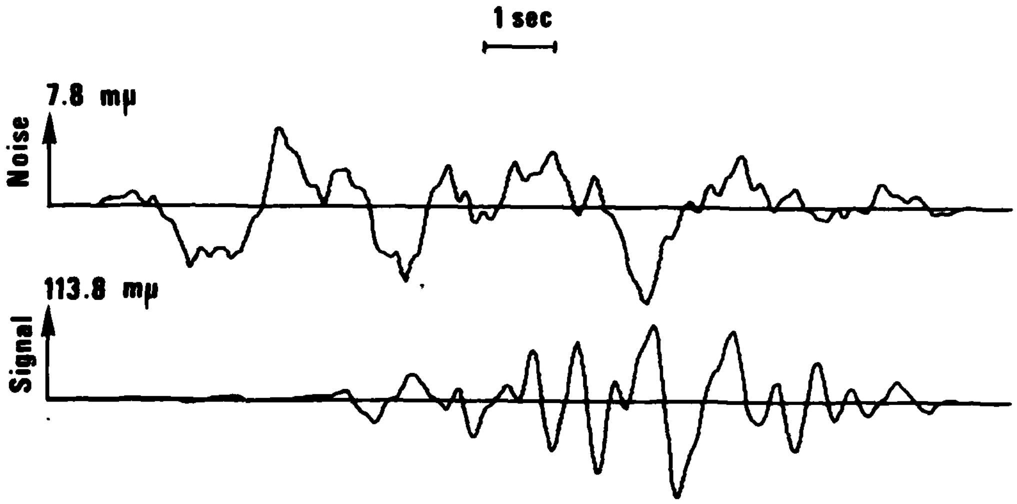

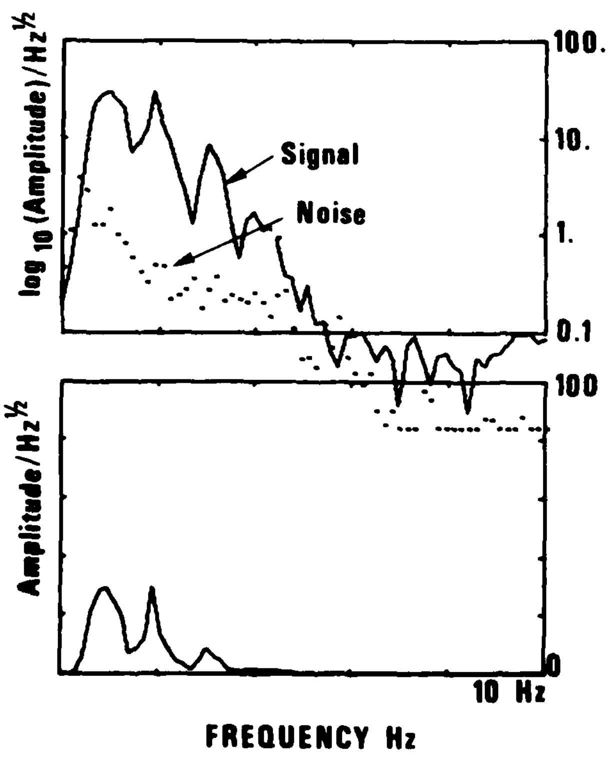

Figure 65,66 Spectra of two events at the C3 subarray of NORSAR. For the same amplitude level at 1 Hz, the level at 5 Hz differs considerably. If nonlinearity were the source of 5 Hz energy for the various events these levels should be the same.

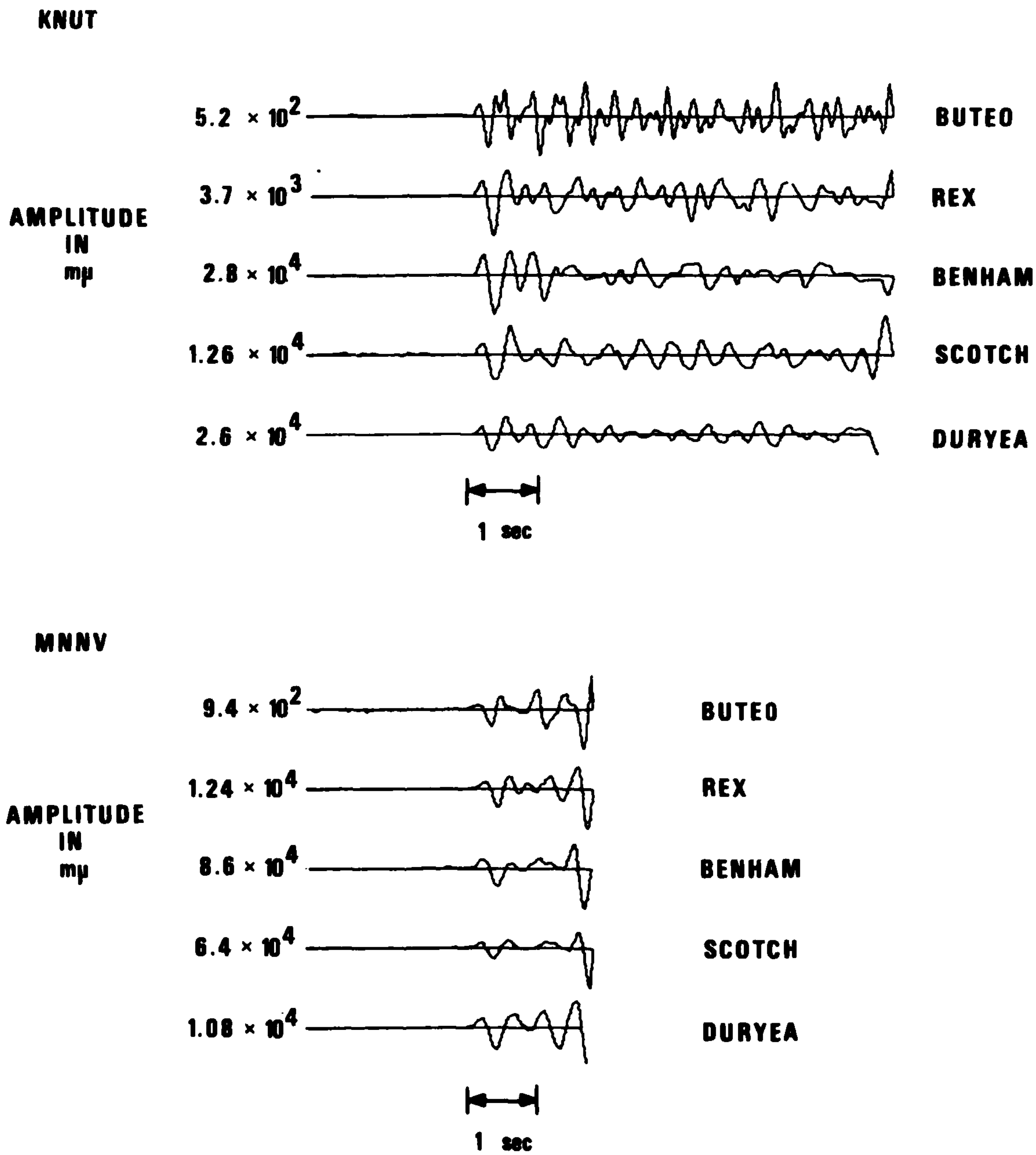

Figure 67 NTS explosions recorded at KNUT and MNNV.

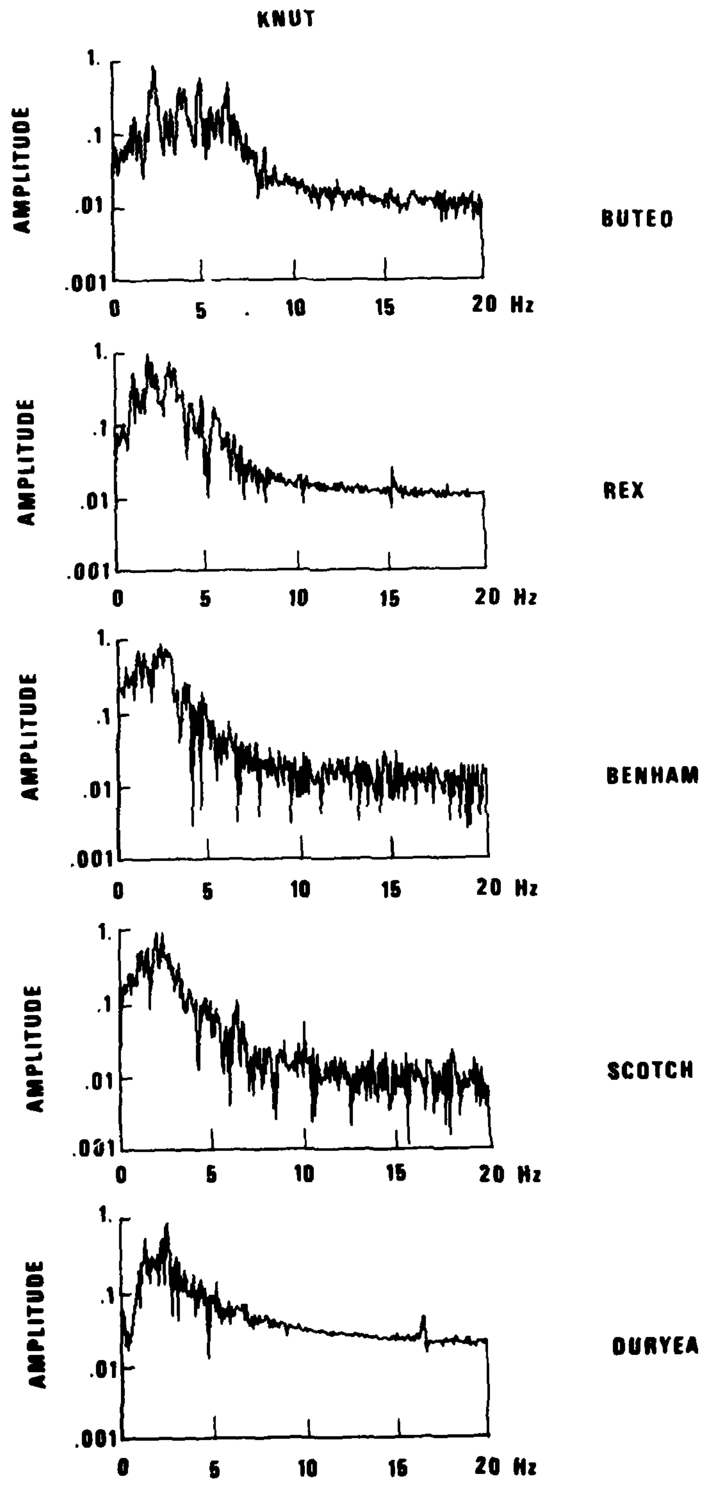

Figure 68 Log amplitude spectra at KNUT for the time windows shown in Figure 67 for BUTEO, REX, BENHAM, SCOTCH, and DURYEA.

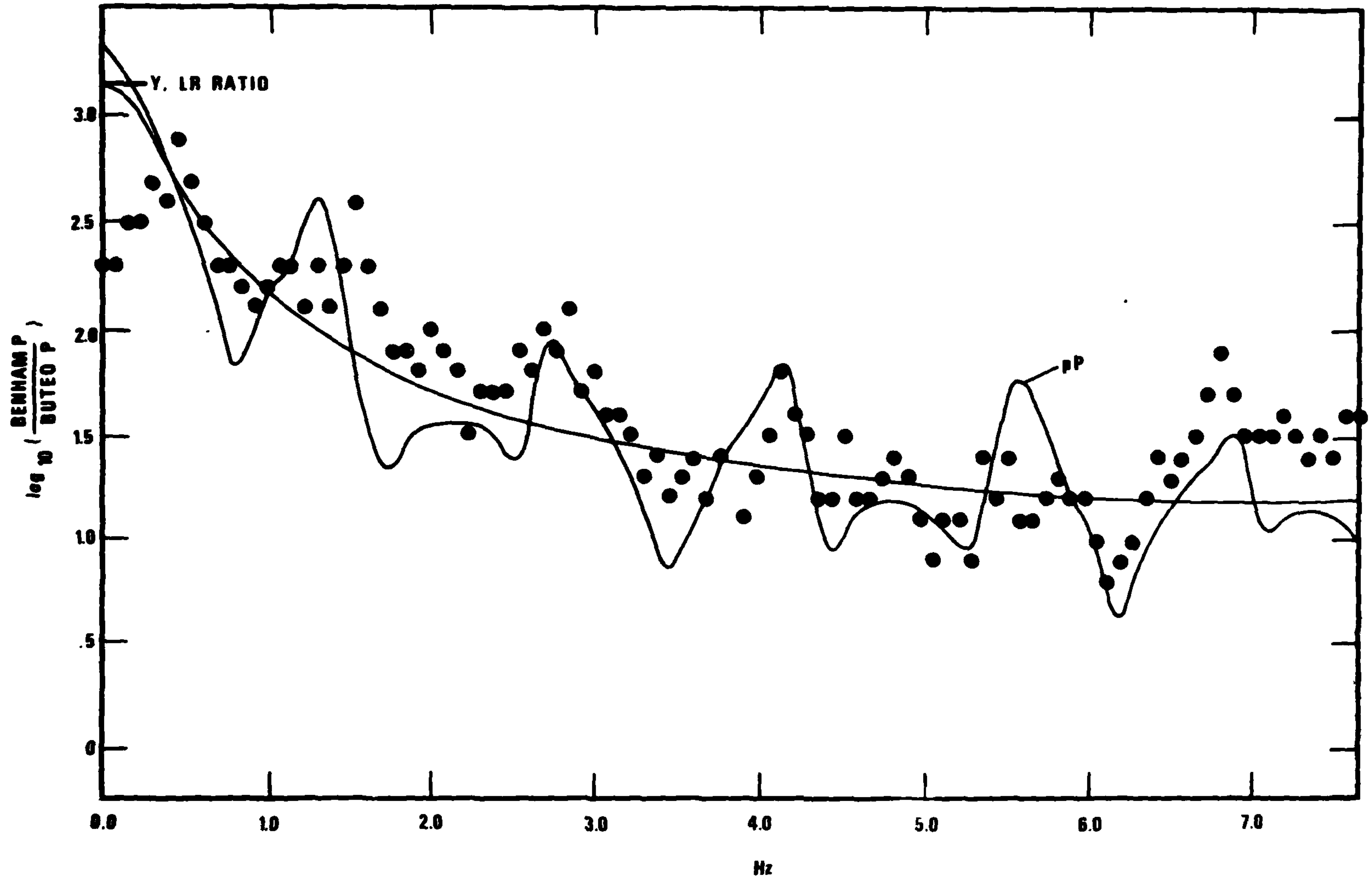

Figure 69 Dots give the observed spectral ratio BENHAM/BUTEO. The theoretical spectral ratios appropriate to the tuff model, B=0, k_o=12 have been superimposed, with and without the effects of pP included.

potential to generate extraneous high frequencies by nonlinearity, should show the shortest S wave periods and the greatest high frequency content. However, in reality the reverse is true. Due to the offsetting inequalities of S wave amplitudes and gains the signals are recorded at roughly the same recording levels on the magnetic tape, and no clipping is detectable.

Since the mechanical system of seismograms is highly linear, most non-linearity comes from the FM tape. (As noted, the calibration signals did not clip on the film that bypassed the FM recording.) Both high gain (in the SWUS) and low gain (in the EUS) should have about the same amount of distortion, yet the frequency contents are visibly unequal.

Additional data is available from the tests performed in the manufacturing plant. As an example, we choose the model 4681 seismograph consisting of the "small Benioff" vertical seismometer and a phototube amplifer. This system was widely used in the LRSM program. Figure 70 from TR-63-55 illustrates the linearity of the recorded amplitude versus input shake table displacement at 1 Hz. The small deviations seen could as well be due to inaccuracies in the shake table driving motors as to the seismometer. This shake table is still in use in Garland. The largest signals were nearly 10 cm peak-to-peak on the graphic display, and no other frequencies were visible even though a 2 mm ripple could have been seen. This places the non-linearity at 700 microns more than 34 dB down. 700 microns is, of course, much larger than any teleseismic signal. Figure 71 shows a complete frequency response for this instrument on a shake table. Between the plotted points there is not much room for a spurious resonance. Other raw data plots of phase and amplitude response from shake tables in TR-59-14 have about two times as many points and still show no resonances. The responses are generally taken at an input displacement of 9.2 microns which is much larger at these frequencies than most teleseismic signals.

We have also examined the develocorder recordings of single TFO elements of an 03 September 1967 event off the coast of Peru. This is shown in Figure 72. The large LR waves with periods of 14 seconds as seen on the short-period instrument arrive around 21:42 and are on scale, with an amplitude of 15 cm peak-to-peak on the viewer. There is also visible 3 to 5 Hz energy from local sources of noise with amplitudes of 1 mm peak-to-peak.

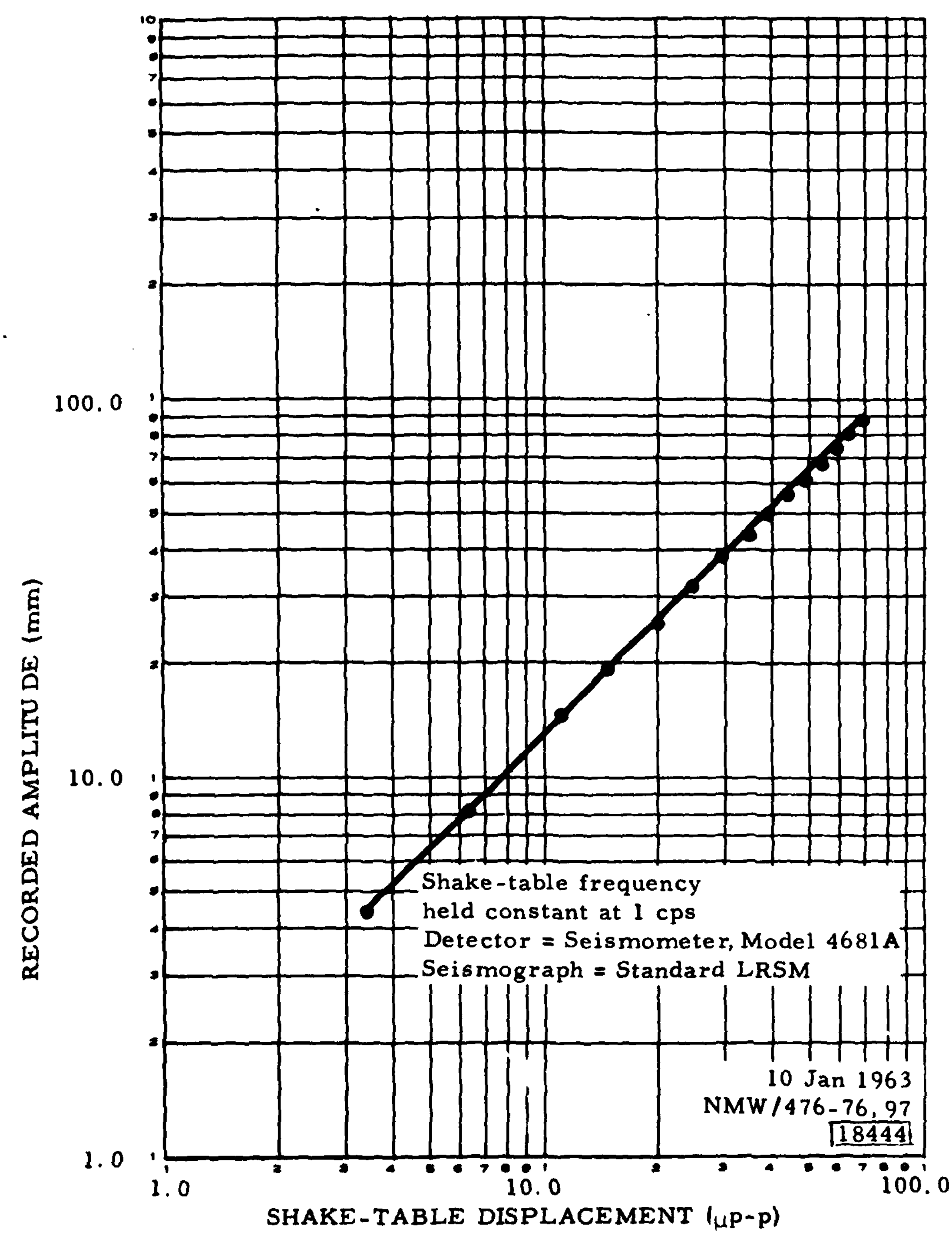

Figure 70 Shake table test results on a "small Benioff" short-period instrument.

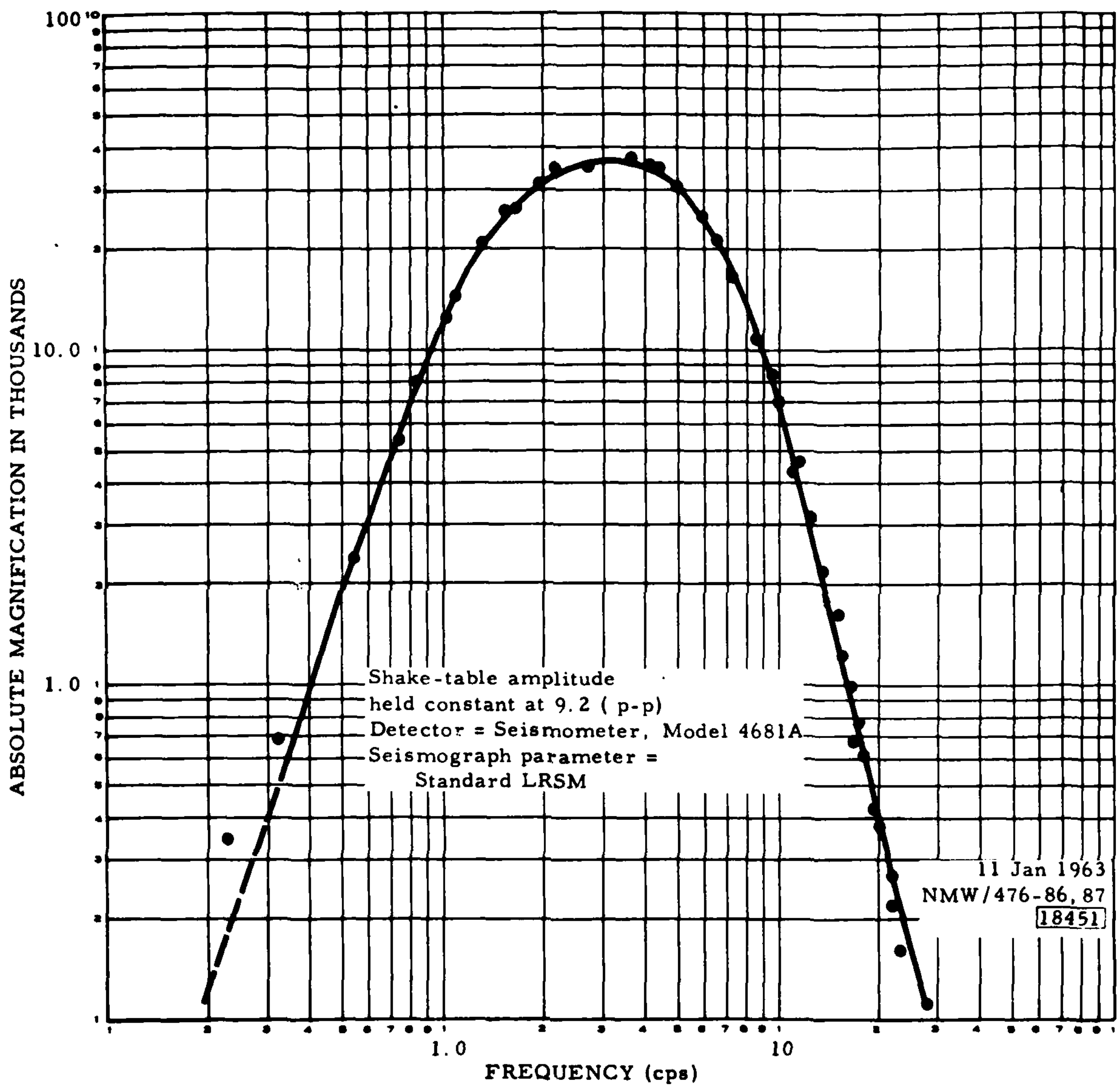

Figure 71 Complete steady state shake table test of the "small Benioff" instrument.

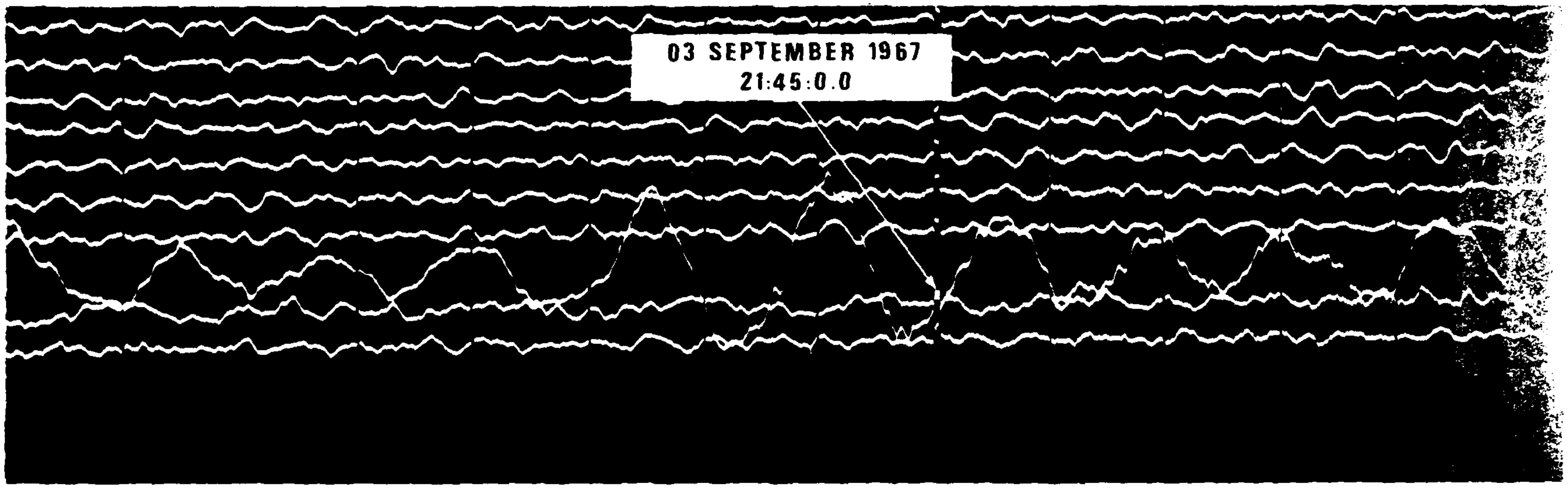

Figure 72 Long-period Rayleigh waves as seen through the short-period *instrument* at TFO. In spite of the high amplitude of the wave exciting the instrument no increase in the high frequency content of the seismogram is seen, and the frequency of the input wave dominates.

This same energy is visible before the arrival of P. In this case, there is no apparent non-linearity of the seismograph system to a level of 44 dB. In terms of non-linearity with respect to ground displacement, taking account of the differing magnifications at 14 seconds and 3 Hz, the linearity is on the order of 44 + 80 = 124 dB. In this case, the LR also includes a non-vertical component of motion that eliminates the possibility of cross talk between components. By analogy, the short-period ($f \sim 1$ Hz) oscillations in the S waves shown in Figure 72 cannot be caused by, say, a huge 0.1 Hz S wave exciting the seismometer. Such a signal would still be dominantly 0.1 Hz in frequency as seen through the short-period instruments.

Further arguments showing that nonlinearity is not an admissible explanation for low t* and that high frequencies are an integral part of a real signal can be summarized as follows:

a) The high frequency content of short-period signals recorded on identical systems varies with geological-geophysical setting.

b) High frequency signals show other meaningful geophysical detail such as surface reflections of pP, sP and travel time triplications.

c) The high frequency content of P and S waves differs for comparable long or intermediate frequency amplitudes.

d) The high frequency content of signals in identical geophysical station settings is of the same order of magnitude regardless of component, make and construction of the instruments and systems, including hydrophones.

In summary, while we do not disagree with Sacks that nonlinearity can, and actually does, introduce harmonics at levels far below that of the predominant signal, we must conclude that in our analyses such effects do not play a significant role.

IMPLICATIONS OF THE FINDINGS OF THIS REPORT TO YIELD ESTIMATION

There is some confusion about the interpretation of the results of the SDCS experiment and the significance of the "discrepancy" between the m_b bias estimates derived from amplitude measurements and spectral differences. There also appears to be a strong feeling, shared by some, that the m_b bias derived from amplitudes is the true measure of bias due to attenuation because of "reciprocity". We feel that a few clarifying remarks are necessary. Beginning with the reciprocity theorem as it is stated in textbooks, we can say that, if we have a dilatational source and a dilatation measuring device, then in any anisotropic, inhomogeneous medium with arbitrary geometry, we can interchange the source and the receiver and obtain <u>exactly the same seismogram</u>, if the source is represented by the same force system and has the same time function. This is clearly not a practical situation, and we shall now explore by more practical examples how this reciprocity breaks down as we move away from the above mentioned situation. Let us assume two granite bodies in two regions and explode, underground, two nuclear devices of the same yield at the same depth (but not at the same time). We then record the seismic waves at the surface near the explosion sites with a vertical seismograph. Although the strict mathematical reciprocity has already broken down, we can still expect to see very similar seismograms since, assuming that the source media are similar, the source time functions are the same and the near source and receiver focusing effects are still approximately reciprocal. If we assume now that one of the sites has a different source medium, we cannot expect to see the same seismogram, because nuclear devices of the same yield do not give the same equivalent elastic source strength and time function in different source media. The amplitudes and the waveforms at the two sites <u>will not</u> be the same. Now if the events are moved away from the recording sites by only a few tens of kilometers, the near source focusing effects will be different, and even if the devices are exploded in the same media, the seismograms can be quite different in amplitude. (The seismograms may not differ in waveform, since near source focusing probably does not affect them as much.) The next step is to move the sites far away from the explosions. Even in identical source media and with identical yields, there can be quite large differences in waveforms and

amplitudes, because both near receiver and source focusing effects will be quite different. If, as in the SDCS experiment, we use sources of uneven azimuthal distribution, as we were forced to do because of the given limitations of global seismicity to determine differences in m_b level, a "discrepancy" between the measured t* and m_b residuals is not surprising but to be expected, because near receiver focusing, which is azimuthally dependent, cannot be averaged out entirely with the available data. (We must note that with certain types of inhomogeneities that consistently focus or defocus teleseismic arrivals, there is no guarantee that even azimuthal weighting would help.) The only way the measured m_b would be a valid measure of "bias" including the Q and focusing effects is if we had a measured source located where the observing stations are located. Therefore, the claim that "reciprocity" requires that the m_b bias measured be the true measure of anelastic loses is fallacious, because stations are not located near the event epicenters.

The relative m_b levels and their confidence limits resulting from this experiment mean relatively little for individual stations. They are probably biased by focusing and, if we had events with more even azimuthal distribution (which would have required many years to accumulate), the results could have been quite different and the mean m_b residuals could even be outside the confidence limits given in this report. Some examples of these anomalies, are the .15 m_b difference between HNME and IFME (which cannot be adequately explained by near surface geology), and the differences between the FANV-GBNM pair and the rest of the WUS stations, although the t* are similar within both groups. Focusing provides a likely explanation for these differences and the references in this report demonstrate that this phenomenon is real and widespread and affects seismic waves in all areas of the world. Common sense dictates, therefore, that while we should not disregard amplitude data, we should interpret it with caution, and rely more on spectral data to determine anelastic losses. Anomalies of m_b are more meaningful if regional averages which can be interpreted in terms of Q are taken (Der et al., 1979; Lay and Helmberger, 1980).

After establishing what the SDCS m_b does not mean, let us discuss what was actually measured. Since spectra are less affected by focusing and other

site effects, we claim that the contribution of Q to the decrease of signal amplitudes from NTS was measured by estimating differences in t* relative to a shield area. Although, according to the best evidence, the Soviet test sites appear to be on shields or stable platforms, the findings of this report do not bear on whether RKON or HNME is a better analog to Kazakh or Novaya Zemlya. Such decisions should be based on facts involving seismic waves originating from those areas. At the SDAC and at large arrays, many years of work on short-period body wave spectra support the idea that the mantle under shield areas is less attenuating than the mantle under tectonic regions. Nevertheless, considerably more work is needed to test the validity, with respect to mantle attenuation, of possible analogs around the world.

The measured m_b residuals in the SDCS experiment are in rough agreement with the t*, but no exact agreement with the available data can be expected, since even the time domain features agree with the interpretation in terms of Q. We assume that the available data was sufficient to average out most, but not all of the focusing effects. This is reassuring, since it would be quite disturbing if the relative signs of the m_b and t* residuals were not consistent with the Q interpretation. Additional S wave information and broad regional studies mentioned in this report also confirm that the Q effects are indeed real.

Although body wave amplitude measurements by themselves are not suitable to measure attenuation for yield estimation, one must ultimately use wave amplitudes for estimating yields. First of all, one should make distinction between the t* effect and the effects of crustal structure, both near receiver and near source focusing. The m_b bias due to <u>attenuation alone</u> in upper mantle under NTS appears to be in the 0.20 to 0.27 magnitude unit range, if one uses the empirical formula $\Delta m_b \sim 1.35\ \Delta t^*$ for the NTS stations. This slightly higher than the actually measured m_b differentials. The formula can also be justified on the basis of synthetic studies of pulses from nuclear explosions. Figure 73 shows that a line with a slope of 1.35 fits curves derived from synthetics of m_b versus t* quite well. This figure also shows that in the 10 kt to 100 kt range some of the effects on m_b due to varying periods discussed in Section B are not important, although they did affect the earthquakes used for measuring Δm_b. For estimating yields throughout the world, upper mantle Q should be thoroughly mapped under the source regions of interest and under the stations used for determining the

yields. Crustal effects under these stations should also be estimated and corrections for these effects should be made.

Effects due to near-source focusing can be determined only for very small source regions for explosions with known yields. In the absence of such information, averages of m_b for a large range of epicentral distances and azimuths will probably eliminate such effects. In general, near-receiver focusing cannot be eliminated unless all receiving stations have many sensors, thus enabling one to outline the causative structures and to derive deterministic formulas for corrections. Since the requirement for the elimination of near-source focusing also demands a large range of azimuths and distances for stations around the source, this calls for many large arrays. We do not consider this a very practical or economical alternative, and one is again reduced to using network averages of m_b.

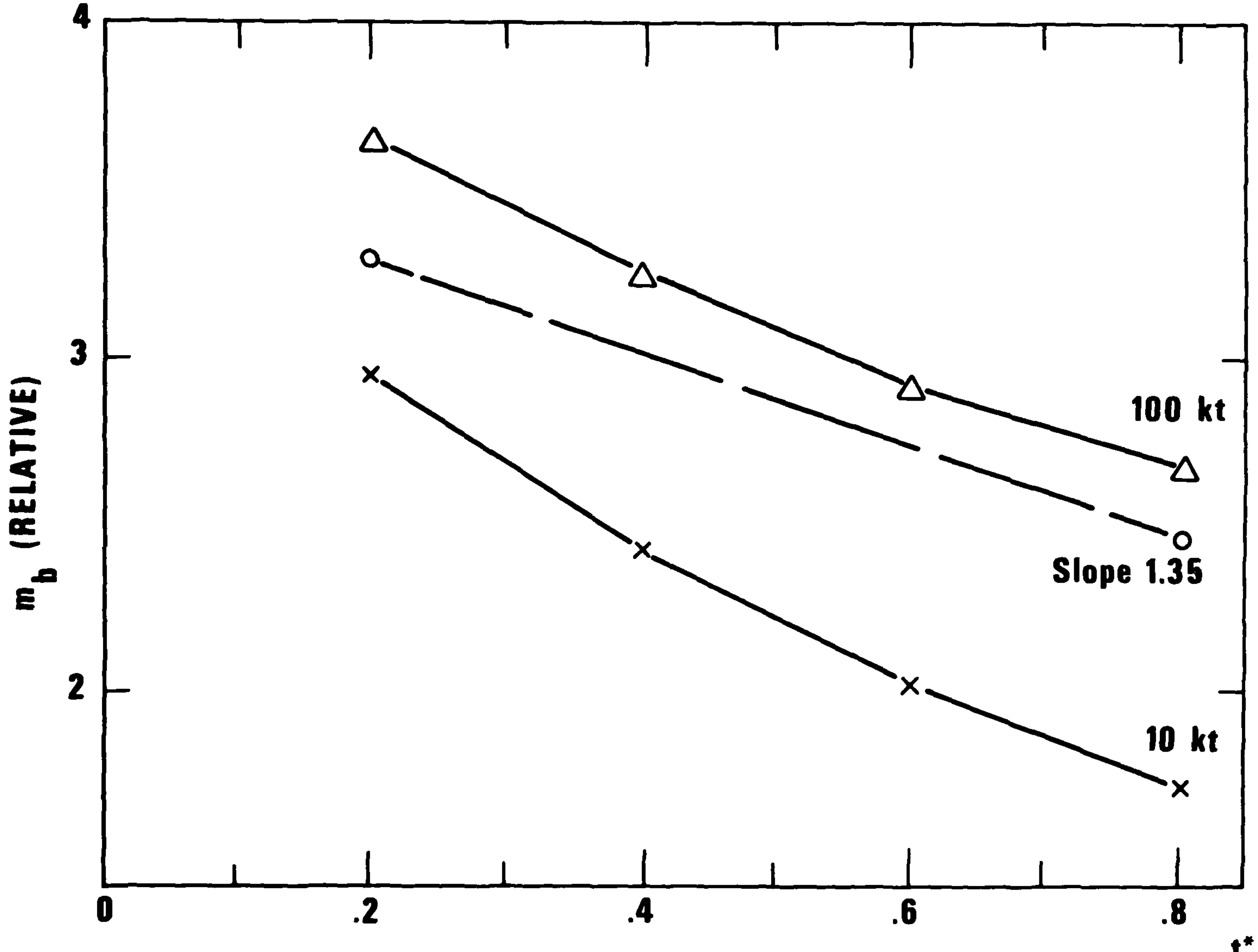

Figure 73 Decrease of m_b computed from synthetic pulses for a 10 kt and a 100 kt nuclear explosion due to increasing t*. The empirical relationship $\Delta m_b \sim 1.35\ \Delta t^*$ is sketched in for comparison. The overall slopes of the three curves are similar.

REFERENCES

Anderson, D. L., A. Ben-Menahem, and C. B. Archambeau, 1965, Attenuation of seismic energy in the upper mantle; J. Geophys. Res., 70, 1441-1448.

Anderson, D. L., and R. S. Hart, 1977, The Q of the Earth; J. Geophys. Res.,

Archambeau, C. B., E. A. Flinn, and D. H. Lambert (1969). Fine Structure of the Upper Mantle, J. Geophys. Res. 74, 5825-5865.

Asada, T., and K. Takano, 1963, Attenuation of short-period P waves in the mantle; J. Phys. Earth, 11, 25-34.

Barazangi, M., W. Pennington, and B. Isacks, 1975, Global study of seismic wave attenuation in the upper mantle behind island arcs using pP waves; J. Geophys. Res., 80, 1075-1092.

Barker, B. W., Z. A. Der and C. P. Mazek (1980). "The Effect of Crustal Structure on the Regional Phases P_g and L_g at NTS" in Studies of Seismic Wave Characteristics at Regional Distances, AL-80-1, Teledyne Geotech, Alexandria, Virginia.

Berteussen, K. A., A. Christofferson, A. Dahle, and E. S. Husebye, 1975, Modeling the geological structures beneath the NORSAR array as a Chernov medium; Exploitation of Seismic Networks, Noordhoff Leiden.

Booth, D. C., P. D. Marshall, and J. B. Young, 1974, Long and short-period amplitudes from earthquakes in the range 0-114; Geophys. J. R. Astr. Soc., 39, 528-538.

Brune, J. N., 1977, Q of shear waves estimated from S-SS spectral ratios; Geophys. Res. Lett, 4, 179-181.

Burdick, L. J., 1978, t* for S waves with a continental ray path; Bull. Seism. Soc. Am., 68, 1013-1030.

Burdick, L. J., and D. V. Helmberger, 1979, Time functions appropriate for nuclear explosions; Bull. Seism. Soc. Am., 69, 957-974.

Butler, R., (1979), An Amplitude Study of Russian Nuclear Events for WWSSN Stations in the United States, Sierra Geophysics, SGI-R-79-001.

Butler, R., Ruff, L. J., Hart, R. S. and G. R. Mellman (1979), Seismic Waveform Analysis of Underground Nuclear Explosions, Sierra Geophysics, SGI-R-79-011.

Butler, R., and L. Ruff, 1980, Teleseismic short-period amplitudes, source and receiver variations; Bull. Seism. Soc. Am., 70, 831-850.

Capon, J., 1974, Characterization of crust and upper mantle structure under LASA as a random medium; Bull. Seism. Soc. Am., 64, 235-266.

REFERENCES (Continued)

Capon, J., and K. A. Berteussen, 1974, A random medium analysis of crust and upper mantle structure under NORSAR; Geophys. Res. Lett., 1, 327-328.

Chang, A., and D. H. von Seggerr), A study of amplitude anomaly and m_b bias at LASA subarrays, SD.. R-79-11, Teledyne-Geotech, Alexandria, Virginia.

Christofferson, A., 1975, Estimation of parameters characterizing random medium; Exploitation of Seismic Networks, Noordhoff, Leiden.

Cleary, J., 1967, Analysis of the amplitudes of short-period P waves recorded by Long Range Measurement Stations in the distance range 30-to 102; J. Geophys. Res., 72, 4705-4712.

Dahle, A., 1975, *Time and amplitude fluctuations of teleseismic P-signals* at NORSAR in view of wave scattering theory; NORSAR Scientific Report No. 4-74/75.

Dahle, A., E. S. Husebye, K. A. Berteussen, and A. Christofferson, 1975, Wave scattering effects and seismic velocity measurements; Exploitation of Seismic Networks, Noordhoff, Leiden.

Der, Z. A., R. P. Masse, and J. P. Gurski, 1975, Regional attenuation of short-period P and S waves in the United States; Geophys. J. R. Astr. Soc., 40, 85-106.

Der, Z. A., and T. W. McElfresh, 1980, Time domain methods, the values of t^*_p and t^*_s in the short-period band and regional variations of the same across the United States; Bull. Seism. Soc. Am., 70, 921-924.

Der, Z. A., and T. W. McElfresh, 1977, The relationship between anelastic attenuation and regional amplitude anomalies of short-period P waves in North America; Bull. Seism. Soc. Am., 67, 1303-1317.

Der, Z. A., Dawkins, M. S., McElfresh, T. W., Goncz, J. H., Gray, C. E. and M. D. Gillispie (1977). Teleseismic P wave amplitudes and spectra at NTS and the Shoal Site as compared to those observed in eastern North America, Preliminary Report, SDAC-TR-77-9, Teledyne Geotech, Alexandria, Virginia.

Der, Z. A., and T. W. McElfresh, 1976, Short-period P wave attenuation along various paths in North America as determined from P wave spectra of the SALMON nuclear explosion; Bull. Seism. Soc. Am., 66, 1609-1622.

Der, Z. A., T. W. McElfresh, and C. P. Mrazek, 1979, Interpretation of short-period P-wave magnitude anomalies at selected LRSM station; Bull. Seism. Soc. Am., 69(4), 1149-1160.

Der, Z. A., and R. R., Blandford. On the absolute value of t^*_s and t^*_p around 1 Hz, Memorandum to Major G. W. Ullrich, VSC, 16 October 79.

REFERENCES (Continued)

Der, Z. A., E. Smart, and A. Chaplin, 1980, Short-period S wave attenuation in the United States; Bull. Seism. Soc. Am., 70, 101-126.

Evernden, J., and D. M. Clark, 1970, Study of teleseismic P. II., Amplitude data; Phys. Earth. Planet. Int., 4, 24-31.

Felix, C. P., W. L. Gilbert, and S. G. Wheeler, 1971, Preliminary results from the NORSAR short-period system, Proceedings from the seminar on seismology and seismic arrays, Royal Norwegian Council for Scientific and Industrial Research.

Fernald, A. T., G. S. Corchary, W. P. Williams, and R. B. Cotten, Surficial deposits of Yucca Flats area, Nevada Test Site, Geol. Soc. Am. Mem. 110, 1968.

Filson, J., and C. W. Frasier, 1972, Multisite estimation of explosive source parameters; J. Geophys. Res., 77, 2045-2061.

Fuchs, K. (1966), The transfer function for P waves for a system consisting of a point source in a layered medium. Bull. Seism. Soc. Am., 56, 75-108.

Haddon, R. A. W., and E. S. Husebye, 1978, Joint interpretation of P wave time and amplitude anomalies in terms of lithospheric heterogeneities; Geophys. J. R. Astr. Soc., 55, 19-44.

Hadley, D. M., 1979, Seismic source functions and att nuation from local and teleseismic observations of the NTS events JORUM and HANDLEY, Sierra Geophysics, SGI-R-79-002, Arcadia, California.

Hanks, T. C., 1980, Source parameters of crustal earthquakes, the corner frequency shift, teleseismic body waves and Q; (unpublished manuscript).

Hays, W. W., and J. R. Murphy, The effect of Yucca fault on seismic wave propagation, Bull. Seismol. Soc. Am., 61, 697-706, 1971.

Healy, D. L., Application of gravity data to geologic problems at Nevada Test Site, Geol. Soc. Am. Mem. 110, 1968.

Helmberger, D. V., 1973, On the structure of the low-velocity zone, Geophys. J. R. Astr. Soc., 34, 251-263.

Houser, F. N., Application of geology to underground nuclear testing, Nevada Test Site, Geol. Soc. Am. Mem. 110, 1968.

Hudson, J. A., (1969), A quantitative evaluation of seismic signals at teleseismic distances, I. Radiation from point sources, Geophys. J. R. A. S., 18, 233-249.

Kelly, K. R., R. W., Ward, Sven Treitel; and R. M. Alford (1976). Synthetic seismograms: A finite-difference approach, Geophysics, 41, 2-27.

Knopoff L., J. A. Gangi (1959). Seismic reciprocity, Geophysics, 24, 681-691.

Knopoff L., (1979). Personal communication

Kovach, R. L., and D. L. Anderson, 1964, Attenuation of shear waves in the upper and lower mantle; Bull. Seism. Soc. Am., 54, 1855-1865.

Lay, T., and D. V. Helmberger, 1980, Body wave amplitude patterns and upper mantle attenuation variations across the United States; (Submitted to Geophys. J. R. Astr. Soc.).

Lay, T., B. Minster, and L. Ruff, 1979, Application of the southern California array to teleseismic amplitude studies; Trans. Am. Geophys. Union EOS, 60, 880.

Lee, W. B., and S. C. Solomon, 1979, Simultaneous inversion of surface wave phase velocity and attenuation, Rayleigh and Love waves over continental and oceanic paths; Bull. Seism. Soc. Am., 69, 65-96.

Lee, W. B., and S. C. Solomon, 1975, Inversion schemes for surface wave attenuation and Q in the crust and the mantle; Geophys. J. R. Astr. Soc., 43, 47-71.

Lundquist, G., 1979, Constraints on the absorption band model of Q, (manuscript), Cooperative Institute for Research in Environmental Sciences, University of Colorado, Boulder, Colorado.

Mack, H. (1969). *Nature of short-period* P *wave* signal variations at LASA, J. Geophys. Res., 74, 3161-3170.

McKeown, F. A., and D. D. Dickey, (1969), Fault displacements and motion related to nuclear explosions. Bull. Seism. Soc. Am., 59, 2253-2269.

Mills, J. M., 1978, Great circle Rayleigh wave attenuation and group velocity, Part IV; Regionalization and pure-path models for shear velocity and attenuation; Phys, Earth. Planet. Inc., 17, 323-352.

Molnar, P., B. E. Tucker, and J. N. Brune, 1973, Corner frequencies of P and S waves and models of earthquake sources: Bull. Seism. Soc. Am., 63, 2091-2104.

Mueller, R. A., and J. R. Murphy, 1971, Seismic characteristics of underground nuclear detonations; Part I. Seismic scaling law of underground detonations; Bull. Seism. Soc. Am., 61, 1975.

Nakanishi, I., 1979, Phase velocity and Q of mantle Rayleigh waves; J. Geophys. Res., 58, 35-59.

Noponen, I., 1975, Compressional wave-power spectrum from seismic sources, Institute of Seismology, University of Helsinki, ISNB-45-0538-7, Contract AFOSR-72-2377 (Final Report).

REFERENCES (Continued)

North, R. G., 1977, Station magnitude bias- Its determination, causes, and effects., ESD-TR-77-85, Lincoln Laboratory, Lexington, Massachusetts.

Oliver, J., and B. Isacks, 1967, Deep earthquake zones, anomalous structures in the upper mantle and the lithosphere; J. Geophys Res., 72, 4259-4275.

Oppenheim, A. V., and R. W. Schafer (1975), Digital signal processing. Prentice Hall, Englewood Cliffs, New Jersey.

Phinney, R. A. (1964). Structure of the Earth's Crust from Spectral Behavior of Long-Period Body Waves, J. Geophys. Res., 69, 2997-3017.

Ramspott, L. D., and N. W. Howard, Average properties of nuclear test areas and media at the USERDA Nevada Test Site, Rep. UCRL-51948, Lawrence Livermore Lab., Livermore, Ca., 1975.

Ringdal, F., 1976, Maximum-likelihood estimation of seismic magnitude; Bull. Seism. Soc. Am., 66, 789-802.

Rivers, W. D., and Z. A. Der, 1980, Worldwide measurements of Q_α using LRSM, SRO, SDCS and array data, (In preparation).

Romanowicz, B. A., and M. Cara, 1980, Reconsideration of the relations between S and P station anomalies in North America; Geophys. Research Letters, 7, 417-420.

Sacks, I. S., 1980, Mantle Q from body waves - difficulties in determining frequency dependence. (Abstract); Trans. Am. Geophys. Union EOS, 61, 299.

Sacks, I. S., and H. Okada, 1974, A comparison of the anelasticity structure beneath western South America and Japan; Phys. Earth Planet. Int., 9, 211-219.

Sailor, R. V., and A. M. Dziewonski, 1978, Measurements and interpretation of normal mode attenuation; Geophys. J. R. Astr. Soc., 53, 559-581.

Sato, R., and A. F. Espinosa, 1967, Dissipation in the earth's mantle and rigidity and viscosity in the earth's core determined from waves multiply reflected from the mantle-core country; Bull. Seism. Soc. Am., 57, 829-856.

Schilt, S., J. Oliver, L. Brown, S. Kaufman, D. Albaugh, J. Brewer, F. Cook, L. Jensen, P. Krumhansl, G. Long, and D. Steiner, 1979, The Heterogeneity of the continental crust: Results from deep seismic reflection profiling using the Vibroseis technique; Review of Geophysics and Space Physics, vol. 17, No. 2, April 1978.

Sengupta, M. K., and B. R. Julian, 1976, P-wave travel times from deep earthquakes; Bull. Seism. Soc. Am., 66, 1555-1579.

Sipkin, S. A., and T. H. Jordan, 1980, Regional variation of Q_{ScS}, BSSA, 70, 1071-1102.

Sipkin, S. A., and T. H. Jordan, 1979, Frequency dependence of Q_{ScS}, Bull. Seism. Soc. Am., 69, 1055-1079.

Solomon, S. C., 1972, Seismic-wave attenuation and partial melting in the upper mantle of North America; J. Geophys. Res., 77, 1483-1502.

Solomon, S. C., and M. N. Tolsöz, 1970, Lateral variation of attenuation of P and S waves beneath the United States; Bull. Seism. Soc. Am., 60, 819-838.

Spence, W. (1974). P wave residual differences and inferences on an upper mantle source for the Silent Canyon Volcanic Centre, Southern Great Basin, Nevada, Geophys. J. R. Astr. Soc., 38, 505-523.

Takano, K., 1971, A note on the attenuation of short-period P and S waves in the mantle; J. Phys. Earth., 19, 155-163.

Taylor, S. R., and M. N. Toksöz, 1979, Three dimensional crust and upper mantle structure of the northeastern United States; J. Geophys. Res., 84, 7627-7644.

Thornborough, A. D., (1971), Current practices and anticipated improvements in PNE. In "Peaceful Nuclear Explosions" International Atomic Energy Agency, Vienna.

von Seggern, D. H., and R. R. Blandford, 1972, Source time functions and spectra from underground nuclear explosions; Geophys. J. R. Astr. Soc., 31, 83-97.

Wickens, A. J., and G. G. R. Buchbinder, 1980, S wave residuals in Canada; Bull. Seism. Soc. Am., 70, 809-822.

Yoshida, M., and M. Tsujiura, 1975, Spectrum and attenuation of multiply reflected core phases; J. Phys. Earth, 23, 31-42.

APPENDIX A

List of Events Used in the SDCS Project Along With Amplitudes, Dominant Periods and Distances

```
14SEP76 15 46  5.2 5.06 0 3 EASTER IS.
26.4S115.8W
   0.0
HN-ME   84.4    74.0   .83 -9
RK-CN   79.6   251.6   .76 -9
CB2NV   63.6    42.7   .94 -9
15SEP76  3 15 20.0 5.84 0 4 AUSTRIA
46.2N  13.3E
   0.0
HN-ME   53.6    70.0   .81 -9
RK-CN   64.4    48.2   .49 -9
CB2NV   85.1    56.7  1.09 -9
NI2NV   85.1   142.7  1.23 -9
15SEP76  9 21 18.4 5.30 0 4 AUSTRIA
46.3N  13.2E
   0.0
HN-ME   53.5    62.8   .78 -9
RK-CN   64.3   100.6   .54 -9
CB2NV   85.0    40.3  1.19 -9
NI2NV   85.0   102.1   .91 -9
29SEP76  3 00 00.0 0.00 1 5 N.Z.
73.5N  53.7E
   0.0
HN-ME   54.7   192.4   .65 -9
RK-CN   54.4   153.3   .44 -9
CB2NV   69.7    39.1   .84 -9
NI-NV   69.7    45.5   .53 -9
NI2NV   69.7    71.8   .48 -9
19SEP76 12 23 31.1 5.27 0 5 S.PANAMA
 7.2N  82.4W
   0.0
HN-ME   40.9    95.2   .71 -9
RK-CN   44.7   262.7  1.01 -9
CB2NV   43.0   180.0  1.45 -9
NI-NV   43.0   477.3  1.03 -9
NI2NV   43.0   449.2   .96 -9
19SEP76 20 57 53.1 5.41 0 5 MEXICO
17.9N100.6W
   0.0
HN-ME   39.0    80.2   .78 -9
RK-CN   33.4    39.4   .61 -9
CB2NV   23.8   320.4   .86 -9
NI-NV   23.8   383.4   .66 -9
NI2NV   23.3   308.4   .73 -9
 29SEP76 10 20 17.6 5.12 0 4 EL SALVADOR
13.2N  89.9W
   0.0
HN-ME   37.8   134.5 1.3   10 27 35.8
RK-CN   37.8   353.3 0.7   10 27 33.5
CB2NV   33.8    62.2 1.04  10 27  0.3
NI-NV   33.8   157.3 0.85  10 27  2.1
06SEP76  9 56 23.2 4.97 0 3 N.ATLANTIC
58.1N  32.1W
   0.0
HN-ME   24.6   138.5   .70 10  1 46.0
RK-CN   35.2    65.4   .75 10  3 13.1
CB2NV   56.0    17.9  1.06 -9
05SEP76 20 11 27.0 5.04 0 3 MEXICO
18.5N101.1W
   0.0
HN-ME   38.6    49.5  1.00 20 13 53.7
RK-CN   32.9    45.3   .80 20 13  0.3
CB2NV   23.0    80.5   .96 -9
05SEP76 20 11 43.6 5.17 0 3 MEXICO
18.7N100.7W
   0.0
HN-ME   36.5   106.8   .96 20 19  7.9
RK-CN   32.7    67.6  1.00 20 13 15.8
CB2NV   23.0  1052.0  1.14 20 16 51.0
```

```
09SEP76 09 27 46.0 5.05 0 3 SVALBARD
77.6N   8.0E
   0.0
BK-ME   42.2   153.7 1.13   9 35 41.8
BK-CN   43.1    25.8  .54   9 35 48.5
CB2NV   60.0    35.1  .71   9 37 57.1
29SEP76 09 52 33.0 5.08 0 4 CUBA
19.3N  80.6W
   0.0
BK-CN   33.1   135.3  .70   9 59 10.6
CB2NV   35.6   120.1  .86   9 59 33.5
NI-NV   35.9   171.6  .61   9 59 36.8
NI2NV   35.8   237.1  .86   9 59 35.7
25SEP76 21 47 20.6 5.13 0 4 EASTER IS.
26.4S115.0W
   0.0
BK-CN   79.5   147.2  .85  21 59 23.1
CB2NV   63.6    32.6 1.28  21 57 52.8
NI-NV   63.6    18.8 1.50  21 57 53.7
NI2NV   63.6    69.3  .94  21 57 53.8
26SEP76 06 35 49.3 4.55 0 3 KAMCHATKA
51.1N157.2E
   0.0
BK-CN   61.7    17.7  .63   6 46  3.8
CB2NV   60.0     8.8  .80   6 45 57.9
NI2NV   60.0    28.3  .56   6 45 57.7
26SEP76 07 13 36.1 4.63 0 4 ARGENTINA
28.1S  64.6W
   0.0
BK-CN   83.0    46.1  .70   7 25 59.3
CB2NV   81.2    29.4  .67   7 25 51.9
NI-NV   81.4    15.0  .67   7 25 53.3
NI2NV   81.4    63.6  .61   7 25 52.6
30SEP76 08 04 10.9 5.21 0 5 CHILE-ARG. BORDER
24.2S  68.2W
   0.0
BK-ME   70.3    43.4 1.30   8 15 28.1
BK-CN   76.3   171.5 1.10   8 16 10.4
CB2NV   76.1   198.9 1.10   8 16  1.4
NI-NV   76.4   583.3  .80   8 16  2.9
NI2NV   76.3   451.2  .80   8 16  2.6
25SEP76 10 40 47.0 4.52 0 4 EASTER IS.
24.6S106.8W
   0.0
BK-CN   76.3    40.3  .70  10 52 44.2
CB2NV   62.4   103.0 1.00  10 51  9.6
NI-NV   62.5    40.1  .90  10 51 12.0
NI2NV   62.5    24.3  .60  10 51 10.6
22SEP76 20 07  1.3 5.30 0 2 N.CHINA
39.9N106.3E
   0.0
BK-ME   93.8    19.5  .90  20 20 20.7
CB2NV   93.6    11.5  .60  20 20 17.6
22SEP76 02 30 30.8 4.78 0 5 ALEUTIANS
51.6N175.9W
  75.0
BK-ME   64.3    45.8  .60   2 41  0.9
BK-CN   46.6   211.0  .40   2 39  7.0
CB2NV   43.7    18.1  .80   2 38 29.4
NI-NV   43.5    80.0  .60   2 38 30.9
NI2NV   43.5    43.3  .80   2 38 30.7
22SEP76 08 20 27.6 5.03 0 4 VOLCANO IS.
23.3N142.1E
 110.0
BK-CN   91.1   249.0  .80   8 33 13.8
CB2NV   84.9   235.1  .60   8 32 50.3
NI-NV   84.6   505.6  .60   8 32 43.5
NI2NV   84.7   569.6  .50   8 32 50.0
```

```
04OCT76 06 59 19.5 4.62 0 4 C.MEXICO
20. N 99. W
   0.0
BK-CN   30.7    35.1  .80  7  5 34.2
CB2NV   22.3    42.7 1.50  7  4 20.3
NT-NV   22.5   140.4 1.10  7  4 23.2
NI2NV   22.6   105.7 1.00  7  4 22.2
04OCT76 23 36 06.0 5.17 0 5 ECUADOR
 0.2S 77.5W
   0.0
HN-ME   47.1    73.0 1.50 23 44 45.8
BK-CN   52.8    36.3  .70 23 45 21.9
CB2NV   51.6    11.6 1.10 23 45 12.7
NI-NV   51.9    51.1  .40 23 45 15.6
NI2NV   51.8    42.9  .50 23 45 14.5
07OCT76 22 01 12.5 4.60 0 4 ECUADOR
 0.8S 80.3W
   0.0
BK-CN   52.9    21.9  .80 22 10 23.7
CB2NV   50.4    22.6  .50 22 10  5.2
NI-NV   50.6   230.2  .30 22 10  8.6
NI2NV   50.5   110.6  .30 22 10  7.0
08OCT76 09 22 46.6 4.55 0 5 KOMANDORSKY IS.
55.1N164.3E
   0.0
HN-ME   69.6    22.2  .70  9 33 57.2
BK-CN   55.9    25.5  .70  9 32 26.3
CB2NV   54.7    88.0  .80  9 32 18.3
NI-NV   54.5    61.0  .60  9 32 17.3
NI2NV   54.4    58.1  .70  9 32 17.8
08OCT76 09 22 56.3 4.53 0 5 KOMA IS.
55.1N164.1E
   0.0
HN-ME   69.6    36.0  .50  9 34  7.5
BK-CN   56.0    25.8  .70  9 32 36.6
CB2NV   54.8   102.0  .90  9 32 29.0
NI-NV   54.6    87.0  .80  9 32 29.1
NI2NV   54.5    75.4  .70  9 32 28.7
08OCT76 14 38 27.9 4.78 0 4 KURILES
43.8N155.7E
   0.0
HN-ME   76.8    44.4  .70 14 50 21.6
BK-CN   63.3    23.3  .60 14 43 58.3
CB2NV   61.4     8.7  .90 14 48 46.0
NI2NV   61.2    26.2  .60 14 48 45.5
23NOV76 05 03 00.0 5.20 1 4 E.KAZ
50.0N 79.0E
   0.0
HN-ME   79.9   241.4  .80  5 15 10.3
BK-CN   79.2   448.5  .50  5 15  5.4
NI-NV   91.9   109.6  .70  5 15 10.8
NI2NV   91.9    78.5  .90  5 16 11.0
09OCT76 12 31 06.6 4.97 0 5 COSTA RICA
10.7N 85.8W
   0.0
HN-ME   38.5    71.6 1.00 12 38 32.4
BK-CN   40.6    40.5  .80 12 38 45.9
CB2NV   37.9   106.7 1.20 12 38 27.6
NI-NV   38.2   424.8 1.20 12 38 30.2
NI2NV   38.1   239.3 1.10 12 38 29.1
09OCT76 02 52 24.3 4.47 0 4 KURILES
45.1N153.5E
   0.0
HN-ME   81.7     9.2  .70  3  4 43.8
BK-CN   67.9    23.0  .70  3  3 23.3
CB2NV   64.9    37.2  .90  3  3  5.9
NI2NV   64.7    52.0  .70  3  3  5.3
```

```
09OCT76 16 02 26.9 4.54 0 5 N.COLUMBIA
 9.4N  77.5W
   0.0
HN-ME   37.7     35.8   .70 16  9 54.0
BK-CN   43.6     31.8   .70 16 10 34.8
CB2NV   44.5      9.6   .80 16 10 43.6
NT-NV   44.8     73.0   .60 16 10 45.9
NT2NV   44.7     25.1   .70 16 10 45.6
09OCT76 19 41 27.1 4.31 0 2 S.PERU
15.2S  71.6W
   0.0
BK-CN   68.8     21.8   .50 19 52 30.6
CB2NV   67.0     18.2   .60 19 52 22.7
09OCT76 21 10 24.1 4.53 0 2 PERU COAST
10.3S  79.5W
   0.0
BK-CN   62.3     28.7   .70 21 20 45.5
CB2NV   58.6      6.7   .70 21 20 23.4
 9OCT76 23 48  9.0 4.39 0 3 C. AMER. COAST
10.0N  91.0W
   0.0
BK-CN   40.9     15.7   .70 23 55 40.9
CB2NV   35.4      7.0   .80 23 55 17.8
NT2NV   35.6     13.6   .60 23 55 19.9
10OCT76 02 58 56.6 4.91 0 4 KURILES
45.4N151.0E
   0.0
HN-ME   82.2     57.1   .90  3 11 19.2
BK-CN   68.7     37.5 1.00   3  9 59.8
CB2NV   66.3     14.4 1.00   3  9 47.3
NT2NV   66.1     18.6   .50  3  9 46.6
10OCT76 06 19 20.8 4.46 0 3 ECUADOR
 0.4S  78.2W
   0.0
BK-CN   52.9     38.1   .70  6 28 35.8
CB2NV   51.4      5.4 1.10   6 28 25.9
NT2NV   51.5     19.4   .60  6 28 29.0
10OCT76 14 32 04.9 4.59 0 3 KURILES
43.2N147.7E
  45.0
BK-CN   71.9     19.2   .50 14 43 30.8
CB2NV   69.4     11.4   .90 14 43  9.7
NT2NV   69.3     15.6   .50 14 43  9.4
 6OCT76  9 12 36.0 5.8  0 3 ECUADOR
 0.6S  78.7W
   0.0
HN-ME   47.7    212.2 2.0    9 21 13.5
BK-CN   53.0    131.2 1.3    9 21 51.9
NT2NV   51.4    226.1 1.2    9 21 44.5
12OCT76  4 24 52.1 4.96 0 4 S. HONSHU, JAPAN
31.2N141.5E
   0.0
BK-CN   84.6     17.6 0.6    4 37 26.2
CB2NV   80.4     38.2 0.9    4 37  5.2
NT-NV   80.1     42.1 1.4    4 37  5.3
NT2NV   80.2     87.5 0.9    4 37  5.1
12OCT76 23 49 24.3 4.41 0 3 W CST COLUMBIA
 2.8N  77.5W
   0.0
HN-ME   44.1     17.9 0.6   23 57 33.5
BK-CN   49.9     64.0 0.6   23 58 16.4
CB2NV   49.3     11.0 0.7   23 58 15.9
13OCT76 17 35 45.1 4.68 0 2 VENEZUELA
10.5N  62.2W
   0.0
BK-CN   47.8     58.6 0.6   17 44 22.8
CB2NV   55.1     15.2 0.8   17 45 20.6
```

```
21OCT76   4 24  16.0 4.62  0 5 N. CHILE
22.1S  70.0W
  0.0
EN-ME    68.2     21.0 0.7    4 35  17.0
ER-CN    75.8     36.2 0.6    4 36   1.6
CB2NV    73.5     23.8 1.0    4 35  50.9
NT-NV    73.9     68.0 0.8    4 35  52.5
NI2NV    73.6     39.9 1.0    4 35  52.1
21OCT76  15  13  22.8 4.92  0 3 ALEUTIANS
52.3N169.3W
 53.0
RR-CN    44.8     16.8 0.4   15 21  31.3
CB2NV    39.6     62.  0.7   15 20  50.4
NI2NV    39.5     69.0 1.0   15 20  48.1
22OCT76   4   4  22.6 4.64  0 5 CST OF NICARAGUA
12.1N  87.6W
 70.0
EN-ME    37.9     32.2 0.9    4 11  34.1
ER-CN    39.1     70.7 0.6    4 11  39.1
CB2NV    35.8     18.1 0.6    4 11  16.0
NT-NV    36.1     36.0 0.6    4 11  19.3
NI2NV    36.0     49.9 0.7    4 11  17.8
22OCT76   5  53  50.9 4.57  0 4 EL SALVADOR
13.2N  88.2W
 79.0
RR-CN    37.9     54.6 0.7    6  0  39.5
CB2NV    34.6     13.1 0.8    6  0  32.5
NT-NV    34.8     43.0 0.7    6  0  35.2
NI2NV    34.7     44.3 0.5    6  0  33.9
22OCT76  18  35  23.9 5.26  0 3 KODIAK REG
56.1N153.3W
  0.0
ER-CN    34.8    118.7 0.5   18 42  16.5
CB2NV    31.2     80.1 1.3   19 41  45.4
NI2NV    31.0    192.3 1.2   13 41  44.7
24OCT76  17  19  55.5 4.60  0 2 CEN. ALASKA
63. N149. W
 70.0
BN-ME    46.4     33.9 0.8   17 28  14.2
CB2NV    32.4     30.5 0.8   17 26  19.3
26OCT76   5  59  56.4 5.34  0 5 KURILE IS
46.1N150.8E
130.0
BN-ME    81.6     89.6 0.6    6 12   0.6
ER-CN    68.3    105.3 0.8    6 10  43.3
CB2NV    66.1     27.6 0.5    6 10  30.5
NT-NV    65.8    270.1 0.6    6 10  23.2
NI2NV    65.9    385.0 0.6    6 10  29.8
28OCT76   9  59  21.3 4.55  0 2 PERU
14.6S  73.7W
  0.0
ER-CN    67.8     26.7 0.7   10 10  19.1
CB2NV    65.4      9.7 0.7   10 10   6.8
 2NOV76  19  23   2.7 4.9   0 3 KURILE IS
47. N151. E
  0.0
BN-ME    80.9    126.4 0.7   19 35  18.9
CB2NV    78.2     22.5 0.9   19 33  49.2
NI2NV    78.1     25.9 0.8   19 33  48.5
12NOV76  14  47  32.7 5.39  0 3 BAFFIN BAY
72. N  70. W
 89.0
EN-ME    26.1    171.6 0.7   14 52  58.3
NT-NV    41.8    181.1 0.7   14 55  15.1
NI2NV    41.8    138.1 0.6   14 55  15.1
15NOV76  14  14  26.6 4.6   0 2 KURILES
45. N148. E
200.0
BN-ME    63.0     43.1 0.5   14 26  30.5
NI2NV    67.8     35.  0.6   14 25   3.6
```

```
17NOV76  5 33 35.5 5.5  0 2 KURILES
51. N156. E
100.0
BK-ME   75.6  408.9 0.7   5 45 10.7
NI2NV   60.5  424.2 0.7   5 43 36.3
22NOV76 20  9   2.7 4.5  0 2 VENEZUELA
 7. N 72. W
  0.0
BK-CN   47.3  120.5 0.5  23 17 33.5
NI-NV   55.    35.2 0.4  23 18  0.0
26NOV76 23 43  12.6 4.8  0 4 PERU-ECUADOR BDR
 2. S 77. W
  0.0
HN-ME   49.2   41.7 0.8  23 52  3.3
BK-CN   55.2   80.0 0.5  23 52 43.3
NI-NV   54.1  269.9 0.6  23 52 36.7
NI2NV   54.0  175.3 0.8  23 52 37.2
 1DEC76 14 15  33.2 5.0  0 3 COSTA RICA
10. N 85. W
  0.0
BK-ME   39.0  213.1 1.3  14 23  2.5
BK-CN   41.6   83.7 1.1  14 23 21.4
NI2NV   39.5  320.8 1.0  14 23  7.6
 1DEC76 17 44  33.8 4.5  0 2 CST OF CENT. AMER.
12. N 90. W
  0.0
BK-CN   36.7   46.5 0.7  17 51 54.9
NI2NV   34.4  129.7 0.6  17 51 25.5
 3DEC76  5 27  34.4 4.9  0 2 CHILE-BOLIVIA
21. S 69. W
 79.0
BK-CN   74.7  145.2 0.7   5 39  2.7
NI2NV   73.1  216.5 1.0   5 38 56.5
 3DEC76 23 10  23.1 4.6  0 2 N. CHILE
22. S 69. W
  0.0
BK-CN   76.5   80.0 0.8  23 22 12.1
NI2NV   73.1   60.1 0.7  23 22  4.4
30NOV76  0 40  57.0 6.3  0 3 CHILE-BOLIVIA
21. S 69. W
 63.0
BN-ME   66.6 1102.7 0.6   0 51 39.4
BK-CN   74.5 4001.4 0.6   0 52 25.8
NI2NV   72.9 1804.5 1.0   0 52 19.4
 4DEC76  5  6  29.7 4.7  0 4 N. CHILE
21. S 69. W
  0.0
BK-CN   74.6   58.5 0.51  5 13  8.1
CB2NV   72.9   62.0 0.8   5 18  0.9
NI-NV   73.1  104.7 0.8   5 18  2.4
NI2NV   73.0   75.2 0.8   5 13  1.9
 4DEC76 12 32  35.4 5.2  0 4 N. CHILE
20. S 69. W
103.0
BN-ME   66.6   80.7 1.3  12 43 12.3
BK-CN   74.5   94.1 0.6  12 44  0.1
NI-NV   72.9  454.2 0.8  12 43 54.3
NI2NV   72.6  333.4 0.9  12 43 54.0
 5DEC76 22  1  22.1 4.84 0 2 BONIN IS.
23. N140. E
393.0
BK-CN   67.6  182.4 0.6  22 13 28.9
NI2NV   63.1  296.7 0.7  22 13  7.7
 6DEC76 19 46   2.4 4.9  0 2 EASTER IS.
34. S112. W
  0.0
BK-CN   66.9   62.6 1.0  13 56 45.5
NI2NV   71.8   46.8 0.9  13 57 26.8
```

```
 7DEC76  9 36 41.4 4.7  0 3 S. HONSHU
34. N137. E
360.0
BK-CN   64.3    25.1 0.8    9 48 34.
NI-NV   81.5   163.4 1.0    9 48 21.2
NI2NV   81.5   387.4 0.8    9 48 21.6
 9DEC76  4 24  6.4 4.3  0 2 EL SALVADOR
14. N 90. W
  0.0
BK-CN   37.2   270.3 0.7    4 31 17.6
NI2NV   33.3    28.1 0.7    4 30 37.3
 9DEC76  9 58 19.7 4.5  0 3 OFF CST OREGON
45. N130. W
  0.0
HN-ME   42.6   149.7 0.8    9 58 56.2
BK-CN   25.1   124.3 0.8    9 56 23.2
NI2NV   12.7   201.9 1.3    9 54  3.0
 9DEC76 15 37 41.0 4.9  0 3 KURILES
44. N148. E
 85.0
HN-ME   64.1    53.2 0.5   15 50  2.7
BK-CN   70.9   111.0 0.6   15 48 43.9
NI2NV   66.6    81.4 0.5   15 48 36.0
20OCT76  8  0  0.0 0.00 1 5 N.Z.
73.0N 55.0E
  0.0
HN-ME   54.6    59.5 0.7    8  9 23.2
BK-CN   54.4   256.1 0.4    8  9 25.9
CB2NV   69.7     6.1 0.6    8 11  9.5
NI-NV   69.7    58.0 0.4    8 11  9.5
NI2NV   69.7    11.9 0.5    8 11  9.7
19DEC76 14 37 30.0 0.00 0 2 KURILES
45.0N154.0E
  0.0
BK-CN   67.9    41.8 0.7   14 48 41.7
NI2NV   64.4    68.1 0.6   14 48 28.0
20DEC76 10 18 58.0 0.00 0 3 COLOMBIA
 7.0N 75.0W
  0.0
HN-ME   39.6   169.4 1.4   10 26 21.5
BK-CN   46.5   228.1 1.3   10 26 43.1
NI-NV   46.2   147.1 0.9   10 26 32.6
15DEC76 12 26  4.0 0.00 0 3 JAPAN
30. N131. E
  0.0
BK-CN   90.0    17.9 0.7   12 39  7.0
NI-NV   87.9    37.9 1.0   12 38 56.4
NI2NV   87.9    32.7 1.1   12 38 56.8
20DEC76 20 33 50.0 0.00 0 5 BR. COLUMBIA
55. N124. W
  0.0
HN-ME   35.6  1160.9 1.25  20 40 43.2
BK-CN   18.6  3078.0 1.3   20 38  9.6
CB2NV   18.6   948.7 1.3   20 36 41.9
NI-NV   18.5  1333.5 1.4   20 36 39.0
NI2NV   18.5  1094.8 1.8   20 36 40.8
20DEC76 21 22 25.0 0.00 0 5 BR. COLUMBIA
56. N124. W
  0.0
HN-ME   36.     63.0 1.0   21 29 10.0
BK-CN   19.    395.4 0.9   21 26 31.5
CB2NV   19.     79.1 1.3   21 25  4.8
NI-NV   19.    271.7 1.2   21 25  3.4
NI2NV   19.    142.3 1.4   21 25  3.5
22DEC76  1  1 42.0 0.00 0 4 VOLCANO IS.
24. N142. E
  0.0
BK-CN   91.    360.6 1.0    1 14 39.2
CB2NV   90.    242.1 1.1    1 14  7.5
NI-NV   85.    377.5 1.1    1 13 55.6
NI2NV   85.    590.1 1.0    1 14  7.1
```

```
13DEC76 23  1 28.0 0.00 0 2 N. PACIFIC
32. N145. E
  0.0
BK-CN   62.4    63.7 0.6  23 14  2.3
NI2NV   77.3   111.3 0.6  23 13 39.3
14DEC76 16  6 56.0 0.00 0 3 JAPAN
31. N130. E
  0.0
BK-CN   89.5   220.0 0.8  16 19 49.8
NI-NV   87.7   472.0 1.6  16 19 39.4
NI2NV   87.8   423.9 1.5  16 19 39.5
27DEC76 18  8  8.0 0.00 0 3 JAPAN
42. N145. E
  0.0
BK-CN   74.     34.4 0.6  18 19 47.6
CB2NV   55.     19.0 0.6  18 19 36.7
NI2NV   56.     28.8 0.6  18 19 36.2
30DEC76  3 57  0.  0.00 1 3 E. KAZ
50. N 79. E
  0.0
BK-CN   79.2    38.6 0.6   4  9  6.7
CB2NV   92.0    14.6 0.8   4 10 14.0
NI-NV   91.8    17.4 0.5   4 10 12.0
31DEC76  9 16 37.  0.00 0 5 JAPAN
40. N145. E
  0.0
HN-ME   66.9    53.0 1.0   9 29 43.0
BK-CN   75.7    45.9 0.7   9 28 34.1
CB2NV   72.9    25.1 1.0   9 28 25.5
NI-NV   72.6    17.0 0.6   9 28 24.5
NI2NV   72.7    27.1 0.7   9 28 25.1
  1JAN77 11 33 42.4 5.13 0 4 JAPAN
30.6N137.2E
483.0
BK-CN   87.6   139.3 0.8  11 45 38.0
CB2NV   83.4    44.7 0.8  11 44 22.7
NI-NV   83.2   127.9 0.8  11 45 21.8
NI2NV   83.3   199.0 0.7  11 45 22.4
  7DEC76  4 57  0.0 0.00 1 4 E. KAZAKH
50. N 79. E
  0.0
HN-ME   79.9   267.9 0.9   5  9 10.7
BK-CN   79.2   582.8 0.4   5  9  5.9
NI-NV   91.9   100.0 0.8   5 10 11.6
NI2NV   91.9   116.6 0.7   5 10 11.4
  5JAN77 10 37 33.6 4.76 0 4 VOLCANO IS.
25.7N142.5E
 92.
BK-CN   66.5    31.4 0.8 10 50 17.9
CB2NV   62.3     5.9 1.0 10 49 49.3
NI-NV   62.0    12.5 0.7 10 49 49.5
NI2NV   62.1    22.9 1.3 10 49 49.0
  5JAN77 22 44 57.0 5.5  0 4 VOLCANO IS.
23.3N143.8E
  0.0
BK-CN   90.7   157.9 0.9 22 57 59.4
CB2NV   64.6   135.9 0.7 22 57 27.6
NI-NV   64.3   181.7 0.9 22 57 27.0
NI2NV   64.4   263.4 0.9 22 57 27.3
  6JAN77  7 55 55.5 5.24 0 5 KURILES
49.3N155.4E
  0.0
HN-ME   76.2    75.6 0.8   8  7 52.0
BK-CN   64.3    76.8 0.6   8  6 29.0
CB2NV   61.5    47.3 1.2   8  6 16.1
NI-NV   61.3    50.2 0.8   8  6 15.7
NI2NV   61.4    59.7 0.8   8  6 15.8
```

```
 6JAN77 16  2  3.6 5.36 0 4 ANDREANOF IS.
51.3N175.4W
   0.0
RK-CN   49.7  212.6 0.5 16 10 43.0
CB2NV   44.5   36.1 0.8 16 10 10.3
N1-NV   44.2   65.4 0.7 16 10 18.8
N12NV   44.3   27.8 0.7 16 10  7.6
22SEP76  0 16   9.3 6.05 0 5 KURILE IS.
44.6N149.1E
  55.0
HN-ME   83.3  675.  0.7    0 28 30.7
RK-CN   70.0 1898.2 1.1    0 27 14.8
CB2NV   67.7  650.3 0.9    0 27  1.5
N1-NV   67.5  798.0 0.78   0 27  0.7
N12NV   67.5 1036.5 0.7    0 27  0.9
17JAN77  6 23 42.6 5.32 0 4 BONIN IS.
26.7N142.6E
  76.
RK-CN   65.6   71.8 1.0    6 36 24.2
CB2NV   61.6   47.2 1.1    6 35 57.1
N1-NV   61.4   64.3 1.1    6 35 56.2
N12NV   61.5   96.4 1.1    6 35 56.5
17JAN77  9 42 22.5 4.68 0 4 S. OF ALASKA
53.6N158.7W
   0.0
RK-CN   36.1   49.4 0.6    9 49 46.7
CB2NV   31.6   29.9 0.8    9 49  3.8
N1-NV   31.4   39.6 0.8    9 49  2.2
N12NV   31.5   33.6 0.7    9 49  2.8
24JAN77  6 11 30.0 4.86 0 5 KURILE IS
45.5N150.9E
  64.
HN-ME   79.8   48.1 0.7    6 23 42.1
RK-CN   66.4   67.1 0.7    6 22 24.3
CB2NV   64.5   15.9 0.9    6 22  9.8
N1-NV   64.3   13.4 0.6    6 21 57.3
N12NV   64.4   22.6 0.7    6 22  3.2
 3FEB77 21 30 53.0 0.00 0 4 RUSSIA-CHINA BDR
43. N130. E
   0.0
HN-ME   65.4   57.8 0.5   21 43 53.4
RK-CN   78.7  290.4 0.4   21 42 53.3
CB2NV   79.8   52.1 0.5   21 43  3.1
N12NV   79.7  261.0 0.5   21 43  4.5
 6FEB77  0 31 29.  0.00 0 3 N. ATLANTIC
24. N 48. W
   0.0
RK-CN   44.1   42.3 0.7    0 39 27.3
CB2NV   58.8   43.4 1.0    0 41  3.7
N12NV   59.0  101.3 0.8    0 41  5.4
13FEB77  5 51 11.  0.00 0 4 KAMCHATKA
52. N160. E
   0.0
HN-ME   73.5  120.4 0.6    6  2 55.4
RK-CN   59.9  139.4 0.6    6  1 30.2
CB2NV   58.1   81.3 0.7    6  1 24.8
N12NV   57.9  187.6 0.8    6  1 24.3
16FEB77  0 50 18.0 0.00 0 3 N ATLANTIC OCEAN
32. N 25. W
   0.0
HN-ME   36.    34.5 0.7    0 56 53.3
RK-CN   53.    85.9 0.9    0 59  8.9
N12NV   72.    16.4 0.7    1  1 11.8
16FEB77  1  5 48.  0.00 0 2 N PACIFIC OCEAN
38. N159. E
   0.0
RK-CN   75.1   20.5 0.5   12 39 57.4
N12NV   70.6   13.4 0.4   12 39 50.2
```

```
17FEB77 13 32   7.0 0.00 0 3 KOMANDORSKI
56. N166. E
  0.0
RK-CN   54.6     94.6 1.0   13 41 52.7
OB2NV   53.5      7.1 1.2   13 41 55.6
NT2NV   53.3     31.9 0.8   13 41 55.1
18FEB77 20 51  26.0 0.00 0 4 JAPAN
34. N142. E
  0.0
HN-ME   55.      66.9 1.2   21  4 57.8
RK-CN   62.     416.4 0.8   21  3 53.5
OB2NV   76.     425.3 1.0   21  3 35.8
NT2NV   76.     903.8 1.0   21  3 35.4
19FEB77  4   1 58.0 0.00 0 3 N PACIFIC OCEAN
31. N147. E
  0.0
RK-CN   62.3     21.0 0.8    4 14 47.6
CB2NV   76.7     24.1 1.2    4 14 29.3
NT2NV   76.5    494.0 1.0    4 14 29.2
19FEB77  5 51   1.  0.00 0 3 KAMCHATKA
51. N156. E
  0.0
RK-CN   62.3     28.7 0.6    6  1 18.1
CB2NV   60.8     93.0 0.8    6  1  8.2
NT2NV   60.6     23.1 0.6    6  1  8.0
19FEB77 22 33  55.0 0.00 0 4 ALEUTIANS
53. N173. E
  0.0
HN-ME   68.0    700.1 0.9   22 45  7.4
RK-CN   53.3    567.1 0.6   22 43 29.7
OB2NV   50.2    232.6 1.0   22 42 21.3
NT2NV   50.1    533.0 1.0   22 43 11.0
19FEB77 22 47   7.  0.00 0 3 ALEUTIANS
49. N175. E
  0.0
RK-CN   54.8     91.6 0.6   22 57  6.3
OB2NV   49.9     21.1 0.5   22 56 47.3
NT2NV   49.7     48.5 0.7   22 56 46.6
20FEB77  7   2  0.0 0.00 0 2 KODIAK IS. REG.
56. N152. W
  0.0
RK-CN   34.1     12.4 0.7    7  9  8.6
CB2NV   30.4      5.6 0.8    7  8 41.9
20FEB77  8   0 36.0 0.00 0 3 ALEUTIANS
51. N174. E
  0.0
RK-CN   54.1    192.0 0.7    8 10 24.7
CB2NV   50.0      6.4 0.5    8 10  5.6
NT2NV   49.9     16.2 0.7    8 10  4.5
 8MAR77 22 46  44.  0.00 0 5 N. BRAZIL
 8. S  63. W
  0.0
HN-ME   54.3    160.5 1.3   22 56  1.0
RK-CN   64.5    290.7 1.0   22 56 44.6
OB2NV   67.0     70.0 1.0   22 56 33.8
NT-NV   67.1    163.3 1.3   -1
NT2NV   67.2    115.9 1.2   22 56 35.3
 9MAR77 14 27   5.  0.00 0 3 N.E. CHINA BDR
42. N130. E
  0.0
HN-ME   90.4    930.1 0.7   14 40  2.0
RK-CN   79.6   5374.3 0.8   14 39  7.6
OB2NV   80.5   2887.5 0.8   14 39 12.0
12MAR77  2 58  55.0 0.00 0 4 N. ATLANTIC RIDGE
32. N  41. W
  0.0
RK-CN   42.6    115.0 1.0    3  6 12.2
CB2NV   60.3    177.9 1.2    3  3  6.2
NT-NV   60.6    294.7 0.8    3  6  9.1
NT2NV   60.5    236.0 1.1    3  6  7.6
```

```
13MAR77  4 55 55.0 0.00 0 5 BRAZIL
 2. S  56. W
   0.0
HN-ME   49.0    56.3 1.1    5  4 55.1
BR-CN   60.9   313.6 0.7    5  5 44.6
CB2NV   66.4   144.2 0.6    5  5 38.6
NT-NV   66.7   220.1 0.6    5  5 40.3
NT2NV   66.6   183.6 0.8    5  5 39.9
13MAR77 21 15 17.0 0.00 0 5 VENEZUELA
 1. N  64. W
   0.0
HN-ME   45.3    57.7 0.9   21 23 44.5
BR-CN   55.8   119.8 0.8   21 24 28.4
CB2NV   60.0   152.3 0.8   21 24 21.0
NT-NV   60.3   314.1 1.0   21 24 23.5
NT2NV   60.2   300.2 0.9   21 24 22.5
15MAR77 21 28  9.0 0.00 0 4 COSTA RICA
 9. N  83. W
   0.0
BR-CN   42.7   180.9 0.7   21 36 28.9
CB2NV   41.1    55.9 0.7   21 34 57.9
NT-NV   41.3   272.5 0.7   21 35  0.0
NT2NV   41.3   200.2 0.7   21 34 59.5
16MAR77  6 22 19.0 0.00 0 4 ALASKA PEN.
56. N155. W
   0.0
BR-CN   35.7    16.5 0.7    6 30 28.4
CB2NV   32.0    13.4 0.8    6 28 53.7
NT-NV   31.8    38.5 0.7    6 28 52.9
NT2NV   31.9    31.4 0.8    6 28 53.5
19MAR77 10 56  6.0 0.00 0 5 KURILES
43. N149. E
   0.0
HN-ME   85.0   434.7 0.7   11  8 51.6
BR-CN   71.5   524.0 0.7   11  7 36.8
CB2NV   68.7   351.9 0.8   11  7 23.7
NT-NV   68.5   392.4 0.8   11  7 22.7
NT2NV   68.6   498.4 0.6   11  7 23.2
 4MAR77 19 21 40.0 0.00 0 4 RUMANIA
44. N  26. E
   0.0
BR-CN   71.7  1055.9 0.6   19 32 59.9
CB2NV   91.8   117.3 0.7   19 34 49.9
NT-NV   91.9   229.9 0.7   19 34 50.8
NT2NV   91.9   239.3 0.8   19 34 50.9
 7MAR77  0 29 11.0 0.00 0 4 N.E. CHINA
43. N114. E
   0.0
BR-CN   83.1    51.3 0.3    0 41 19.8
CB2NV   87.8     7.7 0.7    0 41 17.2
NT-NV   87.6    39.0 0.5    0 41 37.8
NT2NV   87.6    53.8 1.2    0 41 37.5
 7MAR77  9 11 55.0 0.00 0 4 N. PACIFIC
39. N145. E
   0.0
BR-CN   74.7    73.5 0.6    9 23 57.0
CB2NV   70.9   137.3 0.6    9 23 45.3
NT-NV   70.6   220.5 0.7    9 23 44.3
NT2NV   70.7   202.7 0.5    9 23 45.0
21MAR77  4 36 38.0 0.00 0 4 VOLCANO IS.
23. N143. E
   0.0
BR-CN   90.9     9.1 0.7    4 49 36.1
CB2NV   84.4    22.3 1.0    4 48 51.4
NT-NV   84.1    13.8 0.8    4 48 49.4
NT2NV   84.2    41.6 1.0    4 48 51.0
```

```
21MAR77  6 58 18.0 0.00 0 4 MARIANA IS.
21. N141. E
   C.0
BR-CN   93.6     6.9 0.6    7 11 20.9
CB2NV   87.1    29.3 1.0    7 10 37.6
NT-NV   88.8    52.7 0.8    7 10 36.5
NT2NV   86.9    65.4 0.8    7 10 37.0
23MAR77  2 11 25.0 0.00 0 4 CST. VENEZUELA
11. N 69. W
   C.0
BR-CN   44.7 2174.6 0.5    2 19 31.5
CB2NV   49.6  274.5 0.6    2 19 50.6
NT-NV   49.9  665.9 0.7    2 19 53.1
NT2NV   49.8  676.5 0.6    2 19 52.4
23MAR77  3 46 10.0 0.00 0 4 HOKKAIDO
45. N145. E
   C.0
BR-CN   71.6    21.7 0.7    3 57 24.5
CB2NV   70.1    12.7 0.8    3 57 12.0
NT-NV   69.8    31.2 0.7    3 57 23.0
NT2NV   69.9    12.7 0.5    3 57 11.7
26MAR77  4 36 10.0 0.00 0 4 FOX IS.
52. N168. W
   C.0
BR-CN   44.3   167.5 0.9    4 44 22.3
CB2NV   38.8   195.9 1.0    4 43 40.9
NT-NV   38.6   239.0 1.1    4 43 39.3
NT2NV   38.7   216.7 1.1    4 43 39.9
29MAR77  3 57  0.0 0.00 1 3 E. KAZAKH
50. N 78. E
   C.0
BR-CN   78.9    76.4 0.4    4  9  6.5
CB2NV   91.9    33.7 0.7    4 10 13.1
NT-NV   91.8    45.6 0.6    4 10 13.7
 5APR77  7 34 58.1 0.00 0 2 S. PERU
15. S 70. W
   C.0
BR-CN   69.1    24.0 0.6    7 45 52.4
CB2NV   67.8    64.1 0.8    7 45 44.1
 5APR77  7 39 49.5 0.00 0 2 KAMCHATKA
54.3N161.9E
   C.0
BR-CN   57.8    11.0 0.7    7 49 39.6
CB2NV   67.8     5.5 0.6    7 49 26.1
 9APR77 17 16  5.5 0.00 0 2 ARGENTINA
27.9S 67.0W
   C.0
BR-CN   82.0    26.2 0.61 17 28  3.3
CB2NV   79.6     9.5 0.75 17 27 53.1
10APR77  8 31 24.6 0.00 0 3 KURILES
44.6N147.2E
   C.0
BR-CN   71.2    98.0 0.54  8 42 44.1
CB2NV   69.1   135.8 0.91  8 42 32.0
YP-NV   69.    445.4 0.8   8 43  1.9
10APR77 18 45 18.1 0.00 0 2 KAMCHATKA
52.6N158.8E
120.0
BR-CN   60.1    12.7 0.5  18 55 11.9
CB2NV   58.6     5.7 0.42 18 55  3.3
12APR77  3 54 41.7 0.00 0 2 KOMANDORSKY
56. N164. E
   C.0
BR-CN   55.5    25.7 0.6    4  4 18.0
YP-NV   52.0    54.3 0.6    4  4 13.6
13APR77 18 20 38.3 0.00 0 2 RAT IS.
51.5N179.6W
   C.0
BR-CN   50.7    47.2 0.6  18 29 39.4
CB2NV   46.1    95.3 0.8  18 29  5.1
```

```
15APR77 23 35 36.9 0.00 0 2 N. CHILE
22.9S 68.8W
109.0
BK-CN   76.6   193.5 0.7   23 47 17.7
CB2NV   74.7   142.4 1.0   23 47  7.8
16APR77  4  2 18.2 0.00 0 2 ALEUTIANS
52.1N170.5W
  0.0
BK-CN   45.7    25.4 0.8    4 10 39.3
CB2NV   40.4     8.7 0.9    4  9 55.3
17APR77  2 41 10.8 0.00 0 2 CHILE-ARGENTINA
33.4S 68.8W
  0.0
BK-CN   86.9    73.3 0.9    2 53 56.3
CB2NV   83.0    51.6 0.9    2 53 38.5
20APR77  0 19 18.1 0.00 0 2 ALEUTIANS
51. N179. W
 52.0
BK-CN   50.6    14.7 0.45   0 28 10.3
CB2NV   45.7     6.0 0.6    0 27 35.5
20APR77 20  4 29.7 0.00 0 2 JAPAN
30.7N137.5E
  0.0
BK-CN   87.0   916.1 0.82  20 16 23.3
YP-NV   83.    824.8 0.7   20 16  8.2
21APR77  1 45 46.9 0.00 0 3 N. PACIFIC
26.7N142.6E
  0.0
BK-CN   88.1    77.6 1.0    1 59 38.6
CB2NV   82.5    44.8 1.0    1 58 11.6
YP-NV   83.    147.5 0.4    1 58 21.3
22APR77  0 52  5.2 0.00 0 2 KAMCHATKA
52.5N153.8E
406.0
BK-CN   62.2    65.3 0.6    1  1 46.0
CB2NV   61.5   104.2 1.0    1  1 41.7
23APR77  1 32 43.5 0.00 0 2 JAPAN
27.6N127.0E
 20.0
BK-CN   93.9     5.6 0.7    1 45 55.8
CB2NV   92.4     7.0 1.0    1 45 50.6
23APR77 14 49  5.7 0.00 0 3 NEW SIBERIAN IS.
75.0N134.9E
  0.0
BK-CN   60.2    46.4 0.8   14 58  1.6
CB2NV   58.9    44.9 0.8   14 59  7.4
YP-NV   59.     96.9 0.8   14 59  9.3
24APR77 20 42 39.9 0.00 0 2 JAPAN
40.2N142.7E
  0.0
BK-CN   76.7    19.3 0.7   20 54 31.5
CB2NV   74.3     7.2 0.6   20 54 20.2
25APR77  4  6 59.9 0.00 0 2 E. KAZAKH
49.8N 78.3E
  0.0
BK-CN   79.3    39.1 0.48   4 19  6.4
CB2NV   92.2    16.1 0.7    4 20 12.1
26APR77 23  6 38.0 0.00 0 2 KURILES
43.4N146.0E
  0.0
BK-CN   71.8     7.9 1.0   23 19  0.7
CB2NV   69.3    29.7 0.5   23 17 46.9
30APR77 16 22 42.7 0.00 0 2 N. ATLANTIC OCEAN
32.3N 40.4W
  0.0
BK-CN   42.9    10.0 0.6   16 30 41.7
CB2NV   60.7    17.0 1.0   16 32 57.3
30APR77 16 44 15.6 0.00 0 2 ANDREANOF IS.
52.1N173.0W
186.0
BK-CN   47.0    38.6 0.6   16 52 27.8
CB2NV   41.9     7.  0.6   16 51 46.8
```

```
30APR77 20 31 58.0 0.00 0 2 PERU
14.9S 75.3W
 80.0
BK-CN   67.8    49.9 0.7   20 42 44.9
CB2NV   64.6    28.7 0.5   20 42 23.7
30APR77 21 49 45.5 0.00 0 3 ALEUTIANS
52.1N173.4W
 36.0
BK-ME   63.     41.  0.7   22  0  7.5
BK-CN   43.2    87.2 0.4   21 58 13.3
CB2NV   42.2    56.2 0.65  21 57 27.6
 1MAY77  0  9  8.0 0.00 0 2 PERU
 6.1S 77.0W
125.0
BK-CN   56.7   188.  0.63   0 16 50.5
CB2NV   56.6    42.2 0.7    0 13 37.9
 5MAY77 22 14 35.7 0.00 0 2 HOKKAIDO
42.1N142.3E
 52.0
BK-CN   75.0    59.6 0.72  22 26 11.8          38.4 0.5
BK-ME   88.0    38.7 0.8   22 27 19.7
 6MAY77  3 53 37.5 0.00 0 4 KURILES
45.0N152.0E
 70.0
CB2NV   65.4    47.3 0.6    4  4 13.6          43.1 1.0
BK-CN   67.8   163.  0.9    4  4 28.2          89.0 0.7
BK-ME   80.0    78.5 0.8    4  5 46.8
YE-NV   65.5   141.7 0.8    4  4 14.4
 6MAY77 12 52 36.7 0.00 0 2 PERU COAST
15.6S 74.7W
  0.0
CB2NV   65.6    17.  1.0   13  3 21.9           9.3 1.0
BK-CN   66.5    38.4 0.8   13  3 37.9
 6MAY77 20 31 56.7 0.00 0 2 CENT. AMER. COAST
11.9N 88.3W
  0.0
BK-CN   39.2    51.1 0.7   20 39 24.1          45.5 0.7
CB2NV   35.5    44.4 0.4   20 33 55.6          25.7 0.55
 7MAY77  2 13 23.9 0.00 0 2 JAN MAYEN IS.
71.8N  1.3W
  0.0
BK-CN   43.2    76.7 1.2    2 21 32.3          14.8 1.1
CB2NV   61.9    69.7 0.9    2 23 51.7          26.0 0.75
 9MAY77 12 19 16.1 0.00 0 2 N. CHILE
21.9S 69.1W
120.0
CB2NV   73.8    36.5 1.0   12 30 38.6          31.8 0.8
BK-CN   75.9    23.8 0.84  12 30 46.9          23.8 0.84
 9MAY77 15  2 49.  0.00 0 2 E. CHINA SEA
27.2N126.8E
135.0
CB2NV   92.6    27.0 1.4   15 15 47.4          16.0 0.85
BK-CN   94.2    58.7 0.67  15 15 52.6          33.0 0.65
10MAY77  6 49 27.8 0.00 0 2 PERU-BRAZIL BDR
 8.1S 74.8W
  0.0
BK-CN   61.1    10.0 0.5    6 59 42.4          10.0 0.5
CB2NV   59.5     7.2 0.6    6 59 35.7           2.8 0.5
12MAY77 21 37 32.3 0.00 0 3 KURILES
50.1N154.9E
100.0
BK-CN   63.4   229.  0.6   21 47 52.4         214.0 0.6
CB2NV   61.8    37.  0.99  21 47 41.6          30.0 0.7
BK-ME   76.0   263.  0.89  21 49 14.2
12MAY77 11 17 52.1 0.00 0 2 N.E. CHINA
39.4N117.6E
  0.0
CB2NV   88.8    21.7 0.7   11 30 50.2
BK-CN   85.6    50.5 0.59  11 30 32.0
```

```
13MAY77  3  2 38.2 0.00 0 2 MEXICO-GUATEMALA BR
15.0N 91.5W
254.0
BK-CN   34.9   18.2 0.75   3  9  7.1         11.9 0.8
CB2NV   30.3   21.4 0.9    3  8 25.5
13MAY77 13 35  14.4 0.00 0 2 N. PERU
 5.5S 77.0W
 12.0
BK-CN   56.1   31.1 0.6   13 45  5.9         17.9  .4
CB2NV   56.1   14.5 1.05  13 44 53.8         10.7 1.2
14MAY77  6  4  45.9 0.00 0 3 ECUADOR COAST
 1.6N 65.1W
 63.0
BK-CN   45.6   45.6 1.6    6 13 29.2          4.2  .36
CB2NV   45.6   48.0 1.8    6 12 58.1          9.4 1.3
CB3NV   45.6   48.4 1.8    6 12 58.0
22JUL77 16 48  57.6 0.00 0 2 CENT. AMER. CST.
 3.9N 83.4W
  0.0
FA-NV   45.8   21.1 1.7   16 57 17.5
GE-NM   39.4   30.6 1.5   16 56 27.0
22JUL77 17 16  57.1 0.00 0 2 KERMADEC IS.
33.4S179.9W
153.0
FA-NV   93.1   62.2 0.6   17 29 52.5
GE-NM   97.4   15.6 2.0   17 30 11.3
23JUL77 13 45   1.3 0.00 0 4 ALASKA PEN.
54.5N162.4W
 60.0
CB2NV   35.7   55.3 0.91  13 51 53.9         28.4 0.92
CB3NV   35.7   49.2 0.94  13 51 53.8
FA-NV   34.7   21.0 0.8   13 51 44.5
GE-NM   41.2   12.0 0.7   13 52 39.0
24JUL77  5 44  53.3 0.00 0 4 VENEZUELA CST.
11.7N 68.6W
 65.0
CB2NV   49.3    9.7 0.66   5 53 39.6          8.2 0.7
CB3NV   49.3    9.9 0.65   5 53 39.6
FA-NV   49.9    7.9 0.8    5 53 34.5
GE-NM   42.6   27.0 0.7    5 52 47.0
24JUL77  6 23  18.2 0.00 0 7 TONGA IS.
15.2S173.6W
260.0
YK-NV   75.2  200.5 1.22   6 34 30.6
BK-ON   95.5   46.9 1.5    6 36 12.1         46.9 1.7
YK2NV   75.2  244.  1.35   6 34 30.6
CB2NV   75.3   72.9 1.8    6 34 30.5         25.6 1.7
CB3NV   75.3   74.4 1.8    6 34 30.3
FA-NV   75.9  125.0 2.3    6 34 34.0
GE-NM   81.2  128.2 1.8    6 35  3.0
24JUL77 16 19  50.1 0.00 0 4 N. ATLANTIC
17.8N 46.1W
  0.0
CB2NV   63.6    7.6 1.3   16 30 23.7          6.7 1.1
CB3NV   63.6    8.0 1.3   16 30 23.6
FA-NV   63.6    5.9 0.5   16 30 24.0
GE-NM   56.5   11.4 0.8   16 29 35.3
25JUL77  0  5  55.3 0.00 0 3 SAKHALIN IS.
51.7N142.9E
 45.0
CB2NV   67.6   10.0 1.3    0 16 49.8          5.0 0.8
FA-NV   66.5   11.0 1.8    0 16 43.5
GE-NM   72.5    9.0 1.2    0 17 18.0
25JUL77 12 59  45.4 0.00 0 4 FIGI IS
25.6S178.9E
657.0
CB2NV   67.6   21.5 0.8   13 11 13.6         14.3 0.8
CB3NV   67.6   20.4 0.8   13 11 15.6
FA-NV   86.3    5.5 0.7   13 11 22.0
GE-NM   93.3    6.0 1.4   13 11 43.3
```

```
25JUL77 17  5   3.1 0.00 0 2 PERU
11.7S 75.1W
  C.0
FA-NV   63.3    13.1 1.3   17 15 35.5
GE-NM   57.C    11.4 1.0   17 14 50.7
26JUL77  4 25  23.0 0.00 0 4 JAPAN
33.8N141.1E
143.0
CB2NV   75.4    43.4 0.88   4 36 53.1          41.0 0.78
CB3NV   75.4    46.1 0.66   4 36 53.2
FA-NV   74.4    21.4 0.9    4 36 47.5
GE-NM   81.1    39.8 0.8    4 37 24.0
26JUL77  7 43   5.8 0.00 0 4 CHILE-ARGENTINA BDR
31.1S 70.2W
125.0
CB2NV   80.6    21.7 0.81   7 55  5.3          18.5 0.84
CB3NV   80.6    19.9 0.8    7 55  5.4
FA-NV   81.8    26.2 0.7    7 55 11.5
GE-NM   76.1    26.3 0.9    7 54 33.5
26JUL77 10 28   0.0 0.00 0 4 SAMOA IS
15.9S171.9W
 43.C
CB2NV   75.4    16.6 1.08  10 39 39.2          14.0 0.9
CB3NV   75.4    13.9 0.92  10 39 39.2
FA-NV   76.1    27.6 0.7   10 39 43.3
GE-NM   91.1    10.0 1.2   10 40 11.0
26JUL77 16 59  59.9 0.00 0 4 SIBERIA
69.4N 90.4E
  C.0
CB2NV   71.6    20.9 0.96  17 11 23.2          15.5 0.72
CB3NV   71.6    29.5 0.78  17 11 23.1
FA-NV   70.2    22.8 1.0   17 11 13.0
GE-NM   73.1    35.3 0.7   17 11 31.7
27JUL77  2 55   4.4 0.00 0 4 TONGA IS.
16.8S173.5W
  C.0
CB2NV   76.4    25.0 1.0    3  6 54.8          22.6 1.0
CB3NV   76.4    24.3 1.1    3  6 54.8
FA-NV   77.1    26.0 1.0    3  6 59.5
GE-NM   82.2    30.4 1.1    3  7 23.0
29JUL77  9 50  29.0 0.00 0 2 PACIFIC OCEAN
 1.5N107.0W
  C.C
FA-NV   38.1    12.0 1.0    9 57 47.0
GE-NM   35.2    12.9 0.8    9 56 33.5
29JUL77 16 51  10.6 0.00 0 4 TONGA IS.
13.2S175.2W
145.0
CB2NV   79.2    35.0 0.8   17  2 59.6          29.1 0.8
CB3NV   79.2    34.1 0.72  17  2 58.6
FA-NV   79.9    24.0 0.7   17  3  2.0
GE-NM   85.0    19.1 1.1   17  3 28.3
30JUL77  1 56  59.9 0.00 1 2 E. KAZAKH
49.7N 78.2E
  C.0
FA-NV   90.7    12.0 0.7    2 10  6.5
GE-NM   93.5    19.6 0.8    2 10 19.0
30JUL77  5 22  16.3 0.00 0 4 N. PERU
 5.6S 77.3W
  C.C
CB2NV   56.0    12.6 1.1    5 31 55.9          10.8 1.26
CB3NV   56.0    13.1 1.12   5 31 56.1
FA-NV   57.0    18.4 1.3    5 32  3.5
GE-NM   50.7    50.0 0.8    5 31 16.0
30JUL77  5 45  49.1 0.00 0 4 CHILE COAST
30.6S 71.4W
  C.0
CB2NV   79.6    38.6 1.05   5 57 52.3          30.7 1.15
CB3NV   79.6    41.4 1.05   5 57 51.9
FA-NV   80.8    28.8 0.8    5 57 39.0
GE-NM   75.2    54.2 1.0    5 57 26.0
```

```
30JUL77  7 56 36.4 0.00 0 4 EL SALVADOR
13.2N 88.5W
 55.0
CB2NV   34.4    14.0 0.81  8  3 18.2          9.8 0.85
CB3NV   34.4    13.6 0.71  8  3 18.2
FA-NV   35.3    25.2 0.7   6  3 26.7
GE-NM   26.9    31.8 0.8   8  2 29.3
31JUL77  2 41 33.3 0.00 0 2 FIGI IS.
19.4S176.2E
  0.0
FA-NV   85.8    11.5 1.7   2 54 14.0
GE-NM   91.3    10.8 1.1   2 54 41.0
31JUL77 22 10 47.9 0.00 0 2 NEW HEBRIDES
15.0S168.1E
  0.0
FA-NV   86.5     8.5 1.7  22 23 43.4
GE-NM   94.7    27.1 0.6  22 24  8.5
25MAY77 12 09 58.4 0.00 0 4 FIJI IS.
17.3S178.8W
526.
YP-NV   80.3   310.0 1.0  12 21 15.3
YP2NV   80.3   361.0 1.0  12 21 15.3
CE2NV   80.3   163.0 1.2  12 21 15.2         128.0 1.0
CE3NV   80.3   177.0 1.2  12 21 13.3
29MAY77 02 57 00.4 0.00 1 7 E. KAZAKH
49.9N 78.9E
  5.0
GE-NM   93.2     9.5 0.7   3 10 18.3   62
YP-NV   92.0   189.0 1.0  03 10 12.7
YP2NV   92.0   218.0 1.0  03 10 12.6
BR-CN   79.0   546.0 0.5  03 09 06.1         446.0  .55
CB2NV   91.9    95.9 0.9  03 10 11.6          50.0  .96
CB3NV   91.9    93.7 0.8   3 10 11.7
HN-ME   79.7   204.3 1.0  03 09 10.7
29MAY77 02 22 01.7 0.00 0 4 COAST W. PAKISTAN
23.4N 64.6E
  0.0
YP-NV  119.5   843.0 0.4  02 39 34.7
YP2NV  119.5   836.0 0.4  02 39 34.8
CE2NV  119.3    60.1 0.6  02 39 36.5          9.2  .45
CE3NV  119.3    60.5 0.7  02 39 36.7
02JUN77 14 55 33.1 0.00 0 4 ICELAND
63.6N 19.1W
  0.0
GE-NM   56.8     8.0 1.3  15  3 21.0   94
BR-CN   39.7    35.9 1.4  15 03 07.0          23.5 1.3
CB2NV   60.0    22.7 1.6  15 05 43.3
CE3NV   60.0    22.1 0.6  15  5 43.2
02JUN77 16 50 36.1 0.00 0 8 CHILE-BOLIVIA BORDER
20.9S 68.6W
094.0
GE-NM   68.1    11.0 0.9  17  1 25.3   94
YP4NV   73.2   168.5 1.0  17 01 56.7
YP3NV   73.2   126.0 1.0  17 01 56.6
YP-NV   73.2   169.0 1.0  17 01 56.9
YP2NV   73.2   121.3 1.0  17 01 56.9
CE2NV   73.3   122.0 0.9  17 01 57.1          44.0 1.0
BR-CN   75.0   120.0 0.8  17 02 05.1          57.6 0.9
CB3NV   73.3    99.0 1.0  17 01 57.1
05JUN77 02 46 06.8 0.00 010 NEAR COAST N. CHILE
24.0S 70.5W
030.0
FA-NV   75.9     9.0 0.5   2 57 51.0   48
GE-NM   65.9    15.0 1.5   2 57 15.0   99
YP4NV   74.6   126.0 1.0  02 57 44.3
YP3NV   74.6   132.0 1.1  02 57 44.2
YP-NV   74.6   110.0 1.2  02 57 44.0
YP2NV   74.6   129.0 1.2  02 57 44.0
BR-CN   77.6   131.6 1.5  02 57 57.4
HN-ME   70.2    93.0 2.3  02 57 14.6
CE2NV   74.7    68.0 1.6  02 57 34.6
CE3NV   74.7    66.5 1.5  02 57 34.6
```

```
05JUN77 06 41 17.9 0.00 C 9 HOKKAIDO, JAPAN
42.4N142.8E
  C.0
FA-NV   71.8     9.0 0.5   6 52 43.3  550
GE-NM   76.4    43.0 1.0   6 53 22.0 1042
YF4NV   73.0    75.0 0.7  06 52 50.3
YF3NV   73.0    60.0 0.6  06 52 51.0
YF-NV   73.0    61.0 0.6  06 52 50.8
YF2NV   73.0    60.0 0.7  06 52 50.9
BR-CN   74.6    22.5 0.6  06 52 56.7                22.0  .6
CB2NV   72.9    20.0 0.7  06 52 49.9                15.6  .7
CB3NV   72.9    20.6 0.7  06 52 49.9
05JUN77 15 19 13.0 0.00 C 8 NEW BRITAIN
04.6S152.2E
123.0
FA-NV   94.1     5.5 1.0  15 32 18.0    47
GE-NM  101.2     8.0 0.8  15 32 51.0    99
YF4NV   94.2   320.0 0.9  15 32 19.0
YF-NV   94.2   261.0 0.8  15 32 19.1
YF2NV   94.2   308.0 0.8  15 32 19.1
BB-ME  125.8    43.0 1.1  15 38 00.0
CB2NV   94.1   133.0 0.9  15 32 18.1                78.0 1.0
CB3NV   94.1   123.0 0.9  15 32 18.2
08JUN77 13 25 16.0 0.00 C 9 CHILE-BOLIVIA BORDER
22.1S 67.3W
135.0
FA-NV   76.1    16.0 1.3  13 36 48.5    35
GE-NM   69.8    35.0 1.3  13 36 11.3    99
YF-NV   74.8   430.0 1.0  13 36 42.3
YF2NV   74.8   537.0 1.1  13 36 42.5
BB-ME   68.3    80.1 1.2  13 36 01.2
CB2NV   75.0   244.0 1.2  13 36 42.5               196.0 1.2
YF4NV   74.8   408.0 1.4  13 36 42.3
YF3NV   74.8   550.0 1.3  13 36 42.3
09JUN77 14 25 49.0 0.00 C 7 NEAR E COAST HONSHU
33.5N141.5E
063.0
FA-NV   75.0    10.5 1.5  14 37 22.5    35
YF-NV   76.1   400.0 1.3  14 37 29.1
YF2NV   76.1   545.0 1.2  14 37 29.0
CB2NV   76.0   164.0 1.1  14 37 28.2                84.0 1.1
CB3NV   76.0   150.0 1.2  14 37 28.2
YF4NV   76.1   449.0 1.1  14 37 29.0
YF3NV   76.1   487.0 1.2  14 37 29.0
17JUN77 02 29 22.3 0.00 C 6 FIJI ISLANDS
19.7S179.2W
774.0
FA-NV   82.9    36.0 0.8   2 40 27.0    65
YF4NV   82.2   828.0 0.9  02 40 23.4
YF3NV   82.2   651.0 1.0  02 40 23.3
YF-NV   82.2   773.0 1.1  02 40 23.4
YF2NV   82.2   723.0 1.2  02 40 23.4
CB2NV   82.2   382.0 0.9  02 40 23.3
17JUN77 14 45 11.5 0.00 C 5 MARIANA ISLANDS
19.1N145.8E
107.0
FA-NV   84.1    14.0 0.6  14 57 31.6    65
YF-NV   84.8   493.0 1.3  14 57 35.4
YF2NV   84.8   549.0 1.1  14 57 35.4
CB2NV   84.7   204.0 0.9  14 57 34.6               127.0 0.75
CB3NV   84.7   213.0 1.0  14 57 34.6
14JUL77 07 15 35.0 0.00 0 5 ICELAND
64.7N017.1W
  C.0
FA-NV   59.2    12.5 2.0   7 25 39.0  420
GE-NM   57.3    31.  1.3   7 25 24.6  781
CB2NV   60.4     7.4 1.3  07 25 45.9                 3.4 0.8
BR-CN   40.2    18.3 0.9  07 23 13.5                14.7 0.7
CB3NV   60.4     7.5 1.2  07 25 45.9
```

```
21JUL77 07 01 39.3 0.00 0 4 NEW HEBRIDES IS.
18.5S166.5E
337.0
YK-NV   90.1    54.0 1.0   07 13 54.7
CB2NV   90.1    20.0 1.0   07 13 54.4          16.5 0.85
CB3NV   90.1    21.0 1.0   07 13 54.5
YK2NV   90.1    50.0 1.0   07 13 54.7
24JUL77 19 55 38.9 0.00 0 8 MARIANA ISLANDS
19.4N144.9E
438.0
YK-NV   85.3   405.0 0.65  20 07 32.1
YK4NV   85.3   565.0 0.8   20 07 32.0
EK-CN   93.0    15.0 1.0   20 08 34.2           9.0 0.6
CB2NV   85.0   329.3 0.7   20 07 31.3          47.1 0.87
YK3NV   85.3   461.0 0.7   20 07 32.0
YK2NV   85.3   552.0 0.7   20 07 32.2
FA-NV   84.6   116.1 0.6   20  7 23.0
GE-NM   91.9   141.0 1.0   20  3  2.0
25JUL77 04 51 37.7 0.00 0 9 CARIBBEAN SEA
17.8N061.6W
  0.0
YK-NV   35.8    74.0 0.95  04 58 33.3
YK4NV   35.8    63.8 0.8   04 58 33.7
EK-CN   34.4    89.0 1.4   04 53 25.1          52.6 0.9
CB2NV   36.0    39.8 0.95  04 58 40.0
CB3NV   36.0    40.0 0.9   04 58 40.0
YK3NV   35.8    92.7 1.2   04 58 39.5
YK2NV   35.8    67.0 1.1   04 58 33.3
FA-NV   36.6    20.7 0.3    4 58 46.0
GE-NM   29.4    18.0 1.3    4 57 42.7
27JUL77 17 16 58.8 0.00 0 4 MARIANA ISLANDS
21.8N143.0E
219.0
YK-NV   85.2   276.9 0.5   17 29 11.6
YK4NV   85.2   413.9 0.7   17 29 11.4
YK3NV   85.2   323.0 0.7   17 29 11.4
YK2NV   85.2   369.0 0.6   17 29 11.5
29JUL77 11 15 47.3 0.00 0 9 SOLOMON ISLANDS
 8.0S155.6E
 31.0
YK-NV   93.5   465.0 1.0   11 29 04.6
YK4NV   93.5   577.6 1.1   11 29  4.5
CB2NV   93.5   177.0 1.5   11 29 00.0           5.6 0.9
CB3NV   93.5   177.0 1.4   11 28 53.0
EK-ME  126.6   424.0 1.1   11 34 47.6
YK2NV   93.5   646.0 1.1   11 29 04.6
YK3NV   93.5   600.0 1.0   11 29  4.5
FA-NV   93.5   287.8 1.5   11 29  1.5
GE-NM  100.5    16.4 1.5   11 29 35.0
30MAY77 10 20 02.8 0.00 0 7 OFF CST C. AMERICA
 5.9N 86.2W
  0.0
GE-NM   36.3    27.0 1.3   10 27  9.6 1042
YK-NV   41.3    43.9 1.3   10 27 53.5
YK2NV   41.3    51.5 1.3   10 27 52.3
YK4NV   41.3    46.9 1.3   10 27 53.7
YK3NV   41.3    43.8 1.4   10 27 53.3
CB2NV   41.5    18.7 1.4   10 27 54.1
CB3NV   41.5    19.0 1.4   10 27 54.3
30MAY77 15 16 05.1 0.00 0 9 FOX IS. ALEUTIANS
52.3N169.7W
 50.0
GE-NM   45.6    10.0 1.0   15 24 21.0   62
YK-NV   40.0    51.9 0.6   15 23 38.5
YK2NV   40.0    52.9 0.5   15 23 38.3
YK4NV   40.0    65.9 0.8   15 23 37.6
YK3NV   40.0    59.0 0.9   15 23 37.6
CB2NV   39.9    29.0 1.0   15 23 36.1
CB3NV   39.9    25.4 1.3   15 23 36.0
EK-CN   45.0   270.0 1.0   15 24 15.6
EK-ME   61.0    68.0 1.1   15 26 13.3
```

```
28JAN77 04 24 26.0 0.00 0 2 BONIN ISLANDS
29.0N139.0E
   0.0
FR-CN    67.8      21.6 0.5   04 37 16.8
CB2NV    83.6      38.5 0.7   04 36 58.7
15JUL77 06 16 30.5 0.00 0 3 RAT IS. ALEUTIANS
51.5N178.0E
  54.0
CB2NV    47.5       8.7 0.6   06 25 02.4
FR-CN    51.8      42.0 0.5   06 25 33.0
CB3NV    47.5       8.5 0.8   06 25 02.4
 4JUN77 15  0 38.8 0.00 0 4 LAKE BAIKAL REG.
56.3N111.5E
  59.9
CB2NV    78.1       8.4 1.1   15 12 32.4          5.1   .8
CB3NV    78.1       9.2 1.2   15 12 32.4
FA-NV    76.8       6.0 1.3   15 12 24.5  550
GE-NM    69.9      60.0 0.8   15 12 49.0 1042
 4JUN77 18 54 20.7 0.00 0 2 LEEWARD IS.
13.2N  64.0W
   0.0
FA-NV    49.5      16.0 0.7   19  3 14.3  550
GE-NM    42.1      32.0 1.0   19  2 13.0 1042
 5JUN77  6 38  3.5 0.00 0 4 ARGENTINA
23.6S  66.6W
230.0
CB2NV    76.7      35.4 1.0    6 49 29.5          29.9  .9
CB3NV    76.7      32.6 1.06   6 49 29.5
FA-NV    77.8      43.5 0.7    6 49 35.5  550
GE-NM    71.6       9.0 0.8    6 48 59.3   99
 5JUN77 22 23 39.0 0.00 0 3 N. ATLANTIC RIDGE
13.4N  44.7W
   0.0
CB2NV    67.2       8.5 1.3   22 34 36.1          6.1 1.1
FA-NV    67.3       7.5 0.7   22 34 36.3  550
GE-NM    60.1      30.0 1.0   22 33 40.7 1094
 6JUN77  6 38 43.1 0.00 0 4 DOMINICAN REP.
19.4N  69.5W
  11.0
FA-NV    44.6      33.0 1.0    6 46 57.0  550
GE-NM    37.2      26.0 0.7    6 45 55.0 1094
CB2NV    44.1      33.1 1.0    6 46 53.4          2.0 0.5
CB3NV    44.1      31.0 1.2    6 46 53.4          2.0 0.5
 7JUN77 13 31 25.4 0.00 0 4 ARGENTINA
29.8S  67.8W
109.0
FA-NV    82.0      38.0 1.0   13 43 32.0  430
GE-NM    76.1      12.0 1.0   13 43  0.7   99
CB2NV    80.8      39.4 1.1   13 43 26.2          4.4 0.8
CB3NV    80.8      46.3 1.0   13 43 26.3
 8JUN77  1 44 39.0 0.00 0 2 N. PERU COAST
 9.1S  78.9W
   0.0
FA-NV    59.0       5.5 0.7    1 54 40.0  440
GE-NM    52.9      18.0 1.1    1 53 54.3 1094
 9JUN77 14  5 43.7 0.00 0 2 FIJI IS.
21.9S177.1W
248.0
FA-NV    83.1       4.0 0.8   14 17 41.5   35
GE-NM    68.1      22.0 1.0   14 18  6.3 1094
29JUL77  2 51 47.4 0.00 0 2 MEXICO
14.5N  96.9W
   0.0
FA-NV    29.5       4.4 1.3    2 57 47.5
GE-NM    24.0      51.3 0.7    2 56 54.7
 1JUN77  8 57 28.0 0.00 0 3 TONGA IS.
21.1S174.2W
   0.0
GE-NM    56.2      36.0 1.6    9 10  7.3 1042
CB2NV    75.9      23.7 1.04   9  9 37.8          3.5  .85
CB3NV    75.9      26.2 1.16   9  9 37.9
```

```
 1JUN77 12 54 53.5 0.00 0 4 TURKEY
36.3N 31.4E
 88.0
GE-NM   97.5    40.0 0.8   13  8 19.0 1042
CB2NV  100.5     7.3 0.76  13  8 32.8                 5.3  .76
CB3NV  100.5     6.7 0.88  13  8 32.7
BR-CN   80.4   121.3 0.7   13  6 55.7                91.6  .8
11JUN77 20 33 28.4 0.00 0 3 N. ATLANTIC RIDGE
33.9N 39.0W
  0.0
CB2NV   60.9    15.4 1.5   20 43 45.1                 9.3 1.3
CB3NV   60.9    12.9 1.7   20 43 45.1
BR-CN   42.6    20.8 1.6   20 41 27.6                16.9 1.4
12JUN77  8 48  5.1 0.00 0 7 JAPAN
43.0N142.3E
241.0
FA-NV   71.8    35.0 0.8    8 59  3.0  500
GE-NM   76.3    86.0 0.8    8 59 41.3  573
YE-NV   73.0   181.  0.81   8 59 10.9
YE3NV   73.0   208.  0.83   8 59 10.9
CB2NV   72.8    64.4 0.85   8 59  9.4                41.2 0.88
CB3NV   72.9    58.0 0.85   8 59  9.5
BR-CN   74.3    60.5 0.66   8 59 17.6                55.0 0.7
12JUN77 12  0 28.3 0.00 0 4 GULF OF MEX.
22.0N 88.0W
  0.0
FA-NV   29.3    18.0 1.0   12  6 14.0  500
GE-NM   22.2    12.0 0.9   12  5 18.0  573
CB2NV   28.6     8.3 0.65  12  6  5.0                 7.1 0.64
CB3NV   28.6     9.0 0.6   12  6  5.0
12JUN77 12 16 45.8 0.00 0 3 NEW HEBRIDES
19.9S169.4E
 49.0
FA-NV   90.8    15.0 1.0   12 29 42.5  500
CB2NV   90.3    24.6 0.76  12 29 40.3
CB3NV   90.3    24.7 0.53  12 29 40.3
13JUN77  5 28 32.2 0.00 0 5 CENT. AMER. CST.
12.7N 90.5W
 58.0
FA-NV   34.5    36.0 1.0    5 35 12.8  410
GE-NM   28.3     5.5 0.7    5 34 16.6   57
CB2NV   33.5    13.8 1.4    5 35  3.6
CB3NV   33.5    14.4 1.4    5 35  3.6
BR-CN   38.2    51.7 0.8    5 35 40.0                30.1 0.8
13JUN77  8  2 13.4 0.00 0 5 N. CHILE CST.
22.2S 70.0W
108.0
FA-NV   74.7     4.0 0.8    8 13 43.5   30
GE-NM   68.6     5.5 0.7    8 13  6.3   57
CB2NV   73.5    19.1 0.9    8 13 37.1
CB3NV   73.5    21.4 1.16   8 13 37.1
BR-CN   75.9    43.9 0.85   8 13 46.6                33.1 0.89
13JUN77 10  8 44.3 0.00 0 6 TONGA IS.
18.3S174.2W
  0.0
FA-NV   78.6    11.0 2.0   10 20 47.0   30
GE-NM   63.7    85.0 1.3   10 21 14.3  573
YE-NV   77.9    91.0 1.23  10 20 43.8
YE2NV   77.9    99.0 1.2   10 20 43.7
CB2NV   77.9    43.0 1.5   10 20 42.9
CB3NV   77.9    46.0 1.5   10 20 43.0
13JUN77 15 12 52.4 0.00 0 4 KODIAK IS.
57.3N154.5W
 44.0
FA-NV   31.2    16.0 0.9   15 19  8.9  410
GE-NM   37.4    48.0 0.7   15 20  2.0  573
CB2NV   32.4     8.4 0.9   15 19 19.0                 6.9 0.75
CB3NV   32.4     7.2 0.8   15 19 18.0
```

```
19JUN77 17  5 21.6 0.00 0 4 MEXICO
14.9N 93.3W
   0.0
FA-NV   31.1     23.5 0.8   17 11 41.5   398
GE-NM   25.1     19.0 0.8   17 10 47.7    83
CB2NV   30.1      9.4 0.9   17 11 31.8
CB3NV   30.1      8.8 1.1   17 11 31.7
19JUN77 18 17 37.6 0.00 0 5 N. ATLANTIC RIDGE
15.5N 46.7W
   0.0
FA-NV   64.5     26.5 0.7   18 28 16.0   398
GE-NM   57.3     38.0 1.5   18 27 28.3   885
CB2NV   64.4     24.  1.45  18 28 16.5
CB3NV   64.4     24.2 1.5   18 28 16.6
BR-CN   51.5     35.0 1.0   18 26 43.6
20JUN77  0 41 13.9 0.00 0 3 UNIMAK IS.
53.9N164.4W
   0.0
FA-NV   35.8     45.0 0.7    0 48 14.0   425
CB2NV   36.8     39.0 0.9    0 48 23.0               26.8 0.85
CB3NV   36.8     36.9 0.9    0 48 22.9
20JUN77  6 30 54.4 0.00 0 3 N. CHILE
23.9S 69.4W
  90.0
FA-NV   76.3     13.0 0.6    6 42 36.0   425
CB2NV   75.2      8.0 0.88   6 42 29.7                7.3 0.7
CB3NV   75.2      9.7 0.96   6 42 29.4
14MAY77  6 58 51.8 0.00 0 3 ECUADOR CST.
  1.8N 85.4W
  23.0
BR-CN   49.5     30.0 0.89   7  7 38.5                9.5  .9
CB2NV   45.3     11.8 0.8    7  7  7.5                4.3  .9
CB3NV   45.3     11.1 0.9    7  7  7.5
15MAY77  0 21  4.1 0.00 0 4 KURILES
49.9N152.6E
 232.0
BR-CN   64.5    159.2 0.8    0 31 16.9              128.5  .8
CB2NV   63.1     33.6 0.8    0 31  7.8                9.0  .7
CB3NV   63.1     39.1 0.9    0 31  7.8
HN-ME   78.0    306.4 0.7    0 32 37.0
15MAY77 15 50 44.1 0.00 0 3 FOX IS.
52.5N168.2W
   0.0
BR-CN   44.1     32.3 0.5   15 58 54.4               27.5  .8
CB2NV   35.5     56.1 1.32  15 58 12.8               36.2 1.14
CB3NV   35.5     54.7 1.25  15 58 12.8
21JUN77  8 58 22.3 0.00 0 5 TONGA IS.
15.5S174.6W
 306.0
FA-NV   76.9      6.8 0.8    9  9 42.3    65
YF-NV   76.3     91.1 0.97   9  9 38.5
YF2NV   76.3    102.0 0.97   9  9 38.5
CB2NV   76.3    276.0 0.85   9  9 38.5              210.0 0.8
CB3NV   76.3    519.0 0.95   9  9 38.5
22JUN77  7 11 30.2 0.00 0 6 JAPAN
35.4N140.4E
  44.0
FA-NV   77.6     24.0 1.5    7 23 23.5   425
YF-NV   78.7     44.9 0.75   7 23 29.3
YF2NV   78.7     52.9 0.75   7 23 29.6
CB2NV   78.5    102.0 0.78   7 23 28.6               67.0 1.1
CB3NV   78.5    160.0 0.8    7 23 28.5
BR-CN   61.5     21.5 1.10   7 23 43.0               19.9 1.34
22JUN77  8 50 31.2 0.00 0 6 KAMCHATKA
53.7N160.7E
  40.0
FA-NV   56.0     47.0 1.3    9  0  7.3   425
YF-NV   57.2     99.3 0.95   9  0 16.3
YF2NV   57.2    113.7 1.06   9  0 16.2
CB2NV   57.1     75.7 1.23   9  0 14.2               21.2 1.24
CB3NV   57.1    135.5 1.26   9  0 14.1
BR-CN   58.4     67.5 0.74   9  0 23.0               60.1 0.89
```

```
13JUL77  6 35 35.7 0.00 0 3 CHILE-ARGENTINA BDR
29.1S 69.7W
104.0
CB2NV   79.3    22.4 1.1    6 47 30.3          15.4 1.0
CB3NV   79.3    19.5 1.1    6 47 30.3
BR-CN   82.7    30.6 1.0    6 47 45.5          24.8 0.84
19JUL77 13  4   8.9 0.00 0 2 N. COLUMBIA
 7.9N 72.1W
  0.0
CB2NV   49.4     9.6 0.64  13 13  0.2           8.4 0.65
CB3NV   49.4     7.9 0.6   13 13  0.3
20JUL77 13 24 21.1 0.00 0 4 ALASKA PEN.
50.6N161.9W
  0.0
CB2NV   35.5   134.1 1.3   13 31 19.4         111.6 1.1
CB3NV   35.5   129.0 1.4   13 31 19.3
BR-CN   39.8   220.0 1.1   13 31 55.6          84.6 1.2
HN-ME   55.9    84.6 1.2   13 33 58.8
20JUL77 10 36 28.0 0.00 0 8 ANDREANOF IS.
50.1N178.0W
207.0
FA-NV   44.3     8.5 0.6   10 44 20.0  410
GE-NM   51.1    54.0 0.7   10 45 12.6  905
YF4NV   45.3    38.8 0.7   10 44 29.3
YF3NV   45.3    38.1 0.9   10 44 29.3
YF-NV   45.3    30.1 0.8   10 44 29.3
YF2NV   45.3    39.6 0.8   10 44 29.2
CE2NV   45.2     9.9 0.9   10 44 28.0           7.0 0.8
CE3NV   45.2    15.7 0.5   10 44 27.8
21JUL77  2 19 59.2 0.00 0 4 ALASKA PEN.
56.2N157.9W
 33.0
FA-NV   32.5    20.7 0.6    2 26  7.0
GE-NM   38.8     9.0 1.0    2 27 21.6   73
CB2NV   33.6    16.0 0.9    2 26 36.6          13.1 1.0
CE3NV   33.6    20.6 0.9    2 26 36.7
10JUN77  0 41   8.4 0.00 0 2 N.E. CHINA
39.6N118.1E
103.0
FA-NV   87.3     6.0 1.5    0 53 44.0  500
GE-NM   93.0    17.5 0.8    0 54 13.3 1094
10JUN77  2 35 18.6 0.00 0 2 SUMATRA
 2.9S101.5E
 52.0
FA-NV  130.4    17.0 0.5    2 54 25.0  500
GE-NM  137.1    29.0 0.8    2 54 38.3 1094
13JUN77  3  5 33.5 0.00 0 2 MEXICO CST
 8.6N103.7W
  0.0
FA-NV   32.1    14.0 1.8    3 12  1.3  410
GE-NM   28.3    22.0 1.0    3 11 26.6  573
14JUN77 12 52 37.4 0.00 0 2 ARGENTINA
24.9S 66.0W
  0.0
FA-NV   79.0    24.5 0.5   13  4 31.2  410
GE-NM   72.8    27.0 0.7   12 52 37.4  885
15JUN77 13 18   6.9 0.00 0 4 CENT. PACIFIC
 5.1N 99.2W
  0.0
FA-NV   36.9    50.0 0.7   13 25 32.7  410
GE-NM   32.4    13.0 1.0   13 24 38.3   83
CB2NV   35.6    13.0 1.0   13 25 23.0
CE3NV   35.6    14.0 0.9   13 25 23.1
17JUN77  8 26 30.3 0.00 0 4 S. ALASKA
61.5N150.5W
 64.0
FA-NV   31.0    12.0 0.5    8 32 42.5  398
GE-NM   36.5    29.0 0.8    8 33 30.3  885
CB2NV   32.3     9.1 0.78   8 32 53.3           4.1 0.45
CE3NV   32.3     9.3 0.72   8 32 53.5
```

```
19JUN77 10 23 56.0 0.00 0 4 JAPAN
42.1N142.0E
  0.0
FA-NV   72.5    14.0 0.8   10 35 26.0   398
GE-NM   75.1    28.0 0.8   10 36  3.7   885
CB2NV   73.5    11.3 0.9   10 35 31.6               9.3 0.8
CB3NV   73.5    10.4 0.9   10 35 31.8
19JUN77 16 49 41.8 0.00 0 5 CHILE-BOLIVIA BDR
21.0S 68.7W
127.0
FA-NV   74.4    32.0 1.0   17  1  6.3    65
GE-NM   66.2    23.0 1.1   17  0 28.3    83
YP-NV   73.2   514.0 1.1   17  0 59.7
YP2NV   73.2   578.0 1.1   17  0 59.7
BK-ME   67.2    85.0 1.5   17  0 19.9
19JUN77 20 56 42.9 0.00 0 4 MEXICO-GUATEMALA
15.7N 93.0W
145.0
FA-NV   30.7     7.0 1.1   21  2 44.0    65
GE-NM   24.5    19.0 1.1   21  1 50.0    83
CB2NV   29.6    35.0 1.64  21  2 34.7              30.8 1.3
CB3NV   29.6    36.0 1.6   21  2 34.8
19JUN77  7 22 17.4 0.00 0 2 SAMOA IS. REGION
13.3S174.0W
  0.0
FA-NV   74.8     4.2 0.7    7 33 57.4    65
GE-NM   80.2    26.0 1.5    7 34 26.0   885
19JUN77  8 26 34.9 0.00 0 2 WINDWARD IS.
11.1N 62.1W
254.0
FA-NV   55.3     9.5 0.7    8 35 43.5   398
GE-NM   47.9    14.0 0.8    8 34 49.3   885
19JUN77 11 47 22.3 0.00 0 6 KURILES
47.2N151.0E
118.0
FA-NV   64.4    10.0 1.0   11 57 46.0    65
GE-NM   70.9    21.0 0.6   11 58 27.6    83
CB2NV   65.4   100.0 1.4   11 57 52.9              43.0 1.2
CB3NV   65.4    36.0 1.2   11 57 52.9
YP-NV   65.5   497.0 0.7   11 57 54.1
YP2NV   65.5   548.0 1.0   11 57 54.1
20JUN77  3 10 39.0 0.00 0 2 MEXICO-GUATEMALA
15.2N 92.6W
  0.0
FA-NV   31.2    15.0 0.8    3 16 56.0   425
GE-NM   25.0    30.0 1.0    3 16  3.0   885
 1AUG77  0 47 15.9 0.00 0 3 N. COLUMBIA
 7.1N 72.7W
  0.0
BK-CN   47.1    57.0 0.53   0 55 48.9              39.0 0.5
FA-NV   50.3    11.0 0.8    0 56 13.5   687
GE-NM   43.1    17.0 0.7    0 55 18.5  1042
 1AUG77 16 30 37.7 0.00 0 4 CHILE-BOLIVIA BDR.
21.8S 66.6W
150.0
CB2NV   74.0    28.0 1.1   16 41 57.9              21.0 0.9
CB3NV   74.0    32.0 1.05  16 41 57.8
FA-NV   75.1    42.0 0.7   16 42  4.3   688
GE-NM   66.9    10.0 0.7   16 41 26.7    68
 1AUG77 19 12 20.7 0.00 0 4 FIJI IS.
19.3S178.4W
783.0
YP-NV   81.4   194.0 0.85  19 23 16.2
YP2NV   81.4   226.0 0.76  19 23 16.3
YP4NV   81.4   272.0 0.75  19 23 16.2
YP3NV   81.4   262.0 0.7   19 23 16.3
 2AUG77  2 22  6.4 0.00 0 2 ANDREANOF IS.
51.4N175.4W
 26.0
BK-ME   64.2    72.0 0.95   2 32 39.0
BK-CN   48.5   112.0 0.92   2 30 47.2
```

```
 6AUG77  5 26 43.2 0.00 0 2 TONGA REG.
22.0S175.8W
  0.0
CB2NV   81.6    44.0 0.94  5 39  2.7             35.5 0.92
CB3NV   81.5    41.8 1.1   5 39  2.7
 6AUG77 11 52 46.5 0.00 0 8 TONGA IS.
19.5S174.1W
  0.0
FA-NV   78.7    36.0 0.7  12  4 49.7  500
GE-NM   83.7    70.5 1.3  12  5 16.5 1146
YF-NV   77.9    46.7 1.15 12  4 45.9
YF2NV   77.9    49.5 1.22 12  4 45.8
YF4NV   77.9    73.4 1.27 12  4 45.8
YF3NV   77.9    54.6 1.32 12  4 45.7
CB2NV   78.0    34.2 1.06 12  4 45.6             23.  1.04
CB3NV   78.0    32.3 1.19 12  4 45.5
 7AUG77  7  8  2.6 0.00 010 PANAMA-COSTA RICA
 9.6N 82.7W
  0.0
FA-NV   42.9    17.0 1.1   7 16  0.5   47
GE-NM   35.8    11.5 1.5   7 15 13.5  729
YF4NV   41.5   176.8 1.58  7 15 54.8
YF3NV   41.5   209.2 1.47  7 15 54.7
YF-NV   41.4   184.0 1.5   7 15 54.5
YF2NV   41.4   204.0 1.5   7 15 54.5
CB2NV   41.6    91.5 1.6   7 15 52.8             12.5 1.8
CB3NV   41.6    93.0 1.7   7 15 52.9
BX-CN   43.2   708.0 0.9   7 16  3.1
BX-NB   39.6    34.2 0.8   7 15 36.4
 7AUG77 16 46 31.0 0.00 0 2 TONGA IS.
22.3S174.7W
 40.0
CB2NV   81.1     7.4 1.4  16 58 41.4
CB3NV   81.1     8.0 1.4  16 58 41.4
 1AUG77  1 50 57.5 0.00 0 2 CST OF MEXICO
14.4N 98.7W
  0.0
FA-NV   28.7     9.5 0.8   1 56 45.3  688
GE-NM   23.5     3.0 1.3   1 55 55.3   68
 7AUG77 23 26 55.0 0.00 0 9 ANDREANOF IS.
52.2N176.2W
125.0
FA-NV   42.9     7.5 0.8  23 34 42.5   47
GE-NM   49.6    32.5 0.3  23 35 34.3   73
YF4NV   44.0   215.0 0.66 23 34 51.8
YF3NV   44.0   185.0 0.7  23 34 51.8
YF-NV   44.0   176.0 0.64 23 34 51.8
YF2NV   44.0   178.0 0.75 23 34 51.7
CB2NV   43.9   115.0 0.96 23 34 50.6             85.0 0.86
CB3NV   43.9   110.0 0.85 23 34 50.6
BX-CN   48.9    83.8 0.56 23 35 23.7             40.5 0.79
 8AUG77  7  0  6.3 0.00 0 6 CST OF COLUMBIA
 6.9N 77.8W
 22.0
FA-NV   46.9    35.0 1.0   7  8 37.2  500
GE-NM   40.1    41.0 0.9   7  7 40.6 1146
CB2NV   46.1    14.0 0.95  7  8 30.1             12.3 1.00
CB3NV   46.1    14.1 1.1   7  8 30.0             16.8 1.03
BX-NB   40.2   101.8 1.05  7  7 40.8
BX-CN   45.9    59.5 0.9   7  8 24.6             16.8 1.03
 8AUG77 15  5 39.7 0.00 0 4 FIJI IS.
17.2S178.8W
470.0
FA-NV   80.0    60.0 0.7  15 17  4.5  500
GE-NM   88.2    46.0 0.9  15 17 30.1 1146
CB2NV   80.2    50.0 1.15 15 17  1.4             40.2 0.96
CB3NV   80.2    56.0 1.1  15 17  1.5
 8AUG77 22 20 53.7 0.00 0 2 FIGI REG.
21.2S179.4E
350.0
CB2NV   84.2    22.4 0.58 22 32 41.4
CB3NV   84.2    22.8 0.64 22 32 41.3
```

```
 5AUG77  1 38  12.7 0.00 0 6 N. ATLANTIC RIDGE
30.6N  41.5W
   0.0
FA-NV   60.3    12.0 1.3     1 48 25.3   500
GE-NM   54.0    18.5 1.5     1 47 41.2   938
CB2NV   60.6    23.5 1.28    1 48 28.2              14.0   .74
CE3NV   60.6    17.0 1.36    1 48 28.2
BR-CN   43.3    17.6 0.75    1 46 15.3
BM-MB   25.1    29.7 0.94    1 43 44.2
10AUG77  5 36   1.9 0.00 0 4 KODIAK IS.
56.3N152.6W
  52.0
FA-NV   29.8    26.5 2.0     9 42  6.0   500
GE-NM   36.0    30.0 1.1     9 42 59.7   417
CB2NV   31.0    21.0 1.7     9 42 15.3
CE3NV   31.0    21.0 1.74    9 42 15.2
21JUN77 15 32  12.0 0.00 0 2 PERU COAST
14.5S  75.0W
   0.0
FA-NV   65.6    11.0 0.8    15 42 58.0   425
GE-NM   55.5    19.0 1.0    15 42 16.3   833
23JUN77 20 19  13.6 0.00 0 2 KAMCHATKA CST
53.9N163.5E
   0.0
FA-NV   54.4    79.0 0.8    20 28 44.8   440
GE-NM   50.7    15.0 0.7    20 29 30.5    73
27JUN77 18 57  19.7 0.00 0 2 ECUADOR
  1.4S  76.7W
   0.0
FA-NV   54.0    41.0 1.4    19  6 45.0   429
GE-NM   47.5    58.0 0.8    19  5 55.7   854
28JUN77  0 52  25.3 0.00 0 2 CHILE-BOLIVIA BDR
21.4S  68.1W
126.0
FA-NV   75.1     9.0 0.7     1  3 53.0    70
GE-NM   68.8    45.0 0.7     1  3 15.7   854
29JUN77 15 38  34.9 0.00 0 2 N. ATLANTIC RIDGE
22.5N  45.2W
   0.0
FA-NV   61.7    66.5 1.8    15 46 57.3   429
GE-NM   54.8     7.0 1.5    15 46  8.0    73
29JUN77 16 18  12.9 0.00 0 3 N. ATLANTIC RIDGE
22.7N  45.2W
   0.00
FA-NV   61.5    10.5 1.8    16 28 33.3    70
GE-NM   54.3    15.0 1.4    16 27 46.0    73
CB2NV   61.7   153.0 1.6    16 28 34.6             23.0 1.1
29JUN77 19 19  34.7 0.00 0 3 N. ATLANTIC RIDGE
22.6N  45.2W
  13.0
FA-NV   61.8     8.0 2.7    19 28 53.5    70
GE-NM   54.5    18.0 1.8    19 28  6.0    68
CB2NV   61.7   158.0 1.7    19 28 54.6             19.0 1.6
29JUN77  4  6  41.3 0.00 0 2 CHIAPAS MEXICO
12.0N  95.9W
   0.0
FA-NV   32.2    14.0 0.7     4 13 25.7   429
GE-NM   26.7    24.0 1.1     4 12 30.0   833
29JUN77  8 47  15.4 0.00 0 3 ANDREANOF IS.
51.6N176.3W
  45.0
FA-NV   43.0    29.0 1.3     8 55 11.5   429
GE-NM   45.7    10.0 0.8     8 56  4.7    68
CB2NV   44.0    26.0 1.0     8 55 19.8
30JUN77  2 45  55.4 0.00 0 5 N. CHILE
19.2S  69.5W
  17.0
FA-NV   72.5    25.0 1.2     2 57 21.7    70
GE-NM   66.3    10.0 0.7     2 56 42.7    73
CB2NV   71.4   188.0 0.8     2 57 15.4            108.0 1.0
YK-NV   71.3   337.0 1.2     2 57 14.6
YK2NV   71.3   413.0 1.2     2 57 14.5
```

```
30JUN77  8 51 24.7 0.00 0 4 TONGA IS.
15.2S174.6W
  0.0
FA-NV   76.6    5.0 1.0    9  3 14.8    70
GE-NM   81.9   65.0 1.2    9  3 43.0   833
CB2NV   76.0   29.0 1.0    9  3 11.1              25.0 1.0
CB3NV   76.0   26.0 1.1    9  3 11.1
30JUN77 11 13  36.9 0.00 0 2 N. CHILE
27.2S  69.5W
 42.0
FA-NV   79.0   42.0 1.0   11 25 37.3   462
GE-NM   73.1   30.0 0.8   11 25  3.7   833
 1JUL77 12  7   8.2 0.00 0 2 TONGA IS.
17.1S174.1W
  0.0
FA-NV   77.7    4.5 0.8   12 18 59.9    70
GE-NM   82.8    5.0 0.9   12 19 27.7    73
 2JUL77  5  9   2.0 0.00 0 2 N. CHILE CST
25.9S  71.0W
  0.0
FA-NV   77.1   13.5 0.7    5 20 59.0    70
GE-NM   71.3    8.0 1.2    5 20 23.7    52
 2JUL77 15 50  46.9 0.00 0 4 KAMCHATKA CST
53.0N160.2E
 57.0
FA-NV   56.5   43.0 1.1   16  0 26.0   462
GE-NM   62.9   14.0 1.0   16  1  9.0    52
CB2NV   57.8   29.0 1.2   16  0 32.9             20.0 1.1
CB3NV   57.8   26.0 1.3   16  0 33.0
 3JUL77 12 55  39.9 0.00 0 2 FOX IS.
52.4N167.5W
 11.0
FA-NV   37.5   24.0 0.9   13  2 55.4   435
GE-NM   44.3   15.0 0.9   13  3 51.0    52
 3JUL77 17 29  46.9 0.00 0 2 FOX IS.
52.6N167.5W
  0.0
FA-NV   37.5   22.0 0.6   17 37  3.3   435
GE-NM   44.3   10.0 0.9   17 37 58.0    52
 4JUL77  2  7  41.0 0.00 0 2 N. ATLANTIC
57.6N  32.9W
  5.0
FA-NV   54.8    7.0 0.8    2 17 12.3   425
GE-NM   51.6   19.0 1.3    2 16 48.0   573
 5JUL77  1 13  14.7 0.00 0 2 KURILES
50.7N155.8E
  0.0
FA-NV   59.4    9.5 0.5    1 23 19.7   425
GE-NM   65.8   28.0 0.7    1 24  3.0   573
 6JUL77  4 42  21.1 0.00 0 2 S. PANAMA
 5.4N  82.4W
  0.0
FA-NV   45.2   10.0 2.0    4 50 39.6    35
GE-NM   38.7   43.5 1.5    4 49 46.9    78
 6JUL77 10  2  52.9 0.00 0 2 ARGENTINA
27.9S  67.3W
180.0
FA-NV   80.1   19.2 0.8   10 14 47.0   125
GE-NM   74.1   53.5 0.8   10 14 13.5   833
 6JUL77 22 59  59.1 0.00 0 2 TUAMOTU ARCH
22.0S139.2W
  0.0
FA-NV   64.3   27.0 0.7   23 10 34.5   425
GE-NM   66.0   46.5 1.2   23 10 46.4   843
 7JUL77  9 57  32.3 0.00 0 2 TONGA IS.
16.3S174.6W
 90.0
FA-NV   77.5   11.0 0.9   10  9 17.3   440
GE-NM   82.7   24.5 0.8   10  9 45.4   843
```

```
 7JUL77 15  3 37.1 0.00 0 2 EASTER ISLAND
35.0S107.6W
  0.0
FA-NV   74.1    14.0 0.9   15 15 11.2  440
GE-NM   46.5    18.0 2.0   15 14 57.0  843
 9JUL77  7  3 55.5 0.00 0 2 MEXICO
16.9N 95.1W
102.0
FA-NV   28.5     5.0 1.1    7  9 42.0  440
GE-NM   22.5    13.5 0.7    7  8 47.3   68
11JUL77  9 38 32.1 0.00 0 2 RAT IS.
51.2N176.2E
  3.0
FA-NV   47.7    19.0 1.2    9 47 11.2  440
GE-NM   54.4    33.0 1.3    9 48  2.3  865
11JUL77 12 35 49.6 0.00 0 2 KURILES
47.9N155.8E
 77.0
FA-NV   61.2    11.0 1.1   12 45 57.5  440
GE-NM   67.8    35.0 1.3   12 46 41.1  865
11JUL77 15 57 19.0 0.00 0 2 CENT. ALASKA
64.3N146.7W
  0.0
FA-NV   31.6     9.0 1.0   16  3 43.6  440
GE-NM   36.5    10.0 1.0   16  4 26.5   68
16JUL77 12 39 54.9 0.00 0 2 ARGENTINA
23.8S 66.7W
111.0
FA-NV   77.7    31.8 1.0   12 51 40.0
GE-NM   71.5     5.5 1.0   12 51  4.3   68
 3AUG77  2 25 21.5 0.00 0 2 PANAMA-COLUMBIA BDR
 6.4N 77.5W
154.0
FA-NV   46.0    15.5 1.0    2 33 29.7  500
GE-NM   39.1     5.0 0.8    2 32 33.7   83
 3AUG77 12  5 36.8 0.00 0 2 KURILES
49.9N154.5E
 95.0
FA-NV   61.0     7.0 0.7   12 15 41.3   44
GE-NM   67.5    25.0 0.7   12 16 23.5   83
 4AUG77 13 20 50.5 0.00 0 2 CENT. AMERICA CST
11.8N 86.6W
 10.0
FA-NV   36.4     8.0 1.1   13 27 59.7   44
GE-NM   30.0    24.0 1.3   13 27  2.7   78
 9AUG77 12 19 34.6 0.00 0 2 S. PERU
15.4S 72.4W
  0.0
FA-NV   67.6     6.0 1.1   12 30 34.4  500
GE-NM   61.6    22.5 1.0   12 29 53.5  938
11JUN77 11 45 21.1 0.00 0 3 FIJI IS.
16.2S178.5W
  0.0
FA-NV   79.9    21.0 0.7   11 57 32.0  500
CB2NV   79.3    15.3 1.1   11 57 29.0          10.0 0.8
CB3NV   79.3    14.0 1.2   11 57 29.1
17JUN77 22 54 28.4 0.00 0 3 COSTA RICA
10.7N 85.3W
  0.0
GE-NM   32.7     5.0 0.7   23  1  3.7   83
CB2NV   38.3    36.0 0.7   23  1 51.8           6.4 0.6
CB3NV   38.3    38.5 0.7   23  1 51.9
18JUN77 10  4  2.2 0.00 0 5 FIJI IS.
20.2S177.8W
500.0
FA-NV   82.3    37.5 0.7   10 15 32.8   65
YF-NV   81.6   196.0 0.9   10 15 29.3
YF2NV   81.6   261.0 0.8   10 15 29.3
CB2NV   81.7   146.0 0.75  10 15 29.2         109.0 0.75
CB3NV   81.7   149.0 0.7   10 15 29.2
```

```
26JUN77  5 59 26.2 0.00 0 2 FIGI IS.
17.8S178.4W
  0.0
FA-NV   81.0   11.0 0.8    6 11 40.3    75
CB2NV   80.4   67.0 0.85   6 11 33.1             52.0 0.8
26JUN77 10 15 48.9 0.00 0 3 BAHAMA IS.
21.1N 69.7W
  0.0
FA-NV   43.4   43.0 1.0   10 23 52.6   440
CB2NV   43.1   31.0 1.0   10 23 49.7             24.0 1.0
YF-NV   43.0  119.0 0.85  10 23 49.5
13AUG77  3 13 35.1 0.00 0 6 KURILES
44.3N147.9E
 60.0
FA-NV   67.7   18.5 0.9    3 24 27.4   456
GE-NM   74.3    7.0 1.0    3 25  7.9    42
CB2NV   68.7   37.0 0.95   3 24 33.7             28.4 0.8
CB3NV   68.7   33.3 0.95   3 24 33.7
BR-CN   70.9   41.7 0.86   3 24 45.3              4.0 0.36
EN-MB   84.1   24.1 0.74   3 25 53.7
13AUG77  7 57 44.9 0.00 0 5 CENT. CHILE CST
28.3S 71.5W
140.0
FA-NV   78.9   15.0 1.0    8  9 36.0   456
GE-NM   73.1   31.0 1.1    8  9  3.0   521
CB2NV   77.7   12.2 0.85   8  9 29.9             12.1 0.85
CB3NV   77.7   14.7 0.7    8  9 30.0
BR-CN   81.5   30.8 0.67   8  9 41.8             22.5 0.58
13AUG77 19 33 11.7 0.00 0 5 JAPAN
43.2N145.4E
 58.0
FA-NV   69.8   10.0 0.7   19 44 17.0   456
GE-NM   76.4    5.0 0.9   19 44 55.9    68
CB2NV   70.8   22.7 0.83  19 44 23.3             19.5 0.76
CB3NV   70.8   21.4 0.88  19 44 23.3
BR-CN   72.9   49.7 0.64  19 44 34.1             39.4 0.81
14AUG77  4 22 51.9 0.00 0 5 VENEZUELA CST
10.9N 62.6W
119.0
FA-NV   55.0   16.0 1.0    4 32 13.0   456
GE-NM   47.4    4.5 0.7    4 31 19.2    68
CB2NV   54.5   23.7 0.89   4 32 10.4              4.6 0.83
CB3NV   54.5   19.8 1.0    4 32 11.1
BR-CN   47.3   32.5 0.48   4 31 11.7              7.3 0.66
14AUG77 10 58  9.5 0.00 0 5 N. CHILE CST
19.8S 73.6W
  0.0
FA-NV   70.8   41.0 1.0   11  9 30.0   456
GE-NM   64.6    6.0 1.1   11  8 51.3    68
CB2NV   69.6   45.9 0.88  11  9 23.5             39.5 0.88
CB3NV   69.6   42.5 0.91  11  9 23.5
BR-CN   72.6   28.7 0.8   11  9 35.0             21.4 0.83
14AUG77 11 30 33.5 0.00 0 4 N. PERU CST
 8.2S 80.3W
 38.0
GE-NM   51.5   14.0 0.8   11 39 37.0   885
CB2NV   56.4    3.9 1.0   11 40 12.1              3.3 1.3
CB3NV   56.4    3.9 1.0   11 40 12.3
BR-CN   60.2   22.8 0.9   11 40 35.2             17.4 0.88
14AUG77 23 49 15.7 0.00 0 6 SEA OF JAPAN
41.8N138.6E
 30.0
YF4NV   75.8  135.0 1.1    0  1  1.4
YF3NV   75.8  160.0 1.25   0  1  1.3
YF-NV   75.9  104.0 1.1    0  1  1.4
YF2NV   75.9  122.0 1.15   0  1  1.3
CB2NV   75.7  139.0 1.2    0  0 59.5            108.0 1.0
BR-CN   76.8   40.0 0.56   0  1  4.0              7.0 0.55
```

```
15AUG77  0 24 30.9 0.00 0 2 ANDREANCF IS.
51.5N175.6W
   0.0
FA-NV   42.6     7.0 0.7    0 32 29.3   456
GE-NM   49.3    33.5 1.1    0 33 21.8   833
15AUG77  5 41   9.3 0.00 0 7 FIGI IS.
22.9S176.0W
   0.0
FA-NV   63.1    47.0 1.7    5 53 35.3   456
YF4NV   62.3    66.3 1.63   5 53 31.4
YF3NV   62.3    84.0 1.5    5 53 31.2
YF-NV   62.3    76.0 1.4    5 53 31.3
YF2NV   62.3    83.0 1.4    5 53 31.5
CE2NV   62.4    38.2 1.1    5 53 31.3              28.0 1.3
CE3NV   62.4    41.1 1.2    5 53 31.3
15AUG77  5 54   5.4 0.00 0 5 CENT. AMERICA CST
12.9N 91.0W
   0.0
FA-NV   34.1    12.5 0.8    6  0 53.8   456
GE-NM   27.9    22.5 0.7    5 59 57.9   833
CB2NV   33.0    10.4 0.83   6  0 44.7                7.6 0.94
CB3NV   33.0    10.0 0.86   6  0 44.8
BK-CN   36.0    22.5 0.72   6  1 20.9                8.3 0.9
15AUG77 16 43  52.5 0.00 0 2 PERU ECUADOR BDR
 4.3S 80.6W
126.0
FA-NV   54.1    11.0 2.0   16 59  1.5   519
GE-NM   47.9    53.0 1.0   16 58 15.3   864
16AUG77  4 47  14.5 0.00 0 2 TONGA IS.
17.6S170.3W
   0.0
FA-NV   75.6    37.0 1.3    4 59  4.0   519
GE-NM   80.5    60.0 1.0    4 59 31.7   864
20AUG77  2 46  11.4 0.00 0 2 CARIBBEAN SEA
16.7N 66.7W
   0.0
FA-NV   33.6     8.0 1.5    2 52 56.8    94
GE-NM   27.0     5.0 1.0    2 51 56.7   781
20AUG77  3 51  51.4 0.00 0 2 CARIBBEAN SEA
16.4N 66.6W
   7.0
FA-NV   34.1    37.0 1.0    3 58 38.0    94
GE-NM   27.3     9.0 0.7    3 57 37.3   781
20AUG77 18 24  24.4 0.00 0 2 ARGENTINA
28.8S 66.4W
120.0
FA-NV   80.5     9.0 1.5   18 36 26.3    94
GE-NM   74.9     9.0 1.3   18 35 54.0    78
20AUG77 22  0   0.6 0.00 0 6 CENT. SIBERIA
64.1N 99.8E
   0.0
FA-NV   73.4    31.0 1.0   22 11 35.3   950
GE-NM   77.0    16.0 0.66  22 11 57.0    78
CB2NV   74.6    29.0 0.65  22 11 43.8              25.8 0.7
CB3NV   74.6    31.0 0.75  22 11 43.8
BB-ME   69.3    78.0 0.65  22 11 10.9
BK-CN   64.6    57.0 0.67  22 10 39.2              17.0 0.6
21AUG77  3 15  28.4 0.00 0 2 TONGA IS
26.5S175.5W
147.0
CB2NV   64.9    13.0 1.0    3 27 46.4                9.9 1.2
CB3NV   64.9    12.0 1.1    3 27 46.4
21AUG77  4 44  30.1 0.00 0 2 SAMOA IS
14.7S173.3W
   0.0
FA-NV   75.4     5.0 0.8    4 56 14.3   106
GE-NM   80.6     3.5 1.4    4 56 45.0    78
```

```
21AUG77  5 19 39.2 0.00 0 8 HONSHU CST
35.1N141.1E
 14.0
GE-NM    64.2    19.0 0.7   5 32  4.7    78
YF-NV    76.4   136.0 1.3   5 31 33.9
YF2NV    76.4   180.0 1.26  5 31 33.9
YF4NV    76.4   171.0 1.24  5 31 33.9
YF3NV    76.4   175.0 1.35  5 31 33.9
CB2NV    76.3    65.0 1.2   5 31 32.7               29.0 1.14
CB3NV    76.3    60.0 1.2   5 31 32.6
BR-CN    61.5    44.0 1.0   5 31 48.0               35.0 1.2
21AUG77 11 33 41.7 0.00 0 9 GUATEMALA CST
13.6N 90.1W
  0.0
FA-NV    34.1    24.0 1.0  11 40 28.2   106
GE-NM    27.7     7.0 1.1  11 39 32.7    78
YF-NV    32.9   106.0 1.2  11 40 19.2
YF2NV    32.9   140.0 1.25 11 40 19.3
YF4NV    32.3   142.0 1.3  11 40 19.6
YF3NV    32.9   107.0 1.25 11 40 19.4
CB2NV    33.1    63.4 1.11 11 40 19.6               54.5 1.25
CB3NV    33.1    61.0 1.1  11 40 19.6
BR-CN    37.3    83.0 0.75 11 40 53.5                7.6 0.5
23AUG77  3 12 55.6 0.00 0 8 CHILE BOLIVIA BDR
21.5S 68.3W
125.0
FA-NV    75.0    11.0 0.8   3 24 24.0   106
GE-NM    65.8     5.5 0.8   3 23 46.1    68
YF-NV    73.8    96.0 0.93  3 24 17.0
YF2NV    73.8    93.0 1.0   3 24 16.9
YF4NV    73.8   120.0 0.83  3 24 17.1
CB2NV    73.9    64.0 0.95  3 24 17.6
CB3NV    73.9    64.0 0.9   3 24 17.7
BR-CN    75.7   113.0 0.7   3 24 24.4               35.0 1.0
23AUG77  7 35 30.7 0.00 0 2 FIGI IS
14.9S177.3W
  0.0
FA-NV    78.2    21.0 1.6   7 47 31.8   531
GE-NM    63.6     5.0 1.3   7 48  0.7    67
25AUG77 16 54 40.2 0.00 0 2 ARGENTINA
23.8S 66.6W
236.0
FA-NV    77.8    13.0 0.7  17  6 12.5   531
GE-NM    71.6    53.5 1.0  17  5 36.8  1645
26AUG77  7 16  0.8 0.00 010 RAT IS
51.3N176.1E
146.0
FA-NV    47.8    36.0 1.0   7 24 25.7   531
GE-NM    54.5     4.5 1.0   7 25 16.9    73
YF-NV    48.9   121.0 0.75  7 24 35.6
YF2NV    48.9   148.0 0.8   7 24 35.5
YF4NV    48.9   168.0 0.78  7 24 35.6
YF3NV    48.9   164.0 0.7   7 24 35.5
CB2NV    48.8    75.0 0.85  7 24 34.1                8.0 0.8
CB3NV    48.8    75.0 0.8   7 24 34.1
BR-CN    53.0   258.0 0.7   7 25  3.8              120.0 0.9
HA-ME    66.3    52.0 0.7   7 26 47.0
27AUG77  2 54 26.6 0.00 0 2 N. CHILE CST
27.7S 71.0W
  0.0
FA-NV    78.6    20.0 1.0   3  6 29.2   544
GE-NM    72.8    32.0 0.8   3  5 56.0   937
28AUG77 15 40 56.7 0.00 0 7 S. PANAMA
 5.1N 81.4W
  0.0
FA-NV    46.0    45.0 1.0  15 49 15.0   688
GE-NM    39.5    69.0 1.0  15 48 23.0   937
YF4NV    45.0    63.0 1.1  15 49  6.8
YF3NV    45.0    59.0 1.05 15 49  6.7
CB2NV    45.1    21.0 1.1  15 49  7.0               19.0 1.0
CB3NV    45.1    21.0 1.1  15 49  7.0
BR-CN    46.9    27.0 0.85 15 49 23.0               12.0 0.75
```

```
29AUG77 16 36   5.5 0.00 0 2 ARGENTINA
31.8S 69.2W
137.0
FA-NV   62.9     7.0 2.0   16 48 15.2    50
GE-NM   77.2    21.0 1.4   16 47 44.7    83
29AUG77 21  0   8.7 0.00 0 2 ANDREANOF IS
51.7N174.0W
 88.0
FA-NV   41.6    39.0 1.0   21  7 47.5   688
GE-NM   48.3     5.0 1.0   21  6 41.7    78
30AUG77  6 50  41.7 0.00 0 9 CENT. ALASKA
63.2N151.2W
124.0
FA-NV   32.2    73.0 1.3    6 56 59.0   688
GE-NM   37.5    16.0 1.0    6 57 44.1    78
YF-NV   33.7   125.0 1.0    6 57 10.7
YP2NV   33.7   156.0 1.0    6 57 10.7
YF4NV   33.7   164.0 0.95   6 57 11.1
YF3NV   33.7   160.0 0.95   6 57 11.1
OB2NV   33.5    72.0 0.9    6 57  9.2             57.0 0.9
CB3NV   33.5    69.0 1.0    6 57  9.1
RK-CN   32.3    56.0 0.5    6 56 58.6             50.0 0.75
30AUG77 15 12  24.0 0.00 0 2 ANDREANOF IS
51.5N174.1W
  0.0
FA-NV   41.6    26.0 1.2   15 20 16.2   688
GE-NM   48.4    20.0 1.0   15 21  6.3   917
31AUG77  0 42  10.1 0.00 0 2 N. COLOMBIA
 7.4N 76.2W
 58.0
FA-NV   47.6    19.3 2.0    0 50 41.0    63
GE-NM   40.7    33.0 2.0    0 49 47.0    78
 1SEP77  3  0   0.0 0.00 1 8 NOVAYA ZEMLYA
73.3N 54.3E
  0.0
FA-NV   67.9    10.0 0.5    3 11  2.0    59
GE-NM   69.3     6.5 0.8    3 11 10.1    68
YF-NV   69.4   123.0 0.95   3 11 10.7
YP2NV   69.4   151.0 1.1    3 11 10.9
YF4NV   69.4   146.0 1.0    3 11 11.4
YP3NV   69.4   137.0 1.1    3 11 11.3
FR-CN   53.9   568.0 0.7    3  9 26.0            464.0 0.7
BN-ME   54.5   166.0 1.0    3  9 28.0
 1SEP77 10 55  13.3 0.00 0 2 ANDREANOF IS
51.8N172.2W
140.0
FA-NV   40.4     5.5 0.5   11  2 39.9   625
GE-NM   47.2    15.0 0.8   11  3 34.6   833
 1SEP77 17 37   0.9 0.00 0 5 N. COLOMBIA
 6.9N 76.1W
  0.0
FA-NV   48.1     6.0 1.1   17 45 43.0    56
GE-NM   41.1    12.5 1.7   17 44 47.6    68
CB2NV   47.3    70.0 1.25  17 45 36.4             48.0 1.25
CB3NV   47.3    73.0 1.3   17 45 36.4
RK-CN   46.3   101.0 1.1   17 45 25.7             87.0 1.0
 2SEP77  5 56  19.1 0.00 0 5 PANAMA
 7.5N 78.4W
  0.0
FA-NV   46.1    24.5 0.8    6  6 47.0   625
GE-NM   39.2    24.0 1.0    6  5 50.8   833
CB2NV   45.2    12.0 1.2    6  6 40.0              9.0 0.9
CB3NV   45.2    13.0 1.2    6  6 40.0
FR-CN   45.1    75.0 0.75   6  6 35.2             41.0 0.7
 2SEP77  7  9  53.8 0.00 0 5 GALAPAGOS IS
 0.7N 91.1W
  0.0
FA-NV   44.4    30.0 2.3    7 18  6.0   625
GE-NM   39.0    67.5 0.7    7 17 22.1   833
CB2NV   45.2    27.0 1.0    7 17 55.9             21.0 1.0
CB3NV   45.2    26.0 1.0    7 17 55.9
FR-CN   50.2    43.0 0.8    7 18 50.3             34.0 0.7
```

```
 3SEP77 11 56 17.7 0.00 0 8 TONGA IS
15.1S173.5W
   0.0
FA-NV   75.6      4.5 2.0   12  8  4.3    50
GE-NM   61.0     12.0 1.3   12  8 33.7    57
YP4NV   75.1    107.0 1.3   12  8  0.1
YP3NV   75.1    101.0 1.3   12  8  0.3
YP-NV   75.1     89.0 1.3   12  8  0.3
YP2NV   75.1    100.0 1.3   12  8  0.3
CP2NV   75.1     46.0 1.1   12  8  0.1               37.0 1.4
CP3NV   75.2     48.0 1.1   12  8  0.1
 3SEP77 15 24 57.0 0.00 0 2 VENEZUELA
  8.1N 61.7W
   0.0
FA-NV   57.5     13.0 0.8   15 34 51.3   675
GE-NM   50.2     29.0 1.0   15 33 56.9   729
 3SEP77 15 33 45.7 0.00 0 2 DOMINICAN REP.
19.5N  71.0W
   0.0
FA-NV   43.3     13.0 0.8   15 41 48.6   675
GE-NM   36.0     29.0 1.0   15 40 49.0   729
 4SEP77 15 40 59.7 0.00 010 RAT IS
51.0N178.4E
  43.0
FA-NV   46.3      9.5 0.5   15 49 22.4    50
GE-NM   53.1     35.0 1.3   15 50 13.7    57
YP4NV   47.5    260.0 1.0   15 49 32.4
YP3NV   47.5    260.0 1.0   15 49 32.5
YP-NV   47.5    251.0 0.9   15 49 32.1
YP2NV   47.5    339.0 1.0   15 49 32.0
CP2NV   47.3    110.0 1.0   15 49 30.2               20.0 1.1
CP3NV   47.3    148.0 0.8   15 49 30.3
BR-CM   51.9    179.0 0.8   15 50  3.0               18.0 0.8
BR-ME   67.6    143.0 1.15  15 51 49.2
 4SEP77 16 39 47.5 0.00 0 8 S. HONSHU
33.2N140.6E
   0.0
FA-NV   78.9      7.0 1.0   16 51 53.7    50
YP4NV   79.9    326.0 1.25  16 52  0.1
YP3NV   79.9    342.0 1.1   16 52  0.0
YP-NV   79.9    318.0 1.0   16 51 59.0
YP2NV   79.9    321.0 1.2   16 52  0.0
CP2NV   79.6    128.0 1.15  16 51 58.1               27.0 1.1
CP3NV   79.7    122.0 1.2   16 51 58.0
BR-CM   83.3     99.0 1.0   16 52 15.0               21.0 1.1
 4SEP77 17 10 37.0 0.00 0 9 RAT IS.
50.9N178.3E
  16.0
FA-NV   46.4     18.0 0.7   17 18 57.5    50
YP4NV   47.5    826.0 0.9   17 19 13.4
YP3NV   47.5    977.0 1.1   17 19 13.3
YP-NV   47.5    628.0 1.2   17 19 13.0
YP2NV   47.5    745.0 1.15  17 19 13.0
CP2NV   47.4     50.0 0.7   17 19  5.2               38.0 1.3
CP3NV   47.4     77.0 0.7   17 19  5.2
BR-CM   52.0    123.0 0.6   17 19 38.3               62.0 0.6
BR-ME   67.7     80.0 1.15  17 21 23.9
 4SEP77 17 28 50.5 0.00 0 9 RAT IS
50.9N178.1E
  63.0
FA-NV   46.6     17.0 0.8   17 33 15.0    50
YP4NV   47.7    985.0 1.1   17 33 28.0
YP3NV   47.7   1044.0 1.2   17 33 28.0
YP-NV   47.7    913.0 1.1   17 33 28.0
YP2NV   47.7   1159.0 1.1   17 33 28.0
CP2NV   47.6     65.0 0.7   17 33 22.1               16.0 0.8
CP3NV   47.6     52.0 0.6   17 33 22.1
BR-CM   52.1    195.0 0.5   17 33 54.5               65.0 0.6
BR-ME   67.6    130.0 1.5   17 35 40.1
```

```
 4SEP77 18  0 11.2 0.00 0 8 RAT IS
51.0N178.3E
   3.0
FA-NV   46.4    30.0 1.0   18  8 37.0  544
YF-NV   47.5   103.0 0.83  18  8 47.0
YF2NV   47.5   120.0 0.85  18  8 47.0
CE2NV   47.4    34.0 1.0   18  8 44.7               7.0 0.65
CE3NV   47.4    32.0 1.1   18  8 44.7
YF4NV   47.5   118.0 0.75  18  8 47.0
YF3NV   47.5    94.0 0.7   18  8 47.0
BK-CN   51.9    92.0 0.5   18  9 17.1              22.0 0.6
 4SEP77 17 38 21.6 0.00 0 2 RAT IS
51.1N177.6E
  13.0
FA-NV   46.8    11.5 1.1   17 46 52.3   50
GE-NM   53.6    31.5 1.2   17 47 44.2   57
 4SEP77 18 25 55.1 0.00 010 RAT IS
51.1N177.9E
  73.0
FA-NV   46.6     9.0 1.2   18 34 18.0   50
GE-NM   53.4    30.0 1.1   18 35  9.5   57
YF-NV   47.8   287.0 1.0   18 34 27.4
YF2NV   47.8   315.0 1.3   18 34 27.4
CE2NV   47.6   103.0 1.1   18 34 25.7              32.0 1.1
CE3NV   47.6    98.0 1.1   18 34 25.7
YF4NV   47.7   326.0 1.2   18 34 27.4
YF3NV   47.7   384.0 1.25  18 34 27.3
BR-CN   52.1   146.0 0.5   18 34 57.2              13.0 0.5
HA-MB   67.7    34.0 0.5   18 36 43.3
 4SEP77 18 38 28.4 0.00 0 2 RAT IS
51.1N178.3E
  66.0
FA-NV   46.4    31.0 1.1   18 46 50.0  544
GE-NM   53.1    12.0 1.3   18 47 41.1   57
 4SEP77 19 23  1.1 0.00 0 9 RAT IS
51.0N177.7E
  26.0
FA-NV   46.8     5.5 1.3   19 31 30.0   50
GE-NM   53.5    17.0 1.1   19 32 21.7   57
YF-NV   47.9   170.0 1.0   19 31 39.8
YF2NV   47.9   231.0 1.1   19 31 39.7
YF4NV   47.9   244.0 0.9   19 31 39.9
YF3NV   47.9   218.0 1.0   19 31 39.9
CE2NV   47.8    59.0 1.2   19 31 37.5              12.0 0.9
CE3NV   47.8    57.0 1.3   19 31 37.5
BR-CN   52.2    86.0 0.4   19 32  9.1              16.0 0.4
 4SEP77 22 18 35.3 0.00 0 2 RAT IS
51.8N176.4E
   0.0
FA-NV   47.4     5.5 0.7   22 27  5.2  544
GE-NM   54.1    15.0 0.8   22 27 58.0  729
 4SEP77 23 20 48.0 0.00 0 9 RAT IS
51.0N178.5E
  54.0
FA-NV   46.3    16.5 1.8   23 29 11.1   50
YF4NV   47.4   430.0 1.4   23 29 19.6
YF3NV   47.4   386.0 1.5   23 29 19.8
YF-NV   47.4   352.0 1.3   23 29 19.7
YF2NV   47.4   411.0 1.3   23 29 19.7
CE2NV   47.3   128.0 1.6   23 29 18.6             117.0 1.6
CE3NV   47.3   130.0 1.6   23 29 18.4
BR-CN   51.8   255.0 0.5   23 29 50.8              84.0 0.9
HA-MB   67.5   113.0 1.2   23 31 36.8
 5SEP77  0 58  6.2 0.00 0 2 RAT IS
50.6N177.7E
   0.0
FA-NV   46.9    25.0 1.2    1  6 40.3  544
GE-NM   53.6     7.5 1.1    1  7 32.5   68
```

```
 5SEP77 12 52 14.9 0.00 0 9 RAT IS
51.0N177.6E
  55.0
FA-NV   46.7     13.8 1.3   13   0 36.9   544
GE-NM   53.5     64.5 1.0   13   1 28.5   833
YF4NV   47.8     50.0 1.1   13   0 45.4
YF3NV   47.8     49.0 1.1   13   0 45.4
YF-NV   47.8     40.0 1.0   13   0 45.6
YF2NV   47.8     49.0 1.0   13   0 45.7
CE2NV   47.7     17.0 1.1   13   0 44.4                 13.0 1.1
CE3NV   47.7     17.0 1.1   13   0 44.2
BK-CN   52.2     12.0 0.6   13   1 16.9                 11.0 0.6
 5SEP77 22 31     6.2 0.00 0 2 RAT IS
51.1N178.3E
  58.0
FA-NV   46.4      5.0 0.5   22 39 29.8   544
GE-NM   53.1      3.0 0.8   22 40 20.5    68
 6SEP77  6 48 31.0 0.00 0 2 ANDREANOF IS
51.2N178.4W
  75.0
FA-NV   44.3      8.0 0.5    6 56 37.0   513
GE-NM   51.1     21.0 1.0    6 57 29.0   833
 8SEP77  6 36     8.8 0.00 0 5 S. PERU
16.7S 70.5W
   0.0
FA-NV   69.9     12.0 0.7    6 47 21.8   525
GE-NM   63.6     18.5 0.8    6 46 41.1   729
CB2NV   66.9     53.0 0.8    6 47 14.7                  47.0 0.8
CE3NV   66.9     55.0 0.7    6 47 14.7
BK-CN   70.5     15.0 0.5    6 47 22.9
 8SEP77  8  3 53.8 0.00 0 5 MONA PASSAGE
18.5N 66.5W
102.0
FA-NV   45.5     22.0 0.8    8 12  5.3   525
GE-NM   38.2     13.5 0.7    8 11  4.8   729
CB2NV   45.1     82.0 0.8    8 12  1.4                  74.0 0.8
CE3NV   45.1     71.0 1.0    8 12  1.6
BK-CN   37.8     39.0 0.8    8 11 23.5                  28.0 0.8
 9SEP77  2 35     6.2 0.00 0 6 RUSSIA-CHINA BDR
43.0N131.3E
565.0
FA-NV   78.0     10.5 0.7    2 46  8.5    53
GE-NM   64.2     19.0 1.0    2 46 40.7    63
CB2NV   79.1    125.0 0.9    2 46 14.4                  72.0 0.9
CE3NV   79.1    111.0 0.9    2 46 14.3
BK-CN   78.3    360.0 0.6    2 46  8.7                 315.0 0.6
BK-NB   89.6    101.0 0.9    2 47  4.0
 9SEP77 15 58 50.6 0.00 0 3 S. ALASKA
62.0N151.1W
  48.0
FA-NV   31.5     11.3 0.7   16  5 11.4   544
CB2NV   32.8     24.0 0.9   16  5 23.0
CE3NV   32.8     25.0 0.8   16  5 23.9
 9SEP77 21 17 59.2 0.00 0 4 RAT IS
50.9N178.6E
  70.0
FA-NV   46.2     36.0 0.8   21 26 20.3   544
CB2NV   47.2     44.0 0.86  21 26 28.2                  24.0 0.8
CE3NV   47.2     41.0 0.8   21 26 28.0
BK-CN   51.8     38.7 0.55  21 27  0.7                  23.8 0.64
10SEP77  4 39     5.6 0.00 0 5 PERU CST.
14.3S 76.1W
  46.0
FA-NV   64.9      5.0 0.8    4 49 40.5    53
GE-NM   58.8      4.5 1.0    4 48 59.3    72
CB2NV   63.8     33.0 0.9    4 49 33.2
CE3NV   63.8     39.0 1.1    4 49 33.4
BK-CN   66.9     77.5 0.8    4 49 50.4                  67.2 0.9
```

```
10SEP77  9 24  2.2 0.00 0 2 TONGA IS
15.9S174.7W
   0.0
FA-NV   77.2    13.0 0.8    9 35 59.0  544
GE-NM   82.4    17.5 1.1    9 36 26.3 1042
10SEP77 10 21   9.1 0.00 0 9 GUATEMALA
14.1N  91.5W
  31.0
FA-NV   32.8    22.0 1.1   10 27 40.6    53
YP4NV   31.7   269.0 1.35  10 27 30.6
YP3NV   31.7   314.0 1.25  10 27 30.5
YP-NV   31.7   228.0 1.3   10 27 30.3
YP2NV   31.7   277.0 1.25  10 27 30.4
CE2NV   31.8   100.0 1.2   10 27 31.2
CE3NV   31.8    98.0 1.25  10 27 31.3
EN-MB   37.6   495.0 1.0   10 28 22.1
ER-CN   36.8   166.0 0.84  10 28 11.9              22.6 0.94
10SEP77 16  0   0.5 0.00 0 2 LAKE BAIKAL REG
57.2N106.8E
   0.0
FA-NV   77.5     8.0 1.0   16 11 59.4   544
GE-NM   61.8    32.0 0.8   16 12 23.1    72
10SEP77 16 56  28.3 0.00 0 2 MEXICO
14.1N  92.1W
   0.0
FA-NV   32.5    10.0 0.8   17  2  2.0   544
GE-NM   26.3     7.0 1.0   17  2  6.7    72
11SEP77 14  8   4.7 0.00 0 2 SAMOA IS
15.4S172.8W
  15.0
FA-NV   75.6    38.0 2.0   14 19 50.0   531
GE-NM   80.7    11.0 1.3   14 20 18.1    78
11SEP77 14 12  33.1 0.00 0 2 SAMOA IS
15.1S172.8W
  28.0
FA-NV   75.3    40.0 2.0   14 24 15.3   531
GE-NM   80.5     8.8 1.7   14 24 43.5    78
11SEP77 23 19  24.1 0.00 0 2 CRETE
35.1N  23.2E
  18.0
EN-MB   66.4   170.0 1.25  23 30 11.7
ER-CN   77.8   224.0 0.9   23 31 19.8              18.0 0.5
12SEP77 16 48  45.3 0.00 0 3 KURILES
49.3N155.1E
   0.0
FA-NV   60.7     9.3 1.0   16 58 56.6   531
CB2NV   61.8    57.0 1.0   16 59  4.3              52.0 1.0
ER-CN   63.6    27.0 0.9   16 59 16.2              17.0 0.75
12SEP77 23 17  45.4 0.00 0 2 VIRGIN IS
19.5N  64.3W
   0.0
FA-NV   48.5    12.0 0.7   23 26 31.1   544
GE-NM   41.1    23.5 1.0   23 25 32.6   990
12SEP77 23 16  52.7 0.00 0 4 E. SEA OF JAPAN
41.9N138.3E
  29.0
FA-NV   74.8    18.0 1.7   23 28 31.5   544
GE-NM   81.2    71.5 1.1   23 29  8.5   990
CB2NV   75.8    27.0 1.2   23 28 37.3              16.0 1.1
ER-CN   76.8    39.0 1.0   23 28 41.4              35.0 0.9
13SEP77  0 21  49.3 0.00 0 6 TONGA IS
15.4S173.3W
   0.0
FA-NV   75.9    11.0 2.0    0 33 37.0    50
GE-NM   81.1    25.0 1.8    0 34  6.5    73
YP-NV   75.2   111.0 1.6    0 33 33.4
YP2NV   75.2   155.2 1.56   0 33 33.4
YP4NV   75.2   145.0 1.5    0 33 34.1
CB2NV   75.2    66.0 1.8    0 33 32.7              13.0 0.9
```

```
13SEP77  3 33   8.6 0.00 0 2 SAMOA IS.
15.3S172.5W
   0.0
FA-NV   75.6     8.0 0.7    3 44 55.1  544
GE-NM   80.7    20.5 1.1    3 45 25.0  990
13SEP77  3 59  42.0 0.00 0 2 SAMOA IS
15.4S172.5W
   0.0
FA-NV   75.6     4.0 1.5    4 11 28.5   50
GE-NM   80.6    87.0 1.2    4 11 58.6  990
13SEP77  4 55  32.3 0.00 0 4 JAPAN
41.5N142.3E
  82.0
FA-NV   72.7    13.0 0.7    5  6 52.2  544
GE-NM   75.3    48.0 0.8    5  7 30.8  990
CB2NV   73.7    16.0 0.8    5  6 57.7                9.0 0.7
BR-CN   75.6    13.0 0.65   5  7  6.7               10.0 0.95
13SEP77  5 36   7.7 0.00 0 3 CHILE-ARGENTINA BDR
23.1S 67.4W
217.0
FA-NV   76.8     3.2 0.8    5 47 36.3   50
GE-NM   70.6     5.0 1.0    5 47  0.7   73
CB2NV   75.7    31.0 1.0    5 47 30.5               26.0 0.85
13SEP77 14 38  34.7 0.00 0 4 RAT IS
51.2N177.4E
   0.0
FA-NV   46.9    10.5 1.0   14 47  7.1  544
GE-NM   53.6    33.5 0.7   14 47 59.3  990
CB2NV   47.9    12.0 1.1   14 47 14.8
BR-CN   52.3    34.0 0.4   14 47 46.1                9.5 0.5
16SEP77 23 48   7.3 0.00 0 2 AUSTRIA
46.3N 13.1E
   0.0
FA-NV   83.7    44.0 0.8    0  0 39.2  550
GE-NM   81.3    58.0 1.3    0  0 26.5  833
17SEP77 10 46  53.1 0.00 0 6 BONIN IS.
28.7N140.4E
   0.0
FA-NV   81.8    16.5 1.3   10 59 17.7  513
YP4NV   82.8   112.0 0.9   10 59 22.8
YP-NV   82.8   100.0 0.9   10 59 22.6
YP2NV   82.8    97.0 0.9   10 59 22.5
CB2NV   82.7    62.0 0.9   10 59 21.9               40.0 0.85
CB3NV   82.7   103.0 0.9   10 59 21.9
17SEP77 16 28  48.4 0.00 0 4 ALEUTIANS
50.0N173.8W
   0.0
FA-NV   41.6     6.5 0.7   16 36 39.4   44
CB2NV   42.5    63.0 0.9   16 36 47.1               52.0 0.8
CB3NV   42.5   104.0 0.85  16 36 47.1
BR-CN   48.4    47.0 1.0   16 37 31.7
18SEP77  5 44   7.5 0.00 0 8 EL SALVADOR
13.7N 89.5W
  65.0
FA-NV   34.1    11.0 0.8    5 50 48.0   44
GE-NM   27.7     8.5 0.9    5 49 51.3   73
YP4NV   33.0   138.0 1.0    5 50 38.3
YP-NV   33.0   132.0 1.0    5 50 38.0
YP2NV   33.0   150.0 1.0    5 50 38.0
CB2NV   33.1    67.0 1.0    5 50 38.4               37.0 1.2
CB3NV   33.1    87.0 1.0    5 50 38.4
BR-CN   37.3   284.0 0.7    5 51 11.5              172.0 0.8
19SEP77 18 21  23.4 0.00 0 2 CHILE CST
29.7S 71.2W
  22.0
FA-NV   80.2     6.5 1.4   18 33 32.0   44
GE-NM   74.5    14.5 1.3   18 33  0.0   73
21SEP77  3 12  31.0 0.00 0 2 E. SEA OF JAPAN
44.0N137.0E
   0.0
FA-NV   74.2    12.5 1.7    3 23 59.5  488
GE-NM   80.5    13.0 1.0    3 24 33.2  990
```

```
21SEP77 16  5  5.0 0.00 0 2 VENEZUELA CST
 9.0N 62.0W
   0.0
FA-NV   56.7    15.0 1.5   16 14 46.3   488
GE-NM   49.3    28.5 1.3   16 13 51.8   990
21SEP77 17 39  24.0 0.00 0 2 E. CST KAMCHATKA
54.0N161.0E
   0.0
FA-NV   55.7    36.0 1.8   17 49  4.3   488
GE-NM   62.0    10.5 1.5   17 49 48.5    78
23SEP77 11 47   4.0 0.00 0 2 ALASKA PEN.
55.0N157.0W
   0.0
FA-NV   31.7     7.5 0.8   11 53 46.3   531
GE-NM   36.1    15.5 0.8   11 54 43.1   885
 8OCT77  3  3  54.2 5.50 0 5 PERU
 9.3S 74.6W
130.
GC-NV   60.7    34.0 0.8    3 13 51.5    24
GE-NM   55.2    16.5 1.3    3 13 13.8    26
CB2NV   60.6   341.0 1.0    3 13 51.0             231.0 1.1
BK-CM   62.4   396.0 1.0    3 14  0.7             109.0 0.5
BB-ME   55.6   117.0 1.4    3 13 16.9
 9OCT77  2 27  36.4 0.00 0 5 CHILE CST
30.0S 73.3W
   0.0
GC-NV   78.3    16.0 1.0    2 39 40.1   175
GE-NM   73.9     7.5 1.0    2 39 14.5   313
CB2NV   78.2    15.0 1.0    2 39 39.9               9.0 0.7
CE3NV   78.2    14.0 1.0    2 39 39.9
BK-CM   82.6    27.0 1.0    2 39 58.6              20.0 1.0
10OCT77 21  9  14.7 0.00 0 3 S TONGA IS.
25.6S175.5W
   0.0
GC-NV   63.9    16.0 1.3   21 21 45.3   238
CB2NV   64.0     8.0 1.2   21 21 46.2
CE3NV   64.0     7.0 1.4   21 21 46.2
10OCT77 21 21  31.9 0.00 0 3 FIJI REGION
17.7S178.4W
420.0
GC-NV   80.2    28.0 0.8   21 32 58.0   238
CB2NV   80.3    16.0 1.0   21 32 58.5              12.0 0.7
CE3NV   80.3    15.0 1.0   21 32 58.4              13.0 0.9
11OCT77  2  3  37.2 0.00 0 3 S TONGA IS
26.5S174.8W
   0.0
GC-NV   84.2    20.5 1.0    2 16  9.3   238
CB2NV   84.3    13.0 1.2    2 16  9.7              11.0 1.1
CE3NV   84.3    12.0 1.1    2 16 10.0
11OCT77 11 53  46.4 0.00 0 3 S HONSHU
31.0N140.8E
   0.0
GC-NV   80.9     3.8 1.0   12  6  4.2    25
CB2NV   81.0    28.0 1.1   12  6  4.7              16.0 1.0
CE3NV   81.0    28.0 1.15  12  6  4.8
13OCT77 23 16  30.0 0.00 0 5 PERU CST
12.2S 77.9W
 30.0
GC-NV   61.1    18.5 0.8   23 26 41.0   175
GE-NM   56.1    14.5 0.9   23 26  2.7   313
CB2NV   61.0    19.0 0.8   23 26 40.5              10.0 0.9
CE3NV   61.0    17.0 0.85  23 26 40.5
BK-CM   64.5   233.0 0.76  23 27  1.3              83.0 0.85
15OCT77  7 34  31.5 0.00 0 5 MEXICO CST
15.6N 98.6W
   0.0
GC-NV   26.6    27.0 1.2    7 40 10.1   200
GE-NM   22.4    16.5 1.3    7 39 26.3   448
CB2NV   26.5    74.0 1.26   7 40  9.3              17.7 1.1
CE3NV   26.5    77.0 1.25   7 40  9.2
BK-CM   35.5    61.0 1.0    7 41 26.0              39.0 1.1
```

```
16OCT77  1 59 33.7 0.00 C 4 KURILES
47.CN153.8E
  C.0
GC-NW   63.7     14.0 2.7    2 10  9.7  200
GE-NM   69.4     14.0 1.0    2 10 43.8  448
CB2NW   63.8     29.0 2.4    2 10  9.6              6.0 1.8
CB3NW   63.8     31.0 2.5    2 10  9.7
16OCT77  4 25 43.0 0.00 C 5 S. ALASKA
59.9N152.5W
 66.0
GC-NW   32.3      5.0 0.8    4 32  4.2  200
GE-NM   36.5     15.5 0.8    4 32 44.3  448
CB2NW   32.4     17.3 1.15   4 32  4.5             10.3 1.13
CB3NW   32.4     17.3 1.09   4 32  4.6
BR-CN   33.4     30.0 0.75   4 32 13.6
27OCT77 12  6   2.9 0.00 0 3 FIGI IS
18.8S179.2W
  C.0
GC-NW   81.5     22.5 1.3   12 18 19.5  470
CB2NW   81.6     24.7 1.43  12 18 19.4             11.9 1.10
CB3NW   81.6     25.2 1.38  12 18 19.3
29OCT77 10 41   6.4 0.00 C 4 N CHILE CST
20.0S 72.7W
100.0
GC-NW   70.4     16.5 0.6   10 52 11.3  500
GE-NM   65.4     33.0 1.0   10 51 45.5  417
CB2NW   70.3     35.3 0.9   10 52 15.7              7.0 0.8
CB3NW   70.3     33.2 1.0   10 52 15.8
30OCT77  0  1 50.8 0.00 0 4 GUATEMALA CST
13.6N 90.8W
  C.0
GC-NW   32.7     14.0 2.5    0  8 25.   500
GE-NM   27.4      4.0 1.1    0  7 39.2   31
CB2NW   32.6     15.0 1.8    0  6 25.6             12.0 1.6
CB3NW   32.6     15.0 1.8    0  6 25.6
30OCT77  1  4   3.3 0.00 C 3 FIGI IS
21.2S178.5W
  C.0
GC-NW   82.7      5.5 0.7    1 16 29.5   40
CB2NW   82.8     54.0 0.7    1 15 29.8             44.0 0.65
CB3NW   82.8     59.0 0.6    1 16 29.8
 4OCT77 13 45 11.0 0.00 C 4 WINDWARD IS.
12.0N 59.0W
  C.0
GE-NM   49.7      8.0 1.3   13 53 34.5  417
CB2NW   56.7     11.0 0.7   13 54 25.0              4.6 0.9
CB3NW   56.7      9.0 0.8   13 54 25.0
BR-CN   48.0     40.0 0.7   13 53 28.7
 4OCT77 15 39   6.0 0.00 0 4 W. CST. HONSHU
38.CN138.CE
  C.0
GE-NM   84.1      8.0 1.3   15 51 25.8   36
CB2NW   78.4    103.0 1.1   15 50 54.2             76.0 1.2
CB3NW   78.4     99.0 1.2   15 50 54.3
BR-CN   80.3     41.0 1.5   15 31  7.1             35.0 1.2
 7OCT77 21 19 18.2 0.00 C 3 ANDREANOFF IS.
51.3N179.6W
171.C
CB2NW   46.1     21.0 0.8   21 27 28.1             18.0 1.0
CB3NW   46.1     21.0 0.8   21 27 28.2
BR-CN   50.5     37.0 0.45  21 27 59.4             32.0 0.5
16OCT77  6  0 44.8 0.00 C 4 MEXICO CST.
16.0N 93.7W
130.0
GE-NM   23.9      2.5 0.7    6  5 48.5   31
CB2NW   29.0      8.7 1.16   6  6 32.3
CB3NW   29.0      9.6 1.14   6  6 32.4
BR-CN   34.8     15.0 0.55   6  7 21.9              9.0 0.4
```

```
21OCT77 19  9 41.0 0.00 0 4 FOX IS.
53.3N170.0W
  0.0
GC-NV   40.0     18.5 0.9    19 17 25.3     35
GE-NM   45.7     24.5 1.0    19 18 12.1     31
CB2NV   40.0    199.0 1.0    19 17 14.2              134.0 1.1
CB3NV   40.0    180.0 1.1    19 17 14.1
24OCT77  1 45 11.0 0.00 0 3 HONSHU CST.
33.0N137.0E
  0.0
GC-NV   82.1     33.0 1.1     1 57 13.6    450
CB2NV   82.1     27.0 1.0     1 57 26.2               23.3 0.95
CB3NV   82.1     26.0 1.0     1 57 26.2
24OCT77  5 57  5.0 0.00 0 4 N. ATLANTIC
44.0N 39.0W
  0.0
GC-NV   56.8     26.0 1.0     6  8 23.8    450
GE-NM   51.0     78.5 1.0     6  7 49.5    427
CB2NV   56.8     21.0 1.1     6  7 11.2               15.7 0.9
CB3NV   56.8     19.0 1.1     6  7 11.0
24OCT77  7  9 12.0 0.00 0 4 ALASKA PENN.
55.0N158.0W
  0.0
GC-NV   33.3     33.0 0.9     7 16 22.9    450
GE-NM   36.7      4.5 0.8     7 17  6.9     31
CB2NV   33.3     29.0 0.85    7 15 53.7
CB3NV   33.3     27.0 0.85    7 15 53.6
30OCT77 21 38 15.6 0.00 0 3 JAPAN
44.8N145.0E
  0.0
GE-NM   75.7     25.0 1.2    21 50  3.3    417
CB2NV   70.2     13.0 0.7    21 49 30.5
CB3NV   70.2     13.0 0.7    21 49 30.5
 1NOV77  3 54 22.8 0.00 0 3 E. RUSSIA
55.4N130.0E
  0.0
CB2NV   71.6      8.0 0.9     4  5 46.7                6.5 0.9
CB3NV   71.6      8.0 0.9     4  5 46.7
GC-NV   71.6      9.5 0.8     4  5 46.5    500
 2NOV77  1 19 23.9 0.00 0 3 TONGA IS.
15.7S173.5W
  0.0
GE-NM   81.4     33.5 2.5     1 31 42.3    396
CB2NV   75.6     19.0 1.7     1 31  8.7               15.0 1.7
CB3NV   75.6     20.0 1.8     1 31  8.8
 2NOV77  5 51 31.8 0.00 0 3 COSTA RICA
10.6S 85.7W
 22.0
GE-NM   32.5     25.5 0.7     5 56  1.7    396
CB2NV   38.1     37.0 1.1     5 56 50.7               26.0 0.95
CB3NV   38.1     35.0 1.05    5 56 51.0
 2NOV77 14 47 52.0 0.00 0 4 PERU
10.1S 74.6W
  0.0
GE-NM   55.6      6.5 0.8    14 57 31.5     31
CB2NV   61.1     72.0 1.45   14 58  8.3               62.0 1.2
CB3NV   61.1     94.0 1.2    14 58  8.5
BN-CN   63.1    153.0 0.9    14 58 19.1              138.0 1.0
 2NOV77 23 35 58.7 0.00 0 3 FIJI IS.
19.2S179.9E
  0.0
GC-NV   81.7      4.0 1.3    23 48 18.4     74
CB2NV   81.8     23.0 1.2    23 48 18.9
CB3NV   81.8     25.0 1.2    23 48 19.0
 4NOV77  9 53  4.3 5.60 0 4 ANDREANOF IS.
51.7N176.1W
 95.0
GE-NM   49.6      7.0 1.0    10  1 46.8     31
CB2NV   43.6    104.0 0.75   10  1  1.3               29.0 1.4
BN-CN   46.7    525.  0.45   10  1 36.5               15.0 0.5
BN-YB   64.3    149.0 0.8    10  3 30.1
```

```
 4NOV77 10  2  9.5 5.00 0 4 ANDREANOF IS.
51.5N175.6W
  66.0
GE-NM    49.3     32.5 1.3   10 10 53.3   396
CB2NV    48.5     30.0 0.83  10 10  7.5                 26.0 1.0
BR-CN    48.5    196.0 0.5   10 10 46.0               177.0 0.5
BB-MB    64.5     69.0 0.9   10 12 37.6
 4NOV77 12 45 33.7 0.00 C 4 GUATEMALA CST.
13.4N  90.4W
   0.0
GC-NV    33.1      5.5 1.0   12 56 12.5    70
GE-NM    27.7     50.5 1.0   12 55 24.5   396
CB2NV    33.0     38.0 1.1   12 56 11.4                 13.0 1.0
BR-CN    37.5    278.0 0.35  12 56 46.7                 26.0 0.4
 4NOV77 18  7 51.5 0.00 C 2 ANDREANOF IS.
51.4N175.5W
227.0
GE-NM    41.1     36.0 1.2   18 16 20.8   396
CB2NV    43.5     35.0 1.1   18 15 35.5
 5NOV77 14 44  9.2 0.00 C 3 ANDREANOF IS.
51.5N175.6W
  71.0
GC-NV    43.6     10.0 0.6   14 52  6.3    74
CB2NV    43.7     46.4 1.0   14 52  7.0                  7.0 0.6
BR-CN    48.6    485.0 0.5   14 52 44.6                 23.0 0.8
 6NOV77  2 39 35.3 5.50 C 5 E. CST KAMCHATKA
53.4N159.6E
  50.0
GC-NV    57.7     14.0 1.3    2 49 22.3    78
GE-NM    63.0     12.0 0.8    2 49 58.5    31
CB2NV    57.6    107.0 1.3    2 49 22.1                 23.0 1.1
BR-CN    59.0    182.0 0.8    2 49 30.0                 76.0 0.8
BB-MB    72.5     84.0 0.9    2 50 56.5
 8NOV77 14 59  8.3 0.00 C 4 KURILES
47.4N154.3E
   0.0
GC-NV    63.2     21.0 1.3   15  9 39.8   480
GE-NM    68.5     42.0 1.3   15 10 16.0   396
CB2NV    63.3     24.0 1.3   15  9 39.9                 17.0 1.1
CB3NV    63.3     21.0 1.3   15  9 39.9
 9NOV77 21 14 41.5 0.00 C 3 KURILES
47.5N154.4E
  98.0
GE-NM    66.6     19.0 1.1   21 25 37.0   365
CB2NV    63.2      9.0 0.95  21 24 49.1
CB3NV    63.2      8.0 0.9   21 24 49.0
11NOV77  4 29 24.9 0.00 C 4 COSTA RICA
10.4N  84.6W
   0.0
GE-NM    33.3     15.5 0.5    4 36  4.8   417
CB2NV    39.0     13.0 0.9    4 36 53.3                  8.0 0.9
CB3NV    39.0     14.0 0.8    4 36 53.3
BR-CN    41.1     25.0 0.5    4 37  9.0                 20.0 1.2
12NOV77  3 16 44.0 0.00 0 5 KURILES
44.1N148.0E
  34.0
GC-NV    66.7     26.5 0.7    3 27 44.0   450
GE-NM    74.4     30.0 0.7    3 26 16.7   417
CB2NV    66.6     24.0 0.79   3 27 44.3                 16.7 0.79
CB3NV    66.8     23.8 0.67   3 27 44.3
BR-CN    71.0     26.0 0.6    3 27 57.3
12NOV77 13 50  9.6 0.00 C 3 N. CHILE
22.0S  69.2W
   0.0
GC-NV    73.6     10.0 0.8   14  1 46.7   450
CB2NV    73.5     14.0 0.85  14  1 46.2                 12.7 0.8
CB3NV    73.5     13.0 0.9   14  1 46.2
12NOV77 19  4 46.3 0.00 C 3 FIJI REGION
20.4S177.6W
486.0
GC-NV    61.7     17.0 0.8   19 16 14.0    39
CB2NV    61.6    156.0 0.9   19 16 14.3                131.0 0.9
CB3NV    61.6    143.0 0.8   19 16 14.4
```

```
13NOV77  6 42  56.6 5.10 0 5 N. PERU
 7.7S  75.8W
 26.0
GE-NN    53.3    60.0 1.1    8 51 48.3   417
OB2NV    55.6    79.0 0.85   8 52 25.4               65.0 0.9
CE3NV    55.6    75.0 0.9    8 52 25.4
BR-CN    60.5   104.0 0.8    8 52 37.7               85.0 0.9
BR-NB    54.3    83.0 1.1    8 51 55.9
14NOV77 19 29   5.5 4.50 0 5 FOX IS.
52.3N170.6W
 94.0
GE-NN    46.3     5.5 0.7   19 37 23.0    36
CE2NV    40.5    26.0 0.9   19 36 36.9               13.0 0.7
CE3NV    40.5    26.0 0.8   19 36 36.9
BR-CN    45.6    87.4 0.76  19 37 16.2               66.0 1.0
BR-NB    61.5    95.0 1.3   19 39 13.1
16NOV77 10 30  55.3 0.00 0 3 N. CHILE CST
22.8S  70.7W
  0.0
GE-NN    68.7    35.5 0.9   10 42  2.8   395
CE2NV    73.6    21.1 0.9   10 42 33.4
CE3NV    73.6    21.0 0.95  10 42 33.4
16NOV77 19 36  17.6 0.00 C 4 HOKKAIDO JAPAN REG
42.0N142.2E
 76.0
GE-NN    75.0    33.5 0.8   19 43 15.3   417
CE2NV    73.5    21.0 0.9   19 47 43.2               20.0 1.1
CE3NV    73.5    20.0 0.9   19 47 43.2
BR-CN    75.2    71.0 0.8   19 47 51.7               13.0 0.4
17NOV77 17 20  34.1 0.00 C 4 S. HONSHU
33.6N139.8E
105.0
GC-NV    75.9    27.0 1.3   17 32 31.3    78
CE2NV    80.0   270.0 1.1   17 32 32.1              222.0 1.1
CE3NV    80.0   243.0 1.1   17 32 32.1
BR-CN    83.3   236.0 1.3   17 32 46.0              208.0 1.0
20NOV77 18 53  45.6 0.00 C 5 CENT. ALASKA
62.1N152.1W
  0.0
GC-NV    33.2    20.0 0.9   19  0 26.7   470
GE-NN    37.4    48.0 1.1   19  1  2.8   417
CE2NV    33.3    37.0 0.9   19  0 27.0               26.0 0.9
CE3NV    33.3    32.0 1.0   19  0 27.1
BR-CN    32.5    37.0 0.4   19  0 20.0               75.0 0.5
21NOV77  2  9  28.7 0.00 0 4 E. SEA OF JAPAN
42.9N139.0E
244.0
GC-NV    74.2    21.7 1.0    2 20 43.8   470
GE-NN    80.2    44.5 1.0    2 21 14.3   417
CE2NV    74.6    23.0 1.1    2 20 44.2               17.0 1.0
CE3NV    74.6    20.0 1.1    2 20 44.2
21NOV77 21 29  16.0 0.00 C 4 ANDREANOF IS.
52.7N174.6W
239.0
GC-NV    42.6    35.5 0.6   21 36 53.1   470
GE-NN    48.5    49.0 0.9   21 37 37.5   417
CE2NV    42.6    21.0 0.8   21 36 53.7               16.0 0.8
CE3NV    42.6    22.0 0.85  21 36 53.7
22NOV77  6 39  15.5 0.00 C 2 FIJI REGION
19.7S176.2W
  0.0
OB2NV    80.2    20.0 1.1    8 51 33.3
GC-NV    80.1    18.2 1.0    8 51 32.2   470
23NOV77 10  6  32.0 0.00 0 2 ARGENTINA
31.3S  67.1W
  0.0
CE2NV    82.4    15.0 0.8   10 18 55.0
GC-NV    82.5    15.2 0.7   10 18 55.2   470
```

```
23NOV77 10 10 15.0 0.00 0 2 ARGENTINA
31.7S 67.7W
    C.0
CB2NV   82.4    14.0 0.9   10 22 38.2          13.0 0.9
GC-NV   82.5    15.0 0.8   10 22 38.5   470
23NOV77 10 35  19.2 0.00  0 2 ARGENTINA
32.1S 69.6W
    C.0
CB2NV   81.8     9.8 1.0   10 47 41.7
GC-NV   81.8     9.0 1.1   10 47 42.0   470
23NOV77 11   8 41.1 0.00  0 2 ARGENTINA
31.0S 67.6W
    C.0
CB2NV   81.9    47.0 1.1   11 21  0.7          13.0 0.8
GC-NV   82.0    44.0 0.8   11 21  0.3   470
23NOV77 11 44  18.6 0.00  0 2 ARGENTINA
31.5S 67.5W
    C.0
CB2NV   82.3    15.0 0.9   11 56 39.6
GC-NV   82.4    17.8 0.9   11 56 40.0   470
23NOV77 11 46  55.1 0.00  0 2 ARGENTINA
31.6S 67.7W
    C.0
CB2NV   82.3    23.3 0.9   11 59 16.1          22.0 0.8
GC-NV   82.4    21.3 0.7   11 59 16.3   470
23NOV77 11 58  44.5 0.00  0 2 ARGENTINA
30.4S 67.4W
    C.0
CB2NV   81.5   131.0 1.3   12 10 28.1           9.0 0.6
GC-NV   81.6    10.2 1.1   12 10 28.3    35
23NOV77 13   5  0.2 0.00  0 2 ARGENTINA
31.1S 67.7W
    C.0
CB2NV   81.9    96.0 1.3   13 17 20.7          48.0 1.4
GC-NV   82.0    60.0 1.1   13 17 21.2   470
23NOV77 13 38  46.7 0.00  0 2 ARGENTINA
31.3S 66.0W
    C.0
CB2NV   81.9    15.0 1.1   13 51  7.4           8.0 0.8
GC-NV   82.0    15.0 0.8   13 51  7.8   470
23NOV77 16 36   1.2 0.00  0 2 ARGENTINA
31.4S 68.2W
    C.0
CB2NV   81.9   101.0 1.1   16 48 22.5          85.0 1.2
GC-NV   82.0     8.5 0.9   16 48 23.0    35
23NOV77 21 52   3.0 0.00  0 2 ARGENTINA
31.5S 67.6W
    27.0
CB2NV   82.3    35.0 1.0   22  4 20.4          30.0 1.1
GC-NV   82.4    34.5 0.8   22  4 21.0   470
23NOV77 23 27  34.7 0.00  0 2 ARGENTINA
31.7S 67.5W
    C.0
CB2NV   82.5    38.0 1.2   23 39 57.0          28.0 1.2
GC-NV   82.6    31.0 1.0   23 39 57.3   470
24NOV77  1 57  28.0 0.00  0 2 ARGENTINA
32.3S 67.6W
    C.0
CB2NV   82.8    75.0 1.5    2  9 51.3          41.0 1.3
GC-NV   82.9    54.0 1.1    2  9 51.8   470
24NOV77  2 15   3.5 0.00  0 2 ARGENTINA
31.3S 67.7W
    C.0
CB2NV   82.1    38.0 1.1    2 27 25.6           7.0 1.1
GC-NV   82.1    35.5 0.8    2 27 26.7   470
24NOV77 17   0  1.3 0.00  0 2 TUAMOTO ARCH
21.8S139.0W
    C.0
CB2NV   62.8   145.0 1.0   17 10 27.7          88.0 1.0
GC-NV   62.8    17.1 0.8   17 10 27.3    35
```

```
24NOV77 17 56 40.9 0.00 0 2 CHILE-BOLIVIA
21.2S 67.7W
   0.0
CB2NV   74.1    80.0 1.0   18  8 19.3              69.0 1.0
GC-NV   74.1    64.3 1.0   18  8 19.7  470
24NOV77 18 20  12.3 0.00 0 2 ARGENTINA
32.1S  68.2W
   0.0
CB2NV   82.4    71.0 1.0   18 32 34.8
GC-NV   82.5    65.2 0.8   18 32 35.2  470
24NOV77 18 42  38.6 0.00 0 2 ARGENTINA
31.3S  67.5W
   0.0
CB2NV   82.2    79.0 1.3   18 55 59.6              30.0 1.2
GC-NV   82.2     5.8 1.1   18 55  0.0   35
26NOV77 13 52  46.5 0.00 0 2 ARGENTINA
31.2S  67.4W
150.0
CB2NV   82.1    16.0 1.2   14  4 48.7              11.0 0.9
GC-NV   82.8    12.0 1.1   14  4 49.0  520
27NOV77  8 36   1.7 0.00 0 2 KURILES
46.2N 153.1E
   0.0
CB2NV   64.6    31.0 1.1    8 46 41.7              10.0 1.0
GC-NV   64.5    25.9 1.5    8 46 41.1  520
27NOV77  9  8   2.3 0.00 0 2 ARGENTINA
31.5S  69.7W
   0.0
CB2NV   81.2    16.0 0.9    9 20 21.8
GC-NV   81.3    19.0 1.0    9 20 21.5  520
27NOV77 10 19  19.7 0.00 0 2 FIJI REGION
23.2S 178.1W
   0.0
CB2NV   84.0    14.0 1.1   10 31 49.3
GC-NV   83.9    13.8 1.0   10 31 48.7  520
27NOV77 10 46  42.5 0.00 0 2 ALEUTIANS
51.4N 166.2W
   0.0
CB2NV   37.7   106.0 1.0   10 54  0.0              86.0 1.0
GC-NV   37.6     8.0 0.8   10 53 59.2   40
27NOV77 12 40  20.0 0.00 0 2 FIJI REGION
19.8S 178.4W
580.0
CB2NV   81.8   112.3 0.9   12 51 39.0              24.2 0.65
GC-NV   81.7    11.7 0.8   12 51 38.8   40
27NOV77 15  5   9.1 5.20 0 4 ALASKA PENN
58.5N 155.4W
116.0
CB2NV   33.1    70.5 0.71  15 11 34.3              50.7 0.83
GC-NV   33.0    48.0 0.7   15 11 33.7  520
HN-ME   50.8    90.0 0.9   15 13 57.7
HN-CH   35.2   559.0 0.5   15 11 52.0
28NOV77  0 17  25.4 0.00 0 2 ARGENTINA
31.1S  67.7W
  23.0
CB2NV   81.9    75.5 1.22   0 29 41.9              58.7 1.04
GC-NV   82.0     6.8 1.0    0 29 42.4   40
28NOV77  4 19  38.6 0.00 0 2 ARGENTINA
31.3S  67.5W
  45.0
CB2NV   82.4    65.0 0.7    4 31 53.2              38.3 0.62
GC-NV   82.4     6.0 1.1    4 31 55.3   40
28NOV77  6 31  36.9 0.00 0 2 ARGENTINA
31.2S  67.4W
  55.0
CB2NV   82.1   107.0 1.4    6 43 50.7              26.0 0.9
GC-NV   82.2     9.3 1.0    6 43 50.8   40
28NOV77 18 40  27.0 0.00 0 2 ARGENTINA
31.8S  69.5W
153.0
CB2NV   81.6    89.0 1.0   18 52 26.2              79.0 1.0
GC-NV   81.6     7.3 0.8   18 52 26.4   40
```

```
  2DEC77 12 57 15.4 5.70 0 6 S. CST. KAMCHATKA
52.6N159.6E
  39.3
IC-MS   76.7    15.0 0.8   13  9  4.0    65
GE-NM   62.6    12.0 0.7   13  7 42.1    31
OB2NV   57.8    44.0 1.5   13  7  5.8
BN-ME   72.9   156.0 0.8   13  8 41.9
IP-NE   72.9     6.0 0.7   13  8 42.0    21
BR-ON   55.4   125.0 0.9   13 07 15.1
  3DEC77 12 23 56.9 0.00 0 3 COSTA RICA CST.
 8.7N 84.4W
   0.0
IC-MS   22.9    14.0 1.1   12 29  0.0    64
GE-NM   34.8    15.0 1.1   12 30 46.5   385
CB2NV   40.5    49.2 1.74  12 31 36.4
  4DEC77 11 39  4.7 0.00 0 3 SEA OF OKHOTSK
45.3N146.6E
500.0
IC-MS   86.0    24.0 0.5   11 50 54.3    64
GE-NM   72.7     3.5 0.7   11 49 45.0    31
OB2NV   67.3    62.6 0.73  11 49 13.0
  7DEC77  0 32 17.7 0.00 0 4 CHILE ARGENTINA BDR
30.1S 69.1W
   0.0
IC-MS   64.2    47.5 1.0    0 42 51.0    64
GE-NM   75.7     3.5 1.0    0 44  5.0     8
GC-NV   80.5    12.4 0.8    0 44 33.3    38
CB2NV   80.5   137.6 1.1    0 44 32.9
13DEC77  1 14 15.7 0.00 0 5 N. ATLANTIC OCEAN
17.3N 55.0W
   0.0
IC-MS   34.2    26.0 1.5    1 21  3.3    36
GE-NM   45.7     4.0 1.1    1 23 11.8     5
CB2NV   56.8    93.0 0.9    1 24  4.0
BN-ME   30.8   162.0 2.1    1 20 32.6
IP-NE   30.8    50.0 1.2    1 20 33.0   350
13DEC77 10  6 21.2 0.00 0 5 ARGENTINA
31.5S 67.4W
  22.0
IC-MS   66.1    13.5 1.0   10 17  4.0    36
GE-NM   77.7    61.0 1.3   10 19 15.8   417
CB2NV   82.4    47.0 1.2   10 18 40.7
BN-ME   77.6    64.5 1.0   10 18 14.7
IP-NE   77.6    21.0 0.6   10 18 15.1   350
14DEC77  8 55 52.8 0.00 0 2 JAPAN
41.9N147.6E
  90.0
EE-CC   73.2    18.0 1.2    9  7 16.0   109
GE-NM   75.9    48.0 1.0    9  7 33.0   391
20DEC77  8 50 40.6 0.00 0 4 KURILE IS.
48.5N152.9E
 145.0
IC-MS   82.9     5.5 1.0    9  2 49.2     4
IP-NE   76.8    60.  0.8    9  2 28.3    45
BN-ME   76.8   349.0 1.2    9  2 29.2
CB2NV   63.7   105.4 1.1    9  0 57.0
21DEC77  3 47 36.7 0.00 0 2 ARGENTINA
31.4S 68.1W
  46.0
EE-CC   80.4     8.4 1.3    3 59 43.5    47
GE-NM   77.3    10.0 1.3    3 59 30.0    31
22DEC77  2 57 46.8 0.00 0 2 MEXICO CST.
10.9N106.5W
   0.0
EE-CC   29.0    34.0 1.3    3  3 49.0   563
GE-NM   25.9    32.0 1.1    3  3 20.7   360
23DEC77  2 25 25.6 0.00 0 2 ARGENTINA
31.0S 67.7W
   0.0
EE-CC   80.2    27.0 1.3    2 37 37.5   563
GE-NM   77.1    27.5 1.4    2 37 21.1   375
```

```
23DEC77 11 15 45.0 0.00 0 2 NORWEGIAN SEA
72.3N   0.1E
  0.0
HE-CO   57.6    29.0 1.2   11 25 37.4  531
GE-NE   60.2    13.0 1.7   11 25 55.7  375
24DEC77  5 19   1.1 0.00 0 2 ARGENTINA
23.0S  66.6W
  0.0
HE-CC   73.9    32.0 1.1    5 30 38.6  531
GE-NM   70.9    44.5 1.1    5 30 21.3  375
23DEC77 21  2  13.0 0.00 0 2 JAPAN
39.0N143.2E
 41.0
HE-CC   77.6     3.0 1.0   21 14  7.0   40
GE-NB   80.3     9.0 1.1   21 14 21.5   31
27DEC77 15  9  54.0 0.00 0 2 S. ALASKA
60.6N153.7W
175.0
EN-ME   49.2   100.0 0.7   15 18 24.5
IP-ME   49.2    26.0 0.5   15 18 24.7  170
30DEC77 17 35  11.9 0.00 0 2 S. ITALY
40.0N  15.5E
300.0
HN-ME   58.4   840.0 0.9   17 44 37.4
IP-ME   58.4     9.0 0.7   17 44 38.5   10
31DEC77  7 53  21.8 0.00 0 2 PERU
14.7S  71.6W
160.0
HN-ME   60.9   340.0 1.75   8  3 18.8
IP-MB   60.9   250.0 1.3    8  3 17.0
10JAN78  0 50  19.5 5.70 0 3 KURILE IS.
46.6N152.3E
 62.0
HN-ME   80.6   199.0 0.81   1  2 25.6
IP-ME   80.6     5.0 0.7    1  2 25.6   18
BR-CN   67.7    98.5 1.1    1  1  6.2
13JAN78 20  3   5.0 5.80 0 3 KURILE IS.
44.6N149.8E
 48.0
HN-ME   83.3   289.0 0.97  20 15 27.7
IP-MB   83.3     7.5 0.9   20 15 28.0   54
BR-CN   70.5   397.6 0.9   20 14 11.0
17JAN78 11 33  15.3 5.70 0 3 ARGENTINA
31.2S  67.8W
 17.0
HN-MB   77.2   113.0 0.96  11 45  7.7
IP-ME   77.2    11.0 0.9   11 45  6.7  112
BR-ON   64.5   175.0 0.9   11 45 48.3
20JAN78  4 42  56.9 0.00 0 2 CHILE-ARGENTINA BDR
34.5S  70.5W
112.0
EN-ME   80.5   221.0 1.38   4 54 54.7
IP-MB   80.5    29.0 1.2    4 54 54.0  112
24JAN78  8 54  22.9 5.80 0 3 KURILE IS.
44.6N149.7E
 38.0
HN-ME   83.4   156.0 1.04   6  6 46.8
IP-MB   83.4    35.0 0.8    6  6 47.0  105
BR-CN   70.5   283.0 0.9    6  5 30.3
24JAN78 13 18  17.4 5.70 0 3 ARGENTINA
31.7S  68.9W
 21.0
HN-ME   77.7   136.0 0.95  13 30 12.3
IP-ME   77.7    15.0 1.1   13 30 11.7  100
BR-CN   64.7   456.0 0.7   13 30 50.8
24JAN78 17 45  59.7 0.00 0 2 ARGENTINA
27.7S  66.5W
200.0
HN-ME   73.7    63.4 1.07  17 57 11.6
IP-MB   73.7     3.0 1.0   17 57 10.7  100
```

```
29JAN78 21 51 27.7 5.20 0 3 E. CST. KAMCHATKA
53.9N159.2E
   0.0
BN-ME   72.2    83.7 1.33 22  2 55.0
IE-ME   72.2    17.0 1.2  22  2 55.C  110
BR-ON   59.4   105.9 0.9  22 01 29.2
30JAN78  5   0 18.1 4.90 0 5 E. CST. KAMCHATKA
53.9N159.2E
   0.0
BN-ME   72.2    68.9 0.97  5 11 45.3
IE-ME   72.2     3.0 1.0   5 11 45.9  110
BB-CC   60.1    19.0 1.5   5 10 28.8
GE-NM   63.0    15.0 1.1   5 10 48.8  227
BR-CN   59.4    50.7 1.0   5 10 18.6
29DEC77 20 32 41.7 0.00 0 2 ICELAND
64.7N  17.4W
   0.0
BE-CC   55.0    93.9 1.03 20 42 36.7
GE-NM   57.2    63.5 1.0  20 42 30.4  396
 2JAN78 20 57 35.1 0.00 0 3 ANDREANOF IS.
51.1N178.4W
   0.0
BE-CC   46.5   184.9 0.87 21  6 19.6
TC-MS   65.6    16.0 1.1  21  8 21.2   80
GE-NM   51.1    55.0 1.0  21  6 40.7  438
 3JAN78  1 10  0.8 0.00 0 3 ARGENTINA
31.3S 66.0W
   0.0
BE-CC   80.3    41.6 1.45  1 22 14.2
TC-MS   65.7    20.0 2.0   1 20 45.6   80
GE-NM   77.3    55.0 1.1   1 21 58.3  438
 4JAN78  0 57 19.0 0.00 0 2 JAPAN
42.7N142.2E
  23.0
BE-CC   75.7    75.2 0.91  1  9  2.5
GE-NM   78.6     5.1 1.2   1  9 20.3   36
 4JAN78 22 52 17.1 0.00 0 3 COSTA RICA
 9.1N 84.4W
  55.0
BE-CC   37.4    18.0 1.3  22 59 22.0
TC-MS   22.9    31.0 2.0  22 57  8.3   36
GE-NM   34.5    18.0 1.6  22 58 57.3  438
 5JAN78  3 23 16.5 0.00 0 3 S. PACIFIC
22.0S127.1W
   0.0
BE-CC   64.2   174.0 1.4   3 33 51.3
TC-MS   64.2    50.0 1.5   3 33 51.2  200
GE-NM   61.6     6.0 1.2   3 33 33.3   31
28JAN77 22  5 37.3 0.00 0 2 MEXICO
16.1N 95.8W
   0.0
BE-CC   26.1    28.0 1.2  22 11 13.7
GE-NM   22.9     6.9 0.7  22 10 45.3   17
28JAN78 22 38  7.3 0.00 0 2 KAMCHATKA
54.1N159.0E
  16.0
BE-CC   60.1    26.0 1.4  22 48 15.2
GE-NM   63.0    24.0 0.8  22 48 34.8  227
29JAN78  2  5  5.8 0.00 0 2 KURILE IS.
45.9N149.1E
 168.0
BE-CC   69.9   120.0 1.1   2 15 53.3
GE-NM   72.7     3.0 0.9   2 16 16.3   17
29JAN78  2 32 32.8 0.00 0 2 E. CST. KAMCHATKA
54.8N159.6E
 133.0
BE-CC   59.5    13.0 1.3   2 42 22.9
GE-NM   62.4    17.9 1.0   2 42 43.0  227
```

```
29JAN78 18 10  3.6 0.00 0 2 S. OF PANAMA
 4.4N 78.6W
  0.0
BB-CC   44.4    79.0 0.9   18 18 16.6
GE-NN   41.6     3.4 0.9   18 17 54.4    17
30JAN78  7  3 44.5 0.00 0 2 CST. OF PERU
11.0S 80.1W
  0.0
BB-CC   57.2    23.0 1.0    7 13 32.2
GE-NN   54.1    14.0 1.2    7 13 10.2   227
 1FEB78 14 58 48.7 0.00 0 2 KURILE IS.
48.9N153.7E
157.0
BB-CC   65.6    74.0 1.2   15  9 17.9
GE-NN   66.4    47.5 1.0   15  9 35.8   227
 2FEB78  6 51 38.2 0.00 0 2 N.W. OF KURILE IS.
47.6N146.6E
440.0
BB-CC   70.1    14.0 0.8    7  2  8.6
GE-NN   73.0    13.3 0.7    7  2 25.6   227
 3FEB78  8  1 57.9 0.00 0 2 KURILE IS.
44.4N149.9E
  0.0
BB-NE   83.4    75.0 1.0    8 14 27.8
IF-NB   83.5    11.0 1.0    8 14 27.7    91
13FEB78 13  2 54.2 5.20 0 3 E CST KAMCHATKA
56.3N162.6E
 88.0
BB-NE   69.1    43.0 0.8   13 13 52.2
IF-NE   69.2     5.0 0.8   13 14  3.7    26
BR-ON   56.4   110.0 1.0   13 12 23.1
16FEB78  3 47 33.1 0.00 0 2 N CST COLUMBIA
 5.5N 77.6W
 77.0
BB-NE   41.5   118.0 1.0    3 55 11.3
IF-NB   41.4     9.0 0.7    3 55 10.3    42
17FEB78  6 43 31.0 0.00 0 2 CENT. CHILE CST
28.9S 72.4W
 40.0
BB-CO   76.4   105.0 1.4    6 55 16.8
GE-NN   73.3    28.2 1.1    6 54 58.9   188
22FEB78  6  7 37.1 5.80 0 3 GUATEMALA
14.4N 91.2W
 70.0
BB-NB   37.2  1314.6 1.23   6 14 47.8
IF-NE   37.0    14.0 1.0    6 14 40.6     4
BR-CN   36.0   763.0 0.7    6 14 33.1
26FEB78  0  5 42.2 5.40 0 5 KURILE IS.
49.2N155.5E
  0.0
BN-NB   77.4    59.0 1.1    0 17 39.2
IF-NE   77.5    10.0 1.0    0 17 39.2    91
BB-CC   64.5    43.0 1.1    0 16 21.2
GE-NN   63.5    19.8 1.1    0 16 39.5   208
BR-CN   64.4    53.1 0.9    0 16 16.1
26FEB78  9 16 52.6 5.80 0 3 EASTER IS. REG.
26.5S113.6W
 18.0
BB-NE   83.6   153.4 1.47   9 29 20.3
IF-NE   83.4    25.3 1.1    9 29 19.2    91
BR-ON   78.6   234.0 1.3    9 28 55.6
 4MAR78 17 35  7.0 5.40 0 3 GUATEMALA
14.2N 91.2W
 70.0
BB-NB   37.4   231.1 1.51  17 42 13.9
IF-NE   37.2     6.6 0.8   17 42 12.5     7
BR-ON   36.2   263.0 0.8   17 42 05.4
 7MAR78 11 45 37.4 4.80 0 3 N. COLOMBIA
 6.9N 73.0W
155.0
BB-NB   39.5   104.0 0.9   11 52 53.1
IF-NE   39.3    19.0 0.9   11 52 52.0    62
BR-CN   46.7   261.0 0.6   11 53 53.3
```

```
 7MAR78 22 33 44.0 0.00 0 2 CRETE
34.5N 25.2E
  2.0
BR-ME  67.9   67.2 0.59 22 44 45.4
IP-ME  66.1   24.0 0.6  22 44 46.2    62
19MAR78  1 39  19.2 5.90 0 3 MEXICO
17.0N 99.7W
 64.0
BR-ME  39.2  347.0 1.6   1 46 41.5
IP-ME  39.2    7.0 1.3   1 46 40.0    10
BK-ON  33.8  184.0 1.1   1 45 55.9
22MAR78  0 50 34.9 0.00 0 2 KURILE IS.
43.8N146.9E
 47.0
BR-ME  64.3  218.0 2.5   1  3  2.6
IP-ME  64.3   27.0 1.7   1  3  2.5  109
22MAR78 21 34 30.6 0.00 0 2 KURILE IS.
44.0N148.9E
  4.0
BR-ME  64.1  162.4 1.3  21 47  3.9
IP-ME  64.1   20.0 0.8  21 47  4.8  114
23MAR78  0 31  3.8 6.10 0 3 KURILE IS.
44.3N146.7E
 36.0
BR-ME  63.9  334.6 1.3   0 43 30.6
IP-ME  63.9    4.5 0.8   0 43 30.0    10
BK-ON  71.2  533.0 1.0   0 42 14.6
23MAR78  1 49 38.6 5.60 0 3 KURILE IS.
43.9N148.9E
 64.0
BR-ME  64.2   81.2 1.41  2  2  5.1
IP-ME  64.2   14.0 0.7   2  2  6.5  114
BK-ON  71.2   52.3 0.9   2 00 49.1
26MAR78  3 56 59.7 5.60 0 3 E. KAZAKH
49.7N 78.1E
  0.0
BR-ME  79.7   59.8 0.9   4  9 10.4
IP-ME  79.9    9.0 0.8   4  9 11.0    95
BK-CN  60.0  120.0 0.8   4  9  6.6
26MAR78 21  5  0.7 5.40 0 3 E CST KAMCHATKA
53.4N162.9E
 35.0
BR-ME  71.4  162.4 0.97 21 16 17.8
IP-ME  71.4   35.0 0.8  21 16 18.2    95
BK-CN  58.2  150.3 1.0  21 44 48.0
23MAR78 20 17  2.0 5.80 0 3 KURILE IS.
48.8N150.8E
  9.0
BR-ME  76.0  296.8 1.3  20 29  1.8
IP-ME  76.0   50.0 1.2  20 29  3.0  103
BK-CN  65.0  225.0 1.2  20 27 39.4
19MAR78  9 13 11.0 0.00 0 3 W. CHILE RISE
38.2S 93.9W
  0.0
BB-CC  79.1   86.8 1.75  9 25 17.3
TC-MS  69.4    4.5 1.0   9 24 19.0    36
GE-NN  75.9   14.0 2.0   9 24 57.5   188
19MAR78  6 27 35.5 4.60 0 5 N. COLOMBIA
 6.9N 72.9W
172.0
BB-CC  45.7   70.8 0.67  6 35 39.3
TC-MS  28.8    8.0 0.8   6 33 18.0    36
GE-NN  43.2   22.  1.0   6 35 19.5   198
BN-ME  39.9   38.8 0.7   6 34 49.8
BK-CN  46.8  319.0 0.5   6 35 50.0
19MAR78 14 49 42.3 0.00 0 3 KURILE IS.
48.9N154.9E
  0.0
BB-CC  64.9   36.3 0.87 15  0 24.1
TC-MS  61.5    4.0 0.9  15  2  2.5    36
GE-NN  67.8   21.  0.7  15  0 42.2   198
```

```
20MAR78  3 59   8.7 0.00 C 2 S. ALASKA
60.4N153.7W
164.0
FB-CO    34.6    67.2 0.45   4  5 41.5
GE-NM    37.6    19.0 0.6    4  6  7.0   188
20MAR78  7 19  29.4 0.00 0 2 JAPAN
42.4N142.7E
 66.0
FB-CO    75.6    56.4 0.92   7 31  8.6
GE-NM    76.5    17.0 0.6    7 31 23.3   188
20MAR78 15 42  46.0 0.00 0 3 MID-ATLANTIC RIDGE
  1.0N  29.8W
 12.0
FB-CO    80.6    56.7 1.50  15 55  0.0
TC-MS    63.9     9.0 1.2   15 53 19.7    36
GE-NM    79.3    22.0 1.0   15 54 51.6   188
20MAR78 18  9  43.1 0.00 C 3 MID-ATLANTIC RIDGE
  0.8N  29.6W
 13.0
FB-CO    80.8   102.3 2.06  18 21 57.1
TC-MS    64.2     7.5 1.0   18 20 16.3    36
GE-NM    79.6    22.0 1.5   18 21 50.0   188
22MAR78  1 13  33.8 0.00 0 2 KURILE IS.
43.8N149.0E
 45.0
FB-CO    71.2    13.0 1.1    1 24 49.9
GE-NM    74.0    13.0 1.2    1 25  5.0   188
24MAR78 22  9   0.3 0.00 0 3 KURILE IS.
44.1N148.7E
 45.0
FB-CO    71.2   100.5 1.09  22 20 15.0
TC-MS    67.9    12.0 1.3   22 21 45.5    48
GE-NM    74.0    17.0 1.2   22 20 21.5   188
25MAR78 16 55  15.8 0.00 0 2 KURILE IS.
44.3N148.6E
 45.0
FB-CO    71.1    55.0 1.0   17  6 30.0
GE-NM    73.9    24.0 1.4   17  6 45.6   198
25MAR78 23 52  17.2 0.00 0 2 KURILE IS.
43.7N149.4E
 50.0
FB-CO    71.6    49.0 1.1    0  3 34.0
GE-NM    74.4    19.0 1.0    0  3 30.0   188
26MAR78  6  0  16.5 0.00 0 2 KURILE IS.
44.4N149.7E
 20.0
FB-CO    70.4    35.0 1.1    6 11 31.0
GE-NM    73.2    18.0 1.5    6 11 46.9   188
26MAR78  7  9  56.6 0.00 0 2 KURILE IS.
44.5N149.6E
 16.0
FB-CO    70.4    14.0 1.0    7 21 11.1
GE-NM    73.2    11.0 1.0    7 21 27.2   188
26MAR78 11  1  42.1 0.00 0 2 KURILE IS.
44.4N149.3E
  0.0
FB-CO    70.7    32.0 0.9   11 13  0.0
GE-NM    73.4    14.0 1.0   11 13 15.7   188
26MAR78 17 27   5.3 0.00 0 2 N. CHILE
20.8S  69.4W
110.0
FB-CO    70.6    30.0 1.5   17 38  9.4
GE-NM    67.7    12.0 1.3   17 37 50.0   198
26MAR78 17 39  13.0 0.00 C 2 KURILE IS.
44.2N149.1E
 35.0
FB-CO    70.9    31.0 0.9   17 50 28.1
GE-NM    73.7    18.0 1.6   17 50 43.6   188
```

```
26MAR78 19 57 24.5 0.00 0 2 MEXICO
18.6N 95.8W
 58.0
BB-CC  22.4  101.0 1.0  20  2 20.7
GB-NM  15.2   21.0 1.8  20  1 46.0  188
 4APR78 19 33 50.2 0.00 0 2 ARGENTINA
31.3S 66.3W
   0.0
HN-ME  77.3  115.6 0.99 19 45 46.8
IP-MB  77.3    4.0 0.7  19 45 46.0    34
 4APR78 21 11 44.3 0.00 0 2 N. OF PANAMA
10.2N 77.9W
 37.0
EN-MB  36.8  436.3 1.30 21 18 50.7
IP-MB  36.8   20.0 1.1  21 18 49.5    34
 7APR78  7 44 58.3 0.00 0 2 KURILE IS.
44.4N149.4E
 50.0
HN-ME  83.6  273.2 1.00  7 57 22.1
IP-MB  83.6   19.0 0.7   7 57 22.3    36
11APR78 15 30  0.5 0.00 1 2 S. NEVADA
37.2N116.2W
   0.0
EN-MB  36.4  322.0 1.3  15 37  9.2
IP-MB  36.4   55.0 1.0  15 37  8.4  108
11APR78 17 44 59.9 0.00 0 2 CALIF-NEV BDR
36.9N116.2W
   0.0
EN-MB  36.5  359.0 1.2  17 52  9.7
IP-MB  36.5   26.0 1.0  17 52  8.6    54
12APR78  1 22 18.1 0.00 0 2 KURILE IS.
44.1N148.1E
   8.0
HN-ME  64.3   66.0 0.8   1 34 51.0
IP-ME  64.3    7.0 0.7   1 34 51.3    54
12APR78  3 42  4.2 0.00 0 2 KODIAK IS. REG.
56.5N152.6W
   0.0
HN-MB  50.4  137.0 1.2   3 51  4.1
IP-ME  50.4   12.0 1.0   3 51  4.1    54
12APR78 16 51 10.6 0.00 0 2 NICARAGUA CST.
12.8N 87.6W
 70.0
HN-MB  37.0   80.0 1.2  16 58 17.2
IP-MB  37.0   10.0 1.0  16 58 15.8    54
13APR78  6  0 39.4 0.00 0 2 N. ATLANTIC OCEAN
57.0N 36.7W
 27.0
HN-ME  22.2  300.0 1.3   6  5 32.4
IP-MB  22.2   31.0 0.9   6  5 34.5    54
15APR78 17 18 36.2 0.00 0 2 GUATEMALA
14.2N 91.2W
 65.0
HN-MB  37.2  120.0 1.0  17 25 44.4
IP-MB  37.2   52.0 0.9  17 25 42.7    80
20APR78 22 19 28.2 0.00 0 2 KURILE IS.
46.8N151.7E
 72.0
HN-ME  80.8   80.0 0.8  22 31 34.5
IP-MB  80.8   20.0 0.6  22 31 34.3  108
24APR78  4 28 49.3 0.00 0 2 ANDREANOF IS.
51.5N176.1W
 60.0
HN-MB  64.5   91.0 0.8   4 39 19.9
IP-MB  64.5   11.0 0.7   4 39 19.7    70
23APR78  4 28 36.2 0.00 0 2 N. COLOMBIA CST
12.2N 72.5W
 50.0
HN-MB  34.0  123.0 1.1   4 35 17.2
IP-MB  34.0    9.0 0.8   4 35 15.9    70
```

```
 3DEC77 12 35 44.7 0.00 0 2 DOMINICAN REP.
19.6N 69.8W
 90.0
IC-MS   21.2    36.0 1.0   12 40 24.0    64
GE-NM   36.6    11.5 1.1   12 42 45.0   385
 5DEC77 15 43 29.1 0.00 0 2 C. CHILE CST.
31.3S 71.2W
  0.0
IC-MS   64.8     3.0 1.0   15 54  5.1     8
GE-NM   75.9    60.0 1.5   15 55 19.1   385
 6DEC77 17  5  4.9 0.00 0 2 ARGENTINA
31.1S 68.0W
  0.0
IC-MS   65.5    11.0 1.0   17 15 49.0     8
GE-NM   77.1     5.5 1.1   17 17  0.5     8
 7DEC77  3 22 45.8 0.00 0 2 ARGENTINA
31.3S 67.6W
 32.0
IC-MS   65.7    19.5 0.7    3 33 24.2    42
GE-NM   77.3    45.5 1.3    3 34 36.5   448
11DEC77 16 22 12.3 0.00 0 2 VENEZUELA
 9.6N 69.7W
 31.0
IC-MS   28.4    66.0 1.0   16 28  4.6    31
GE-NM   43.4     2.0 0.8   16 30 14.5     7
 1JAN78 10 51  6.0 0.00 0 2 ARGENTINA
31.0S 68.9W
 83.0
IC-MS   65.1    12.0 1.2   11  1 38.6    80
GE-NM   76.6    30.0 1.8   11  2  1.3   438
 2JAN78  8 27 42.5 0.00 0 2 CHILE-ARGENTINA BDR
38.0S 71.0W
133.0
IC-MS   71.3    17.0 1.1    8 38 46.6    80
GE-NM   81.8    56.0 1.0    8 39 46.9   438
 3JAN78  6 31  1.3 0.00 0 2 ARGENTINA
31.1S 67.6W
  0.0
IC-MS   65.6    13.0 1.2    6 41 44.6    80
GE-NM   77.2    21.0 1.2    6 42 57.4   438
05APR78 23 29 56.1 0.00 0 2 NE COAST HONSHU
35.1N142.6E
 49.0
RE-CO   61.5    44.0 1.0   -9
GE-NM   64.2    24.0 1.0   23 42 23.6   158
06APR78 08 39 57.1 0.00 0 2 HOKKAIDO, JAPAN
41.5N142.6E
106.0
RB-CO   76.3    21.0 0.6   -9
GE-NM   75.1     6.0 1.5   08 31 52.8   158
07APR78 07 44 58.3 0.00 0 3 KURILE ISLANDS
44.4N149.4E
 50.0
RE-CO   70.6    26.0 0.7   -9
GE-NM   73.4    21.0 0.7   07 56 25.6   158
EN-ME   93.6    17.3 0.6   07 57 22.1
07APR78 08 29 53.0 0.00 0 2 KURILE ISLANDS
44.3N149.4E
 00.0
RE-CO   70.7    46.0 0.9   -9
GE-NM   74.7    11.0 0.6   08 41 27.5   158
12APR78 03 42 04.2 0.00 0 3 KODIAK ISL REG
56.5N152.6W
 00.0
RE-CO   33.1   132.0 1.3   -9
GE-NM   36.0     7.0 1.1   03 49 07.6    16
HN-ME   50.4    35.0 0.6   03 51 04.1
13APR78 06 00 39.4 0.00 0 3 N ATL OCEAN
57.0N 36.7W
 27.0
RB-CO   48.0   103.0 0.8   -9
GE-NM   49.7    78.0 1.0   06 09 31.3   616
HN-ME   22.2   206.0 0.9   06 05 32.4
```

```
11APR78 05 12 53.3 0.00 C 2 UNIMAK ISL REG
53.6N163.8W
 48.0
FE-CC   39.3    43.0 1.2   -9
GE-NM   42.C     9.0 0.6   05 20 45.C   83
03APR78 03 06 48.1 0.00 C 2 S OF PANAMA
3.1N 78.9W
 53.0
FE-CC   45.4    29.0 0.9   -9
GE-NM   42.5    12.0 0.7   03 14 37.3  192
03APR78 07 51 30.8 0.00 C 2 E COAST HONSHU
39.6N144.4E
 68.0
FE-CC   72.7    48.0 1.4   -9
GE-NM   79.3     9.0 0.8   06 33 30.0   35
03APR78 11 28 23.4 0.00 C 2 S PACIFIC OCEAN
35.9S101.1W
 00.0
FE-CO   76.C    41.0 1.9   -9
GE-NM   72.8    12.0 1.3   11 39 52.0  192
04APR78 21 11 44.3 0.00 C 3 N OF PANAMA
10.2N 77.9W
 37.0
FB-CO   40.1   290.0 1.0   -9
GE-NM   37.4    20.0 2.0   21 18 55.2   35
HN-ME   36.8    88.6 1.1   21 18 50.7
13APR78 04 01 41.1 0.00 C 2 KURILE ISLANDS
44.4N149.1E
 50.0
FE-CC   70.8    13.0 1.0   -9
GE-NM   73.6    22.0 0.8   04 13 09.0  575
19APR78 07 32 53.5 0.00 C 2 S OF HONSHU
30.8N141.8E
 41.0
FE-CO   84.0    26.0 1.0   -9
GE-NM   86.6    18.0 1.0   07 45 33.7  575
20APR78 22 19 28.2 0.00 C 3 KURILE ISLANDS
46.8N151.6E
 72.0
FE-CC   68.C   140.0 1.0   -9
GE-NM   70.8    15.0 0.8   22 30 36.0   46
HN-ME   80.8    62.0 0.6   22 31 34.5
23APR78 23 40 01.3 0.00 C 2 OAXACA, MEXICO
16.9N 97.9W
 40.0
FB-CC   24.6   139.0 1.0   -9
GE-NM   21.4    10.0 0.7   23 44 46.0   33
24APR78 04 28 49.3 0.00 C 3 ANDREANOFF ISL
51.5N176.1W
 60.0
FE-CC   47.C    60.0 1.00  -9
GE-NM   49.6    24.0 1.0   04 37 35.6  433
HN-ME   64.5    59.0 0.7   04 39 19.9
26APR78 03 28 19.3 0.00 0 2 GUERRERO MEX. COAST
16.5N 99.0W
 40.0
FB-CO   24.7    66.0 1.0   -9
GE-NM   21.5     7.0 0.7   03 33 04.4   31
26APR78 21 01 05.3 0.00 C 2 NICARAGUAN COAST
12.0N 86.5W
 109.0
HB-CC   33.8    55.0 1.2   -9
GE-NM   30.9    14.0 0.5   21 07 22.3  140
27APR78 01 41 15.5 0.00 C 2 KODIAK ISL REG
56.6N152.7W
 00.0
HB-CO   33.2    14.0 0.8   -9
GE-NM   36.1     5.0 1.0   01 48 18.6  140
```

```
28APR78 C4 28 36.2 0.00 0 3 COLUMBIAN COAST
12.2N 72.5W
 50.0
EB-CO   41.9    30.0 1.6   -9
GE-NM   39.6     3.0 0.7   C4 36 03.7    10
BN-ME   34.C    77.0 0.7   04 35 17.2
05MAY78 05 32  48.5 5.10  0 2 C ALASKA
63.2N151.0W
127.0
EN-ME   47.0    91.0 0.8   05 41 07.2
IF-ME   47.0    36.0 0.5   05 41 07.6   182
09MAY78 07 31  06.0 5.10  0 2 KAMCHATKA
52.5N158.1E
 87.0
EN-ME   73.7    13.0 0.6   07 42 31.1
IF-ME   73.7    10.0 0.6   07 42 33.0   182
11MAY78 00 23  38.0 5.70  0 2 ANDREANOF IS
51.6N176.0W
 48.C
HN-ME   64.4   234.0 1.1   03 34 C9.8
IF-ME   64.4    43.0 0.6   00 34 C9.4   182
11MAY78 23 18  37.6 5.00  0 2 COAST CHIAPAS,MEX
14.6N 92.0W
119.0
EN-ME   37.4    69.0 1.1   23 25 39.3
IF-ME   37.2    13.0 0.7   23 24 27.1   182
14MAY78 08 32  20.2 4.90  0 2 MEX/GUATMLA BDR
15.8N 92.0W
105.0
HN-ME   36.4    73.0 0.9   03 39 15.6
IF-ME   36.2    29.0 0.6   C8 39 15.5   182
23MAY78 13 10  33.1 5.5C  0 2 PERUVIAN COAST
10.2S 78.6W
 30.0
EN-ME   57.2   237.0 1.5   13 20 13.7
IF-ME   57.C     5.0 0.6   13 20 13.C    16
31MAY78 01 07  26.1 5.70  0 2 NICARAGUAN COAST
12.7N 87.4W
 50.0
HN-ME   37.3   752.0 1.6   01 14 30.6
IF-ME   37.1    26.0 1.1   01 14 30.0    16
02JUN78 20 41  45.7 5.00  0 2 VANCCUVER IS.
50.2N127.5W
 17.0
EN-ME   38.8   112.0 1.2   20 49 10.5
IF-ME   38.7    18.0 1.2   20 49 C9.7   173
06JUN78 03 58  33.9 5.50  0 2 E. COAST KAMCHATKA
51.1N157.5E
 56.C
HN-ME   75.1   156.0 1.3   04 10 10.7
IF-ME   75.2     4.0 1.1   04 10 10.6    18
C9JUN78 07 35  00.9 5.20  0 2 PERU-BRAZ BRDR
 7.7S 74.4W
155.0
HN-ME   54.2    34.0 0.8   07 44 08.6
IF-ME   54.C    21.0 0.7   07 44 08.6   173
09JUN78 18 04  26.7 5.30  0 2 CHILE-ARG BRDR
29.5S 69.CW
120.0
EN-ME   75.7    59.0 0.8   18 15 57.3
IF-ME   75.5    14.0 0.8   18 15 56.0   173
11JUN78 02 57  00.1 5.90  0 2 E KAZAKH SSR
49.9N 78.7E
  C.C
HN-ME   75.7    93.0 0.8   03 C9 11.0
IF-ME   75.9     4.0 0.9   03 C9 11.3   173
13JUN78 C8 18  29.6 5.60  0 2 S OF PANAMA
 5.4N 82.6W
 60.0
HN-ME   42.7    18.0 0.5   08 26 20.9
IF-ME   42.5     7.5 0.7   08 26 18.0   173
```

```
15JUN78 09 28 58.3 5.40 0 2 KURILE IS
44.0N149.1E
 55.0
EN-ME  64.0    48.0 0.8  09 41 23.8
IE-ME  64.1    28.0 0.6  09 41 23.0   173
19JUN78 10 31 06.2 5.30 0 2 GREECE
40.7N 23.2E
 00.0
HN-ME  62.7    25.0 1.3  10 41 33.2
IE-ME  62.9    15.0 1.2  10 41 35.0   190
20JUN78 20 03 23.6 6.20 0 2 GREECE
40.3N 20.3E
 00.0
EN-ME  62.7    28.0 0.6  20 13 50.4
IE-ME  62.5     3.0 0.8  20 13 52.0   18
01JAN78 22 52 17.1 5.20 0 2 COSTA RICA
09.1N 84.4W
055.0
EN-ME  39.4    53.8 1.0  22 59 39.0
RK-CN  42.0   103.0 0.9  23 00 01.4
06JAN79 07 08 46.2 5.00 0 2 ANDREANOF
51.7N176.1W
057.0
HN-ME  64.4    50.9 1.1  07 19 14.8
RR-ON  49.1   128.3 0.6  07 17 25.8
01FEB78 23 36 50.2 5.60 0 2 KURILES
45.2N120.1E
020.0
EN-ME  69.7    96.0 1.0  23 49 12.5
RK-CN  90.3   126.0 1.0  23 47 55.6
23FEB78 16 59 59.9 5.60 1 2 NEVADA
36.9N115.9W
000.0
EN-ME  36.4   248.0 1.5  17 07 08.3
RK-CN  20.9  1444.0 1.5  17 04 45.3
19MAR78 03 46 59.8 0.00 1 2 KAMCHATKA
43.9N 77.8E
000.0
HN-ME  79.5    44.5 0.9  03 59 08.9
RK-CN  79.7    35.6 0.6  03 59 05.1
```

APPENDIX B

Histograms of Magnitude Differentials Δm_b for Various Pairs of SDCS Stations

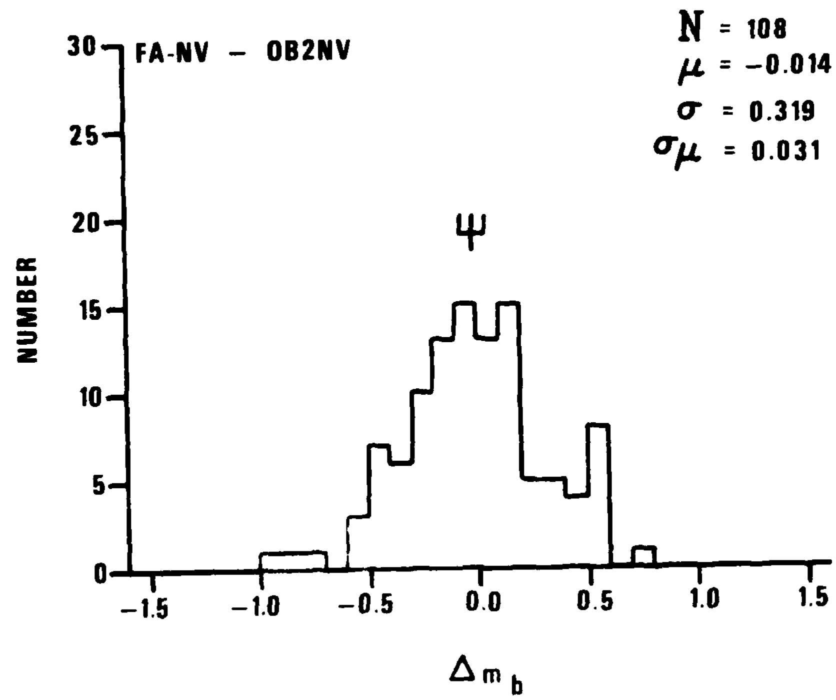
FA-NV – OB2NV
N = 108
μ = −0.014
σ = 0.319
σμ = 0.031
NUMBER
Δ m b
0
5
10
15
20
25
30
−1.5
−1.0
−0.5
0.0
0.5
1.0
1.5

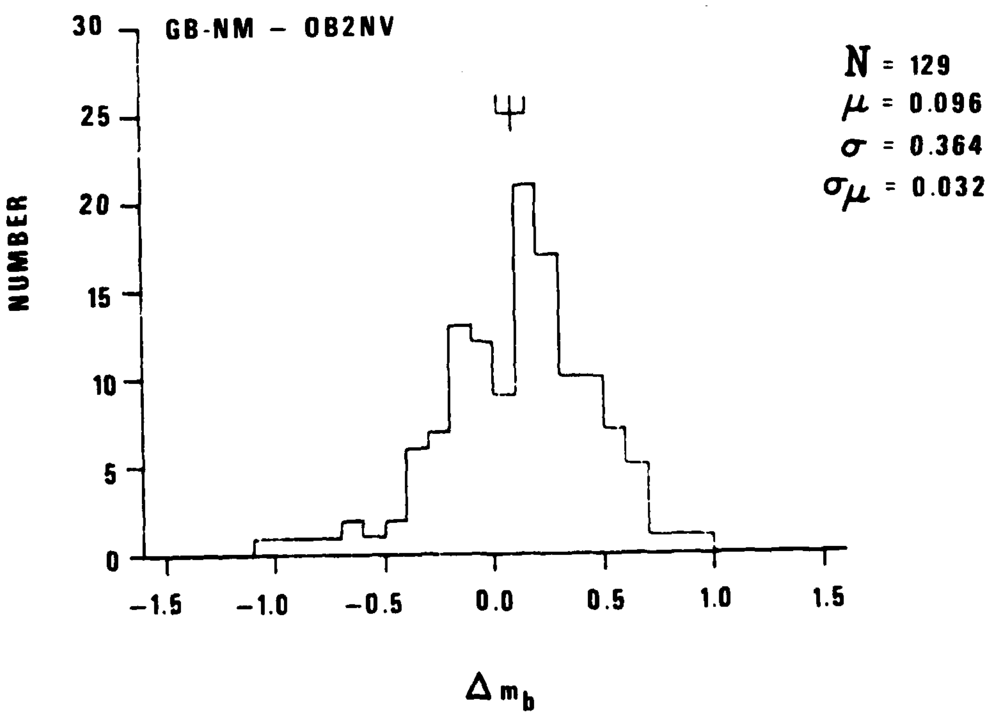
GB-NM – OB2NV
N = 129
μ = 0.096
σ = 0.364
σμ = 0.032
NUMBER
Δ m b
0
5
10
15
20
25
30
−1.5
−1.0
−0.5
0.0
0.5
1.0
1.5

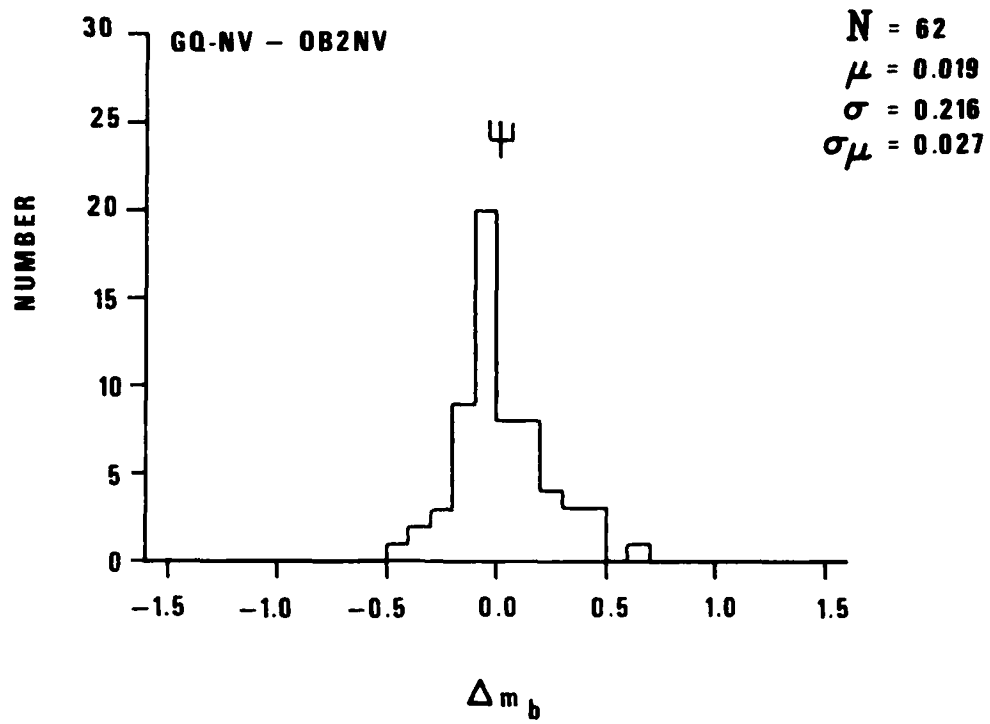
GQ-NV – OB2NV
N = 62
μ = 0.019
σ = 0.216
σμ = 0.027
NUMBER
30
25
20
15
10
5
0
−1.5
−1.0
−0.5
0.0
0.5
1.0
1.5
Δ m b

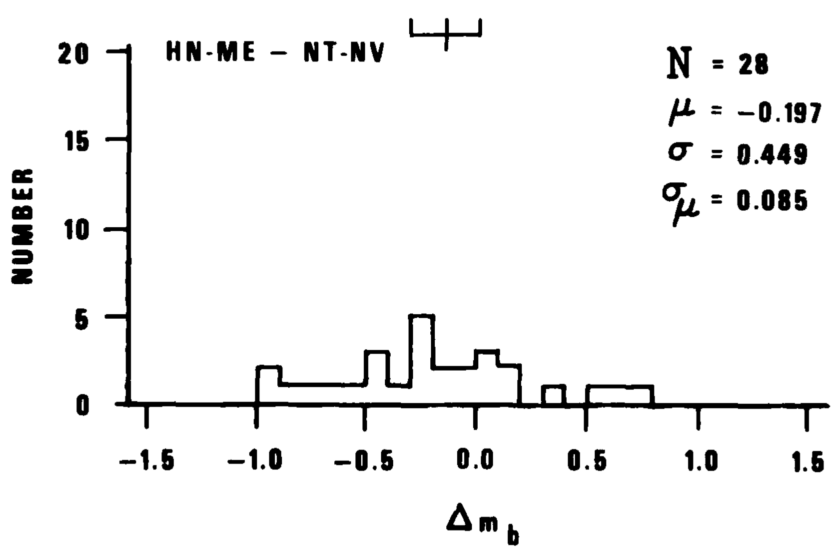
HN-ME – NT-NV
N = 28
μ = −0.197
σ = 0.449
σμ = 0.085
NUMBER
20
15
10
5
0
−1.5
−1.0
−0.5
0.0
0.5
1.0
1.5
Δ m b

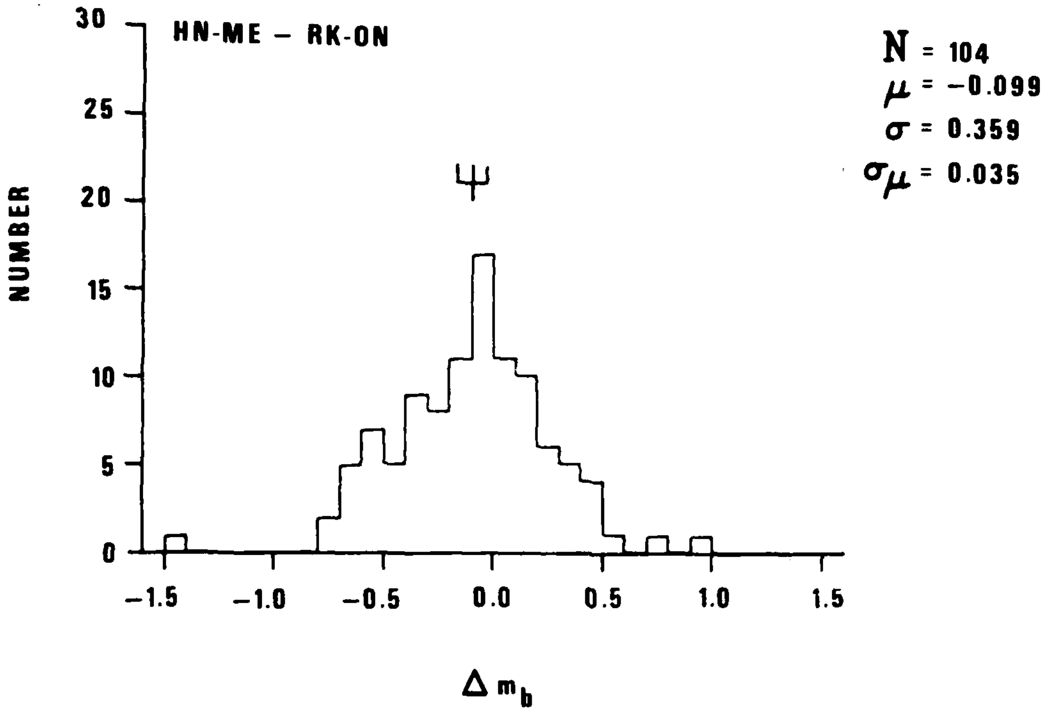
HN-ME – RK-ON
N = 104
μ = −0.099
σ = 0.359
σμ = 0.035
NUMBER
30
25
20
15
10
5
0
−1.5
−1.0
−0.5
0.0
0.5
1.0
1.5
Δ m_b

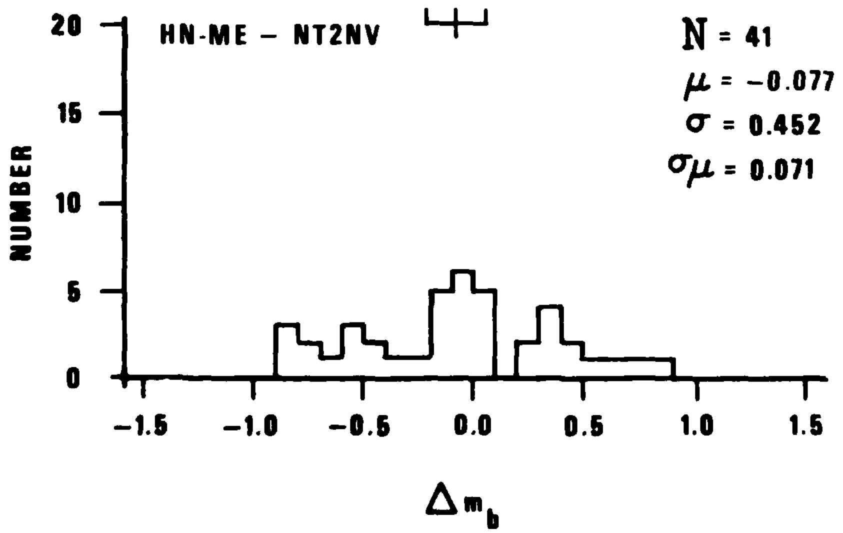
HN-ME – NT2NV
N = 41
μ = −0.077
σ = 0.452
σμ = 0.071
NUMBER
20
15
10
5
0
−1.5
−1.0
−0.5
0.0
0.5
1.0
1.5
Δ m_b

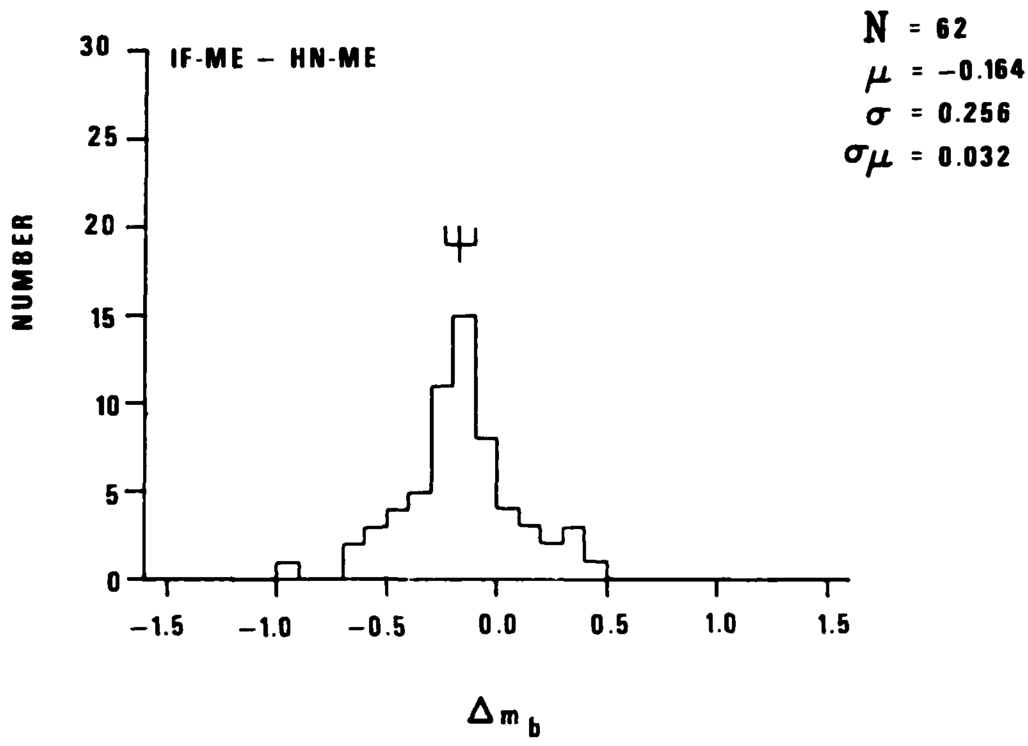
N = 62
μ = −0.164
σ = 0.256
σμ = 0.032
IF-ME − HN-ME
NUMBER
30
25
20
15
10
5
0
−1.5
−1.0
−0.5
0.0
0.5
1.0
1.5
Δm b

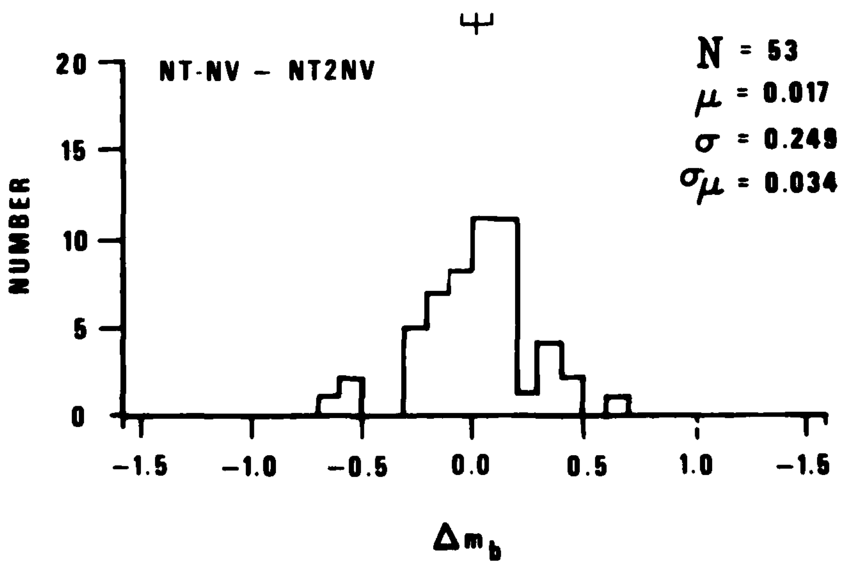
N = 53
μ = 0.017
σ = 0.249
σμ = 0.034
NT-NV − NT2NV
NUMBER
20
15
10
5
0
−1.5
−1.0
−0.5
0.0
0.5
1.0
−1.5
Δm b

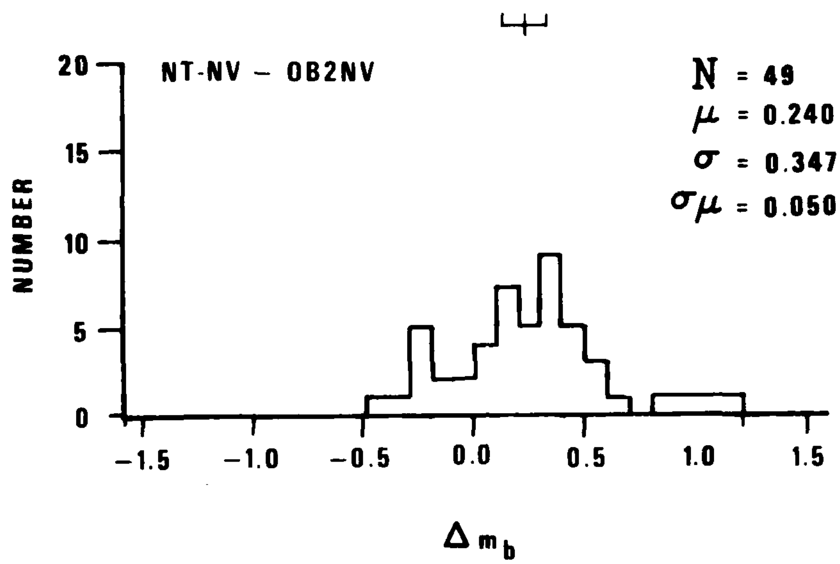
NT-NV – OB2NV
N = 49
μ = 0.240
σ = 0.347
σμ = 0.050
NUMBER
20
15
10
5
0
−1.5
−1.0
−0.5
0.0
0.5
1.0
1.5
Δ m b

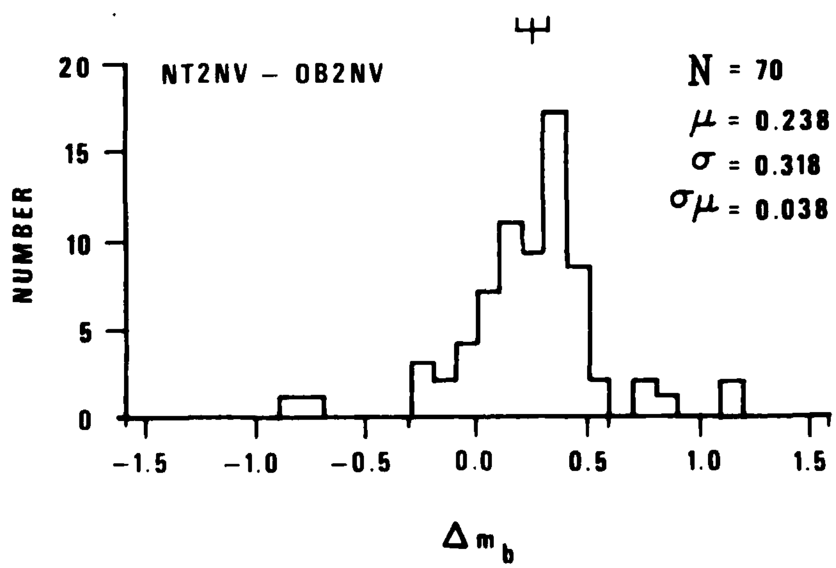
NT2NV – OB2NV
N = 70
μ = 0.238
σ = 0.318
σμ = 0.038
NUMBER
20
15
10
5
0
−1.5
−1.0
−0.5
0.0
0.5
1.0
1.5
Δ m b

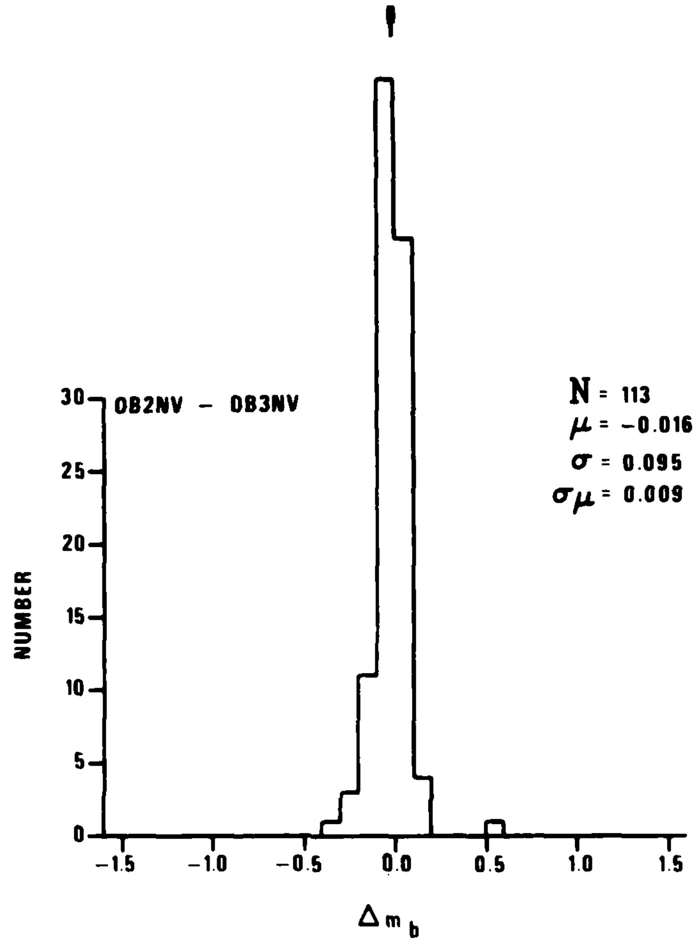
OB2NV – OB3NV
N = 113
μ = −0.016
σ = 0.095
$\sigma\mu$ = 0.009
NUMBER
30
25
20
15
10
5
0
−1.5
−1.0
−0.5
0.0
0.5
1.0
1.5
Δm_b

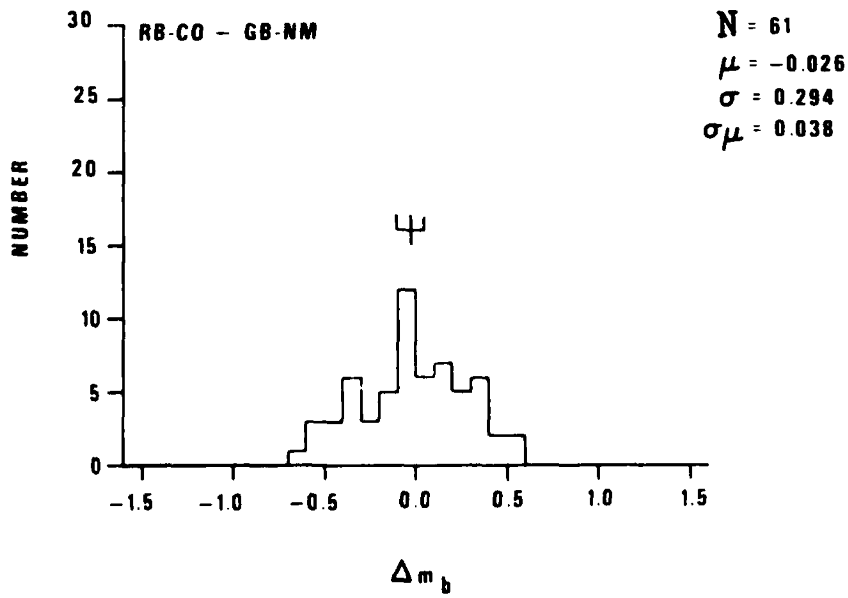
RB-CO – GB-NM
N = 61
μ = −0.026
σ = 0.294
$\sigma\mu$ = 0.038
NUMBER
30
25
20
15
10
5
0
−1.5
−1.0
−0.5
0.0
0.5
1.0
1.5
Δm_b

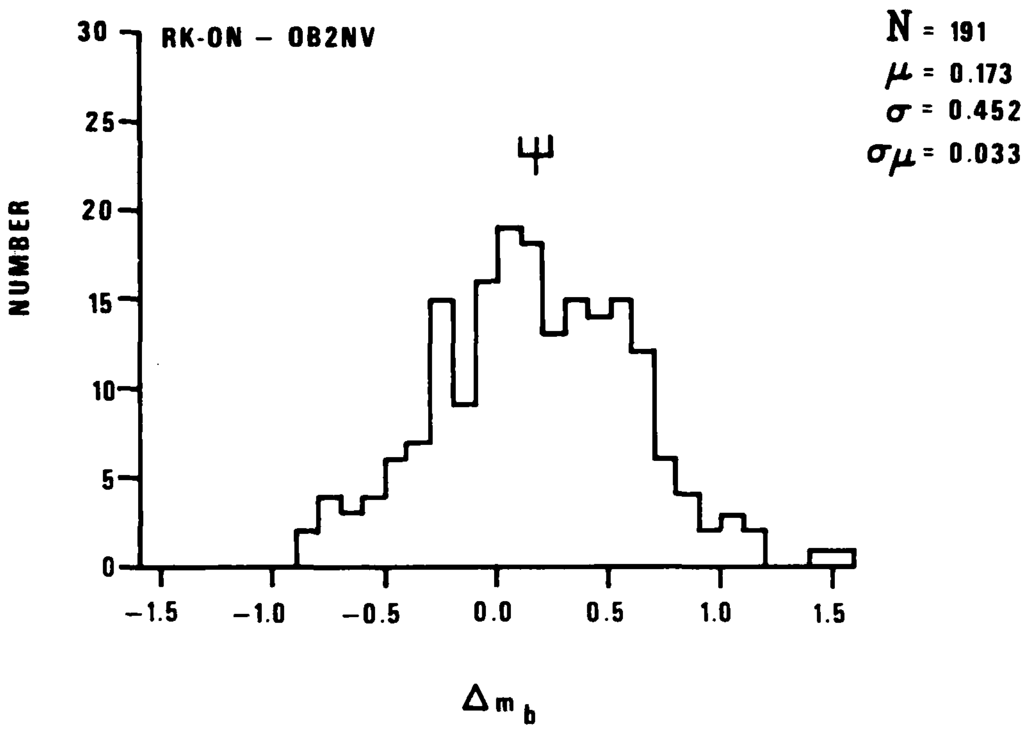
RK-ON – OB2NV
N = 191
μ = 0.173
σ = 0.452
σμ = 0.033
NUMBER
30
25
20
15
10
5
0
−1.5
−1.0
−0.5
0.0
0.5
1.0
1.5
Δ m b

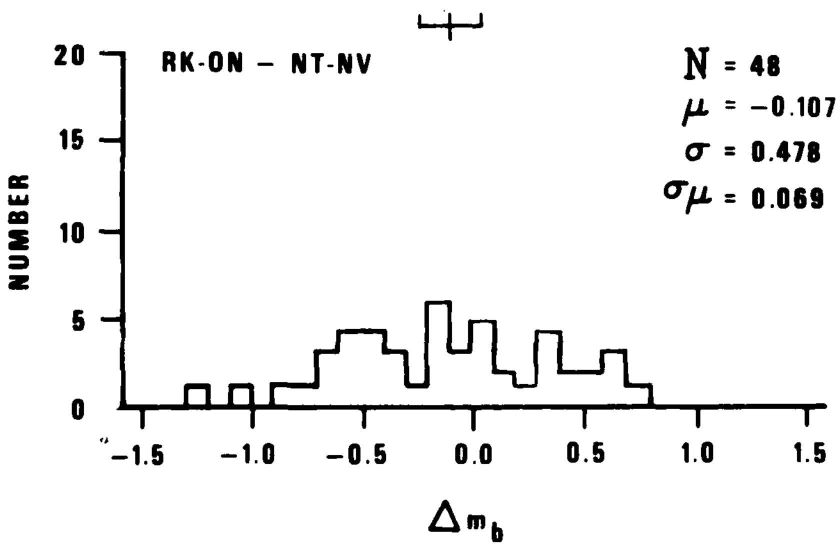
RK-ON – NT-NV
N = 48
μ = −0.107
σ = 0.478
σμ = 0.069
NUMBER
20
15
10
5
0
−1.5
−1.0
−0.5
0.0
0.5
1.0
1.5
Δ m b

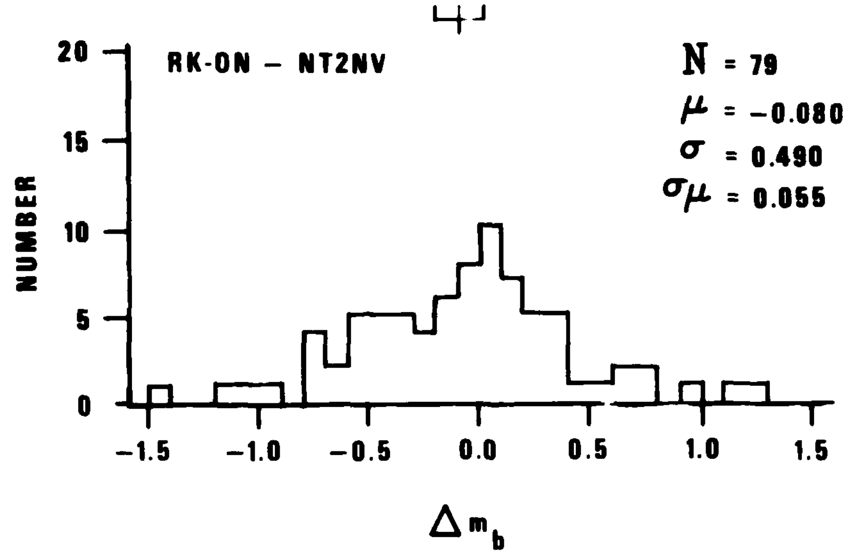
RK-ON – NT2NV
N = 79
μ = -0.080
σ = 0.490
σμ = 0.055
NUMBER
20
15
10
5
0
-1.5
-1.0
-0.5
0.0
0.5
1.0
1.5
Δ m b

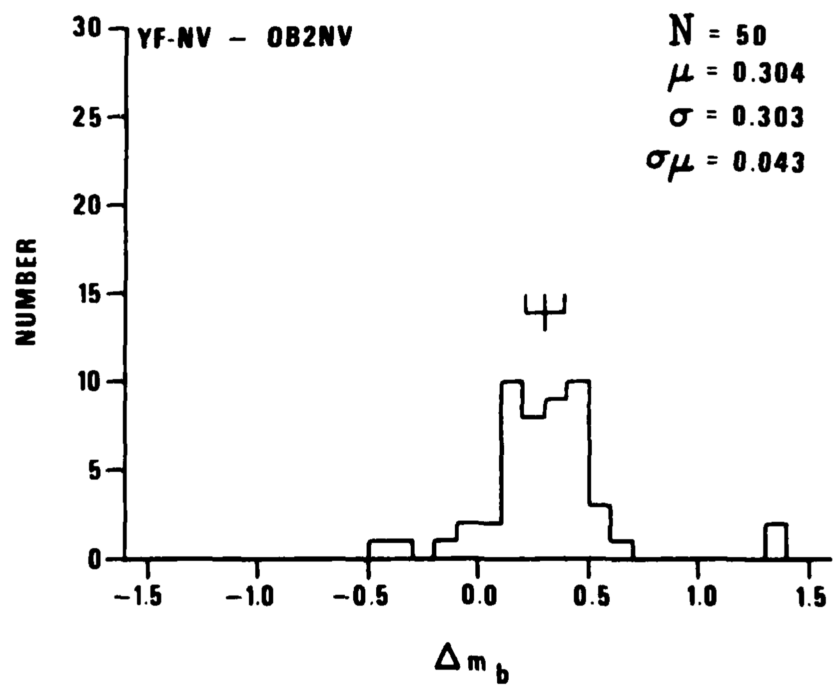
YF-NV – OB2NV
N = 50
μ = 0.304
σ = 0.303
σμ = 0.043
NUMBER
30
25
20
15
10
5
0
-1.5
-1.0
-0.5
0.0
0.5
1.0
1.5
Δ m b

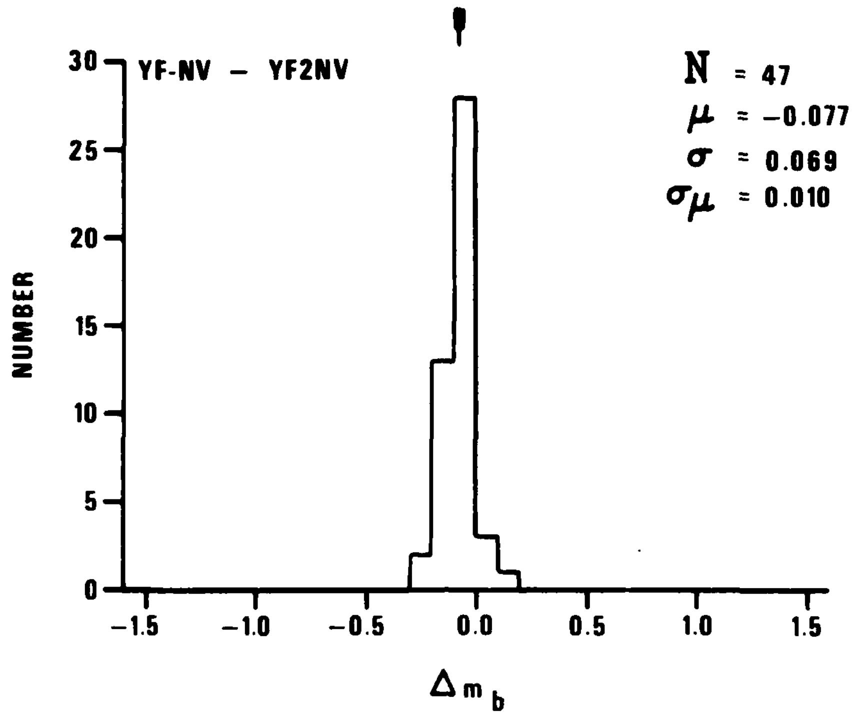
YF-NV – YF2NV
N = 47
μ = −0.077
σ = 0.069
σμ = 0.010
NUMBER
Δ m b

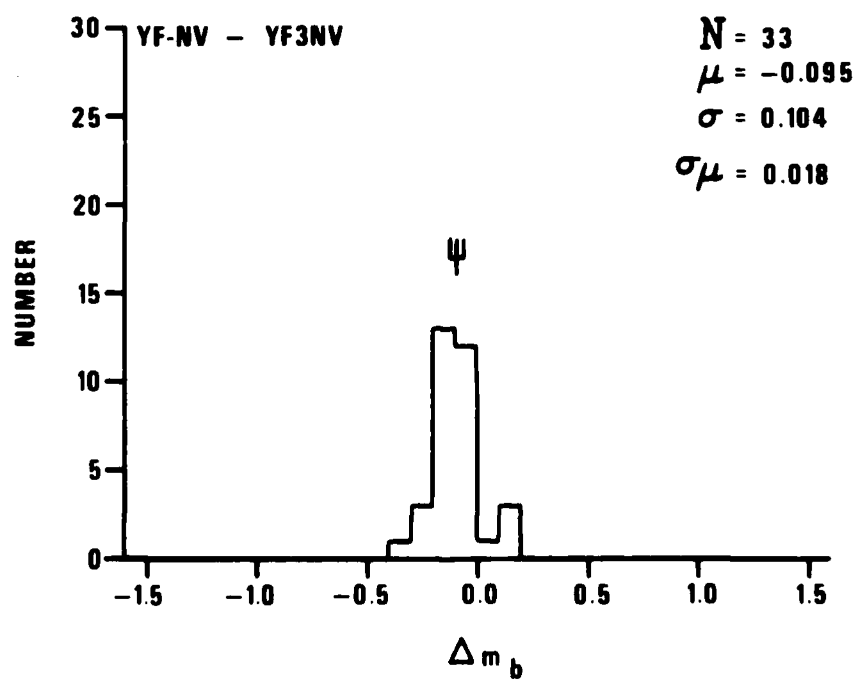
YF-NV – YF3NV
N = 33
μ = −0.095
σ = 0.104
σμ = 0.018
NUMBER
Δ m b

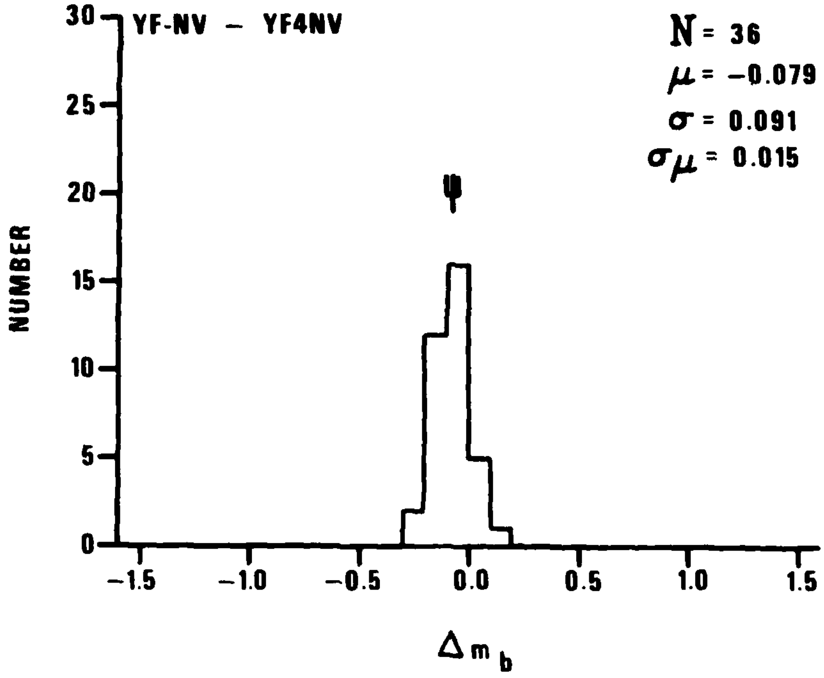
YF-NV – YF4NV
N = 36
μ = −0.079
σ = 0.091
σμ = 0.015
NUMBER
30
25
20
15
10
5
0
−1.5
−1.0
−0.5
0.0
0.5
1.0
1.5
Δ m b

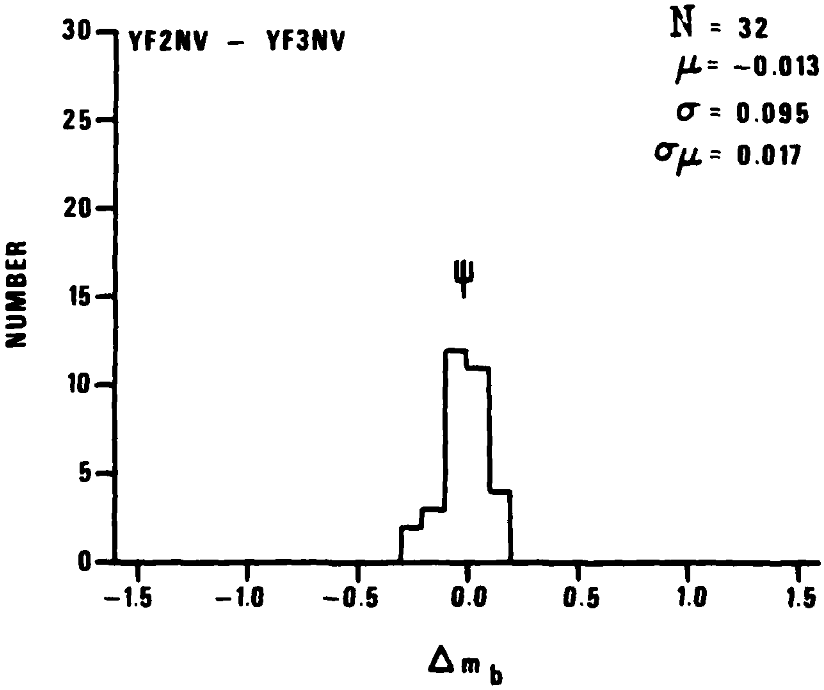
YF2NV – YF3NV
N = 32
μ = −0.013
σ = 0.095
σμ = 0.017
NUMBER
30
25
20
15
10
5
0
−1.5
−1.0
−0.5
0.0
0.5
1.0
1.5
Δ m b

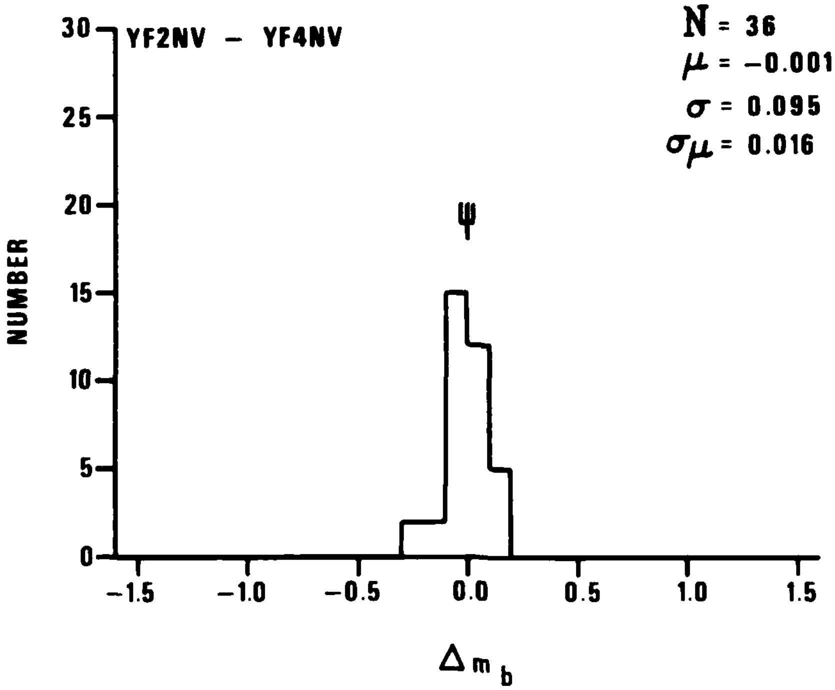

YF2NV – YF4NV
N = 36
μ = −0.001
σ = 0.095
σμ = 0.016
NUMBER
30
25
20
15
10
5
0
−1.5
−1.0
−0.5
0.0
0.5
1.0
1.5
Δ m b

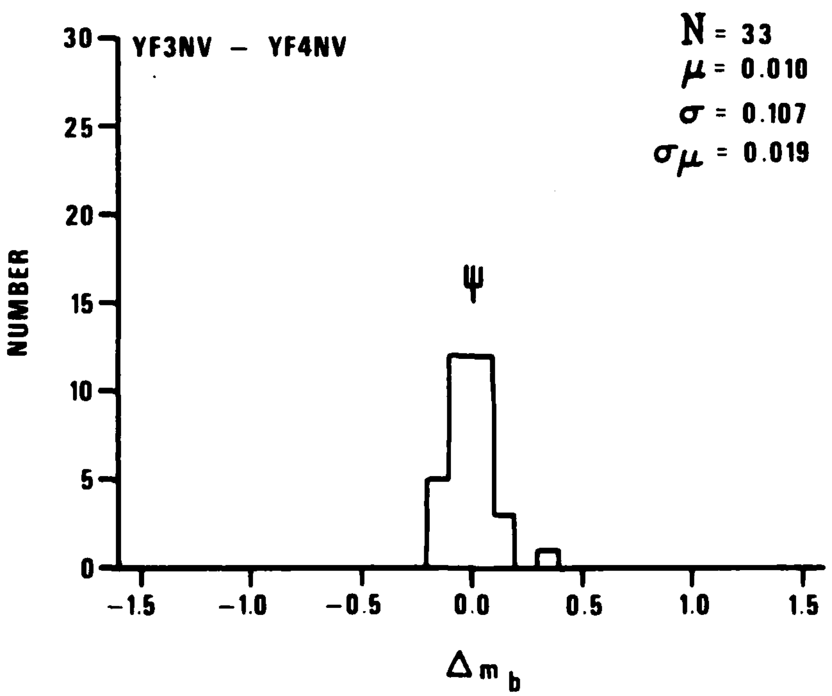

YF3NV – YF4NV
N = 33
μ = 0.010
σ = 0.107
σμ = 0.019
NUMBER
30
25
20
15
10
5
0
−1.5
−1.0
−0.5
0.0
0.5
1.0
1.5
Δ m b

APPENDIX C

Histograms of Trace Amplitude Differentials ΔA_{tr} for Various Pairs of SDCS Stations

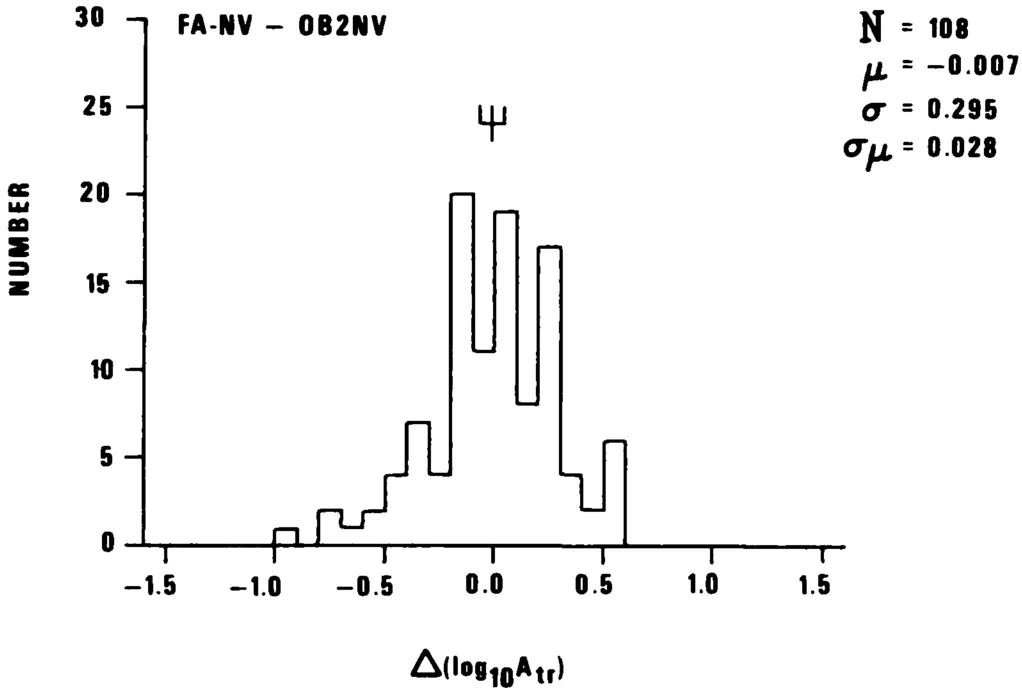
FA-NV – OB2NV
N = 108
μ = −0.007
σ = 0.295
σμ = 0.028
NUMBER
Δ(log10Atr)

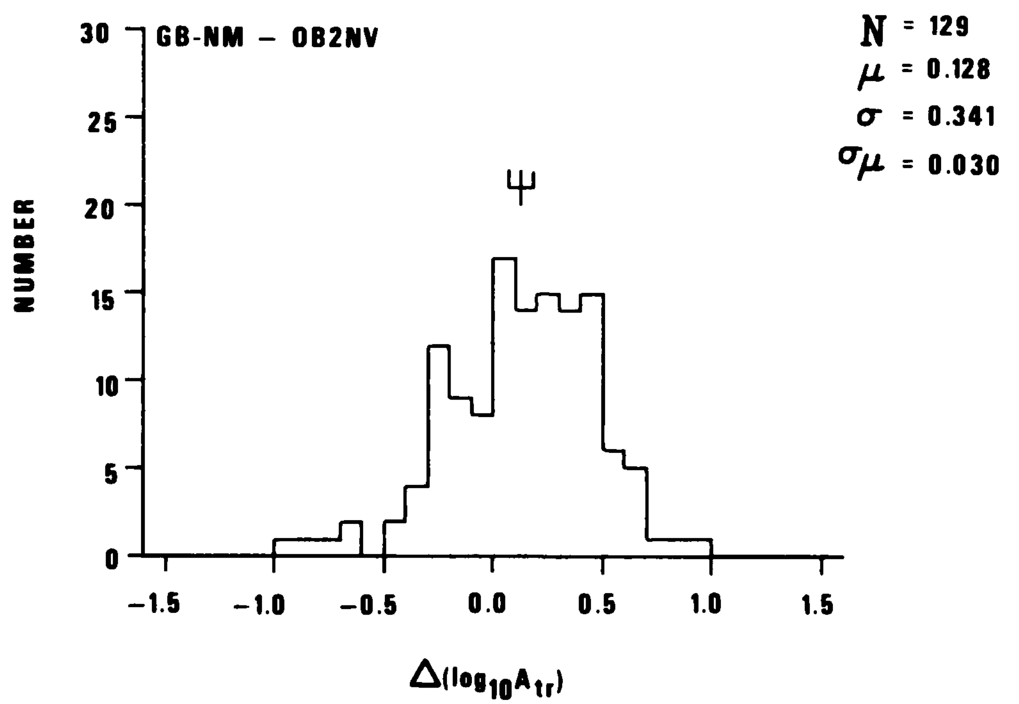
GB-NM – OB2NV
N = 129
μ = 0.128
σ = 0.341
σμ = 0.030
NUMBER
Δ(log10Atr)

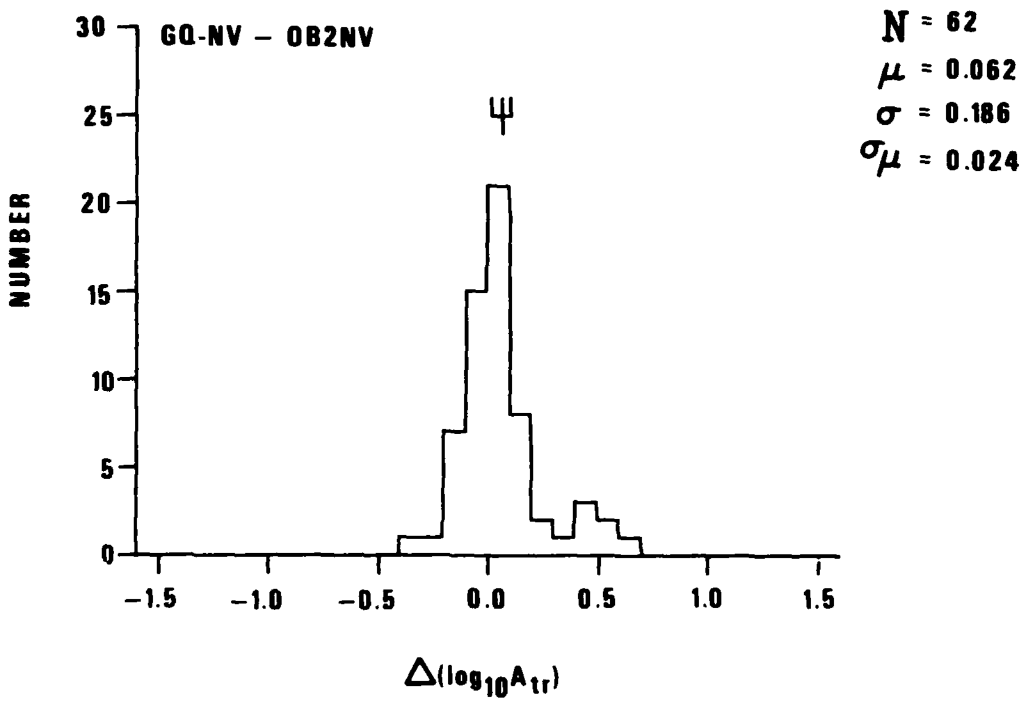
GQ-NV – OB2NV
NUMBER
30
25
20
15
10
5
0
−1.5
−1.0
−0.5
0.0
0.5
1.0
1.5
Δ(log10Atr)
N = 62
μ = 0.062
σ = 0.186
σμ = 0.024

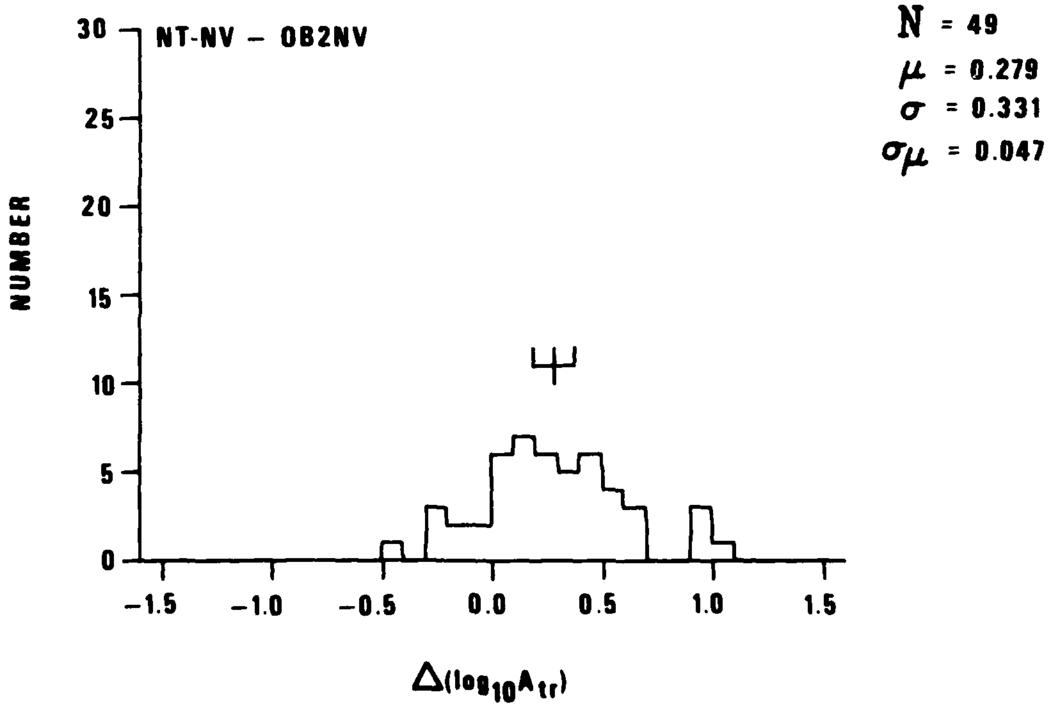
NT-NV – OB2NV
NUMBER
30
25
20
15
10
5
0
−1.5
−1.0
−0.5
0.0
0.5
1.0
1.5
Δ(log10Atr)
N = 49
μ = 0.279
σ = 0.331
σμ = 0.047

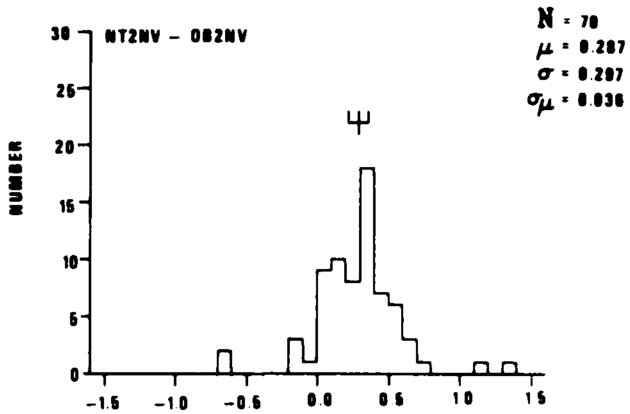
NT2NV - OB2NV
N = 70
μ = 0.287
σ = 0.297
σμ = 0.036
NUMBER
30
25
20
15
10
5
0
-1.5
-1.0
-0.5
0.0
0.5
1.0
1.5

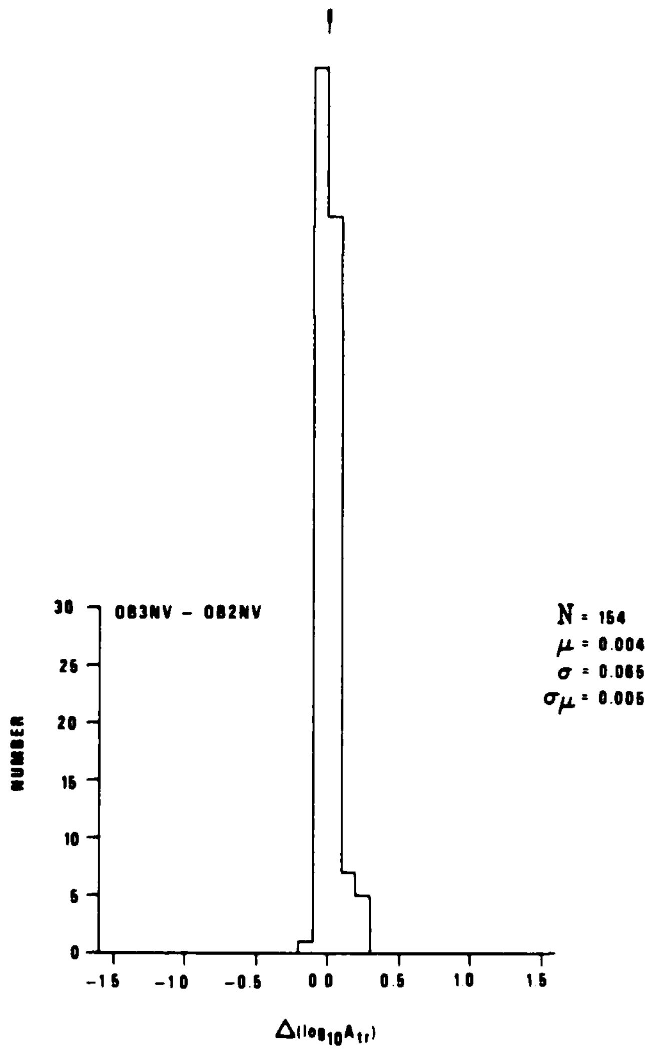
OB3NV - OB2NV
N = 154
μ = 0.004
σ = 0.065
σμ = 0.005
NUMBER
30
25
20
15
10
5
0
-1.5
-1.0
-0.5
0.0
0.5
1.0
1.5
Δ(log10 Atr)

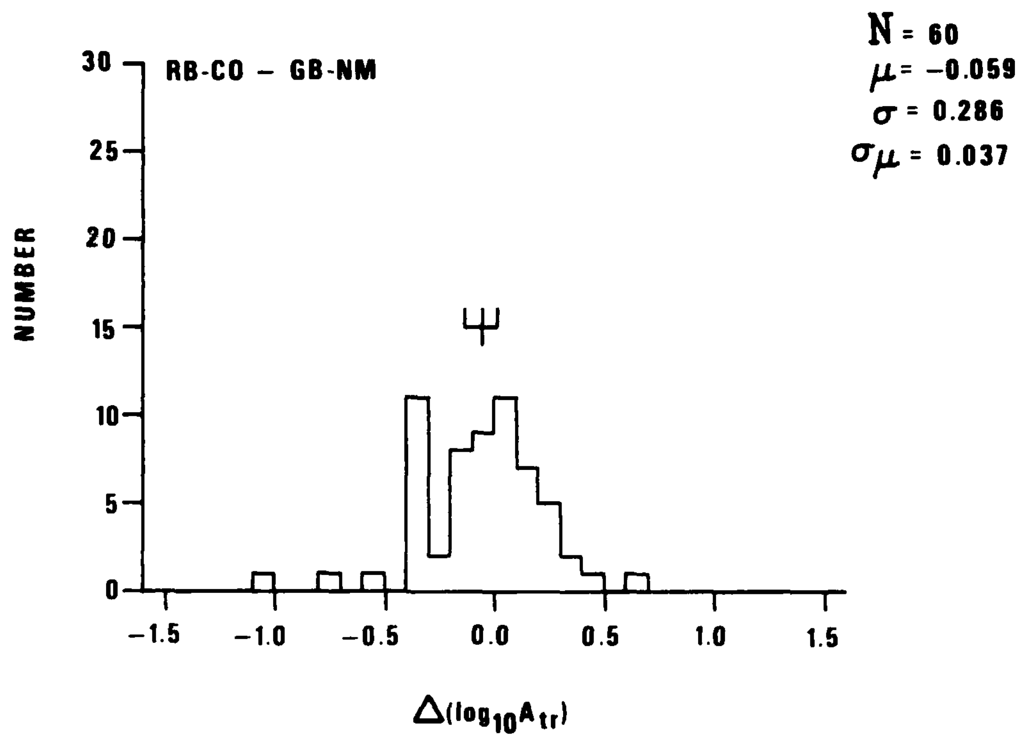

RB-CO – GB-NM
N = 60
μ = −0.059
σ = 0.286
σμ = 0.037
NUMBER
30
25
20
15
10
5
0
−1.5
−1.0
−0.5
0.0
0.5
1.0
1.5
Δ(log10Atr)

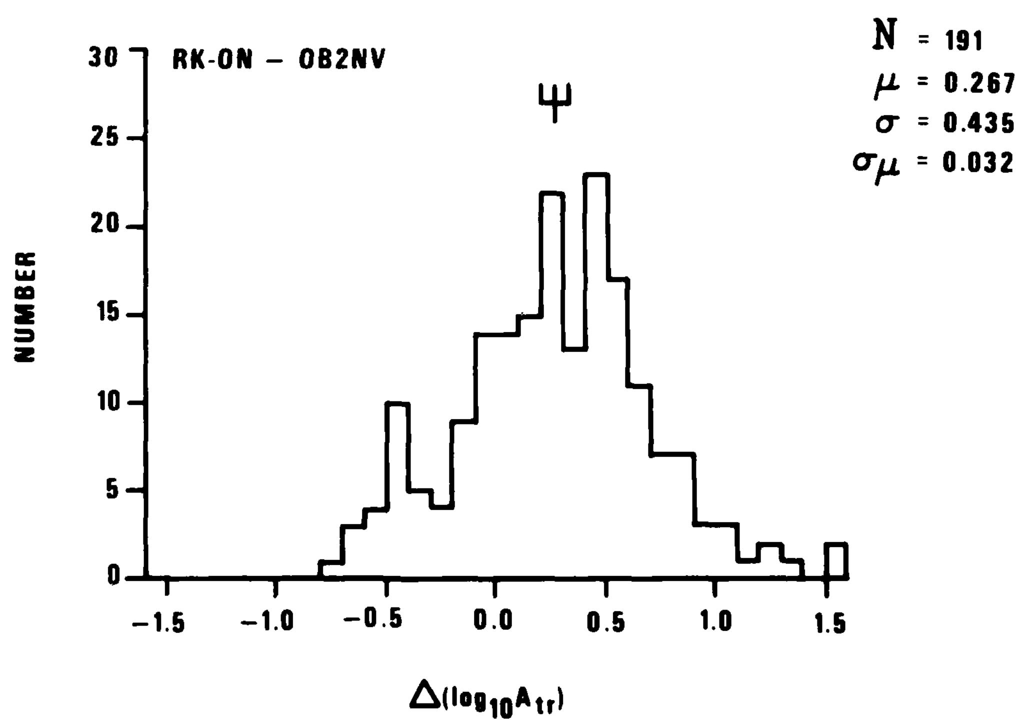

RK-ON – OB2NV
N = 191
μ = 0.267
σ = 0.435
σμ = 0.032
NUMBER
30
25
20
15
10
5
0
−1.5
−1.0
−0.5
0.0
0.5
1.0
1.5
Δ(log10Atr)

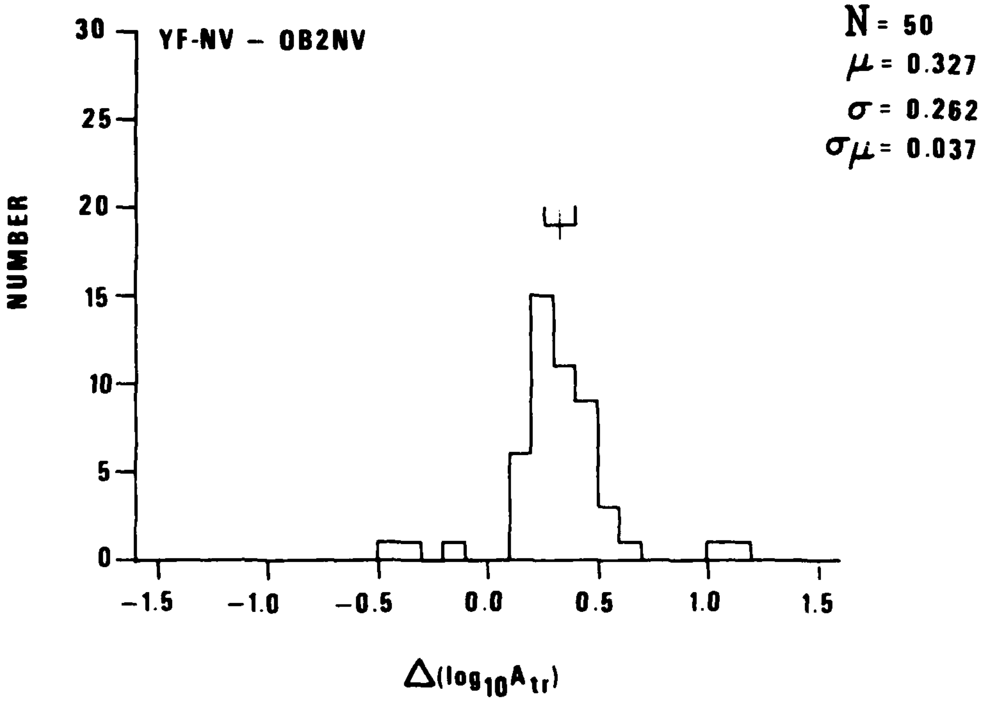
YF-NV – OB2NV
NUMBER
30
25
20
15
10
5
0
−1.5
−1.0
−0.5
0.0
0.5
1.0
1.5
Δ(log10 Atr)
N = 50
μ = 0.327
σ = 0.262
σμ = 0.037

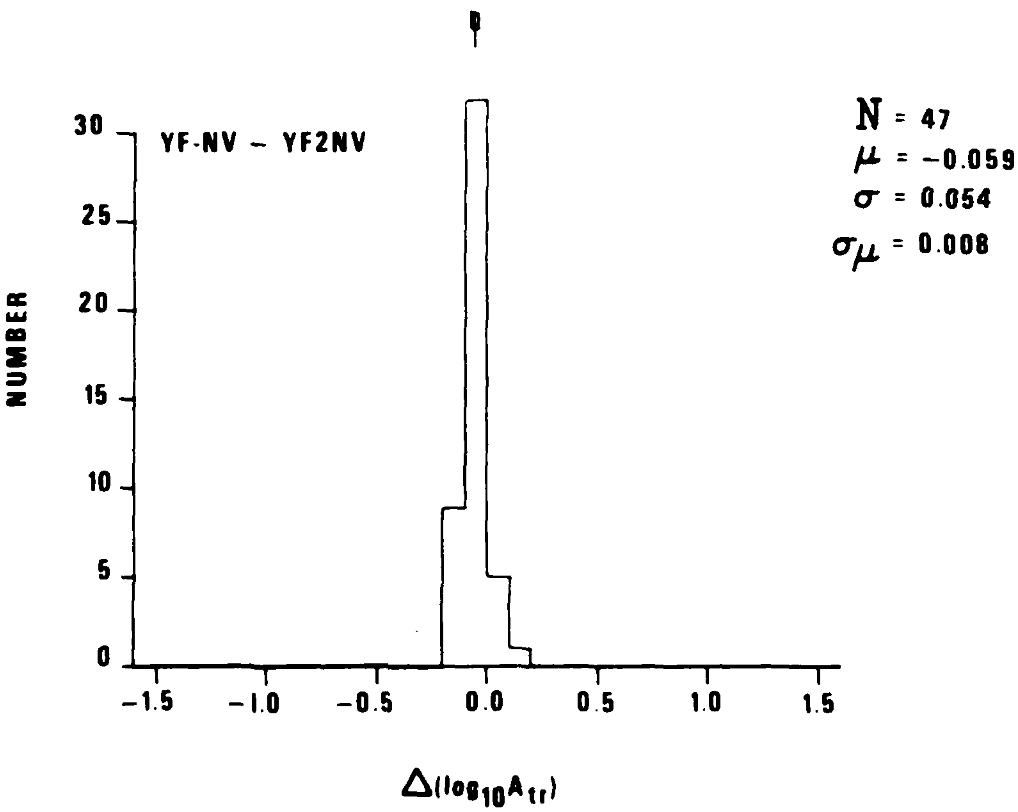
YF-NV – YF2NV
NUMBER
30
25
20
15
10
5
0
−1.5
−1.0
−0.5
0.0
0.5
1.0
1.5
Δ(log10 Atr)
N = 47
μ = −0.059
σ = 0.054
σμ = 0.008

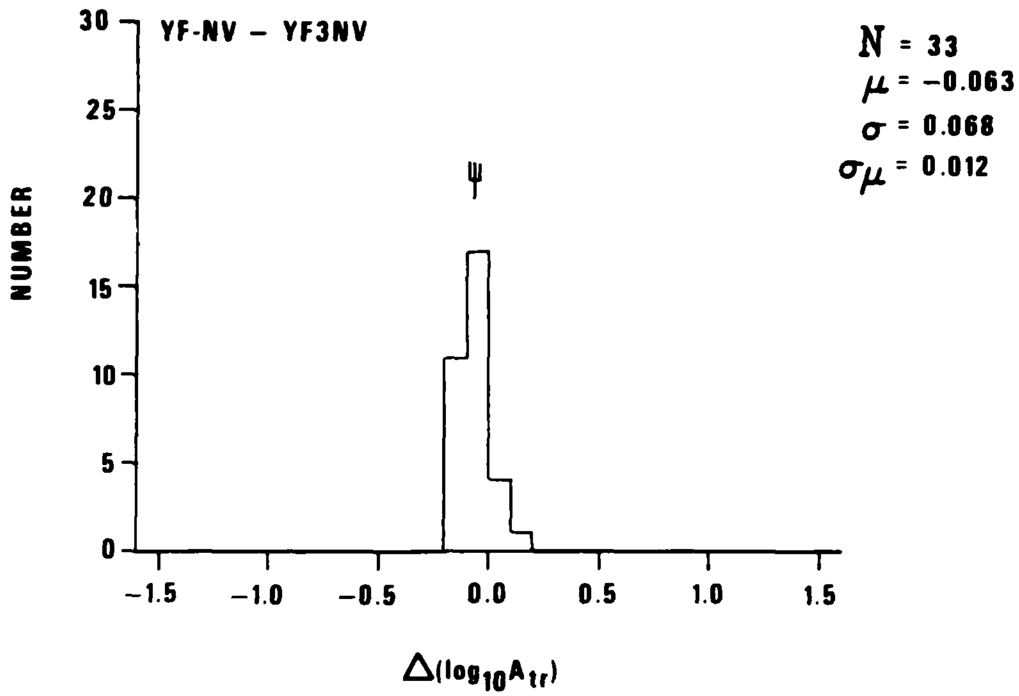
YF-NV − YF3NV
N = 33
μ = −0.063
σ = 0.068
σμ = 0.012
NUMBER
30
25
20
15
10
5
0
−1.5
−1.0
−0.5
0.0
0.5
1.0
1.5
Δ(log10 Atr)

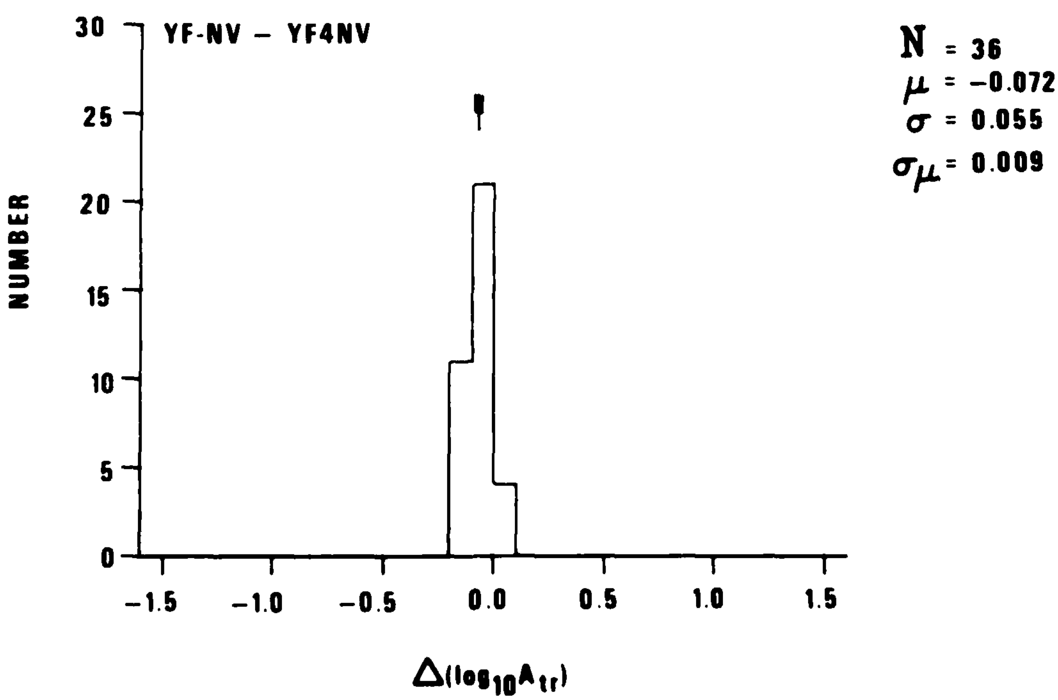
YF-NV − YF4NV
N = 36
μ = −0.072
σ = 0.055
σμ = 0.009
NUMBER
30
25
20
15
10
5
0
−1.5
−1.0
−0.5
0.0
0.5
1.0
1.5
Δ(log10 Atr)

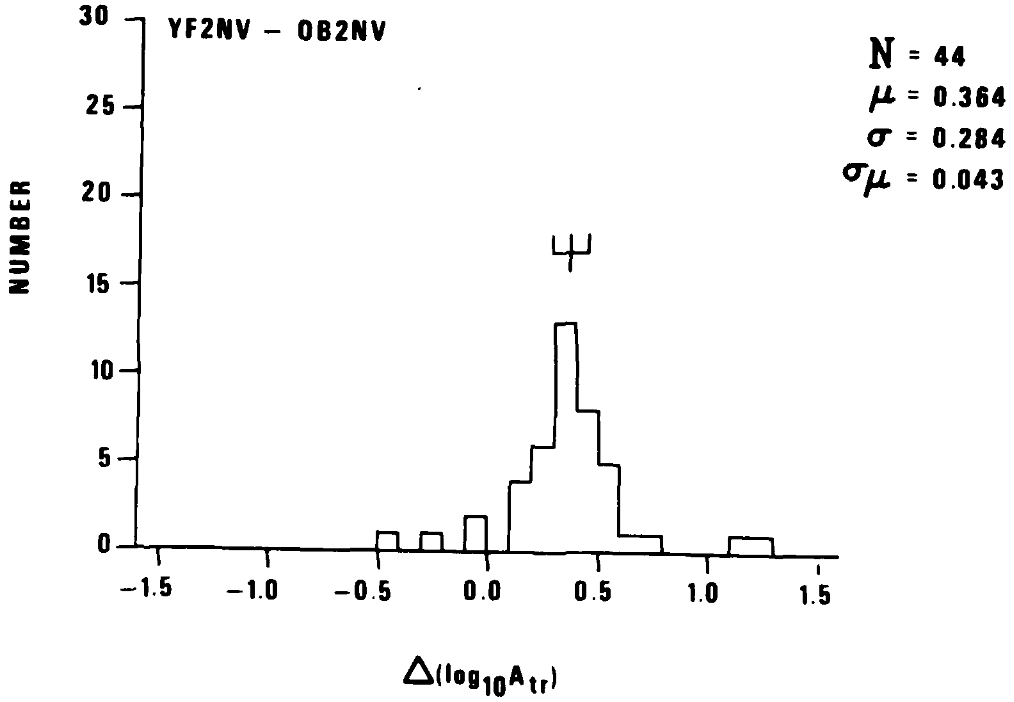
30
25
20
15
10
5
0
YF2NV – OB2NV
NUMBER
N = 44
μ = 0.364
σ = 0.284
σμ = 0.043
−1.5
−1.0
−0.5
0.0
0.5
1.0
1.5
Δ(log10Atr)

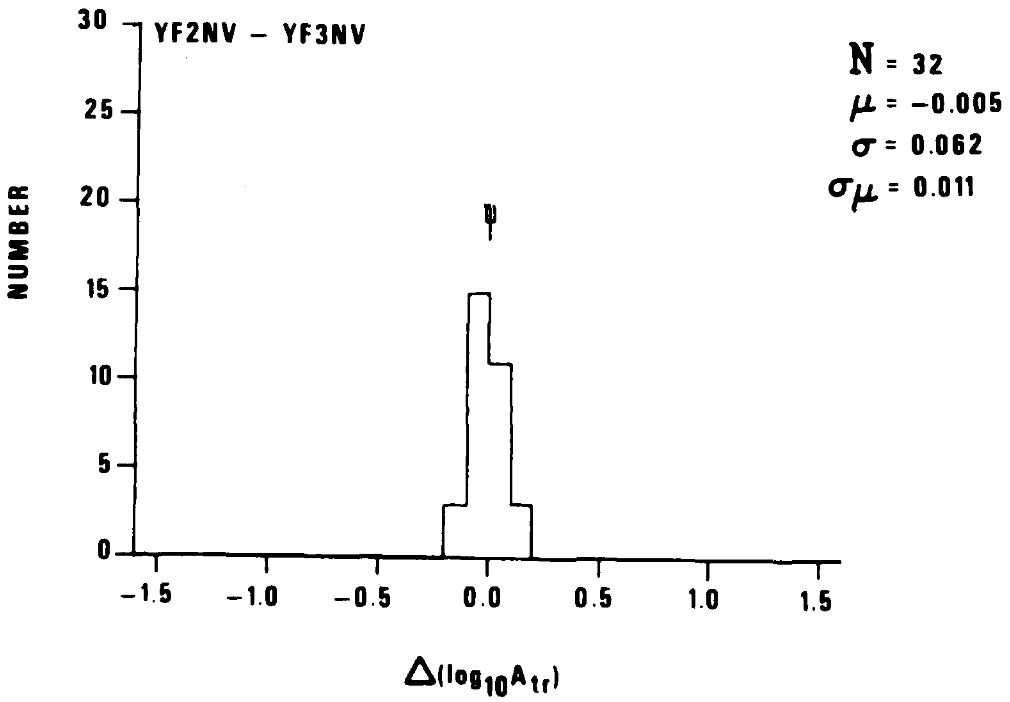
30
25
20
15
10
5
0
YF2NV – YF3NV
NUMBER
N = 32
μ = −0.005
σ = 0.062
σμ = 0.011
−1.5
−1.0
−0.5
0.0
0.5
1.0
1.5
Δ(log10Atr)

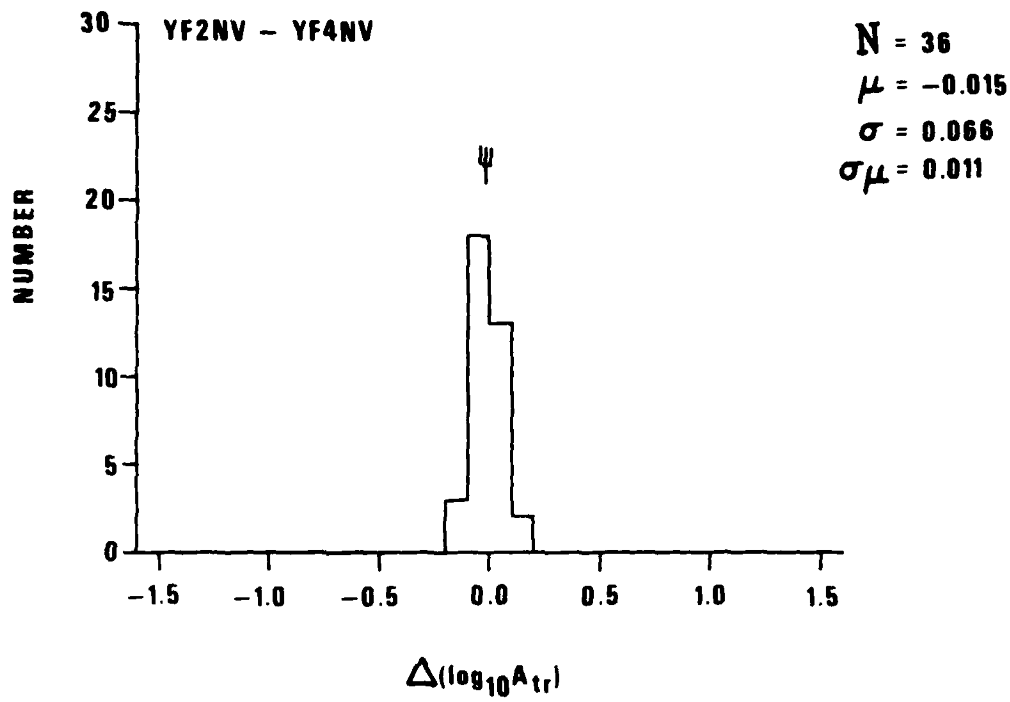

YF2NV – YF4NV
N = 36
μ = –0.015
σ = 0.066
σμ = 0.011
NUMBER
30
25
20
15
10
5
0
–1.5
–1.0
–0.5
0.0
0.5
1.0
1.5
Δ(log10Atr)

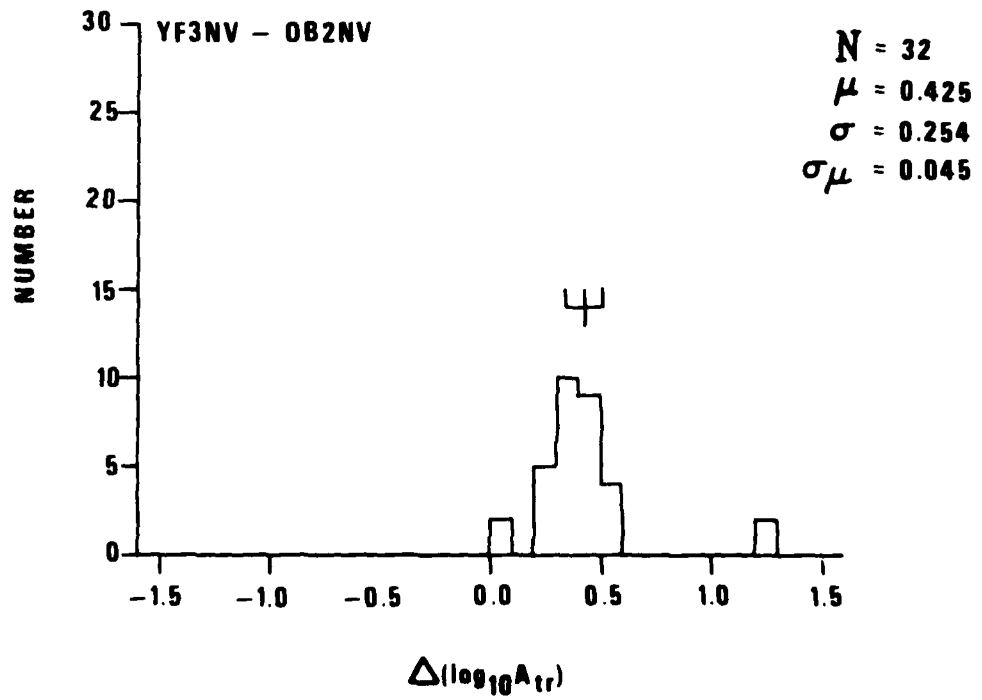

YF3NV – OB2NV
N = 32
μ = 0.425
σ = 0.254
σμ = 0.045
NUMBER
30
25
20
15
10
5
0
–1.5
–1.0
–0.5
0.0
0.5
1.0
1.5
Δ(log10Atr)

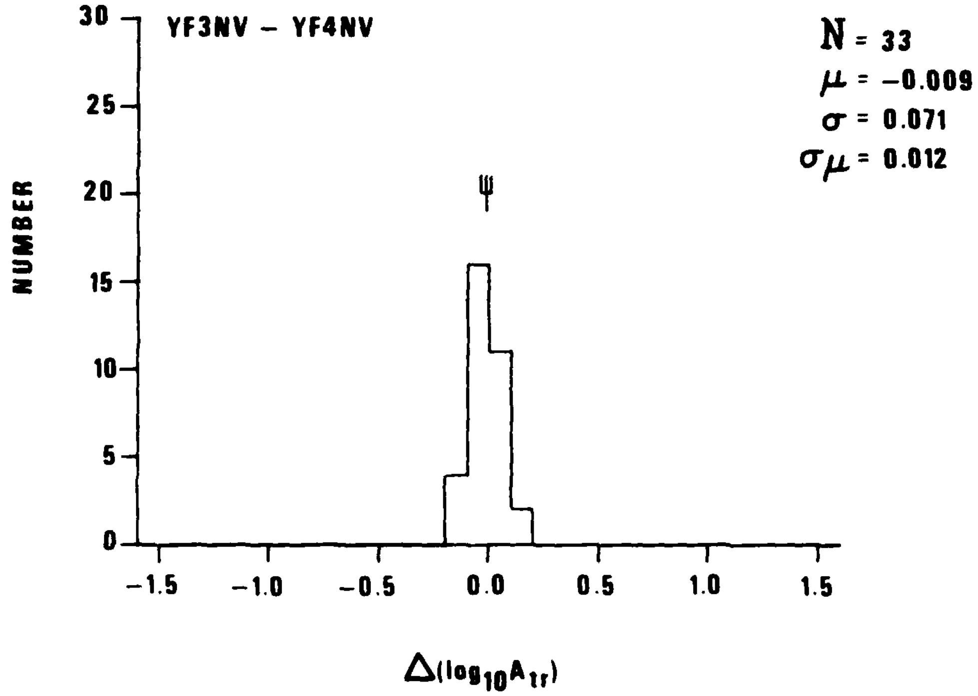
YF3NV – YF4NV
N = 33
μ = –0.009
σ = 0.071
σμ = 0.012
NUMBER
Δ(log10Atr)

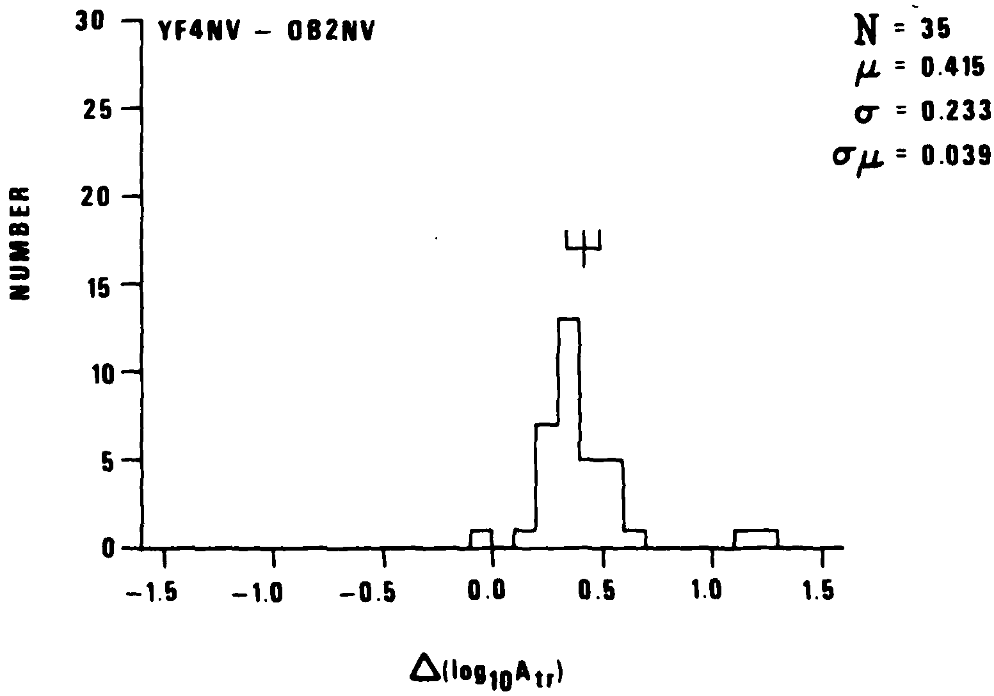
YF4NV – OB2NV
N = 35
μ = 0.415
σ = 0.233
σμ = 0.039
NUMBER
Δ(log10Atr)

APPENDIX D

Histograms of Differentials Δt^* for Various Pairs of SDCS Stations

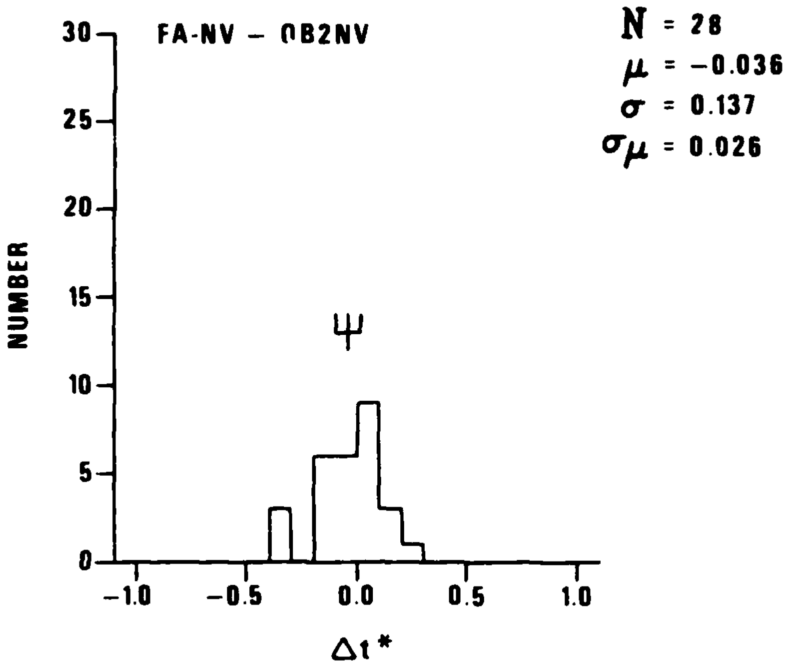
FA-NV – OB2NV
N = 28
μ = −0.036
σ = 0.137
σμ = 0.026
NUMBER
30
25
20
15
10
5
0
−1.0
−0.5
0.0
0.5
1.0
Δt*

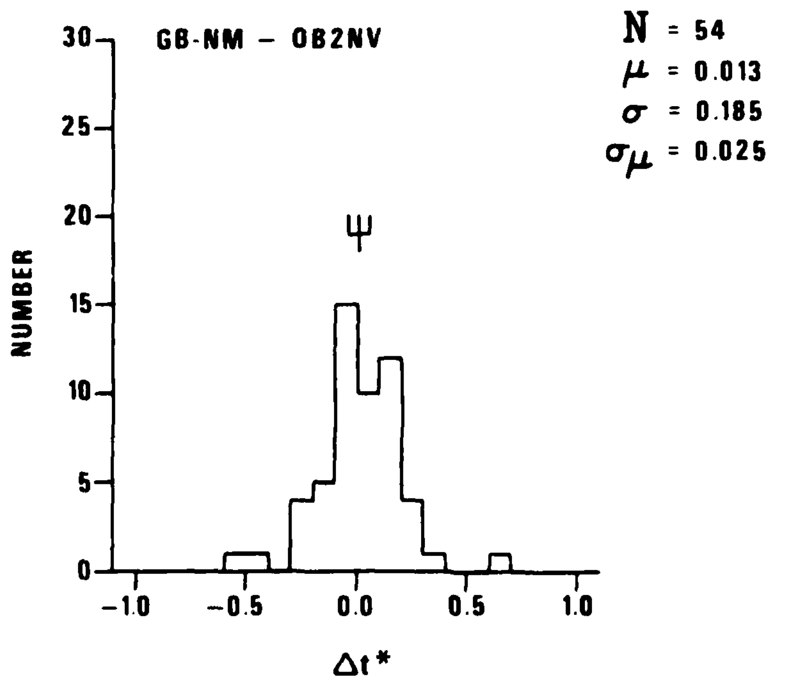
GB-NM – OB2NV
N = 54
μ = 0.013
σ = 0.185
σμ = 0.025
NUMBER
30
25
20
15
10
5
0
−1.0
−0.5
0.0
0.5
1.0
Δt*

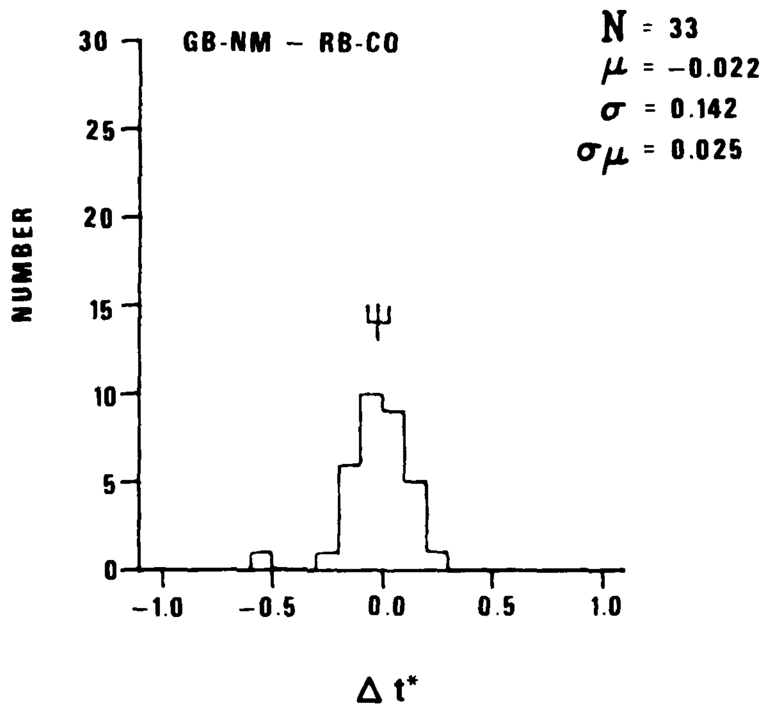
GB-NM – RB-CO
N = 33
μ = −0.022
σ = 0.142
σμ = 0.025
NUMBER
30
25
20
15
10
5
0
−1.0
−0.5
0.0
0.5
1.0
Δ t*

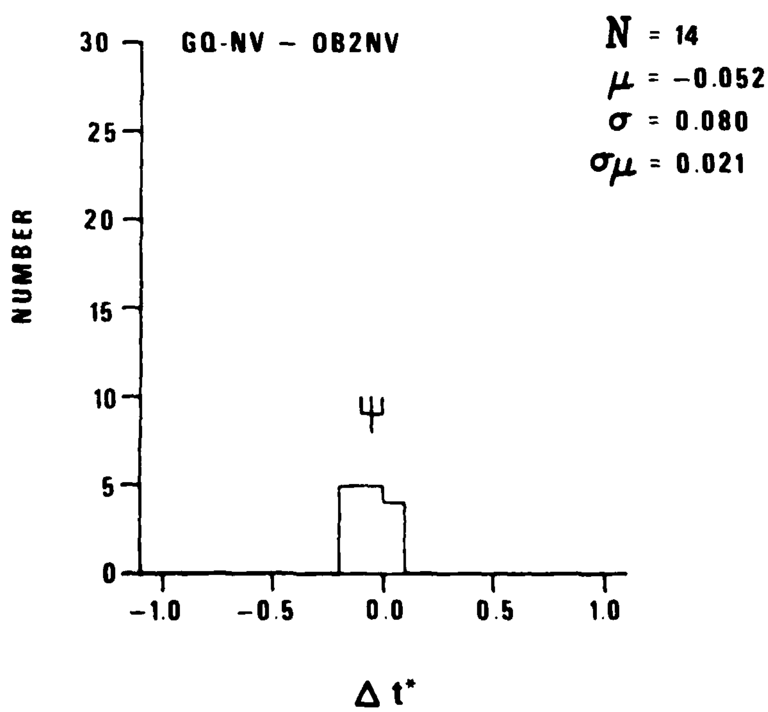
GQ-NV – OB2NV
N = 14
μ = −0.052
σ = 0.080
σμ = 0.021
NUMBER
30
25
20
15
10
5
0
−1.0
−0.5
0.0
0.5
1.0
Δ t*

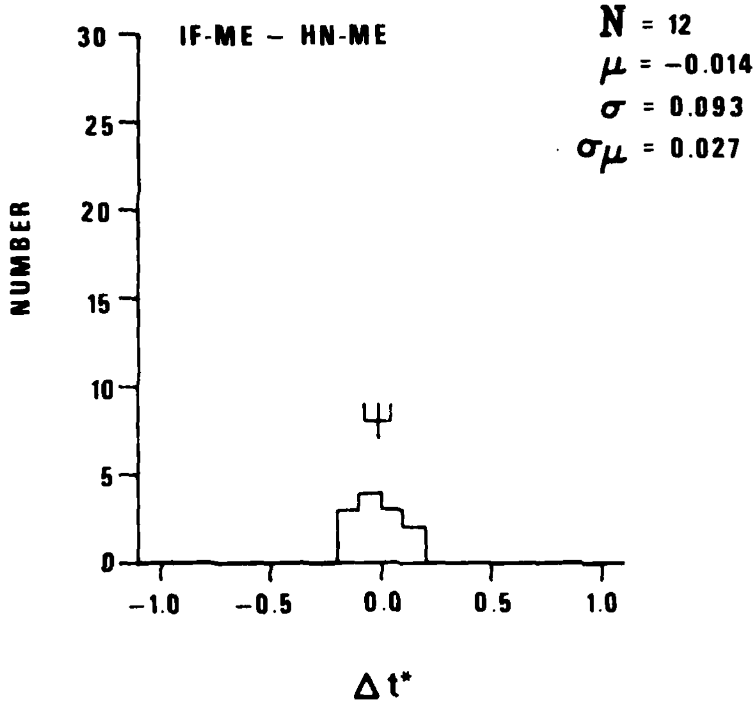
IF-ME – HN-ME
N = 12
μ = −0.014
σ = 0.093
σμ = 0.027
NUMBER
30
25
20
15
10
5
0
−1.0
−0.5
0.0
0.5
1.0
Δt*

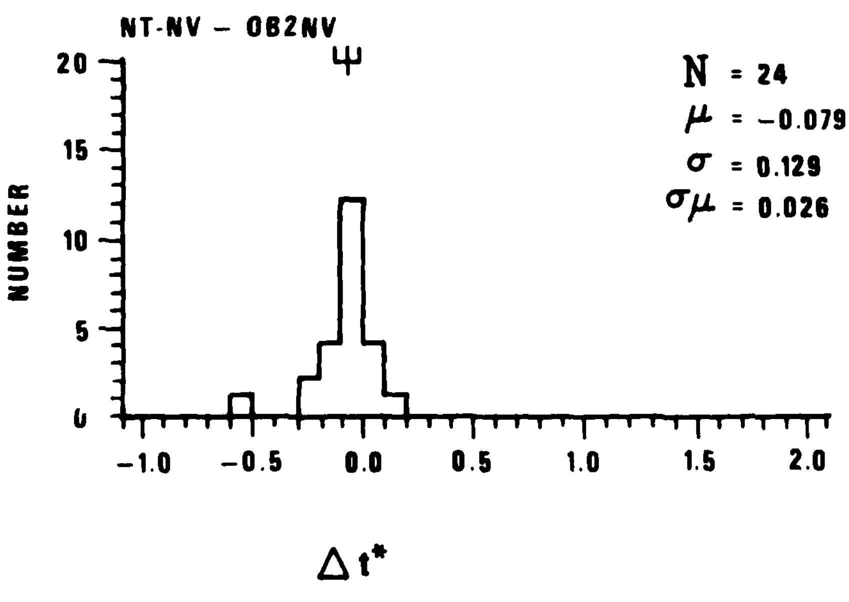
NT-NV – OB2NV
N = 24
μ = −0.079
σ = 0.129
σμ = 0.026
NUMBER
20
15
10
5
0
−1.0
−0.5
0.0
0.5
1.0
1.5
2.0
Δt*

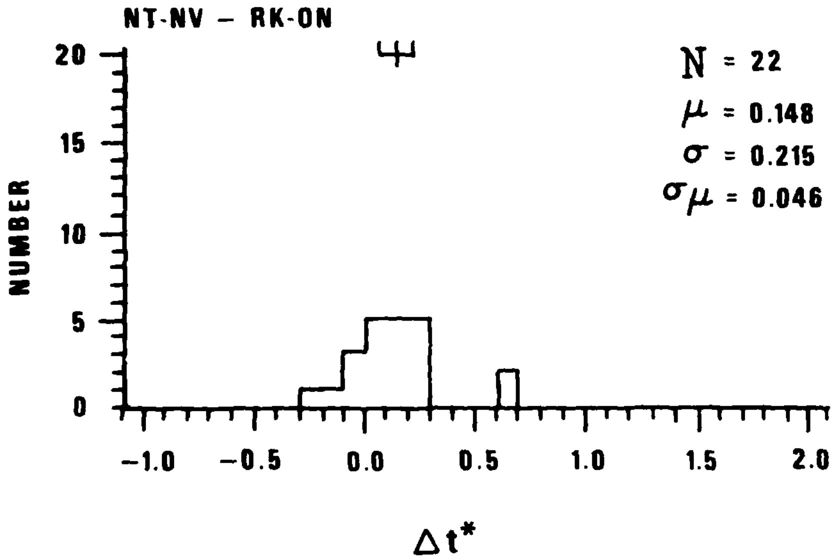
NT-NV – RK-ON
N = 22
μ = 0.148
σ = 0.215
σμ = 0.046
NUMBER
20
15
10
5
0
−1.0
−0.5
0.0
0.5
1.0
1.5
2.0
Δt*

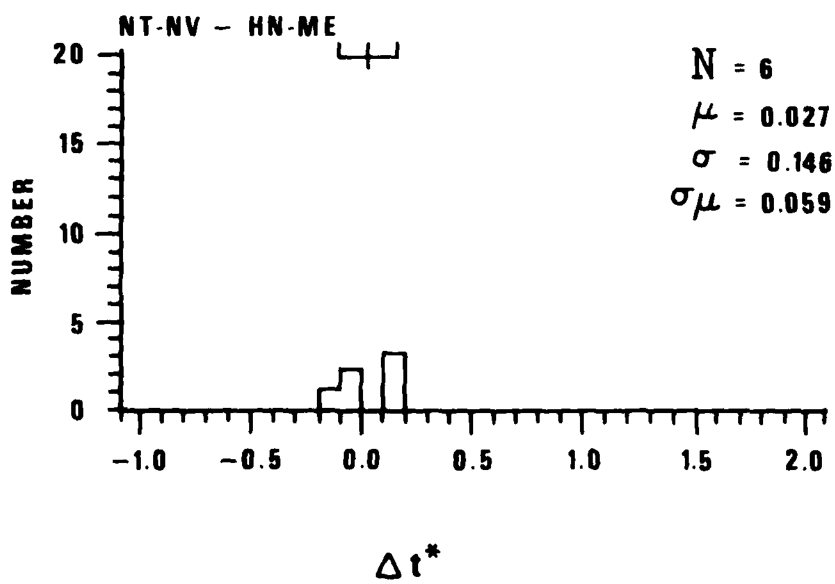
NT-NV – HN-ME
N = 6
μ = 0.027
σ = 0.146
σμ = 0.059
NUMBER
20
15
10
5
0
−1.0
−0.5
0.0
0.5
1.0
1.5
2.0
Δt*

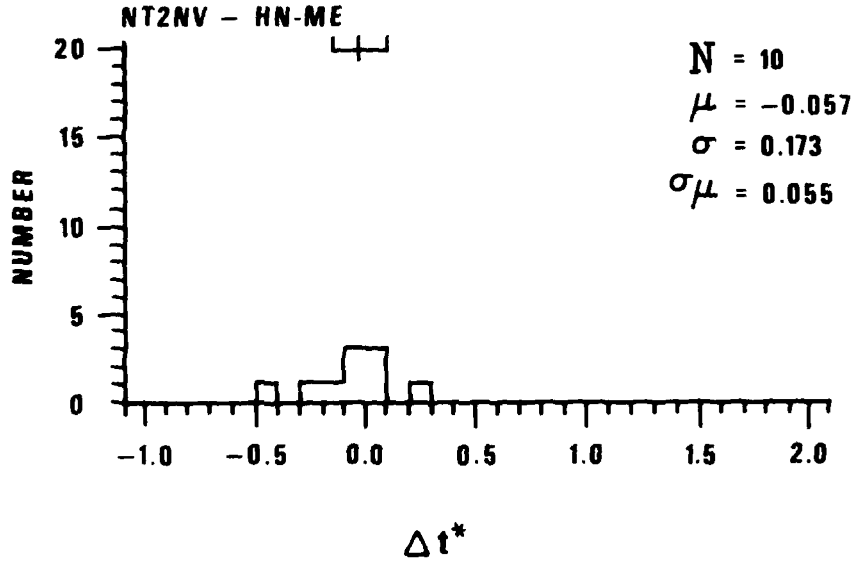
NT2NV – HN-ME
N = 10
μ = –0.057
σ = 0.173
σμ = 0.055
NUMBER
20
15
10
5
0
–1.0
–0.5
0.0
0.5
1.0
1.5
2.0
Δt*

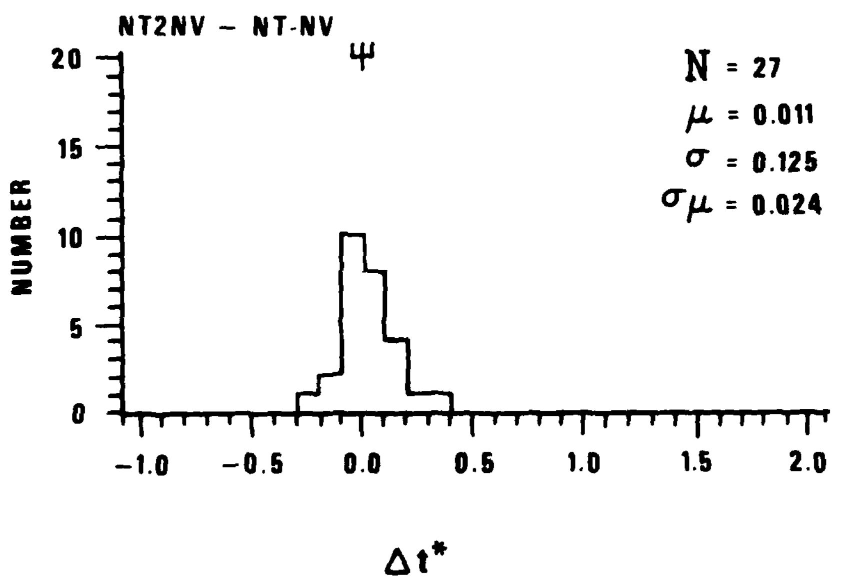
NT2NV – NT-NV
N = 27
μ = 0.011
σ = 0.125
σμ = 0.024
NUMBER
20
15
10
5
0
–1.0
–0.5
0.0
0.5
1.0
1.5
2.0
Δt*

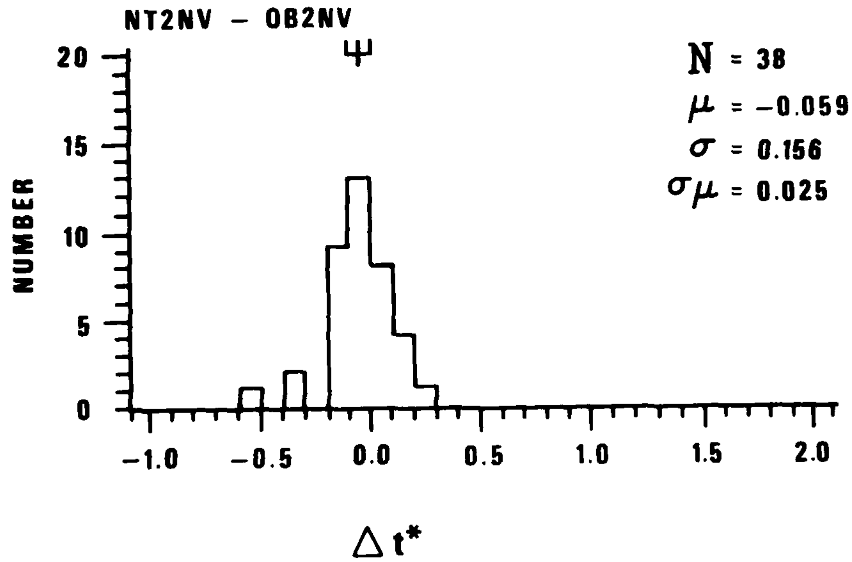

NT2NV – OB2NV
N = 38
μ = –0.059
σ = 0.156
σμ = 0.025
NUMBER
20
15
10
5
0
–1.0
–0.5
0.0
0.5
1.0
1.5
2.0
Δt*

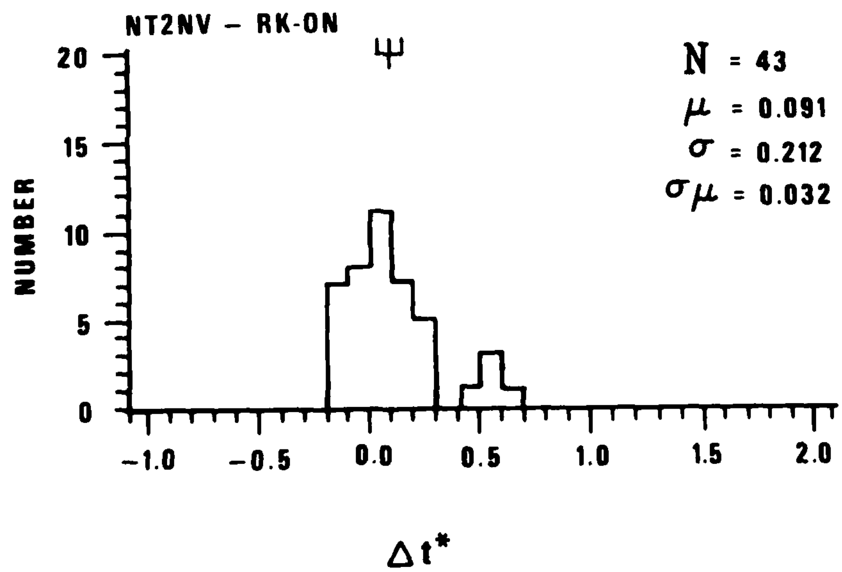

NT2NV – RK-ON
N = 43
μ = 0.091
σ = 0.212
σμ = 0.032
NUMBER
20
15
10
5
0
–1.0
–0.5
0.0
0.5
1.0
1.5
2.0
Δt*

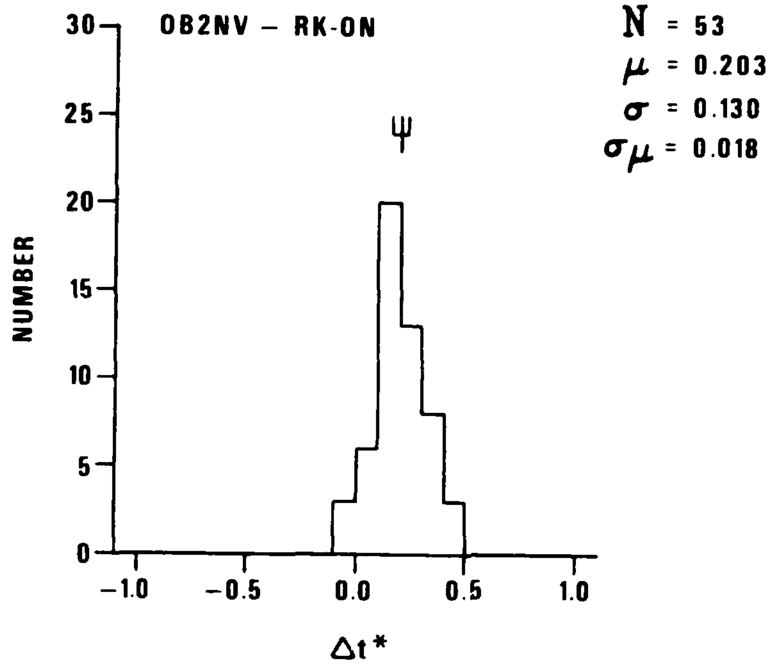
OB2NV – RK-ON
NUMBER
Δt*
N = 53
μ = 0.203
σ = 0.130
σμ = 0.018

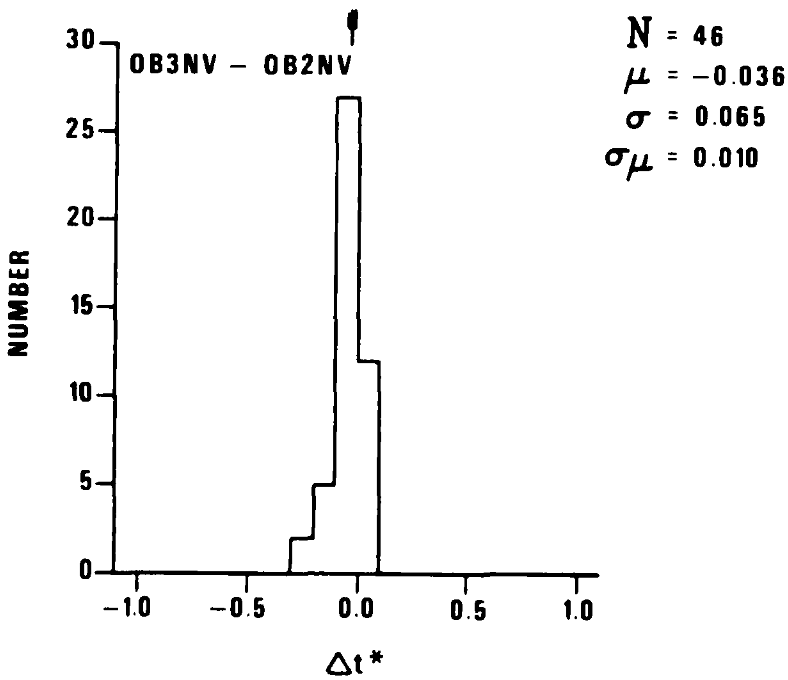
OB3NV – OB2NV
NUMBER
Δt*
N = 46
μ = −0.036
σ = 0.065
σμ = 0.010

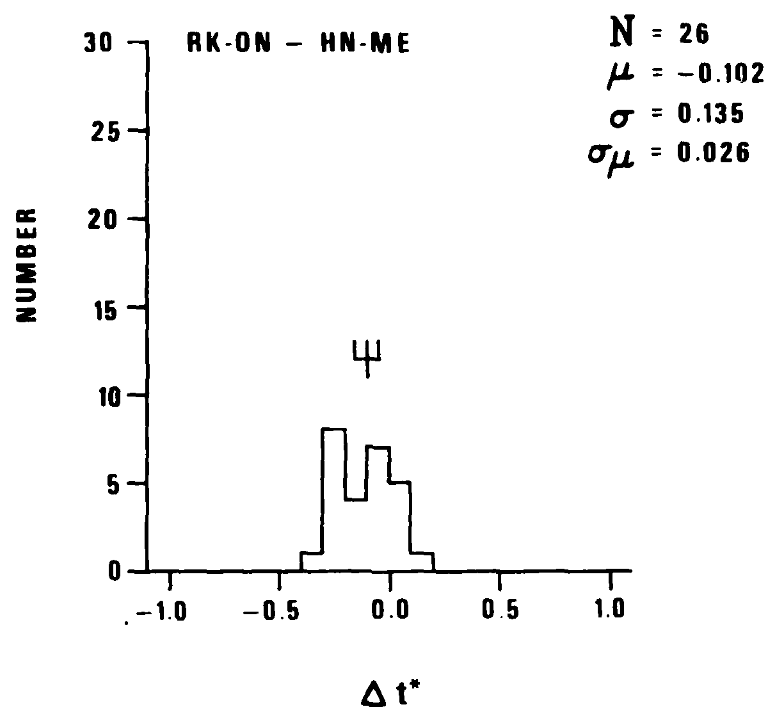
RK-ON – HN-ME
N = 26
μ = −0.102
σ = 0.135
σμ = 0.026
NUMBER
30
25
20
15
10
5
0
−1.0
−0.5
0.0
0.5
1.0
Δ t*

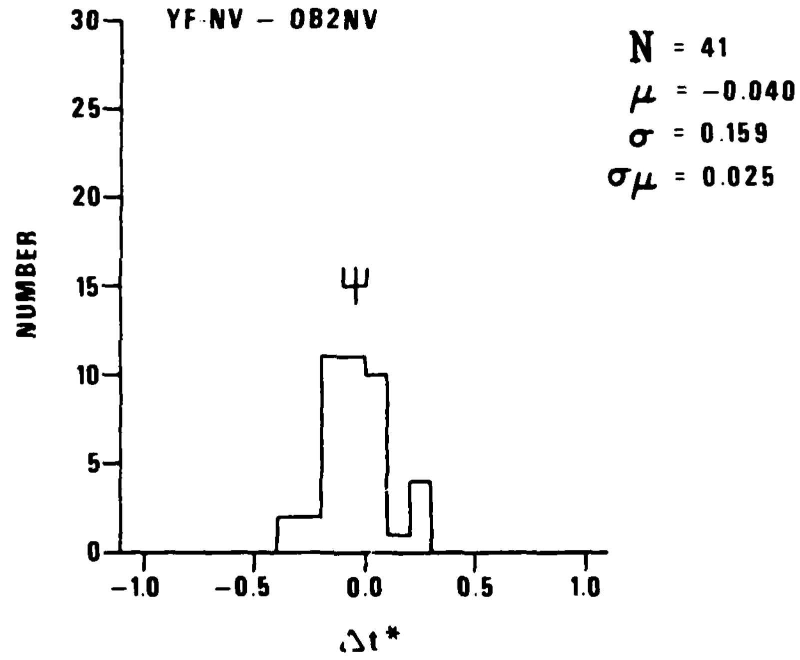
YF-NV – OB2NV
N = 41
μ = −0.040
σ = 0.159
σμ = 0.025
NUMBER
30
25
20
15
10
5
0
−1.0
−0.5
0.0
0.5
1.0
Δt*

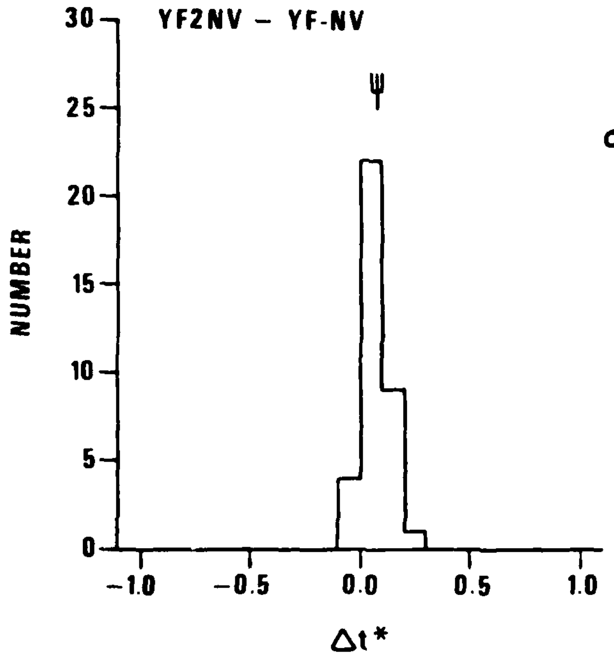

N = 36
μ = 0.076
σ = 0.069
σ_μ = 0.012

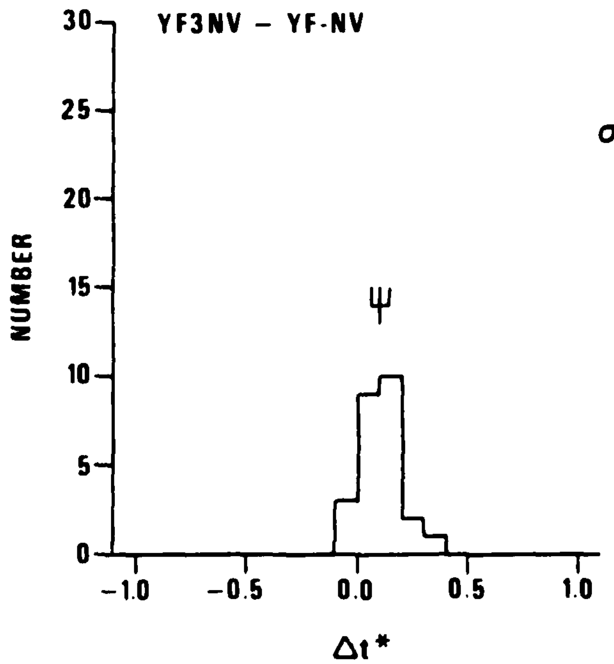

N = 25
μ = 0.108
σ = 0.091
σ_μ = 0.018

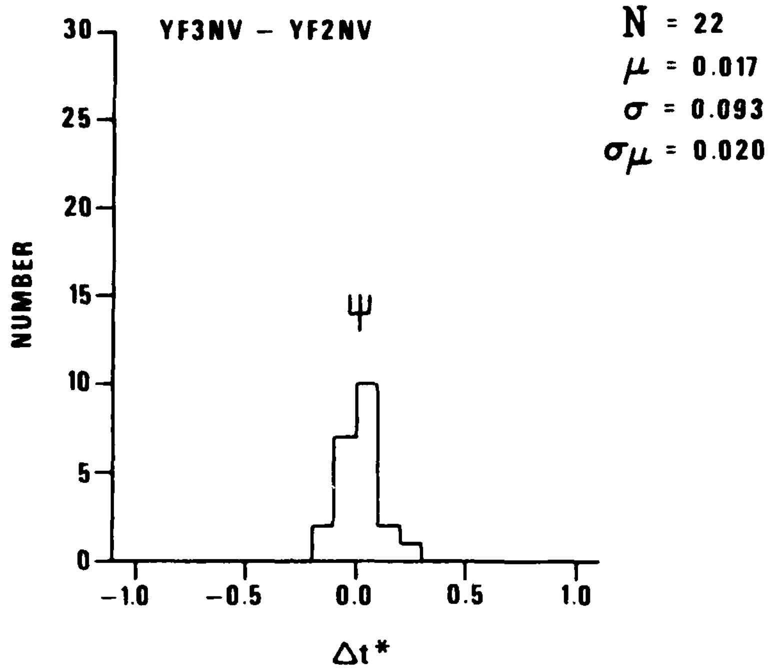
YF3NV – YF2NV
N = 22
μ = 0.017
σ = 0.093
σμ = 0.020
NUMBER
Δt*

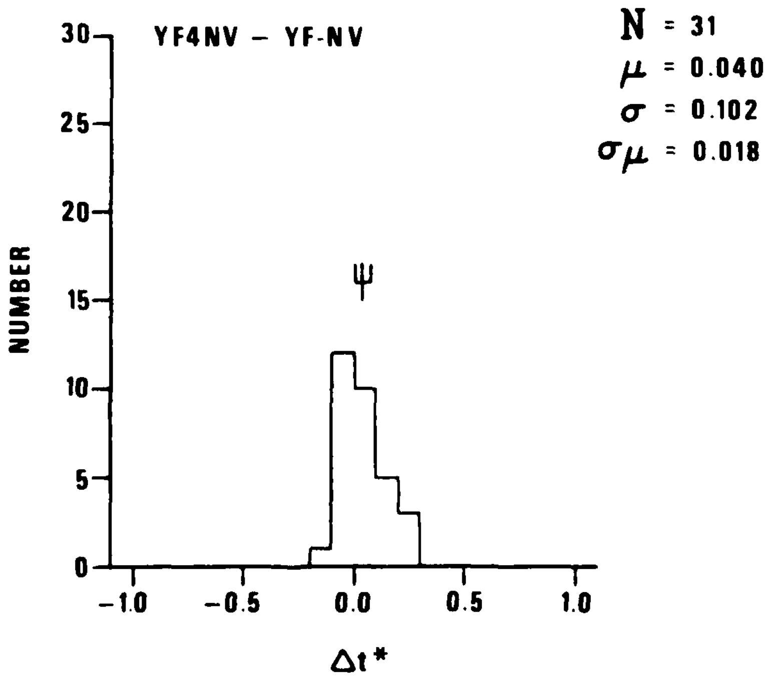
YF4NV – YF-NV
N = 31
μ = 0.040
σ = 0.102
σμ = 0.018
NUMBER
Δt*

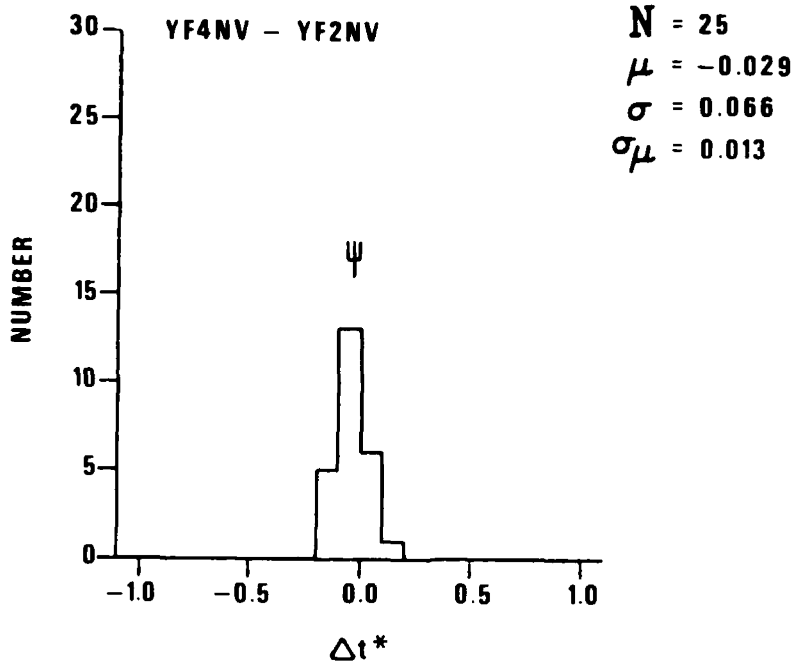
YF4NV – YF2NV
N = 25
μ = −0.029
σ = 0.066
σμ = 0.013
NUMBER
Δt*

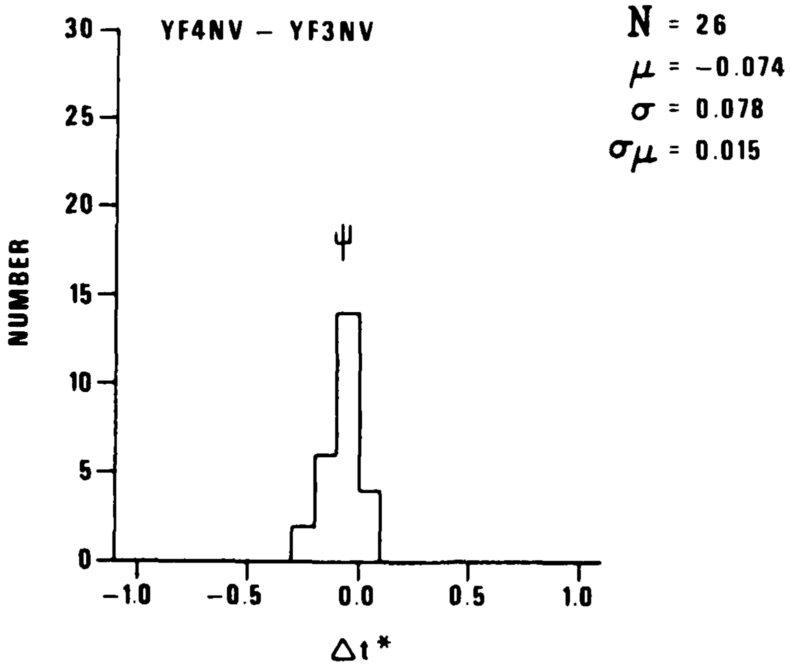
YF4NV – YF3NV
N = 26
μ = −0.074
σ = 0.078
σμ = 0.015
NUMBER
Δt*

APPENDIX E

Histograms of Dominant Period Differentials ΔT for Various Pairs of SDCS Stations

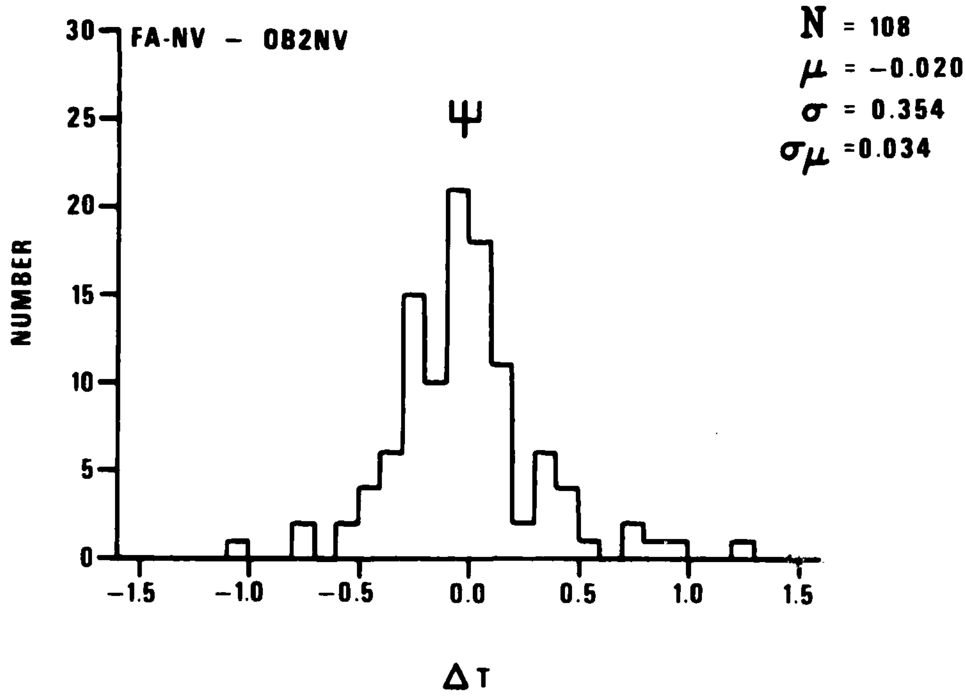
FA-NV – OB2NV
N = 108
μ = –0.020
σ = 0.354
σμ =0.034
NUMBER
0
5
10
15
20
25
30
–1.5
–1.0
–0.5
0.0
0.5
1.0
1.5
ΔT

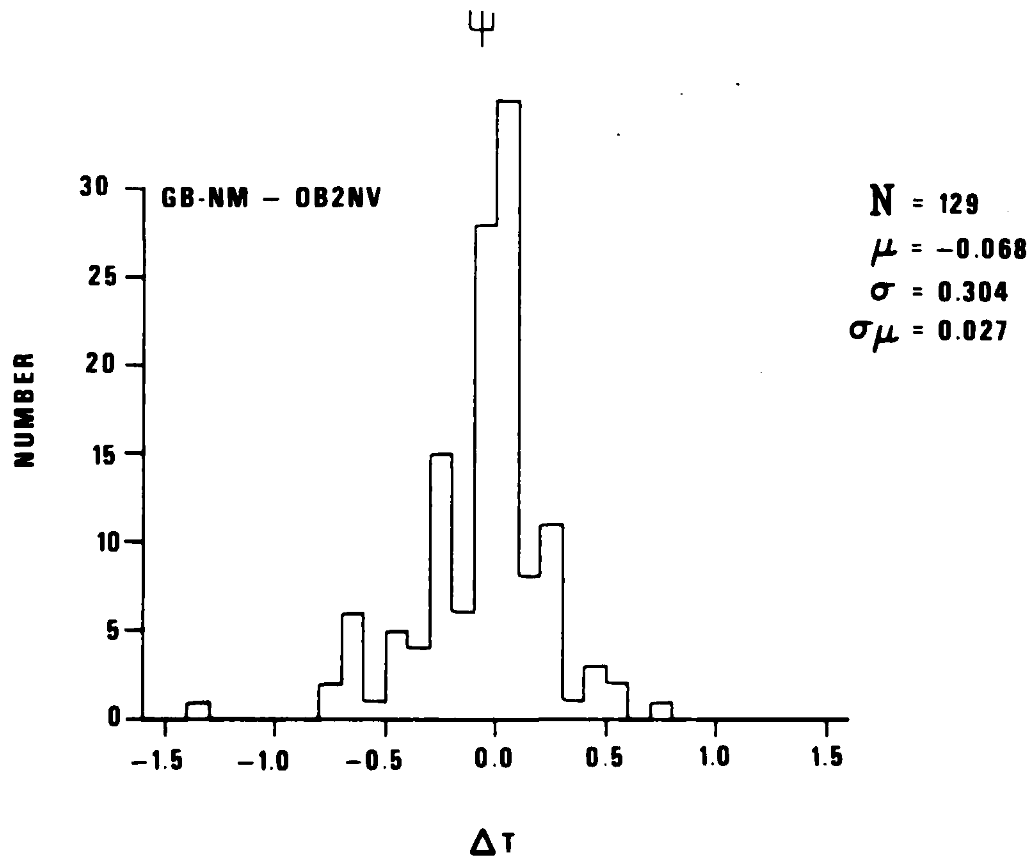
GB-NM – OB2NV
N = 129
μ = –0.068
σ = 0.304
σμ = 0.027
NUMBER
0
5
10
15
20
25
30
–1.5
–1.0
–0.5
0.0
0.5
1.0
1.5
ΔT

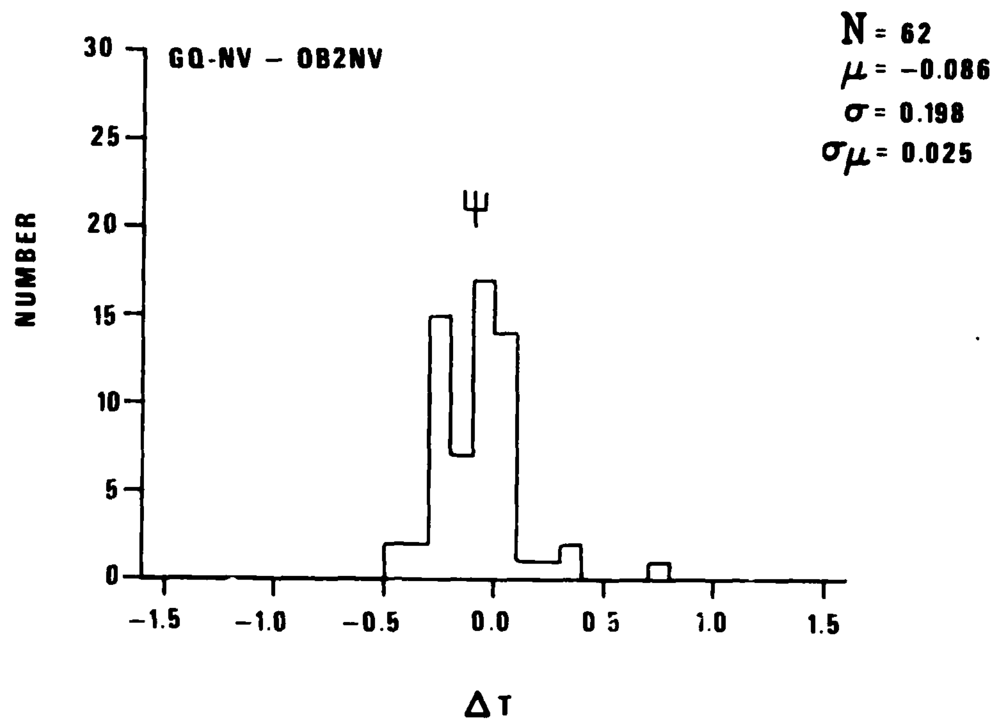
GQ-NV – OB2NV
N = 62
μ = −0.086
σ = 0.198
σμ = 0.025
NUMBER
ΔT
30
25
20
15
10
5
0
−1.5
−1.0
−0.5
0.0
0.5
1.0
1.5

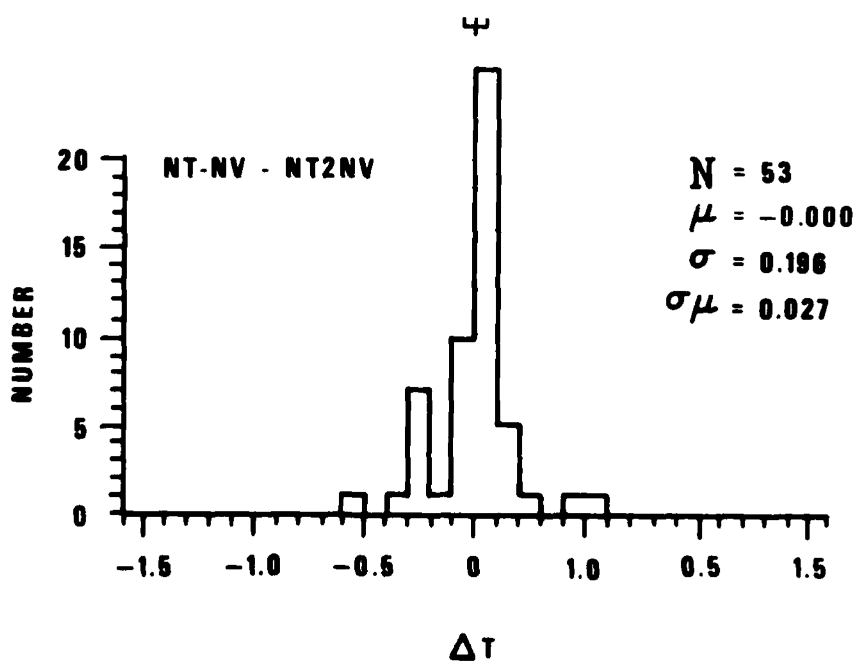
NT-NV - NT2NV
N = 53
μ = −0.000
σ = 0.196
σμ = 0.027
NUMBER
ΔT
20
15
10
5
0
−1.5
−1.0
−0.5
0
1.0
0.5
1.5

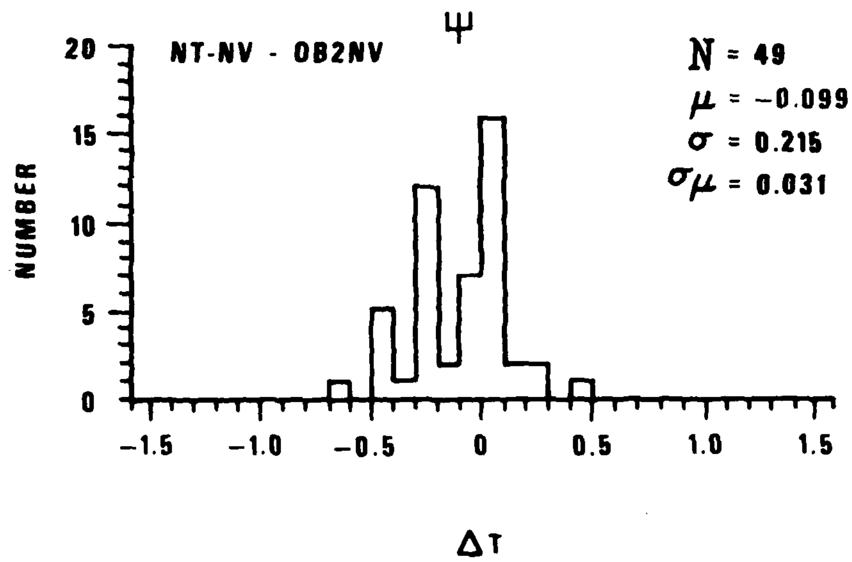
Ψ
NT-NV - OB2NV
N = 49
μ = −0.099
σ = 0.215
σμ = 0.031
NUMBER
ΔT

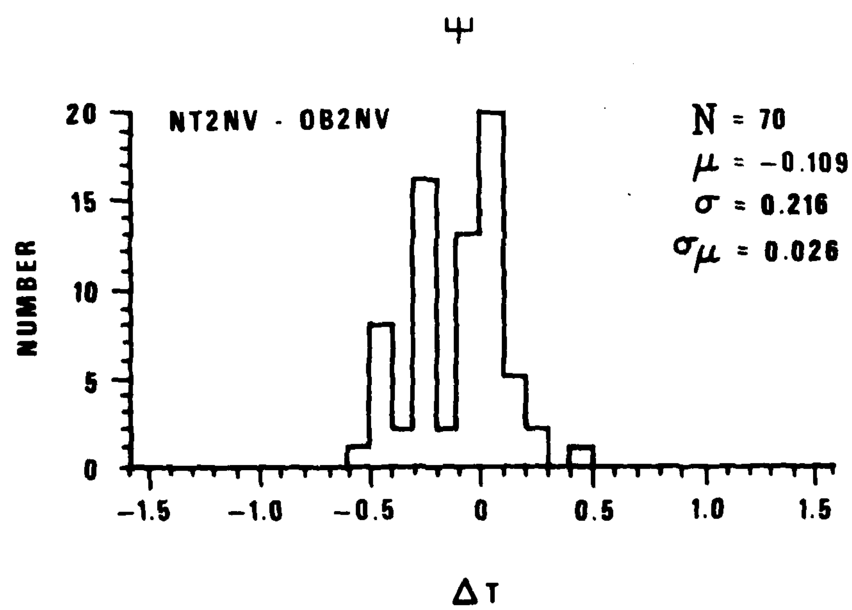
Ψ
NT2NV - OB2NV
N = 70
μ = −0.109
σ = 0.216
σμ = 0.026
NUMBER
ΔT

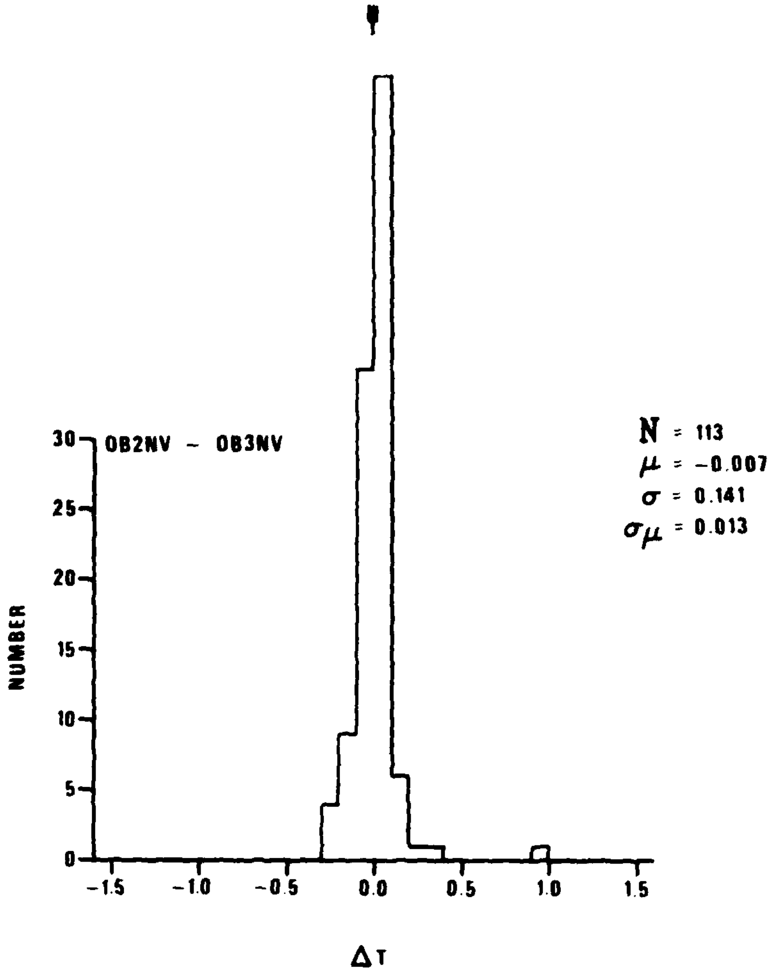

OB2NV – OB3NV
N = 113
μ = -0.007
σ = 0.141
σμ = 0.013
NUMBER
ΔT

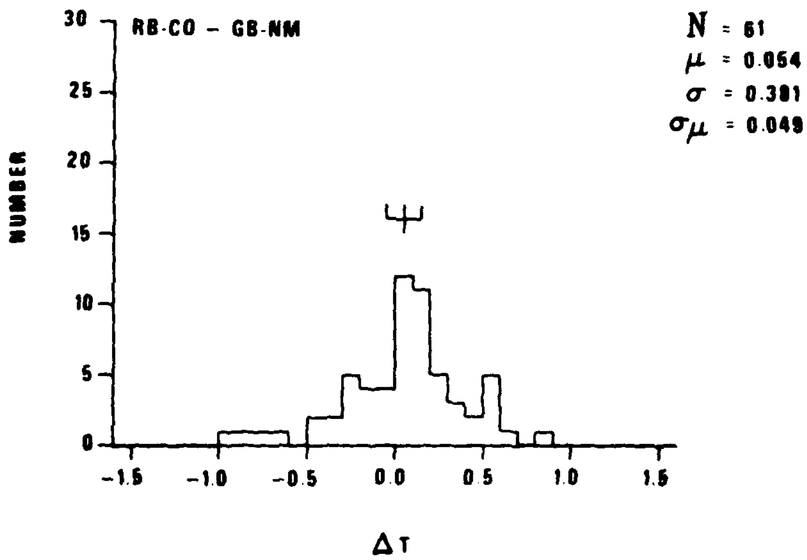

RB-CO – GB-NM
N = 61
μ = 0.054
σ = 0.381
σμ = 0.049
NUMBER
ΔT

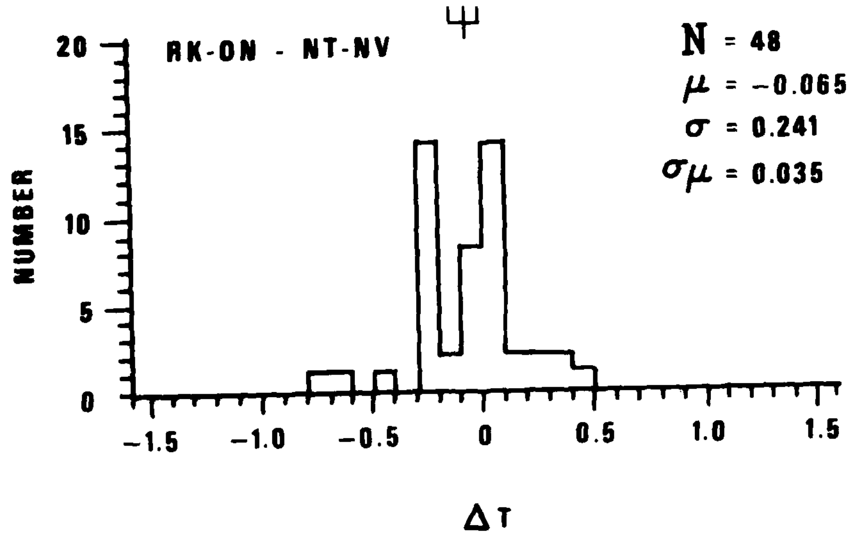

RK-ON - NT-NV
N = 48
μ = −0.065
σ = 0.241
σμ = 0.035
NUMBER
20
15
10
5
0
−1.5
−1.0
−0.5
0
0.5
1.0
1.5
ΔT

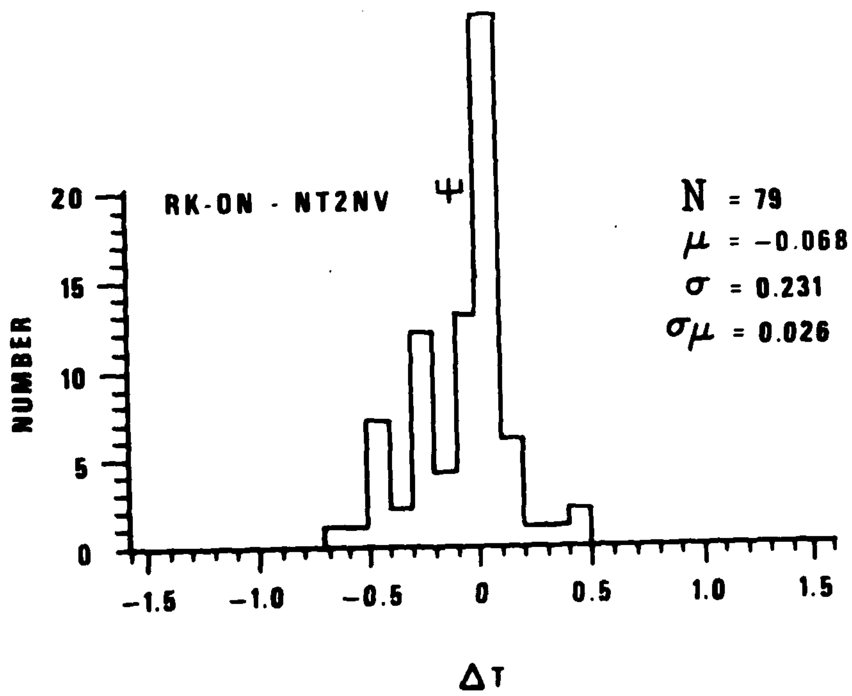

RK-ON - NT2NV
N = 79
μ = −0.068
σ = 0.231
σμ = 0.026
NUMBER
20
15
10
5
0
−1.5
−1.0
−0.5
0
0.5
1.0
1.5
ΔT

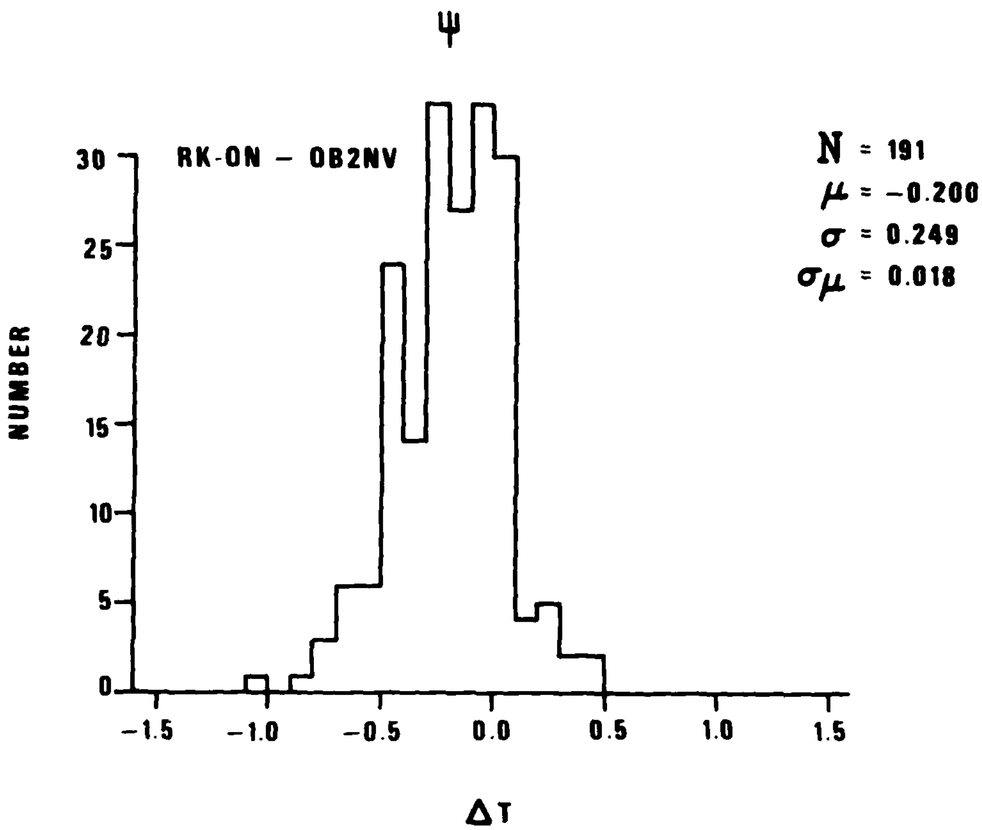

RK-ON — OB2NV
N = 191
μ = −0.200
σ = 0.249
σμ = 0.018
NUMBER
ΔT

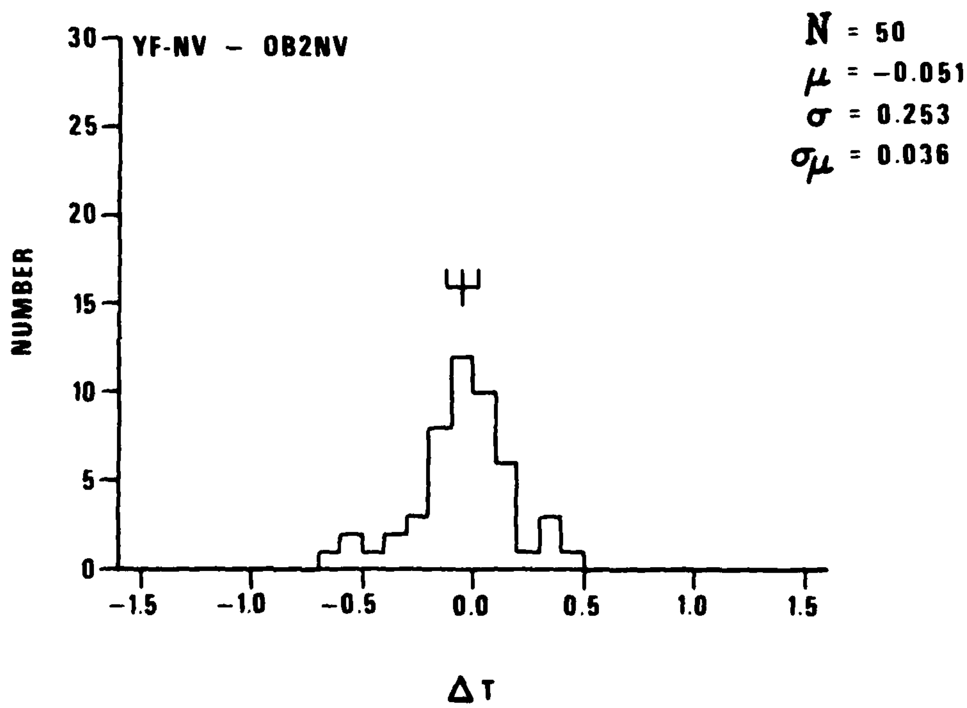

YF-NV — OB2NV
N = 50
μ = −0.051
σ = 0.253
σμ = 0.036
NUMBER
ΔT

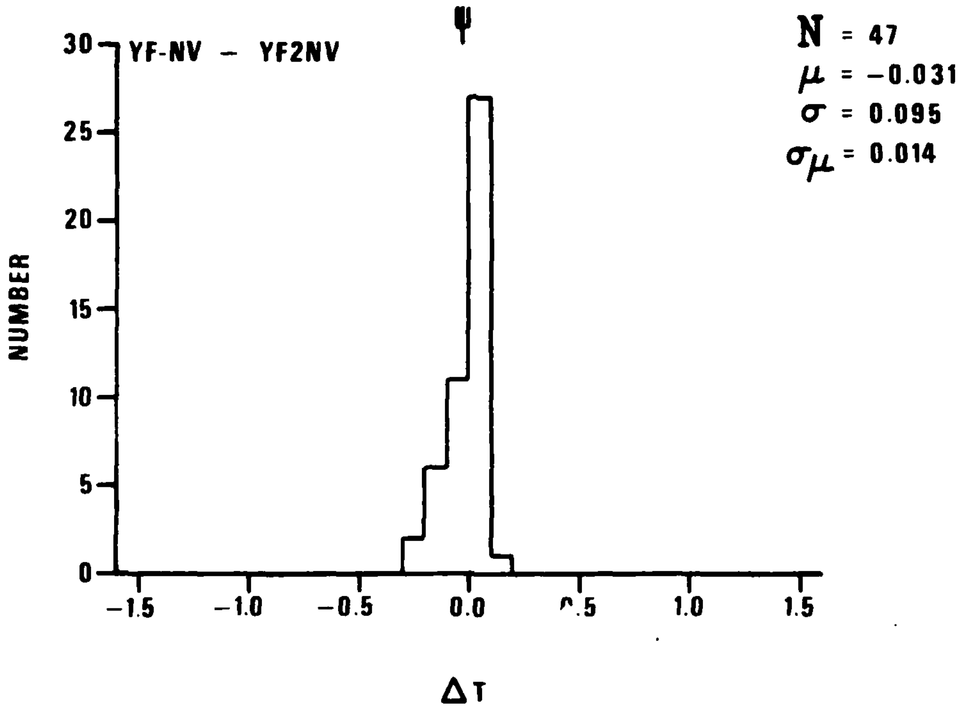
YF-NV – YF2NV
N = 47
μ = −0.031
σ = 0.095
σ_μ = 0.014
NUMBER
30
25
20
15
10
5
0
−1.5
−1.0
−0.5
0.0
1.0
1.5
ΔT

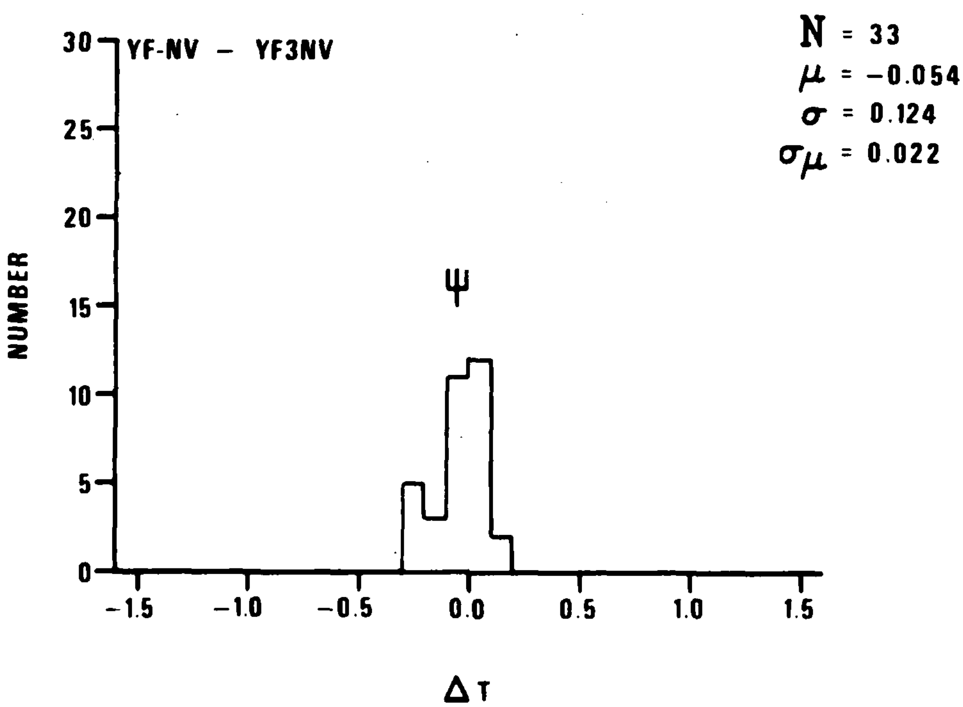
YF-NV – YF3NV
N = 33
μ = −0.054
σ = 0.124
σ_μ = 0.022
NUMBER
30
25
20
15
10
5
0
−1.5
−1.0
−0.5
0.0
0.5
1.0
1.5
ΔT

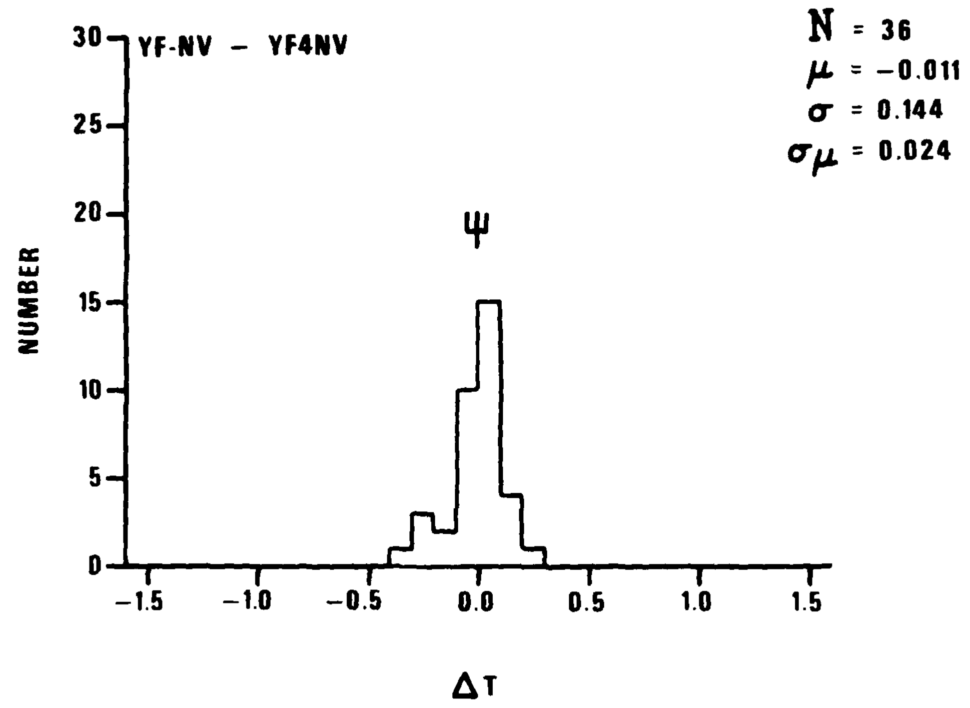
YF-NV – YF4NV
N = 36
μ = −0.011
σ = 0.144
σμ = 0.024
NUMBER
ΔT
30
25
20
15
10
5
0
−1.5
−1.0
−0.5
0.0
0.5
1.0
1.5

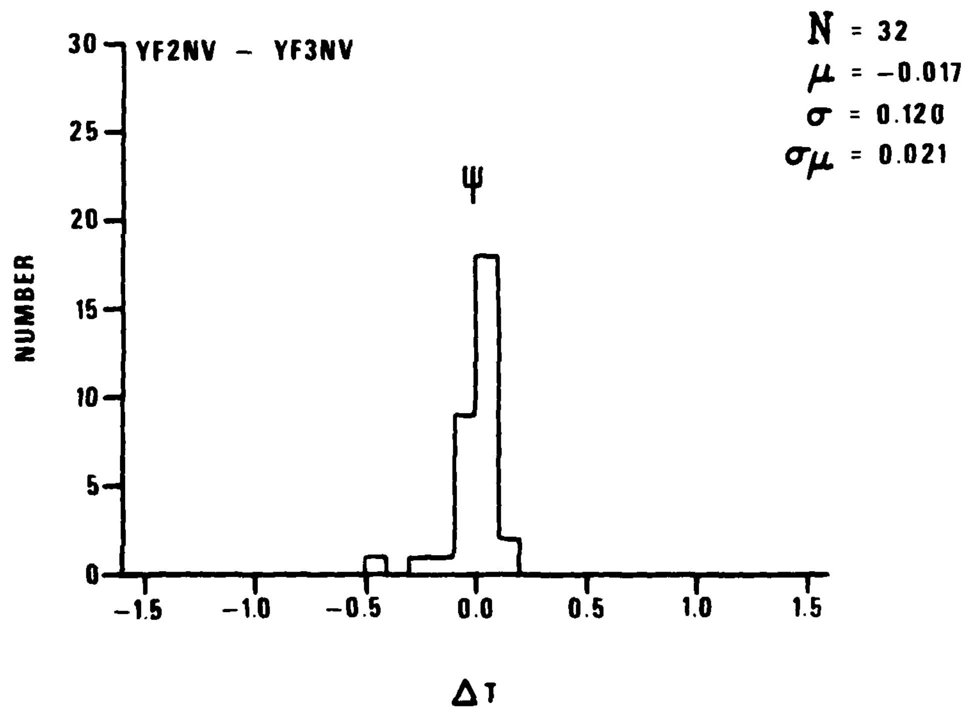
YF2NV – YF3NV
N = 32
μ = −0.017
σ = 0.120
σμ = 0.021
NUMBER
ΔT
30
25
20
15
10
5
0
−1.5
−1.0
−0.5
0.0
0.5
1.0
1.5

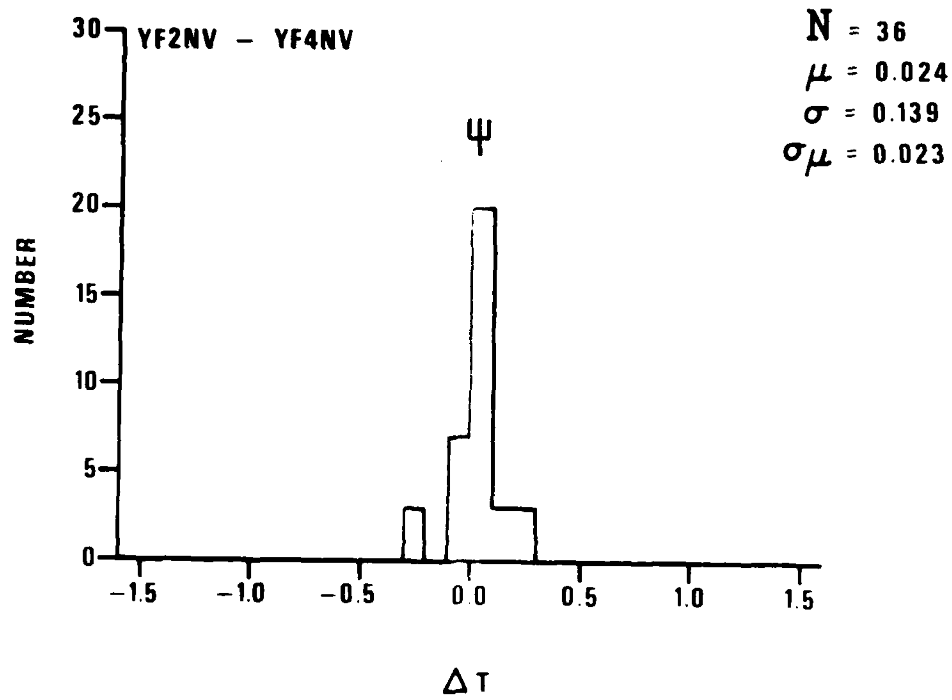

YF2NV - YF4NV
N = 36
μ = 0.024
σ = 0.139
σμ = 0.023
NUMBER
30
25
20
15
10
5
0
-1.5
-1.0
-0.5
0.0
0.5
1.0
1.5
ΔT

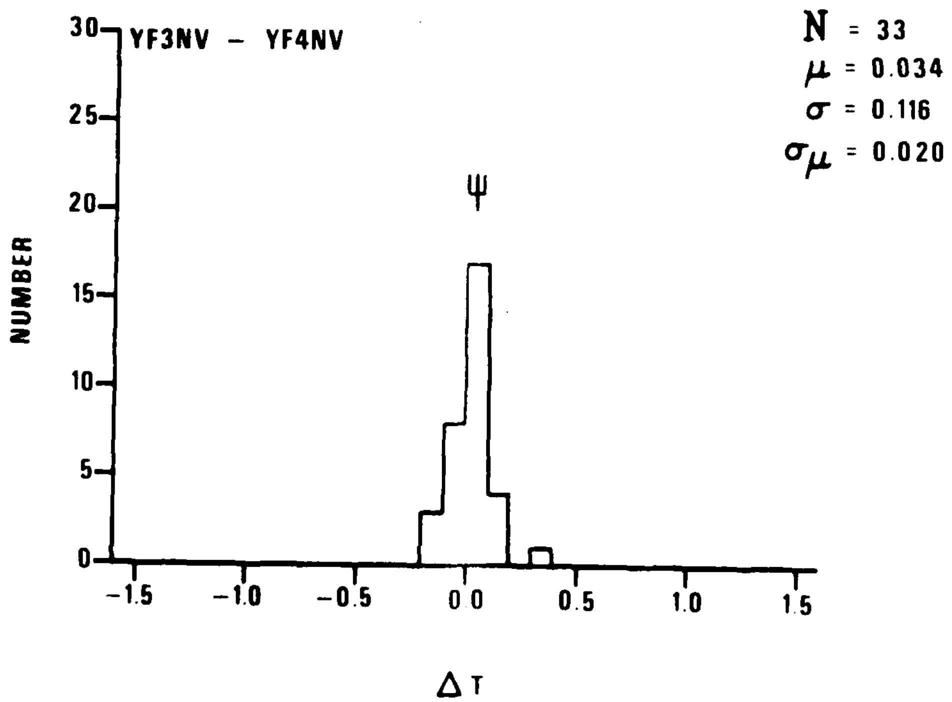

YF3NV - YF4NV
N = 33
μ = 0.034
σ = 0.116
σμ = 0.020
NUMBER
30
25
20
15
10
5
0
-1.5
-1.0
-0.5
0.0
0.5
1.0
1.5
ΔT

APPENDIX F

Histograms of Travel Time Differentials for Various Pairs of SDCS Stations

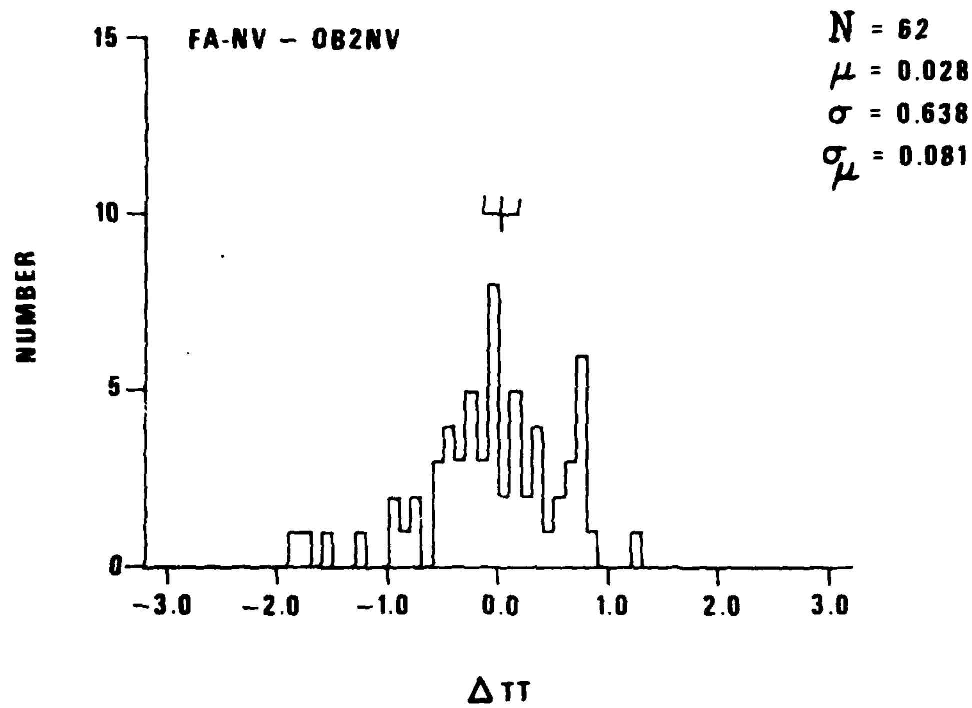

FA-NV – OB2NV
N = 62
μ = 0.028
σ = 0.638
σμ = 0.081
15
10
5
0
NUMBER
–3.0
–2.0
–1.0
0.0
1.0
2.0
3.0
Δ TT

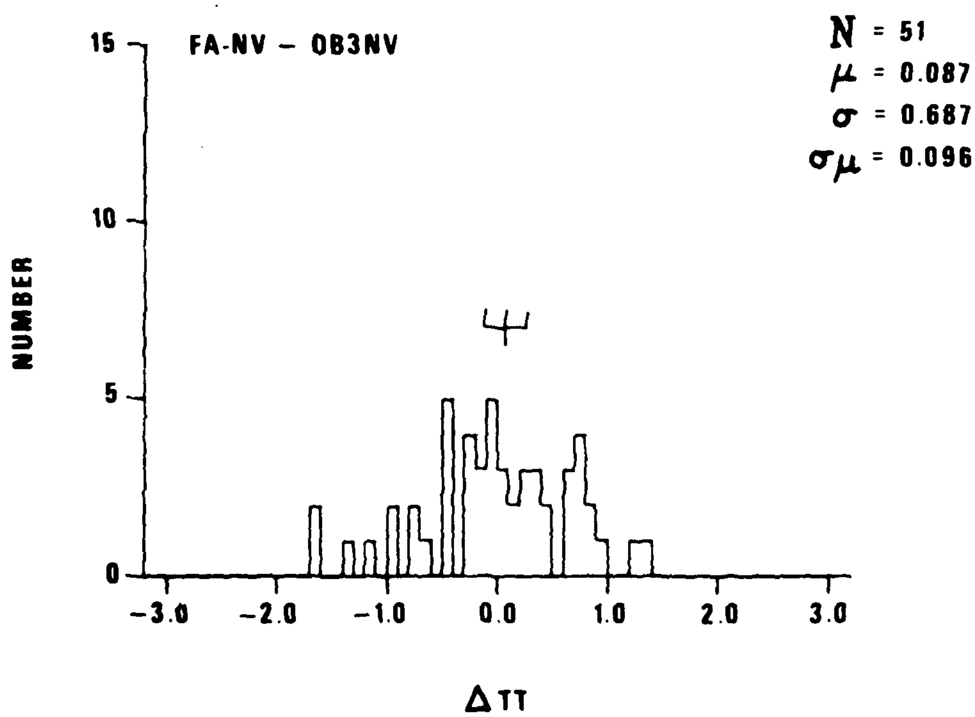

FA-NV – OB3NV
N = 51
μ = 0.087
σ = 0.687
σμ = 0.096
15
10
5
0
NUMBER
–3.0
–2.0
–1.0
0.0
1.0
2.0
3.0
Δ TT

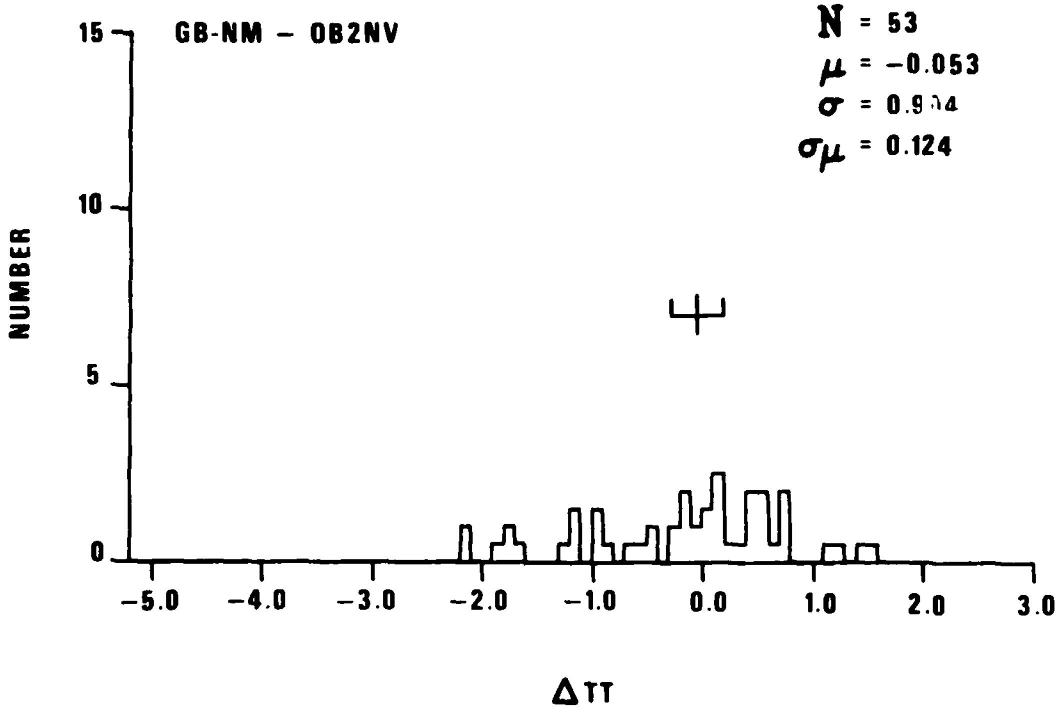
GB-NM – OB2NV
N = 53
μ = –0.053
σ = 0.9
σμ = 0.124
15
10
5
0
NUMBER
–5.0
–4.0
–3.0
–2.0
–1.0
0.0
1.0
2.0
3.0
ΔTT

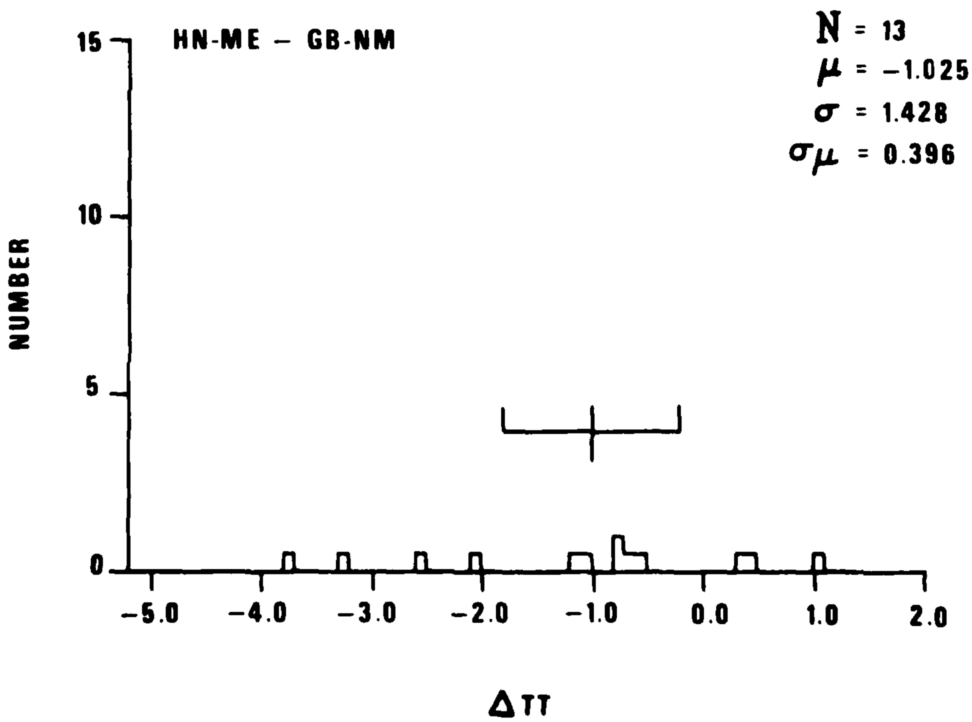
HN-ME – GB-NM
N = 13
μ = –1.025
σ = 1.428
σμ = 0.396
15
10
5
0
NUMBER
–5.0
–4.0
–3.0
–2.0
–1.0
0.0
1.0
2.0
ΔTT

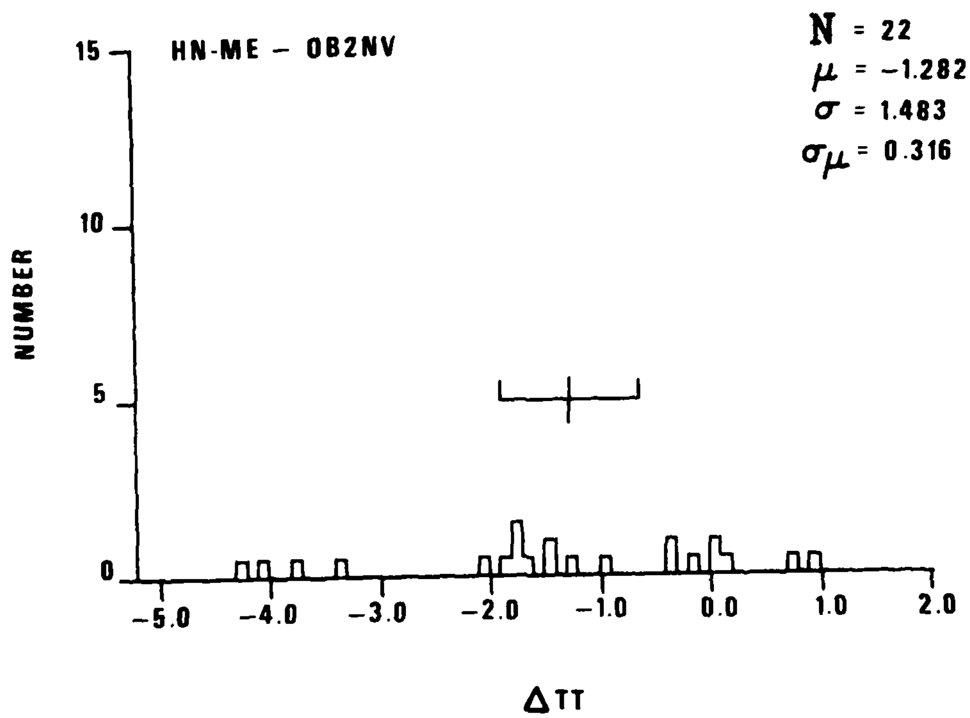
HN-ME – OB2NV
N = 22
μ = −1.282
σ = 1.483
σμ = 0.316
NUMBER
15
10
5
0
−5.0
−4.0
−3.0
−2.0
−1.0
0.0
1.0
2.0
ΔTT

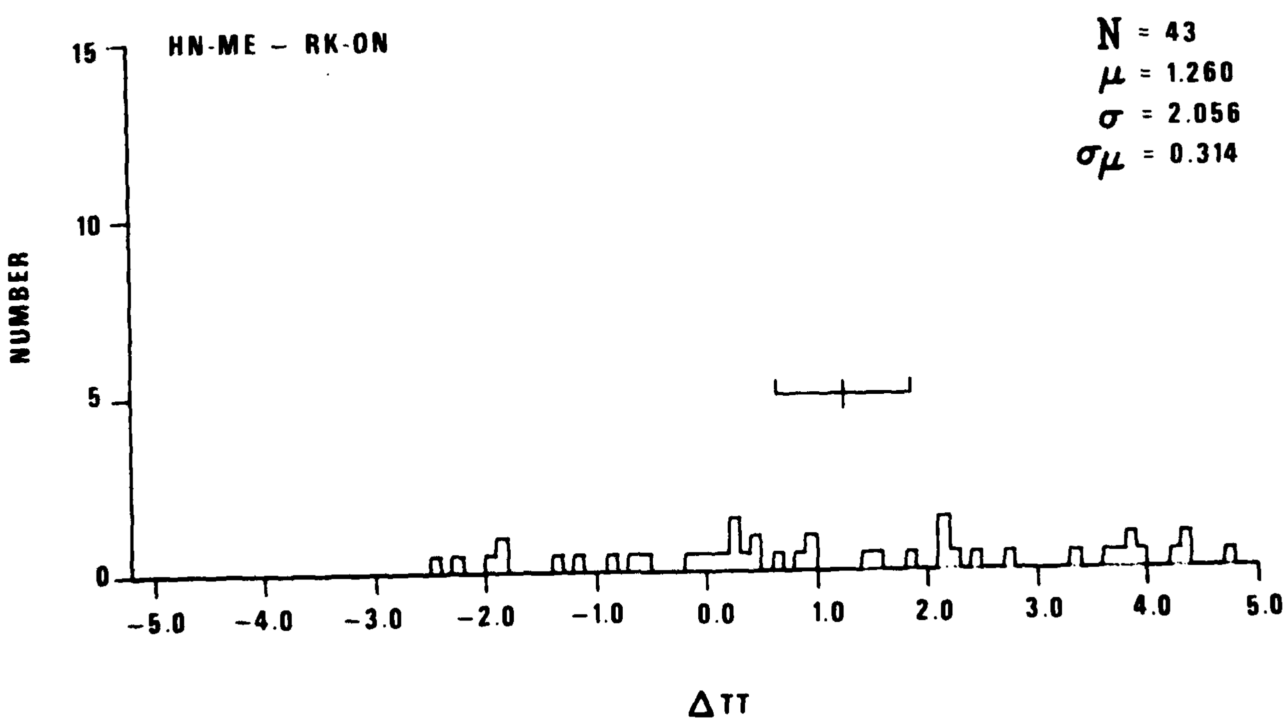
HN-ME – RK-ON
N = 43
μ = 1.260
σ = 2.056
σμ = 0.314
NUMBER
15
10
5
0
−5.0
−4.0
−3.0
−2.0
−1.0
0.0
1.0
2.0
3.0
4.0
5.0
ΔTT

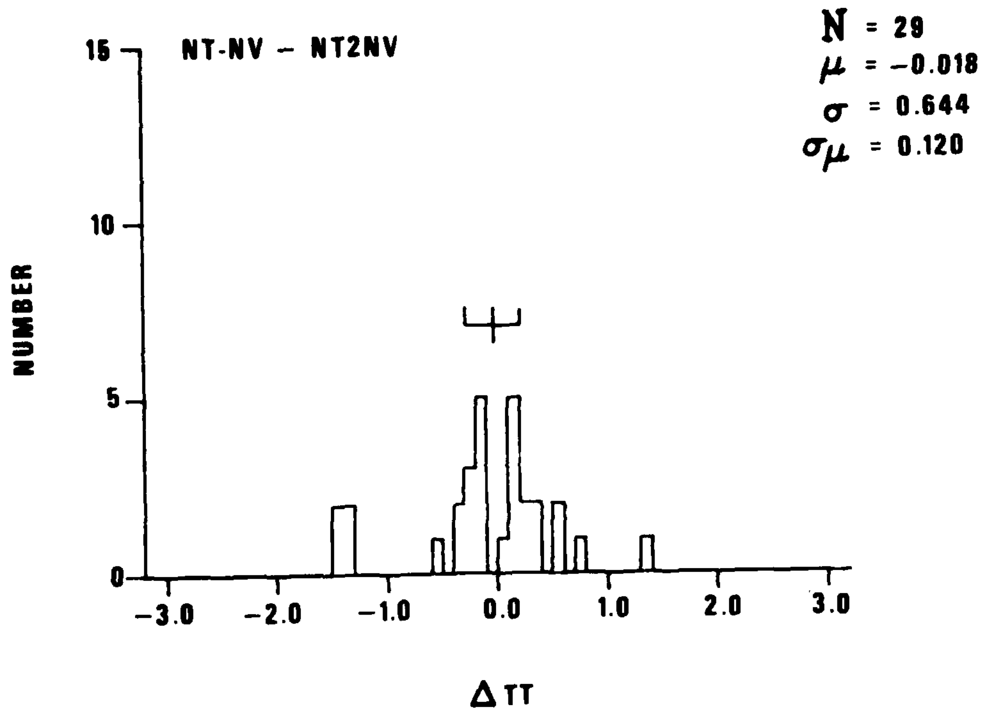

NT-NV – NT2NV
N = 29
μ = –0.018
σ = 0.644
σμ = 0.120
NUMBER
15
10
5
0
–3.0
–2.0
–1.0
0.0
1.0
2.0
3.0
Δ TT

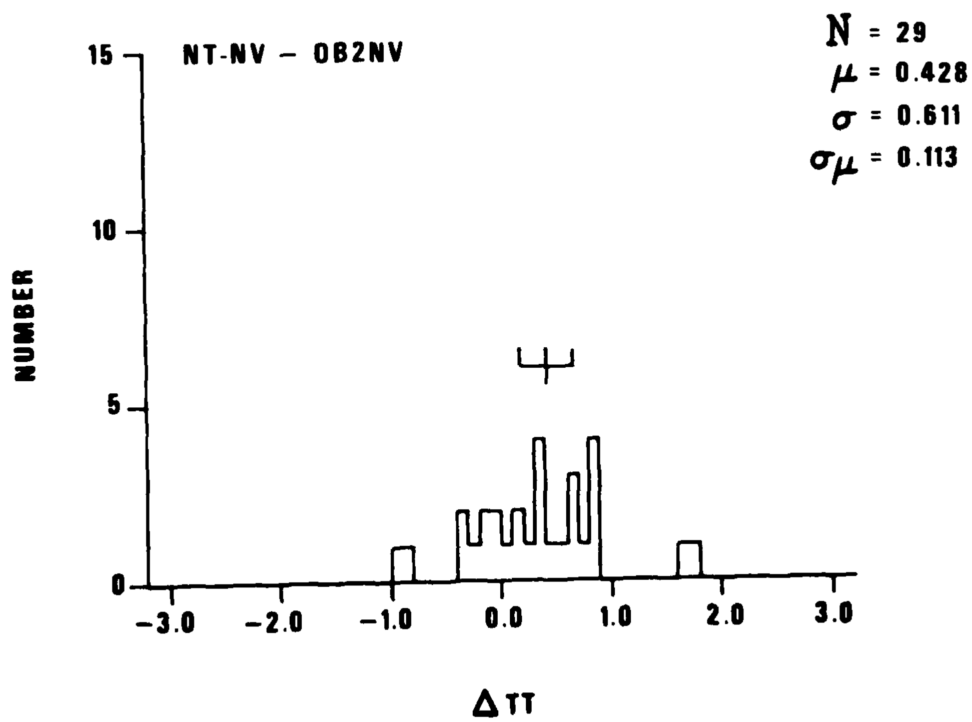

NT-NV – OB2NV
N = 29
μ = 0.428
σ = 0.611
σμ = 0.113
NUMBER
15
10
5
0
–3.0
–2.0
–1.0
0.0
1.0
2.0
3.0
Δ TT

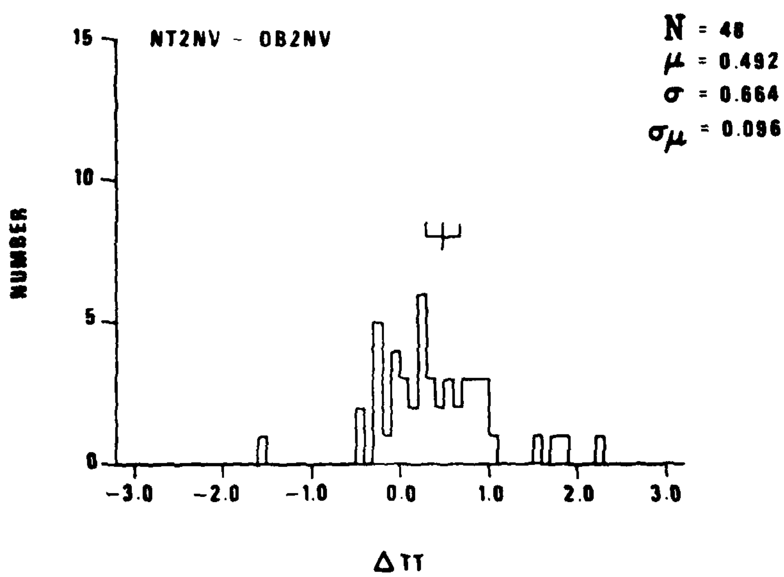
NT2NV - OB2NV
N = 48
μ = 0.492
σ = 0.664
σμ = 0.096
15
10
5
0
NUMBER
-3.0
-2.0
-1.0
0.0
1.0
2.0
3.0
Δ TT

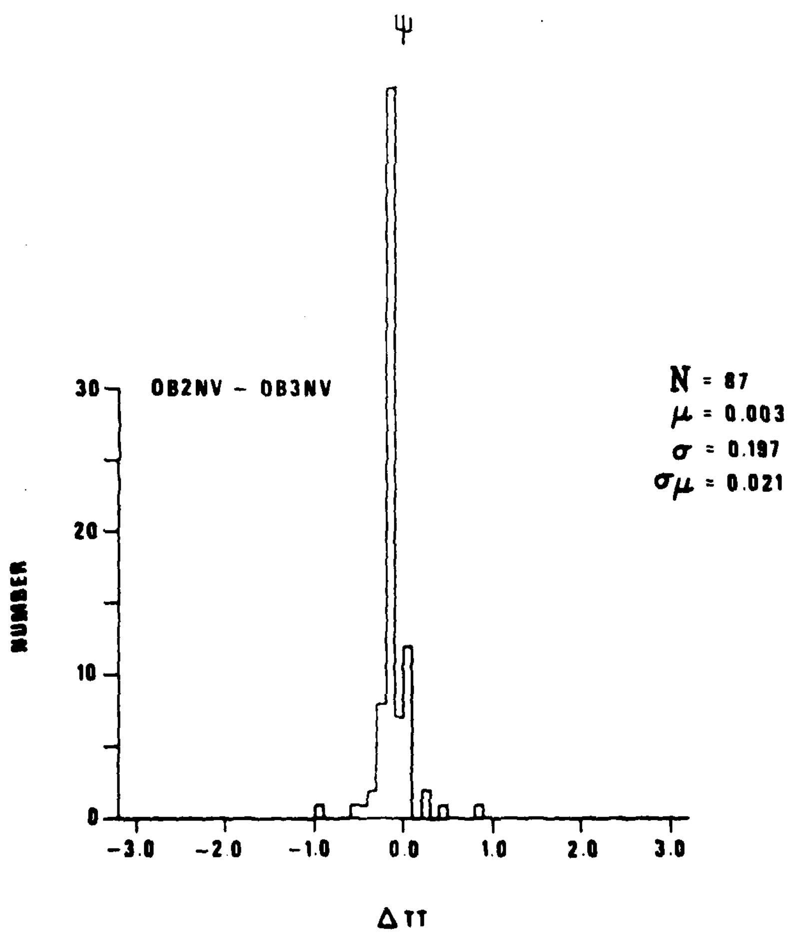
OB2NV - OB3NV
N = 87
μ = 0.003
σ = 0.197
σμ = 0.021
30
20
10
0
NUMBER
-3.0
-2.0
-1.0
0.0
1.0
2.0
3.0
Δ TT

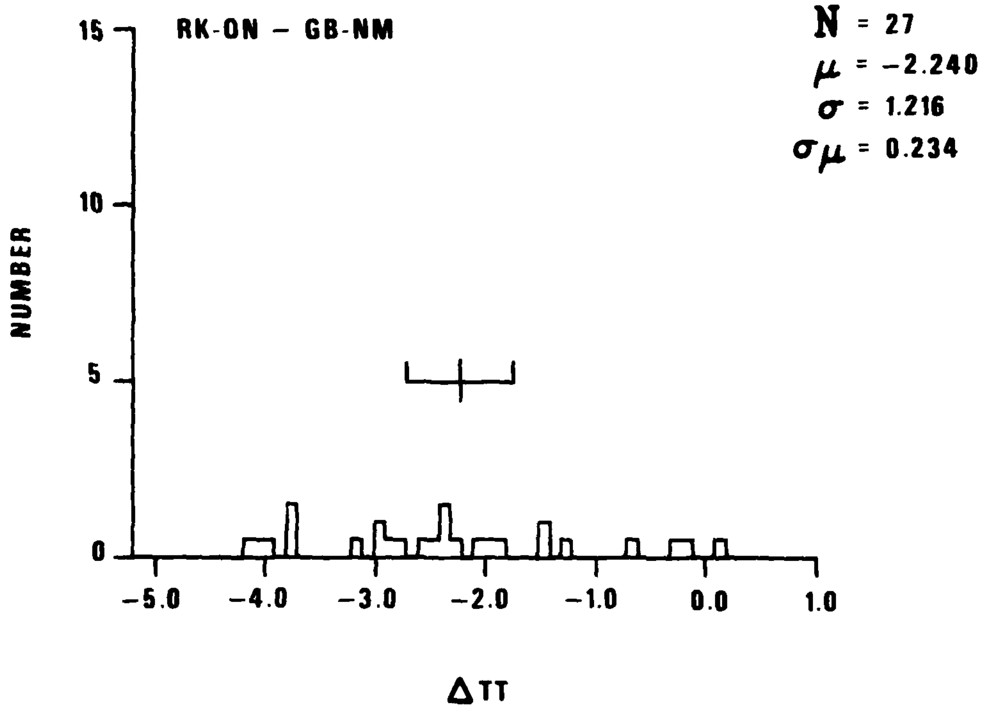

RK-ON – GB-NM
N = 27
μ = −2.240
σ = 1.216
σμ = 0.234
15
10
5
0
NUMBER
−5.0
−4.0
−3.0
−2.0
−1.0
0.0
1.0
ΔTT

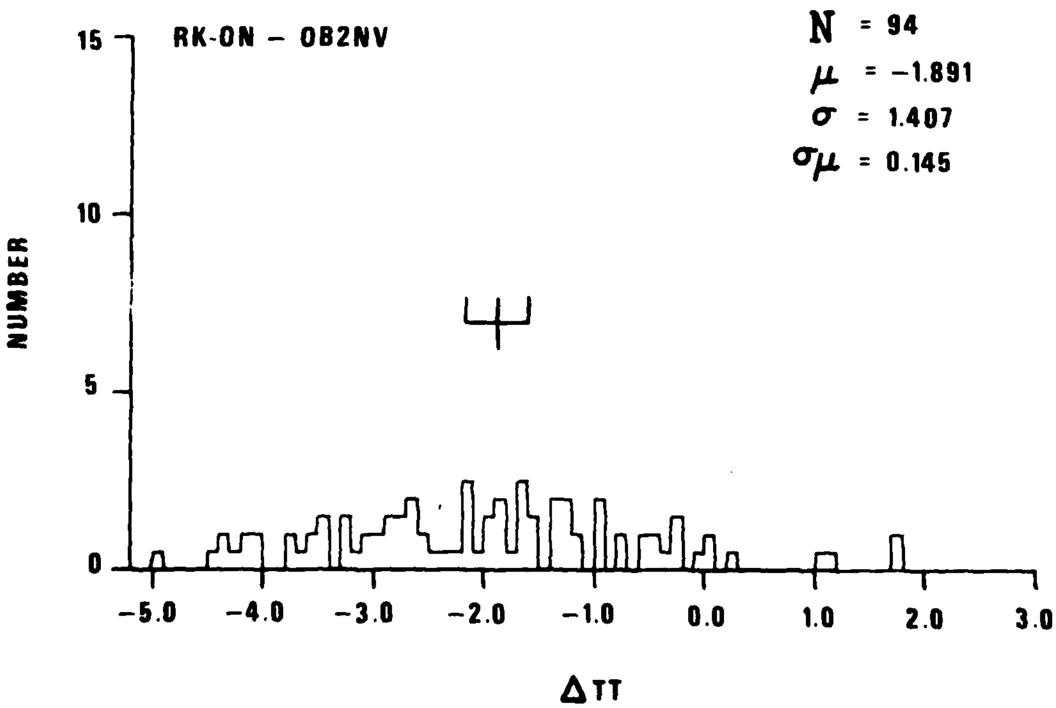

RK-ON – OB2NV
N = 94
μ = −1.891
σ = 1.407
σμ = 0.145
15
10
5
0
NUMBER
−5.0
−4.0
−3.0
−2.0
−1.0
0.0
1.0
2.0
3.0
ΔTT

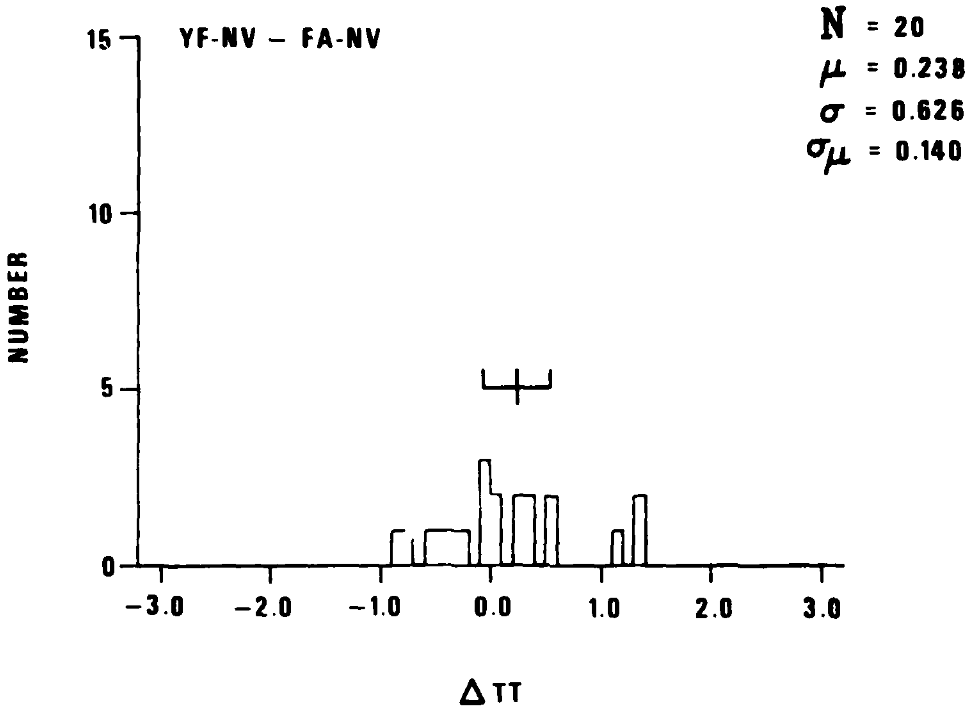
YF-NV – FA-NV
N = 20
μ = 0.238
σ = 0.626
σμ = 0.140
NUMBER
15
10
5
0
−3.0
−2.0
−1.0
0.0
1.0
2.0
3.0
Δ TT

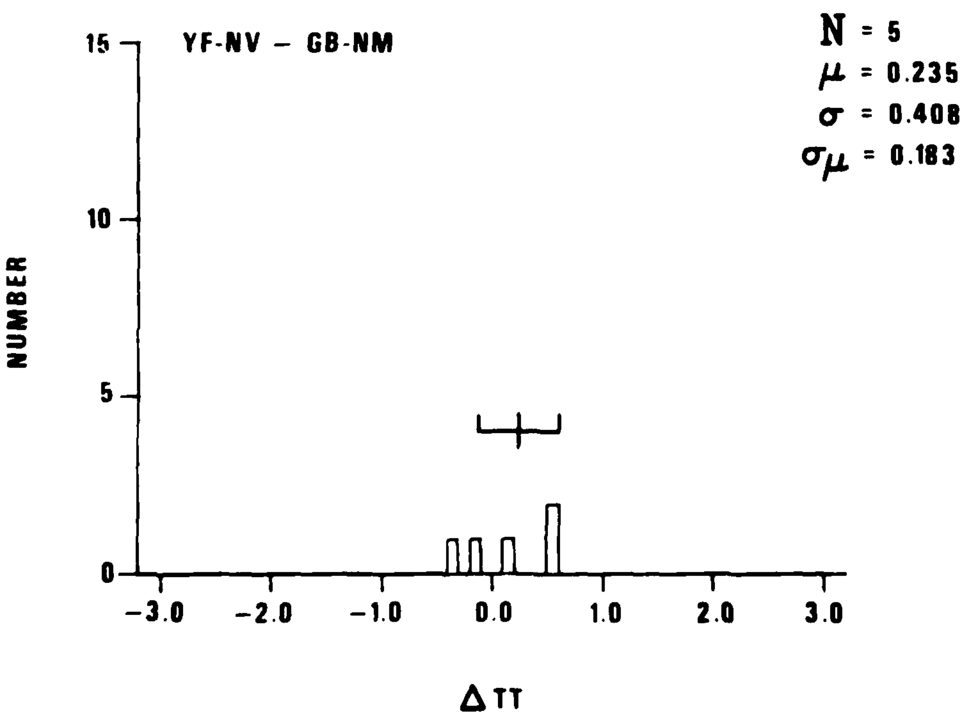
YF-NV – GB-NM
N = 5
μ = 0.235
σ = 0.408
σμ = 0.183
NUMBER
15
10
5
0
−3.0
−2.0
−1.0
0.0
1.0
2.0
3.0
Δ TT

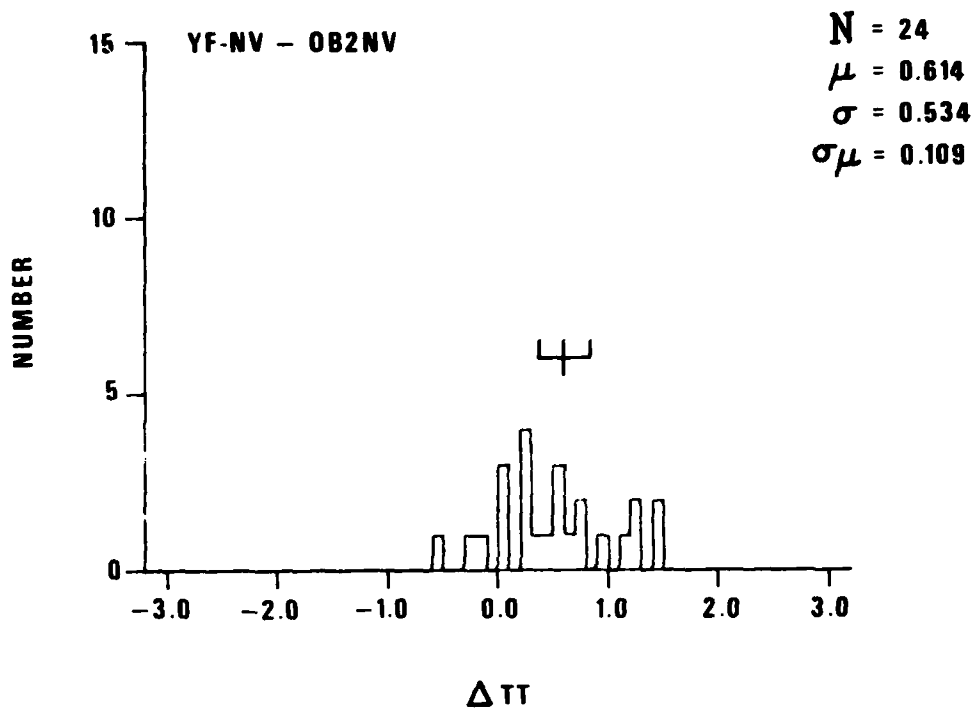
YF-NV – OB2NV
N = 24
μ = 0.614
σ = 0.534
σμ = 0.109
NUMBER
15
10
5
0
−3.0
−2.0
−1.0
0.0
1.0
2.0
3.0
ΔTT

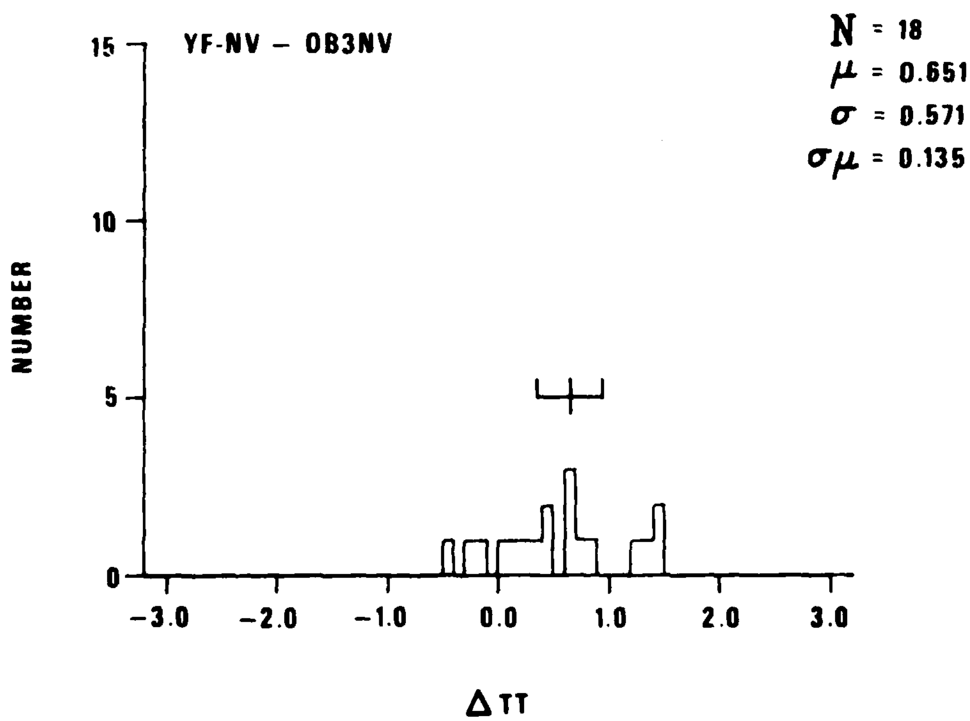
YF-NV – OB3NV
N = 18
μ = 0.651
σ = 0.571
σμ = 0.135
NUMBER
15
10
5
0
−3.0
−2.0
−1.0
0.0
1.0
2.0
3.0
ΔTT

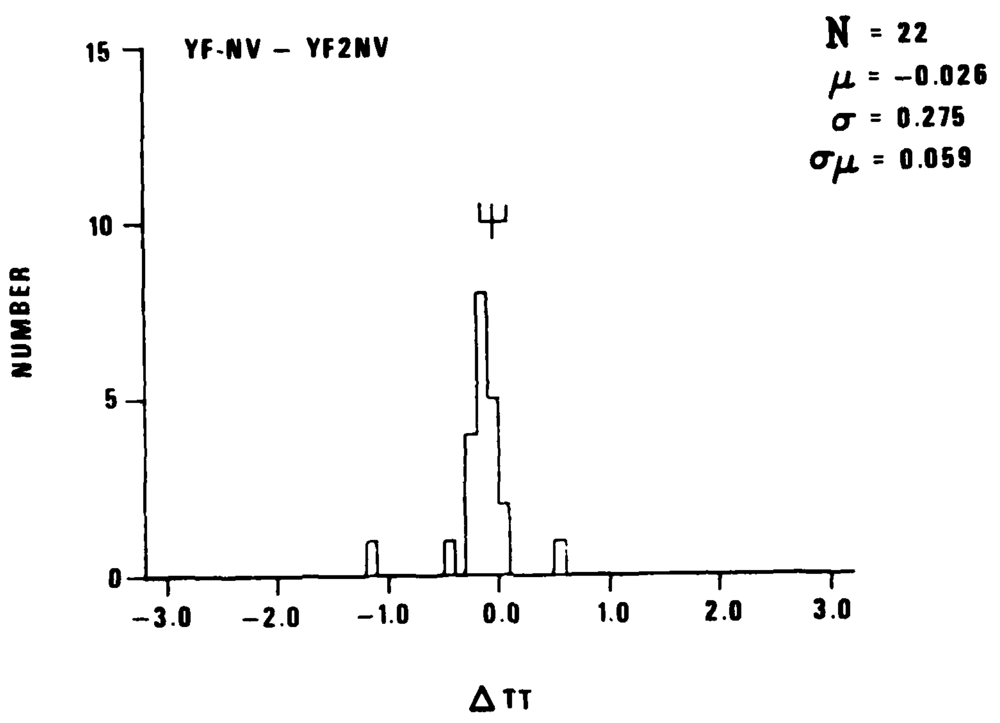

YF-NV – YF2NV
N = 22
μ = –0.026
σ = 0.275
σμ = 0.059
15
10
5
0
NUMBER
–3.0
–2.0
–1.0
0.0
1.0
2.0
3.0
Δ TT

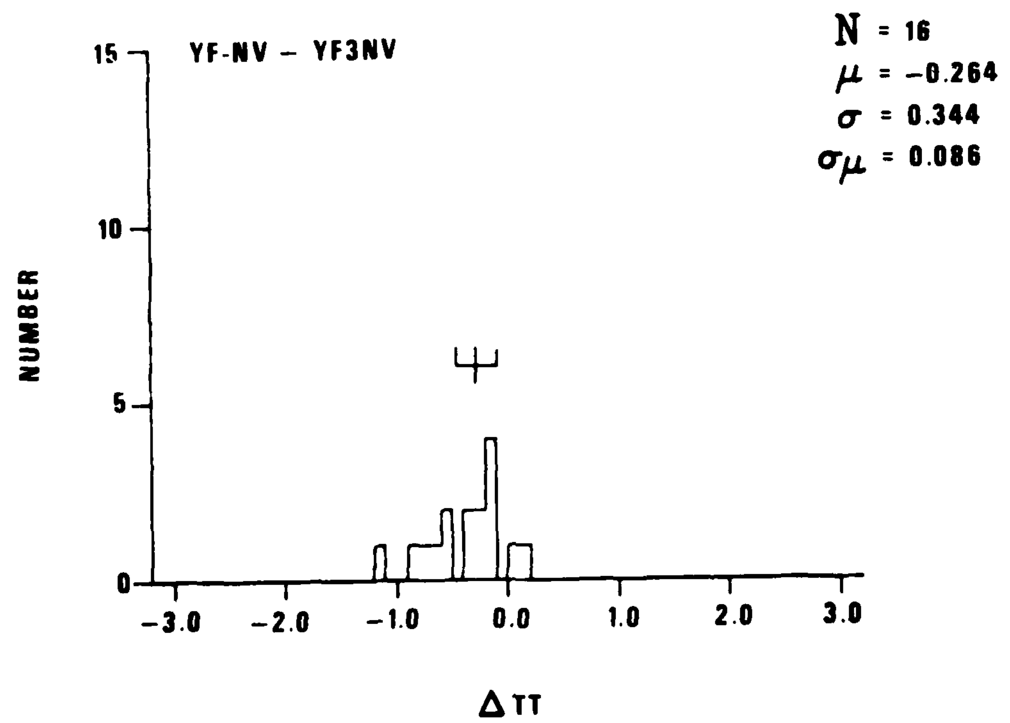

YF-NV – YF3NV
N = 16
μ = –0.264
σ = 0.344
σμ = 0.086
15
10
5
0
NUMBER
–3.0
–2.0
–1.0
0.0
1.0
2.0
3.0
Δ TT

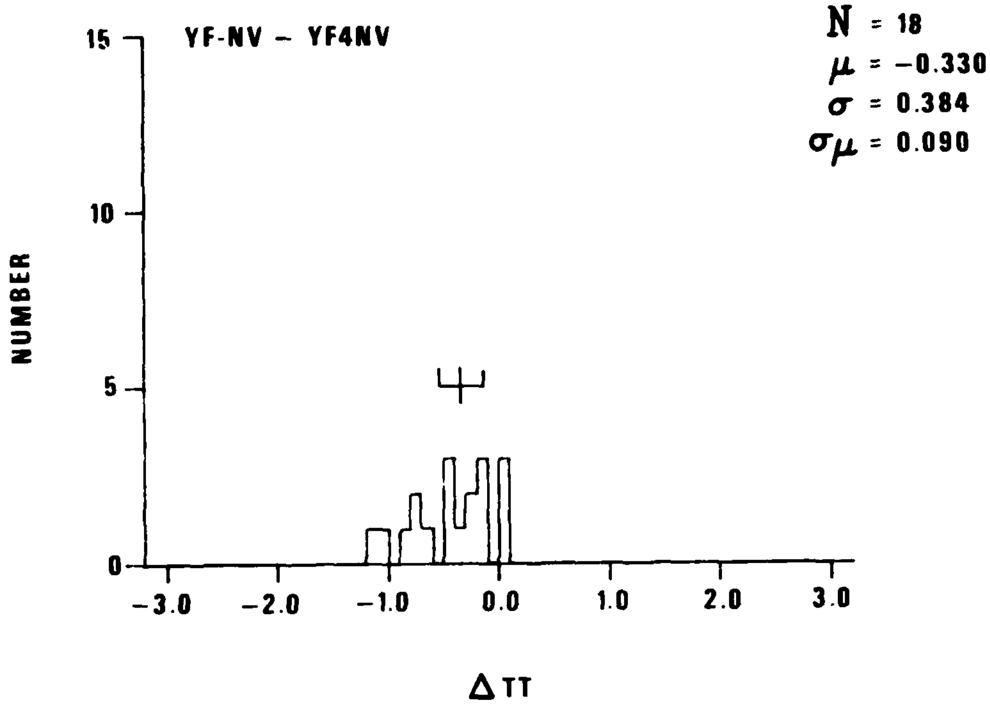
YF-NV – YF4NV
N = 18
μ = −0.330
σ = 0.384
σμ = 0.090
NUMBER
15
10
5
0
−3.0
−2.0
−1.0
0.0
1.0
2.0
3.0
Δ TT

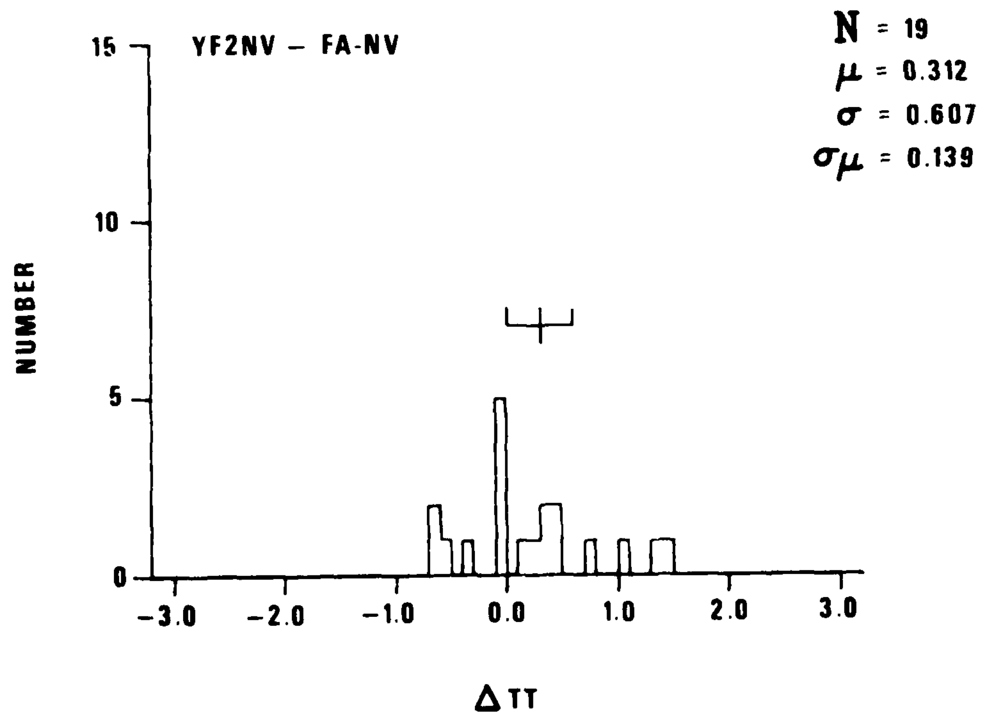
YF2NV – FA-NV
N = 19
μ = 0.312
σ = 0.607
σμ = 0.139
NUMBER
15
10
5
0
−3.0
−2.0
−1.0
0.0
1.0
2.0
3.0
Δ TT

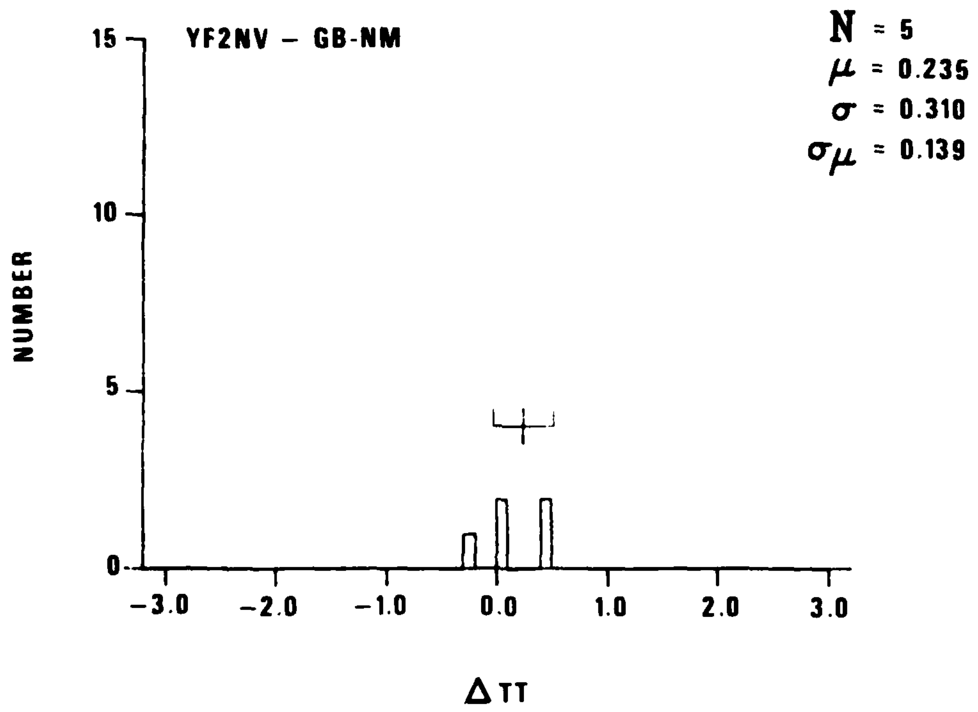
YF2NV – GB-NM
N = 5
μ = 0.235
σ = 0.310
σμ = 0.139
NUMBER
15
10
5
0
–3.0
–2.0
–1.0
0.0
1.0
2.0
3.0
Δ TT

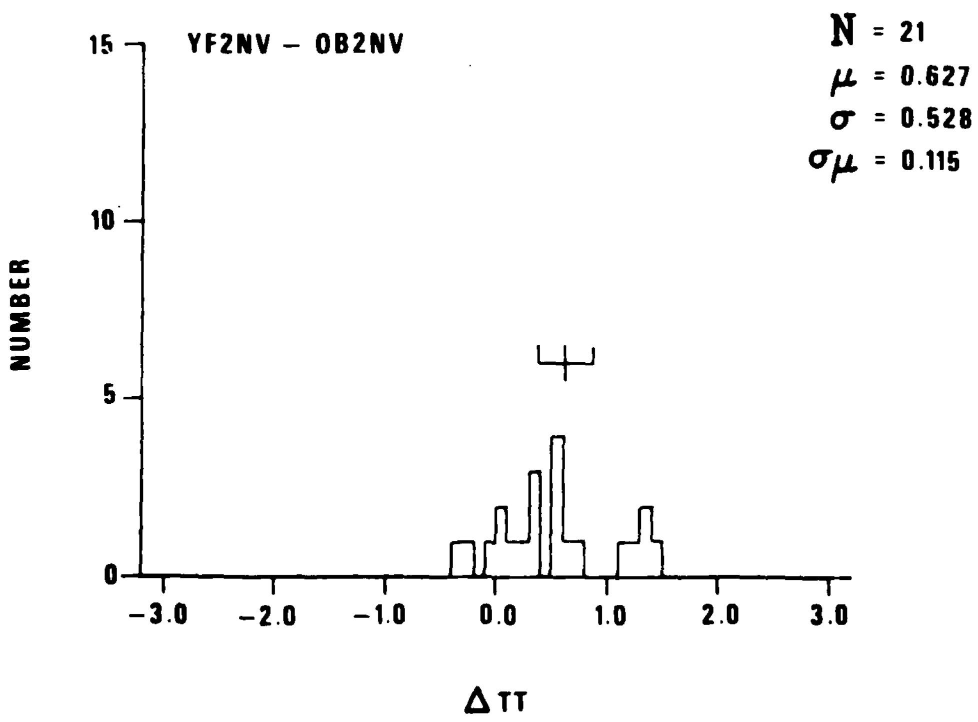
YF2NV – OB2NV
N = 21
μ = 0.627
σ = 0.528
σμ = 0.115
NUMBER
15
10
5
0
–3.0
–2.0
–1.0
0.0
1.0
2.0
3.0
Δ TT

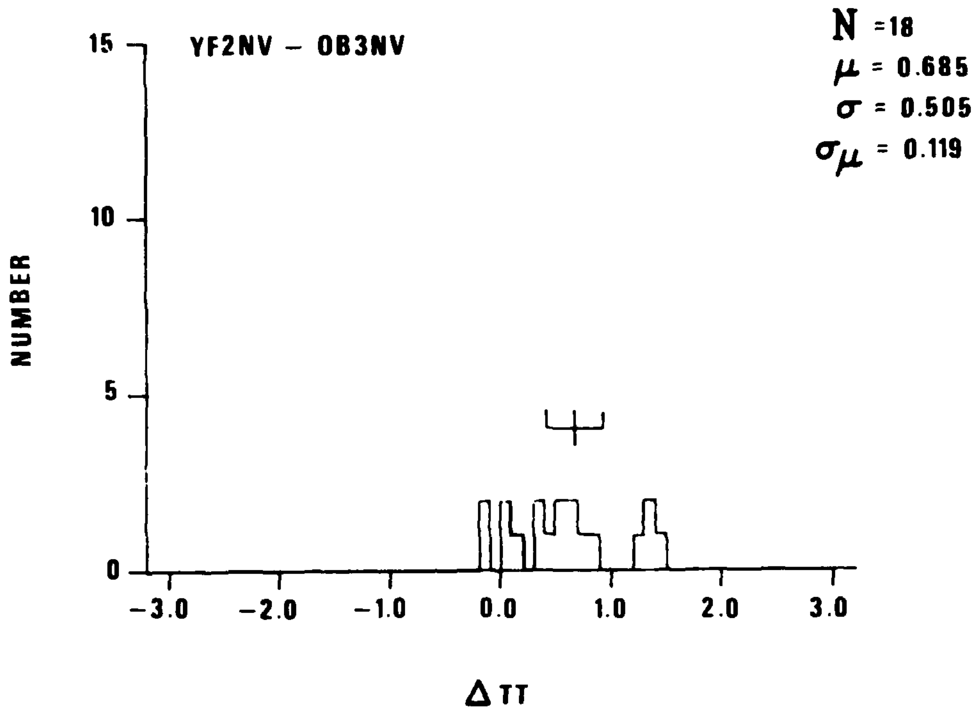
YF2NV – OB3NV
N =18
μ = 0.685
σ = 0.505
σμ = 0.119
NUMBER
15
10
5
0
−3.0
−2.0
−1.0
0.0
1.0
2.0
3.0
Δ TT

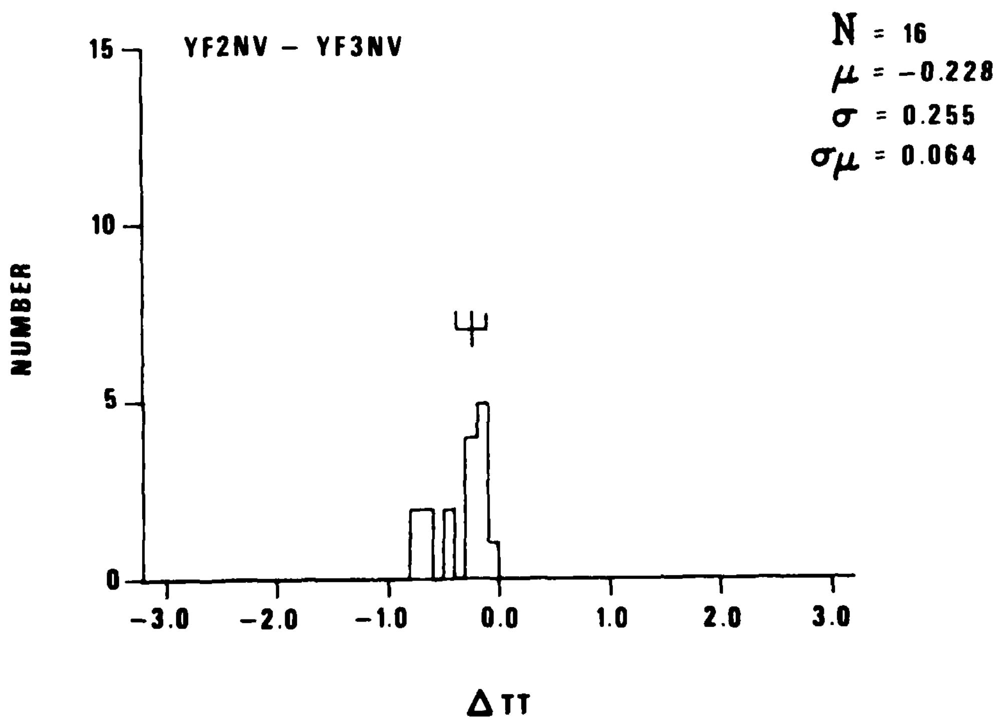
YF2NV – YF3NV
N = 16
μ = −0.228
σ = 0.255
σμ = 0.064
NUMBER
15
10
5
0
−3.0
−2.0
−1.0
0.0
1.0
2.0
3.0
Δ TT

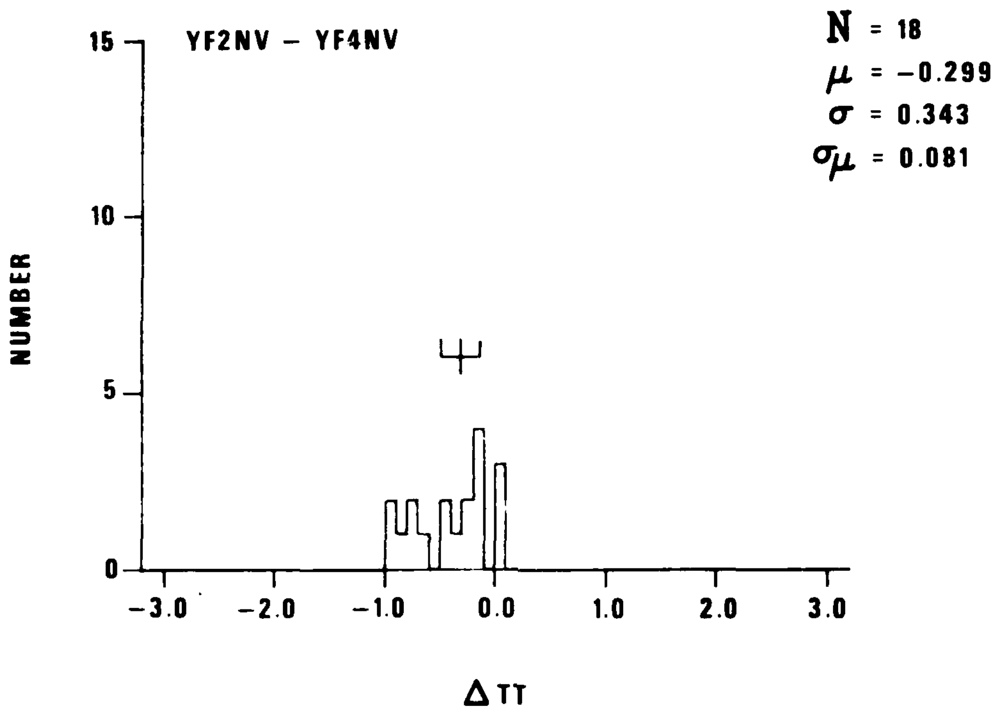
YF2NV – YF4NV
N = 18
μ = −0.299
σ = 0.343
σμ = 0.081
NUMBER
15
10
5
0
−3.0
−2.0
−1.0
0.0
1.0
2.0
3.0
ΔTT

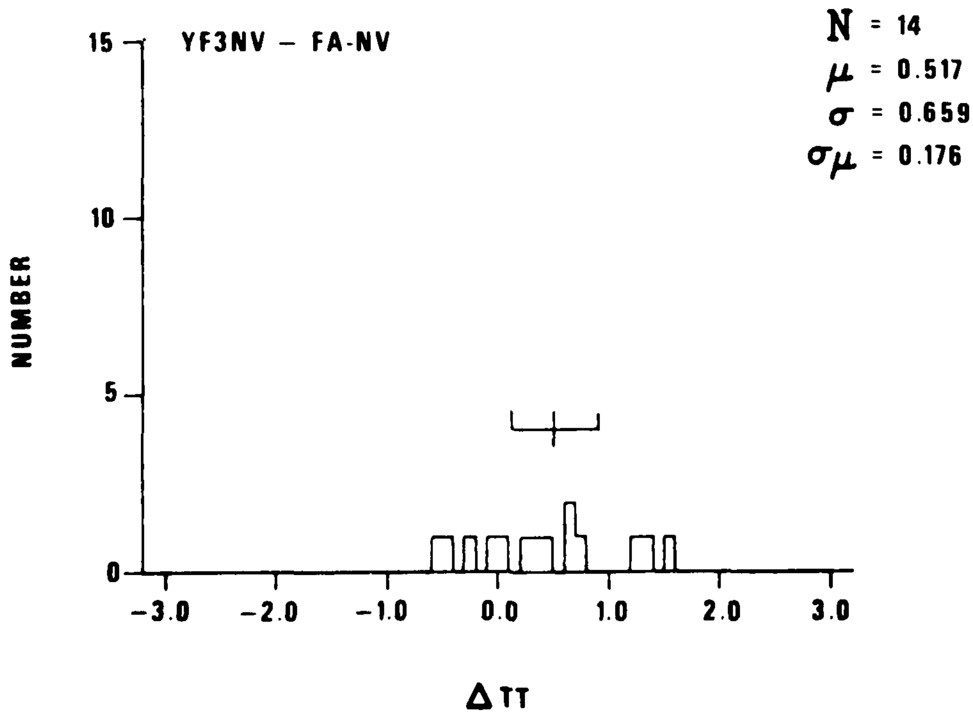
YF3NV – FA-NV
N = 14
μ = 0.517
σ = 0.659
σμ = 0.176
NUMBER
15
10
5
0
−3.0
−2.0
−1.0
0.0
1.0
2.0
3.0
ΔTT

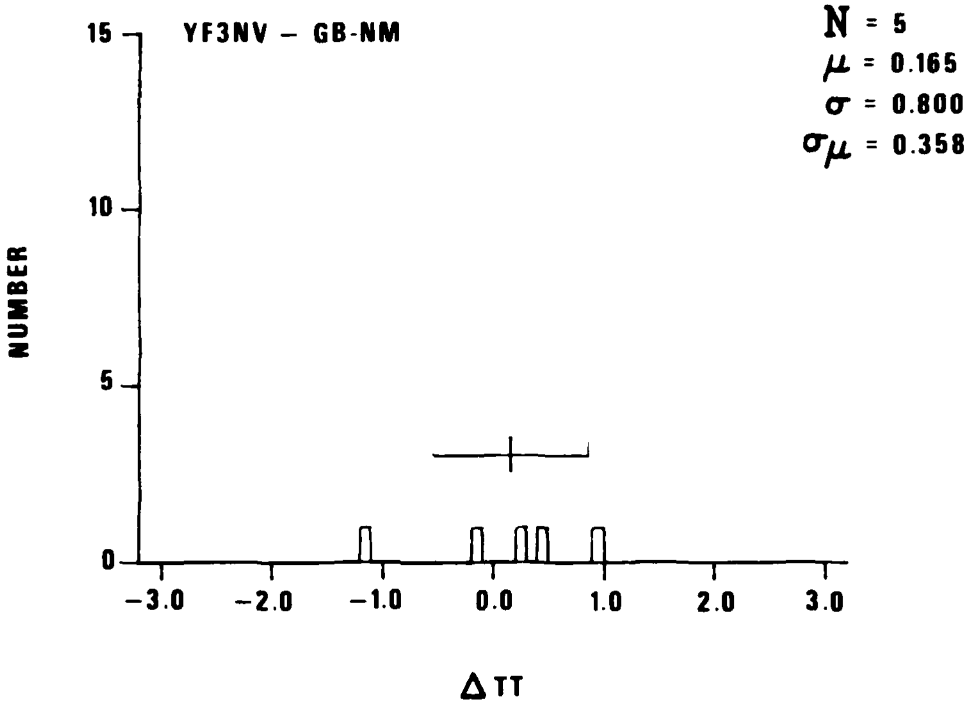

YF3NV – GB-NM
N = 5
μ = 0.165
σ = 0.800
σμ = 0.358
15
10
5
0
NUMBER
−3.0
−2.0
−1.0
0.0
1.0
2.0
3.0
ΔTT

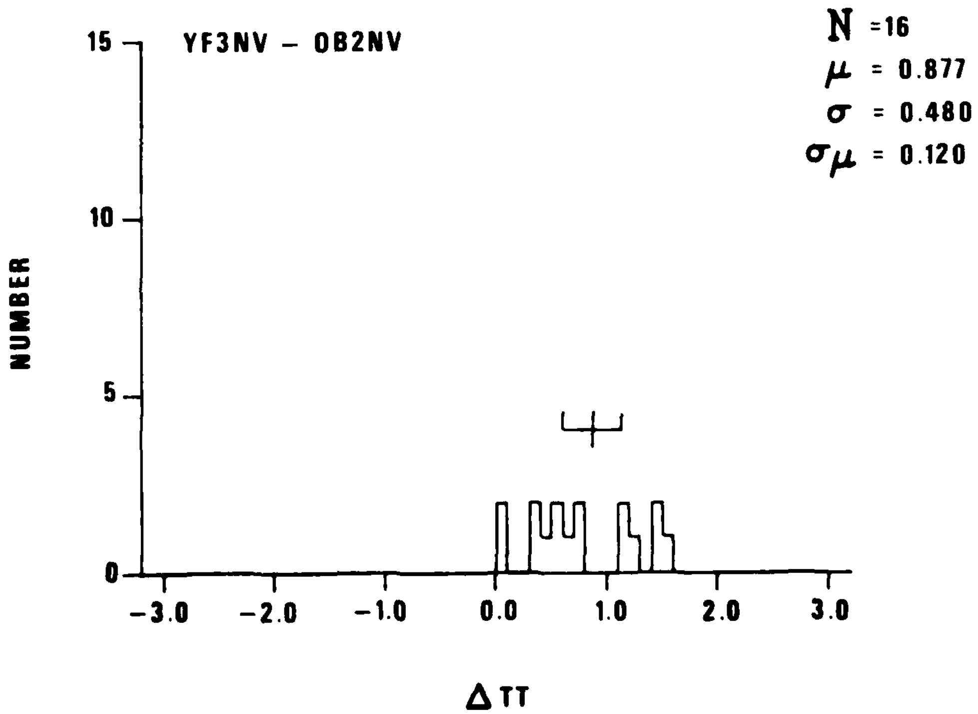

YF3NV – OB2NV
N =16
μ = 0.877
σ = 0.480
σμ = 0.120
15
10
5
0
NUMBER
−3.0
−2.0
−1.0
0.0
1.0
2.0
3.0
ΔTT

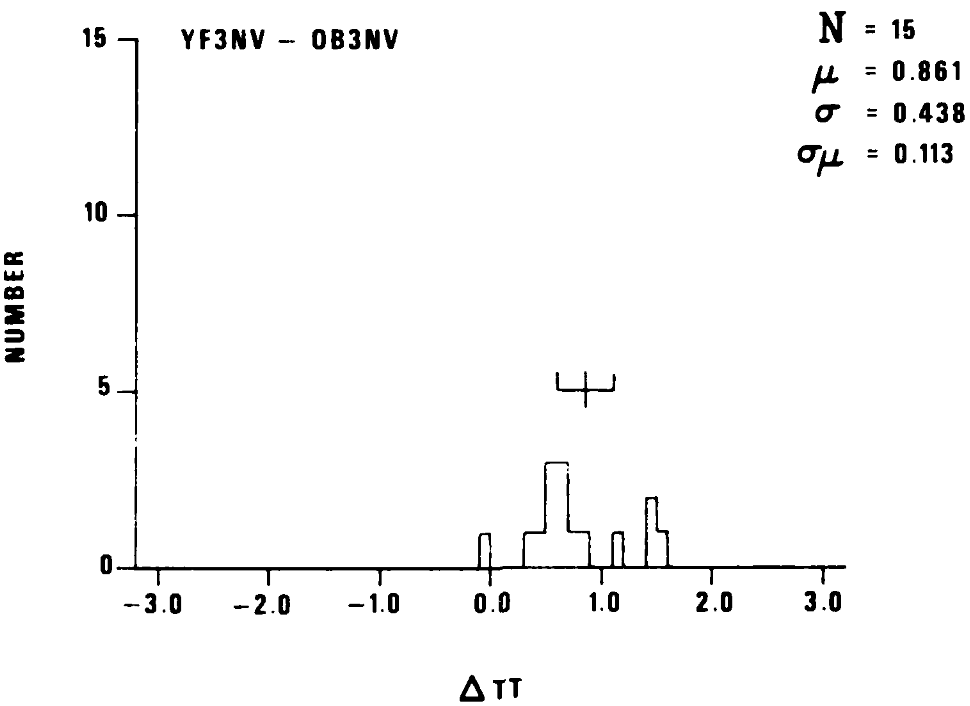
YF3NV – OB3NV
N = 15
μ = 0.861
σ = 0.438
σμ = 0.113
NUMBER
15
10
5
0
−3.0
−2.0
−1.0
0.0
1.0
2.0
3.0
Δ TT

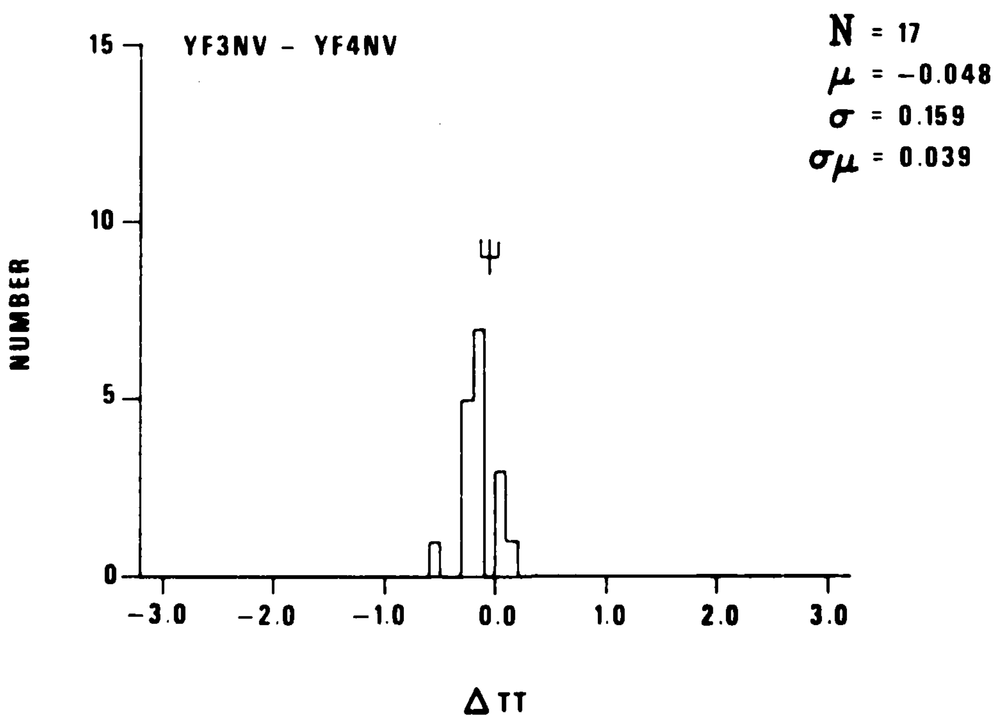
YF3NV – YF4NV
N = 17
μ = −0.048
σ = 0.159
σμ = 0.039
NUMBER
15
10
5
0
−3.0
−2.0
−1.0
0.0
1.0
2.0
3.0
Δ TT

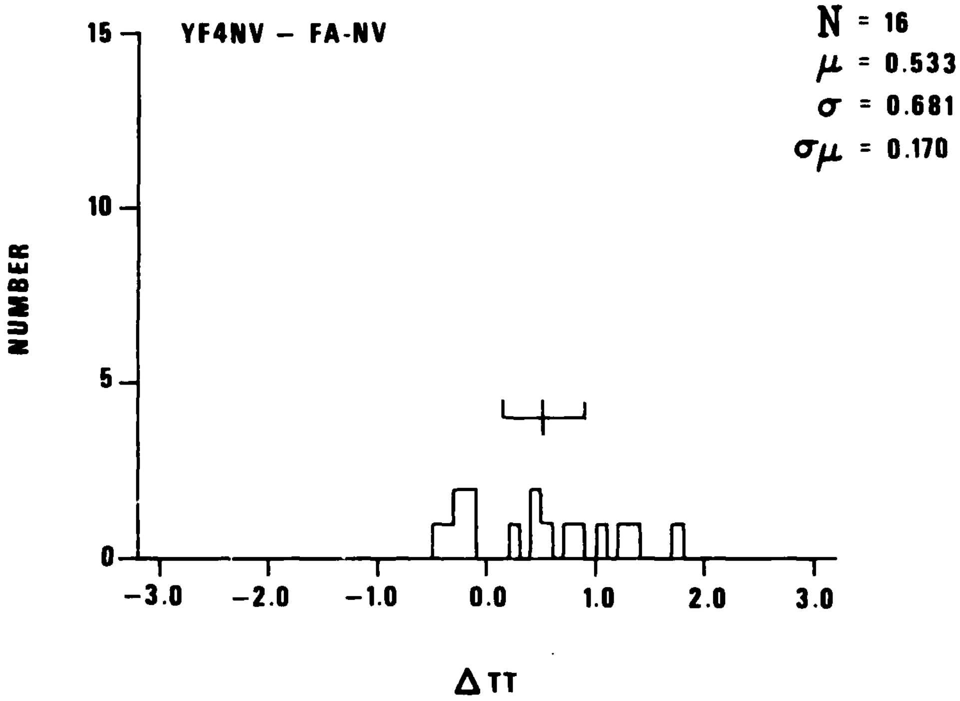
YF4NV – FA-NV
N = 16
μ = 0.533
σ = 0.681
σμ = 0.170
NUMBER
15
10
5
0
−3.0
−2.0
−1.0
0.0
1.0
2.0
3.0
Δ TT

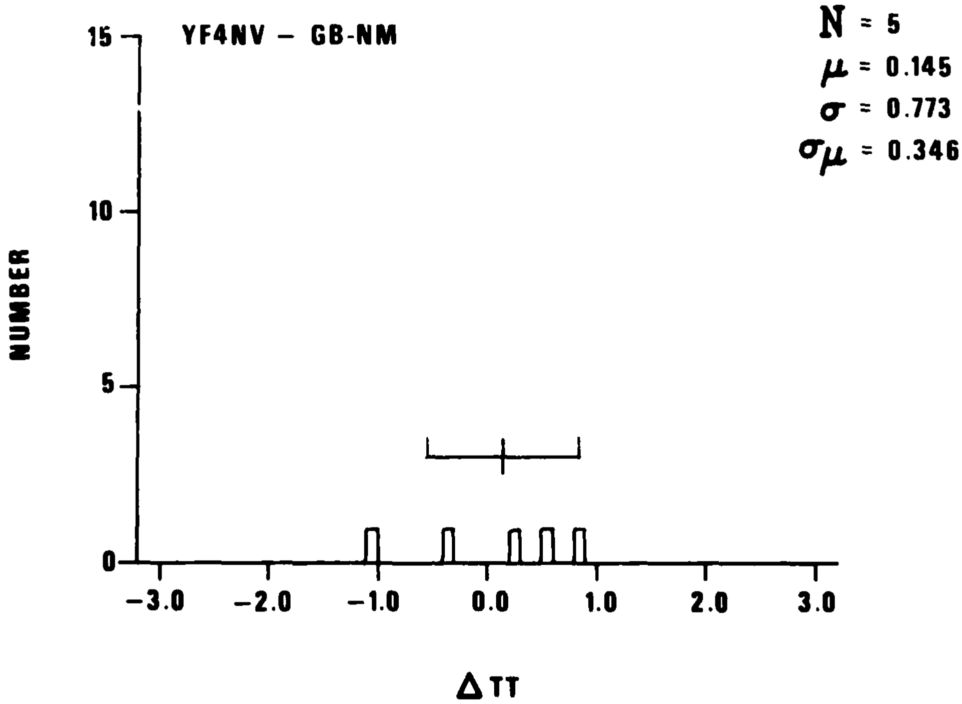
YF4NV – GB-NM
N = 5
μ = 0.145
σ = 0.773
σμ = 0.346
NUMBER
15
10
5
0
−3.0
−2.0
−1.0
0.0
1.0
2.0
3.0
Δ TT

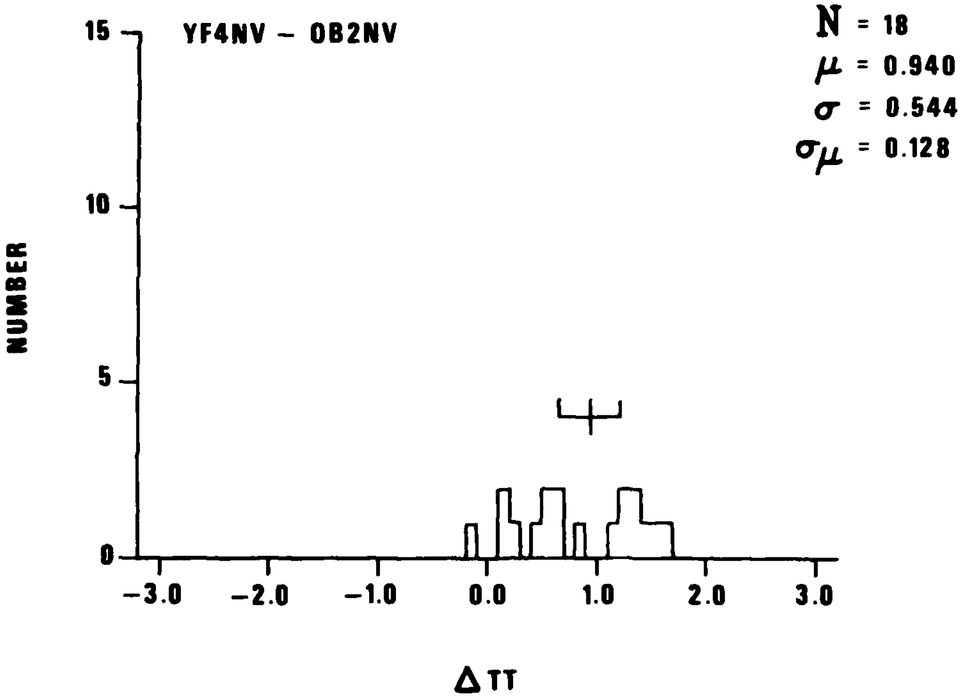
YF4NV – OB2NV
N = 18
μ = 0.940
σ = 0.544
σμ = 0.128
NUMBER
15
10
5
0
−3.0
−2.0
−1.0
0.0
1.0
2.0
3.0
ΔTT

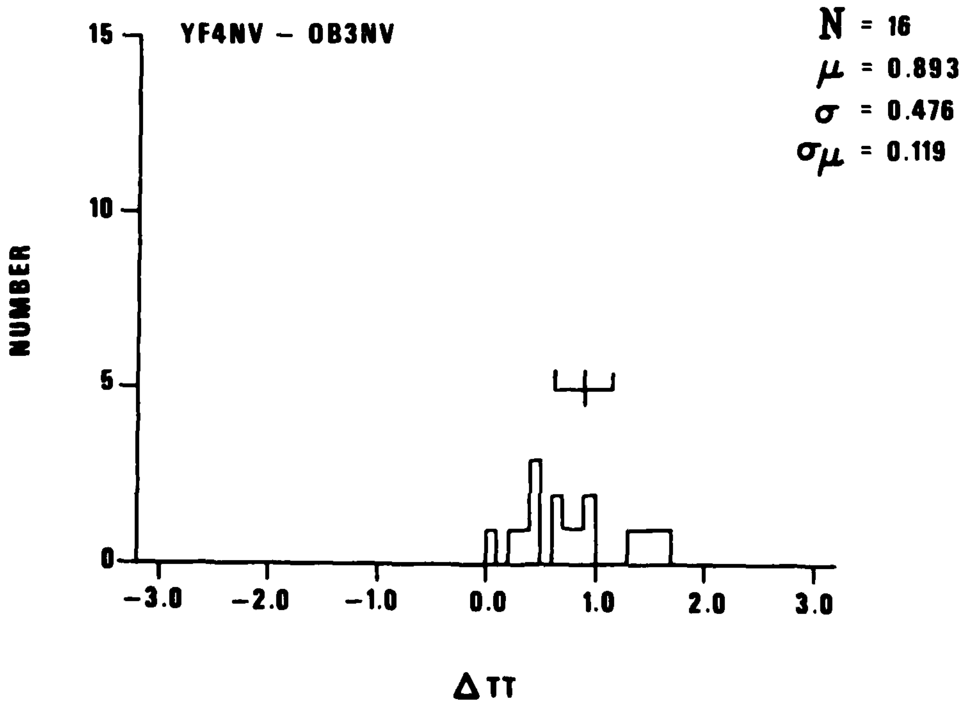
YF4NV – OB3NV
N = 16
μ = 0.893
σ = 0.476
σμ = 0.119
NUMBER
15
10
5
0
−3.0
−2.0
−1.0
0.0
1.0
2.0
3.0
ΔTT

SUPPLEMENTARY

INFORMATION

M E M O R A N D U M

TO: All Recipients of VSC-TR-81-14

FROM: Z. A. Der and T. W. McElfresh

DATE: 26 October 1982

SUBJECT: Explanation of amplitude data in VSC-TR-81-14

The raw station data presented in Appendix A of the final SDCS report (VSC-TR-81-14) has the format:

					Arrival				
STA	Δ	A	T	H	M	S	GAIN	A_b	T_b
IF-ME	77.2	11.0	0.9	11	45	6.7	112		

where STA = station name

Δ = station to event distance (deg)

A = maximum signal amplitude* (first three cycles)

T = dominant period of corresponding cycle (sec)

H = hour

M = minute

S = second

(H, M, S: Arrival Time)

GAIN = gain factor (see below)

A_b = b-phase amplitude, if measured

T_b = b-phase period, if measured

*Attention is called to the Amplitude and GAIN columns. If no gain factor is given, then the amplitude A is understood to be in units of nanometers. This is the case for those stations having digital recording equipment.

If a gain factor is listed for a station, then the amplitude A is in millimeters as measured directly from the film viewer. In this case, the amplitude in nanometers can be computed using the equation:

$$A_{nm} = 500\ A_{mm}/\mathrm{GAIN}$$

This conversion was applied by the computer program that produced the histograms of magnitude differentials Δm_b and trace amplitude differentials ΔA_{tr} shown in Appendices B and C. Thus the histograms and results of the report are valid as stated.

The few repeated events in Appendix A are due to the arrival and processing of various subsets of the data at different times. This also accounts for the events not being listed chronologically.

The authors regret any confusion that this may have caused our readers. We are planning to re-issue the data shown in Appendix A in a unified format in the near future.

ZAD-TWM/paw